

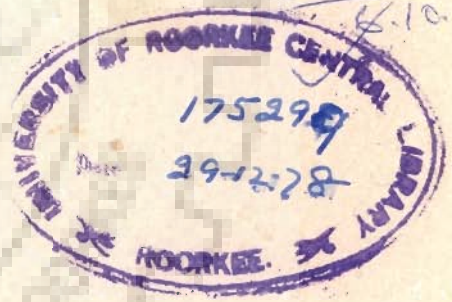
(T)

F-78
YOG

STUDIES ON GAS-SOLIDS FLUIDIZATION WITH VERTICAL INTERNAL BAFFLES

A THESIS
submitted in fulfilment
of the requirements for the Degree
of
DOCTOR OF PHILOSOPHY
in
CHEMICAL ENGINEERING

BY
YOGESH CHANDRA



DEPARTMENT OF CHEMICAL ENGINEERING
UNIVERSITY OF ROORKEE
ROORKEE, 247672 (INDIA)
May, 1978

C E R T I F I C A T E

It is certified that thesis entitled 'STUDIES ON GAS-SOLIDS FLUIDIZATION WITH VERTICAL INTERNAL BAFFLES' which is being submitted by Sri Yogesh Chandra, in fulfilment of the requirements for the award of the degree of DOCTOR OF PHILOSOPHY in CHEMICAL ENGINEERING at the University of Roorkee, Roorkee, is a record of candidate's own work carried out by him under the supervision and guidance of the undersigned. The matter embodied in this thesis has not been submitted for the award of any other degree.

This is further certified that the candidate has worked for a period of about Four years since July, 1974, for preparing this thesis.

N. J. Rao

(N. J. RAO)
Reader
Department of
Chemical Engg.
University of
Roorkee, Roorkee
INDIA.

P. S. Panesar

(P. S. PANESAR)
Professor, Q.I.P.
University of
Roorkee, Roorkee
INDIA.

N. Gopal Krishna

(N. GOPAL KRISHNA)
Professor and Head
Department of
Chemical Engg.
University of
Roorkee, Roorkee
INDIA.

May 17 , 1978.

S U M M A R Y

The thesis entitled 'Studies on gas-solids fluidization with internal vertical baffles' is presented in six chapters. In Chapter I, the literature review relating to fluidization characteristics, bed pressure drop, minimum fluidizing velocity, bed expansion, fluidization characteristics in continuous fluidization and bed hold ups is reported. The present studies on the effect of vertical baffles on fluidization characteristics, bed expansion and quality of fluidization in batch and continuous gas-solids fluidization and studies on bed hold-up using mixed sized particles are indicated.

In Chapter II, is presented the physical and flow properties of solids like particle diameter, particle density, static bed porosity, sphericity and solids angle of repose for material like spherical glass beads, bauxite, limestone and baryte.

Chapter III deals with the studies on batch fluidization in 70 mm I.D. perspex column having 12, 7 and 3 Nos. of 6 mm diameter stainless steel rods as internal vertical baffles having an effective length of 610 mm. Aluminium grid plate having 10% openings is used as air distributor and to support the particles. Spherical glass beads, crushed bauxite, limestone and baryte in

the size range of 1540 microns to 385 microns have been studied. The bed pressure drop has been measured as a function of air flow rate in the fixed bed, at the onset of fluidization and in the fluidized bed zones. It is observed that bed pressure drop increases with increase in air flow rate in fixed bed zone and it remains essentially constant after the onset of fluidization. The variation of pressure drop with air flow rate is compared with fluidized beds with and without baffles. It is observed that pressure drop in baffled bed is more than that in the unbaffled bed. This increase in the pressure drop is due to the additional skin friction caused due to the presence of baffles in the bed. The pressure coefficient ($\Delta PA/W$) is observed to be more in the fluidized beds with baffles as compared to that with unbaffled beds indicating better fluidization. Keeping the same conditions of solids loading per unit area and the equivalent diameter of the column, effect of a single baffle on fluidization characteristics has been studied. The bed pressure drop has been measured at different air flow rates in the fixed bed, at the onset of fluidization and in fluidized bed zones. When compared, pressure drop in fixed bed zone with single equivalent baffle and in multibaffled bed is found to be of same magnitude. However, at and beyond onset of fluidization, pressure drop is more in the multibaffled fluidized bed as compared to that in the

bed with single equivalent baffle. This is indicative of the presence of channelling tendencies in the latter. Quality of fluidization is improved by introducing several baffles in the bed as the slugging is reduced in the bed.

A dimensionless correlation has been proposed to predict the overall pressure drop in the fluidized bed with vertical baffles, at and beyond onset of fluidization as,

$$\frac{\Delta P A}{W} = 0.923 + k_1 (Re_{eq})^2 + k_2 (Re_T)^2$$

$$k_1 = 3.72 \times 10^{-8}$$

$$k_2 = 3.46 \times 10^{-10}$$

The correlation predicts the pressure drop within $\pm 10\%$ of the experimental values.

A minimum distance of six particle diameters between two adjacent baffles is found essential for initiating the movement of particles. At a distance greater than ten particle diameters, however, smooth and uniform fluidization is achieved.

The experimental values of the minimum fluidizing velocities in the baffled beds have been found to differ widely from the values predicted using Leva's correlation for cylindrical columns without baffles. A dimensionless

correlation incorporating various parameters like the term d_o/D_p , solids and fluid physical properties and geometry of the apparatus, has been proposed for predicting the minimum fluidizing velocity as

$$\frac{D_p G_{mf}}{\mu_f} = 6.2 \times 10^{-2} (Ar)^{0.624} \left(\frac{D_e}{D_p}\right)^{-0.12} \left(\frac{d_o}{D_p}\right)^{-0.13} \left(\frac{L}{d_o}\right)^{0.04}$$

The predicted values are found to be well within $\pm 20\%$ of the experimental values.

Studies on the effect of vertical internal baffles on the bed expansion and fluctuation ratio have been conducted. The bed expansion and fluctuation ratio will be lower in beds with vertical internal baffles as bubbling is reduced because of the presence of baffles. A dimensionless correlation has been proposed as

$$\epsilon = 0.065 (Fr)^{-0.22} (Re)^{0.4} \left(\frac{d_o}{D_p}\right)^{0.69} \left(\frac{\rho_s - \rho_f}{\rho_f}\right)^{-0.11}$$

for predicting the expanded bed height in baffled beds within $\pm 15\%$ deviation from the experimental values and is valid for $4 < Re_p < 175$.

The fluctuation ratios for different solids for a given reduced mass velocity of air (G_f/G_{mf}) are observed to be lower in baffled beds as compared to unbaffled beds, indicating better quality of fluidization in the former. The quality of fluidization in a fluidized

bed can be measured by the fluctuation ratio of the levels in the bed. Fluctuation ratio has been correlated as an exponential function of $(G_f - G_{mf})/G_{mf}$ as earlier done by Lewis et al [126] as

$$r = e^{m(G_f - G_{mf})/G_{mf}}$$

where m is the slope of the line on semilog plot and is a function of particle diameter. The predicted values of fluctuation ratios are found to be within $\pm 15\%$ of the experimental values.

In Chapter IV, studies on continuous gas-solids fluidization in column fitted with multibaffles (as described in Chapter III) with provision to feed the material continuously from top and remove the solids from bottom, have been given. Studies have been carried out using different solids in the size range of 977 to 385 microns and feed rate varying from 6.9×10^{-3} to 1.52×10^{-2} kg/s. Introduction of vertical baffles in the bed increases the pressure drop because of extra skin friction due to additional baffle surface and fluidized particles. A dimensionless correlation has been proposed to predict the bed pressure drop within $\pm 20\%$ deviation from the experimental values as

$$\frac{\Delta P}{P_f L} = 52.5 (Fr)^{0.33} (Re)^{0.08} \left(\frac{D_e}{D_p}\right)^{-0.1} (R)^{0.3} \left(\frac{P_s - P_f}{P_f}\right)^{0.17}$$

It is observed that for a given solids feed rate, the lower bed densities could be obtained at high air velocities in countercurrent operation of gas and solids. When compared, the bed density is observed to be higher in fluidized beds with vertical baffles than in unbaffled beds for a given solids loading ratio. A dimensionless correlation incorporating various parameters has been proposed for predicting the bed density in baffled beds as

$$\frac{\rho_{bd}}{\rho_f} = 342 (\text{Fr})^{-0.15} (\text{Re})^{-0.008} \left(\frac{d_o}{D_p}\right)^{0.27} \left(\frac{\rho_s - \rho_f}{\rho_f}\right)^{0.11}$$

The predicted values are found to lie within $\pm 10\%$ of the experimental values.

Chapter V deals with the studies on the mean residence time and hold up of particles using mixed sized feeds in continuous systems with vertical internal baffles. The effect of air flow rate, solids feed rate, bed height and feed composition of solids on residence time and hold up of particles has been studied. The hold up ratio in the bed (defined as the ratio of the mean residence time of larger particles to that of small particles) is observed to be higher in beds with baffles as compared to that in unbaffled beds. At air flow rates between $1.6 - 1.8 U_{mf}$ the bed hold up ratio tends to remain steady in the unbaffled beds whereas a steady increase in the bed hold up ratio with increase in air flow rates even beyond

1.8 U_{mf} is observed in the beds with vertical baffles. This is indicative that in case of baffled beds, the hold up of larger particles increases as compared to that of the small particles. A correlation for predicting the hold up ratio has been proposed as,

$$H(2,1) = 0.44 \left(\frac{U_f}{U_{mf}} \right)^{0.26} \left(\frac{W}{w_s} / \frac{V}{V_f} \right)^{0.10}$$

The predicted values of the bed hold up ratios are found to lie well within $\pm 7\%$ of the experimental values.

In Chapter VI are given the conclusions based on the present study and the scope for further work.

The computer programmes used are given in appendices I and II.

A C K N O W L E D G E M E N T

The author wishes to express his deep sense of gratitude and indebtedness to Dr.N.Gopal Krishna, Professor and Head, Dr.P.S.Panesar, Professor and Dr.N.J.Rao, Reader of the department of Chemical Engineering, University of Roorkee, Roorkee, for their valuable and expert guidance and inspiration throughout the preparation of this thesis.

Many thanks are extended to:

- Sri Surendra Kumar, a colleague of the author for his help in computer work and stimulating discussions during the preparation of this thesis.
- Sarvasri C.P.Mathur, B.K.Arora, Jugendra Singh and C.M.Bhatnagar of Unit Operations Laboratories and fabrication section and other staff of the laboratories for their help during experimentation.
- The staff of the computer centre at S.E.R.C., Roorkee for their cooperation in computer work.
- Sri U.K.Mishra who did typing work with devotion.
- All friends for their constant encouragement during the work and
- finally, to his wife for her unflinching help in checking the manuscripts and constant encouragement during the preparation of this thesis.

C O N T E N T S

		Page
	SUMMARY	i
	ACKNOWLEDGEMENTS	viii
	CONTENTS	ix
	NOMENCLATURE	xii
CHAPTER I	INTRODUCTION-LITERATURE REVIEW	2
	1.1 Batch Fluidization	5
	1.1.1 Minimum Fluidizing Velocity	6
	1.2 Continuous Fluidization	21
	1.3 Fluidized Beds with Baffles	27
	1.4 Proposed Work	38
	1.4.1 Batch Fluidization with Baffles	38
	1.4.2 Continuous Fluidization with Baffles	39
	1.4.3 Hold-up Studies with Baffles	39
CHAPTER II	FLOW PROPERTIES OF SOLIDS	41
	2.1 Particle Size	42
	2.2 Density	43
	2.3 Porosity	43
	2.4 Sphericity	43
	2.5 Angle of Repose	44

CHAPTER III	BATCH FLUIDIZATION WITH VERTICAL BAFFLES	...	47
3.1	Experimental Set Up	...	48
3.2	Procedure	...	51
3.3	Results and Discussion	...	55
3.3.1	Batch Fluidized Bed without Baffles	...	55
3.3.2	Batch Fluidized Bed with Vertical Internal Baffles	...	57
3.3.2.1	Bed Expansion Behaviour	...	58
3.3.2.2	Effect of Baffle Spacing	...	59
3.3.3	Batch Fluidized Bed with Single Baffle	...	61
3.3.4	Correlations	...	62
3.3.4.1	Minimum Fluidizing Velocity	...	63
3.3.4.2	Pressure Drop	...	64
3.3.4.3	Bed Expansion	...	66
3.3.4.4	Quality of Fluidization	...	67
3.4	Conclusion	...	68
CHAPTER IV	CONTINUOUS FLUIDIZATION WITH VERTICAL BAFFLES	...	143
4.1	Experimental Set Up	...	144
4.2	Procedure	...	149
4.3	Results and Discussion	...	152
4.3.1	Continuous Fluidization Without Baffles	...	152
4.3.2	Continuous Fluidization with vertical baffles	...	152
4.3.2.1	Pressure Drop	...	152
4.3.2.2	Bed Density	...	153

4.3.3	Correlations Proposed	...	155
4.3.3.1	Pressure Drop	...	155
4.3.3.2	Bed Density	...	157
4.4	Conclusion	...	159
CHAPTER V	HOLD-UP STUDIES IN CONTINUOUS SYSTEMS WITH VERTICAL BAFFLES	...	206
5.1	Experimental Set Up	...	207
5.2	Procedure	...	212
5.3	Results and Discussion	...	214
5.3.1	Hold-Up Ratio without Baffles	...	216
5.3.2	Hold-Up Ratio with Vertical Baffles	...	217
5.3.3	Mechanism of Particle Movement in Continuous Systems with Mixed Sized Feeds	...	218
5.3.4	Correlation	...	222
5.3.4.1	Correlation Proposed	...	223
5.4	Conclusion	...	225
CHAPTER VI	CONCLUSIONS AND RECOMMENDATION	...	254
6.1	Batch Fluidized Beds with Vertical Internal Baffles	...	255
6.2	Continuous Fluidized Beds with Vertical Internal Baffles	...	257
6.3	Hold-Up Studies in Continuous Systems with Mixed Feeds	...	257
6.4	Scope for Further Work	...	259
APPENDIX-I	Computer Program	...	261
APPENDIX-II	Computer Program	...	264
	R E F E R E N C E S	...	265

N O M E N C L A T U R E

A	Cross sectional area available for fluidization, m^2
Ar	Archimedes Number, $g D_p^3 (\rho_s - \rho_f) / \nu_f^2 \rho_f$
B	Form factor, $f (D_p)$
B _o	Beranek Number, $U_t^3 \rho_f / g \nu_f \rho_s$
C _D	Drag Coefficient, $D_p g \rho_f (\rho_s - \rho_f) / 2 G_{mf}^2$
d _o	Distance between two adjacent baffles, mm
D _e	Equivalent diameter of column, mm
D _p	Particle diameter, micron
D _{peq}	Equivalent diameter of particles, micron
D _{pmax}	Diameter of the largest size particle, micron
Fe	Federov Number, $D_p [4/3 g (\rho_s - \rho_f) / \nu_f^2 \rho_f]^{1/3}$
Fr	Froude Number, $U_f^2 / g D_p$
F _{cc}	Chilton-Colburn factor
g	Acceleration due to gravity, $9.81 m/s^2$
g _c	Conversion factor
G _f	Fluid mass velocity, $kg/m^2.s$
G _{mf}	Minimum fluidizing mass velocity, $kg/m^2.s$
h _D	Static bed height to column diameter ratio
H(2,1)	Hold up ratio between large and small size particles
K _{ΔP}	Dimensionless group, $C_D Re^2$
K _{ΔP}	Dimensionless group, $F_{cc} \cdot Re^2$
L	Static bed height, mm
r	Fluctuation ratio, $\frac{\text{Highest bed level}}{\text{Lowest bed level}}$
R	Solids loading ratio, (W_s/W_g)

Re	Reynolds Number, $D G_f/\mu_f$
Re_{mf}	Reynolds Number at onset of fluidization
Re_t	Reynolds Number at terminal velocity
Re_{eq}	Reynolds Number based on equivalent diameter of column
Re_T	Reynolds Number based on column diameter
Re_p	Reynolds Number based on particle diameter
S_R	Free area (grid opening) expressed as percentage of bed area
T_G	Gas contact time in bed (V_s/V_f), s
U_f	Linear velocity of fluid, m/s
U_{mf}	Fluid velocity at onset of fluidization, m/s
U_{op}	Operating fluid velocity, m/s
U_t	Terminal velocity of particles, m/s
V_s	Volume of solid particles, m^3
V_f	Volumetric flow rate of fluid, m^3/s
W	Weight of solids charged, kg
W_g	Air flow rate, kg/s
W_s	Solids feed rate, kg/s
ΔP	Pressure drop, N/m^2
ΔP_f	Pressure drop due to friction, N/m^2
ΔP_B	Pressure drop due to baffles, N/m^2
ΔP_G	Pressure drop due to grid, N/m^2

Greek Symbols

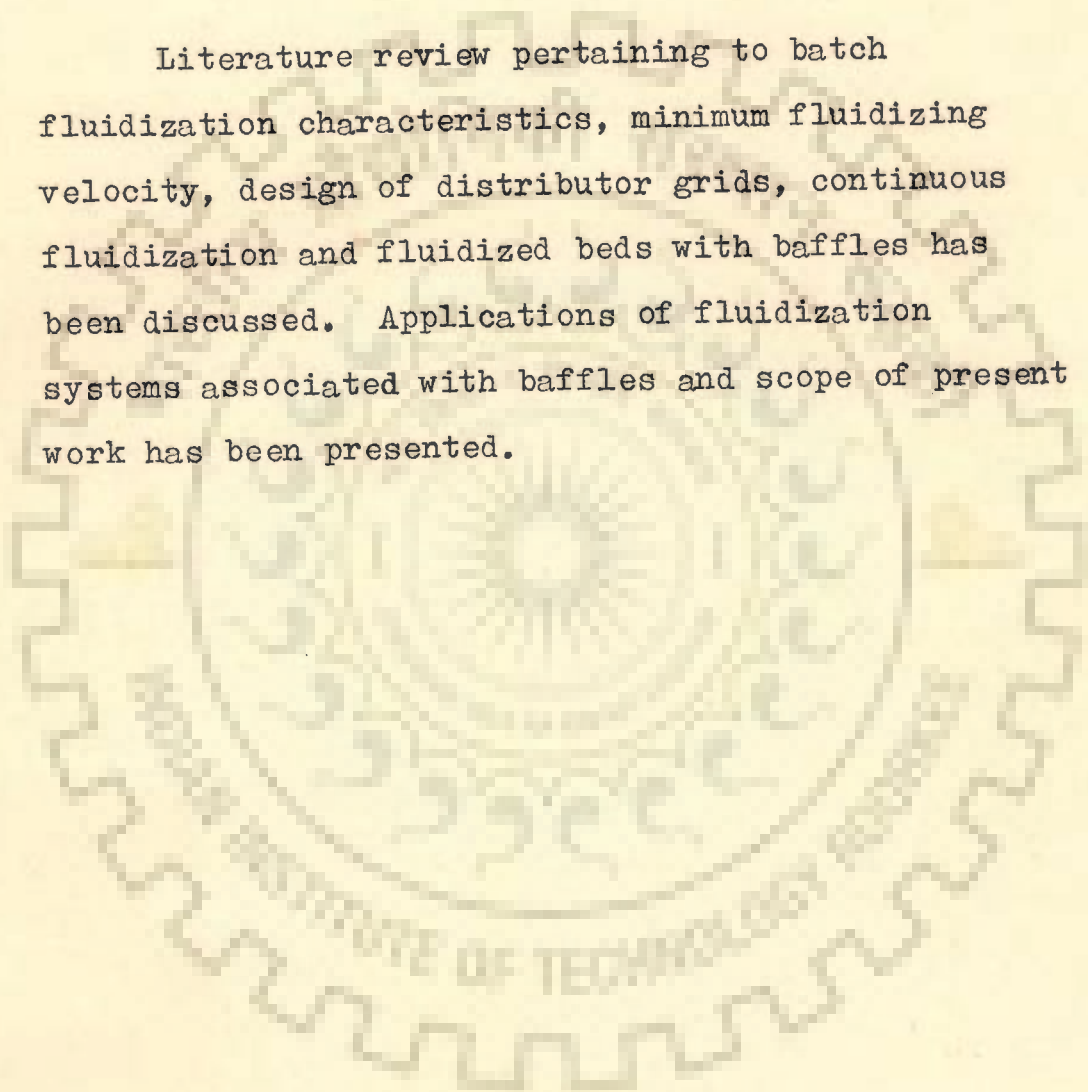
α_0	Constant	
ϵ	Bed voidage	
ϵ_{mf}	Bed voidage at onset of fluidization	
ϵ_0	Static bed voidage	
φ_s	Sphericity	
θ	Angle of repose of solids, degree	
μ_f	Fluid viscosity,	kg/m.s.
ν_f	Kinematic viscosity of fluid,	m ² /s
ρ_{bd}	Bed density,	kg/m ³
ρ_f	Density of fluid,	kg/m ³
ρ_s	Density of solids,	kg/m ³
τ_s	W/w, mean residence time of particles,	s
τ_B	τ_s/T_G dimensionless time parameter	
\bar{t}	Mean residence time,	s

Subscripts

1	Small size particles
2	Large size particles

C H A P T E R - IA B S T R A C T

Literature review pertaining to batch fluidization characteristics, minimum fluidizing velocity, design of distributor grids, continuous fluidization and fluidized beds with baffles has been discussed. Applications of fluidization systems associated with baffles and scope of present work has been presented.



CHAPTER - IINTRODUCTION

Fluidization finds wide applications in the process industries like Petroleum, heavy chemical and metallurgical industries. Fluidized beds have a number of attractive features. Due to intimate contact between solids and fluid, better heat and mass transfer rates are obtained. The mobility of solid phase in the fluidized beds, ensures almost isothermal conditions and makes it amenable to the control of chemical reactions. The mobility of solid phase also enables the continuous feeding and withdrawing of solid material to or from the fluidized beds. Although the principle of operation of gas-solids fluidized bed was employed as early as 1921 in the German winkler gas generator, it was not until 1941, when the fluidized catalytic cracker was first developed in U.S.A., that the technique became widely known. Since then the technique has been applied to various processes e.g. pyrites roasting, lime calcining and drying.

The term 'fluidization' applied to a bed of granular solids implies the conversion of that bed from a settled state at rest, where it behaves as a coherent porous solid, to a state where it behaves as a fluid

with properties of flow and surface levelling and that each particle of solids becomes mobile, individually and independently.

The ideal state of fluidization, where the whole of a bed of particles behaves as a homogeneous fluid is probably not attainable and the term is largely applied to the bed of particles maintained in a state of motion by an upward current of fluid.

The general picture presented through literature [3,4] shows that the fluidization by gases follows a different path from that of the liquid fluidization. The physical flow phenomenon noticed in fluidized beds is divided into two distinct categories, viz. particulate fluidization associated with liquid fluidized systems and aggregative fluidization associated with gaseous fluidizing media. Different characteristics are ascribed to these two categories of fluidized systems. Industrial fluidized bed reactors are mostly gas-solids systems having more non-ideal behaviour.

If through a bed of solid particles resting on a supporting grid, an increasing flow of gas is passed, a point is eventually reached when the bed can no longer remain static. When the solid particles start the slightest movement, the phenomenon is termed as incipient fluidization. At this stage the particles unlock

themselves from the bed and become freely supported on the rising current of gas. With further increase in the gas velocity, the bed takes on a more and more fluid like appearance. The particles are no longer constrained in a fixed bed, but are free to move throughout the bed which looks like a liquid having a mobile state. As the gas velocity is further increased, the solids circulation within the bed becomes more turbulent. At still higher gas velocities the gas stops coming out through the gas-solids mixture uniformly but instead it now starts flowing through the bed in the form of bubbles. Under such condition the whole bed appears like a boiling liquid. These bubbles carry with them a wake of particles and when they split, the particles are ejected into the free space above the bed. However, if the gas velocity is made to exceed the particle terminal velocity, the particles ejected from the bubbles will be entrained in the flowing gas stream. This is known as Pneumatic conveying.

With gas as the fluidizing medium, the bed expansion is observed to be smooth just at the incipient fluidization. As the flow rate is increased, the particles carried upwards by the upmoving bubbles are thrown out by the bursting of bubbles and the action becomes more and more agitated and violent. This is called bubbling or 'aggregative' fluidization. However,

liquid solids systems behave more homogeneously and the bed expansion is smooth with increasing liquid velocity resulting in 'Homogeneous' or 'particulate' fluidization.

1.1 BATCH FLUIDIZATION

Fluidized beds can be operated as batch or continuous systems. In batch fluidized systems, solids are handled as batch and gas is continuously passed through the bed. In continuous fluidization the solids enter continuously from one end and get discharged at the other end while they come in contact with continuously flowing fluid during the transit. The contact of the gas with solids is once through and quality of solids product is uniform. The time of operation is usually governed by the system requirements.

Pressure drop in fixed bed has been studied extensively [7-13]. Ergun [11] proposed a generalized correlation for predicting the fixed bed pressure drop as follows:

$$\frac{\Delta P}{L} g_c = 150 \frac{(1-\epsilon)^2}{\epsilon^3} \frac{\mu_f U_f}{D_p^2} + 1.75 \frac{(1-\epsilon)}{\epsilon^3} \frac{\rho_f U_f^2}{D_p} \dots (1.1)$$

The first term in the above expression accounts essentially for the viscous energy losses and the second term is related primarily to the kinetic energy losses.

It is generally assumed that the bed pressure drop is equal to the apparent weight of the solid particles. This may however, lead to erroneous results in view of certain inherent tendencies present in a fluidized bed e.g. channelling, bubbling and slugging. The channelling tendencies arising from the preferential flow paths developed due to non-uniform voids and poor gas distribution affect the pressure drop severely. Adler and Happel [13] observed that the bed pressure drop reduces considerably and so also the fluid-solids contact. The bubbling phenomenon in the bed causes fluctuations in the pressure drop. The slugging tendencies in the bed would increase the pressure drop and seriously affect the quality of fluidization.

1.1.1 Minimum fluidizing velocity is one of the important design characteristics of a fluidized bed which explains the transition from fixed bed to fluidized bed conditions. It may be defined as the mass flow rate of fluid sufficient to suspend the bed of solids. The expressions for predicting the minimum fluidizing velocity have been obtained based on the following principles.

- i) At the incipient fluidizing conditions, the bed behaves like a fixed bed and the pressure drop across the bed is equal to the apparent weight of the bed per unit cross sectional area.

- ii) The conditions at the onset of fluidization are similar to that of free falling conditions of the particles [31].
- iii) The drag force acting on the particles is equal to the submerged weight of the particles.

Leva, Grummer and Weintraub [17] considered the incipient fluidizing conditions to be the extreme points in the fixed bed condition and suggested a correlation for predicting minimum fluidizing velocity in terms of the physical properties like shape factor and bed voidage at minimum fluidizing conditions as

$$G_{mf} = \frac{0.005 D_p^2 (P_s - P_f) P_f g_c \epsilon_{mf}^3 \phi_s^2}{(1 - \epsilon_{mf})} \dots (1.2)$$

Leva [3] modified the above correlation by expressing the unknown quantities ϵ_{mf} and ϕ_s as function of Re , and gave an empirical correlation

$$G_{mf} = 688 D_p^{1.82} [P_f (P_s - P_f)]^{0.94} / \mu_f^{0.88} \dots (1.3)$$

where G_{mf} is in pounds per square foot per hour; D_p is in inches, P in pounds per cubic foot and μ in c.p.

Based on a large number of experimental data covering a wide variety of systems, Wen and Yu [18]

used the following expressions for shape factor and voidage at minimum fluidizing conditions.

$$\frac{1-\epsilon_{mf}}{\epsilon_{mf}^3 \varphi_s^2} = 11 \quad \text{and} \quad \frac{1}{\varphi_s \epsilon_{mf}^3} = 14. \quad \dots (1.4)$$

They expressed the minimum fluidizing velocity in terms of Reynolds number as

$$\frac{D_p G_{mf}}{\mu_f} = \left[(33.7)^2 + \frac{0.0408 D_p^3 \rho_f (\rho_s - \rho_f) g^{1/2}}{\mu_f^2} \right] - 33.7 \quad \dots (1.5)$$

This correlation is found to predict values of G_{mf} generally agreeable with the measured values. However, this is based on solids and fluid properties mainly and does not take into account the possible effects of column diameter. In this regard, works of Miller and Log Winuk [19], Vanheerden et al [20], Johnson [21] and Wilhelm and Kwauk [5] are also noteworthy. Akopian and Kastkin [22], Bena et al [23], Erkova et al [25] used Archimedes number to express the minimum fluidizing velocity. Winterstein et al [26] introduced Froude group in the correlation.

Narasimhan [29], Pinchbeck and Popper [30], Goddard and Richardson [27], have proposed correlations for predicting minimum fluidizing velocity using the concept of free falling velocity.

Beranek and Sokol [28] defined the ratio of minimum fluidizing velocity to terminal velocity in terms of a dimensionless group B_0 (called Beranek number) which represents criteria for the free fall of spherical particles. Zabrodsky [40] correlated the minimum fluidizing velocity in terms of terminal velocity and Federov number $D_p [4g(\rho_s - \rho_f)/3 \mu_{ff}^2]^{1/3}$. Bourgois and Grenier [31] have expressed their correlation for the minimum fluidizing velocity in terms of Re_t/Re_{mf} and physical properties of the material, based on the assumption that the wall effect is negligible. Investigations based on drag force considerations were carried out by Davies and Richardson [32], Frantz [33], Baerg et al [34] Pillai and Raja Rao [35] and Bal Krishnan and Raja Rao [36] and correlations were proposed to predict the minimum fluidizing velocity.

Beilin [24] and others tried to predict the minimum fluidizing velocity based on empirical correlations with reasonable accuracy for the given system. A review [39] of the literature shows that quite a good number of correlations exist for predicting the minimum fluidizing velocity and the results do not agree well with each other. Table 1.1 gives the correlations proposed by various authors with range of applicability.

Motamedei and Jameson [37] tried to measure minimum

fluidizing velocity on the basis of two phase theory of fluidization and concluded that the only safe way to obtain minimum fluidizing velocity is to measure it for individual gas-solids systems. Murthy and Raja Rao [38] also visualized the importance of measuring the minimum fluidizing velocity for individual gas-solids system.

TABLE 1.1

Prediction of Minimum Fluidization Velocity
(onset of Fluidization Velocity)

Author	Correlations	Range of Applicability
1	2	3
1. Akopian and Kasatkin [22]	$Re = \frac{0.009 \epsilon_0^3 \cdot Ar}{\varphi_0 (1 - \epsilon_0)}$ $Re = 0.367 \frac{\epsilon_0^3}{\varphi_s (1 - \epsilon_0)} Ar^{0.57}$	$Re \leq 35$ $70 \leq Re \leq 700$
2. Aliev, Indyokov and Rustanov [42]	$U_{mf} = (5.1 \times 10^{-4}) \frac{D_p^2 (P_s - P_F)}{\mu_F}$	$n = f(D_p)$
3. Beilin [24]	$Re = 0.046 Ar^{0.587}$	
4. Bena, Ilavasky and Kossaczky [23]	$Re = \frac{0.00138 Ar}{(Ar + 19.0)^{0.11}}$	$Re < 39$ $Ar < 10^5$

1	2	3
5. Beranek and Sokol [28]	$U_{mf}/U_t = 0.019 \pm 0.003$	$Bo < 0.3$
	$U_{mf}/U_t = 0.022 Bo^{0.2}$	$0.3 < Bo < 10$
	$U_{mf}/U_t = 0.09 \pm 0.005$	$Bo > 10^3$
6. Winterstein and Rose [26]	$Fr \frac{\rho_F}{\rho_s} = \epsilon_0^3 \frac{Re}{150(1-\epsilon_0)} + 1.75Re$	
7. Ginzburg and Rezchikov [43]	$Re = 0.01 Fe^{1.98}$	
8. Graf [44]	$U_{mf} = \frac{0.000565 D_p^2 (\rho_s - \rho_F) g}{\mu_F}$	$Re < 10$
9. Grishin [45]	$Re = 0.01 Fe^{1.98}$	
10. Dementiev [46]	$Re^{1.82} = 0.065 \alpha_0 \epsilon_0^{2+K} Ar$	$15 < Re < 600$
	$K = 15.3 (\epsilon_0 - 0.35)^{1.3}$	
11. Johnson [21]	$G_{mf} = \frac{D_p^2 \varphi_s g (\rho_s - \rho_F) \rho_F \epsilon^5}{18 \mu_F [1+0.5(1-\epsilon)]}$	$Re < 2$
	$G_{mf} = 0.171 D_p \varphi_s \rho_s \frac{\epsilon}{1-\epsilon}$	
	$\frac{g^2 \rho_F \epsilon^6}{\mu_F (1-\epsilon) [1+0.5(1-\epsilon)]}$	$Re > 2$

1	2	3
12. Erkova and Smirnov [25]	$Re = 5.44 \times 10^{-4} Ar.$	Laminar Zone
13. Zabrodsky [47]	$U_{mf} = 0.476/U_t = 0.1 Fe^{0.115}$	
14. Boguslavskii et al [48]	$U_{mf} = 0.00034(D_p)^{1.6} \frac{\rho_s - \rho_F}{\rho_F}$	
15. Leva, Weintraub, Grummer, Polchick and Storch [49]	$G_{mf} = \frac{0.005(D_p)^2 g \rho_f [\rho_s - \rho_F]}{\mu_f^2 (1 - \epsilon_0)^2}$	Re < 10
16. Leva, Shirai, and Wen [50]	$G_{mf} = 0.00923 D_p^{1.82} [\rho_F (\rho_s - \rho_F)]^{0.94}$	Re < 5
	(or Nomograph based on this equation)	
17. Loeffler and Ruth [51]	$U_{mf}/U_t = \frac{\epsilon^3/(1-\epsilon)}{5.7 + \epsilon^2/(1-\epsilon)}$	Laminar Zone
18. Miller and Logwinuk [19]	$G_{mf} = \frac{0.00125 D_p^2 (\rho_s - \rho_F)^{0.9} \rho_F^{1.1} g}{\mu_F}$	
19. Petrov [52]	$Re = \frac{Ar \epsilon^{m/2}}{18 + 1.933 Ar^{0.4}}$	m = f (Ar) .

1	2	3
20. Pinchbeck and Popper [30]	$Re_t/Re_{mf} = \frac{8.21 \times 10^3}{Ar} + \frac{\sqrt{36 + 2/3 Ar}}{0.00073 Ar}$	
21. Rowe [53]	$U_{mf}/U_t = 68.5$	
22. Smirnov [54]	$Re_{mf}/Re_t = \frac{5.4 \times 10^{-4} Ar}{-6 + \sqrt{6 + 2/3 Ar}}$	Laminar Zone
23. Smirnov [54]	$Re = 5.4 + 10^{-4} Ar$	
24. Straneo and Cappi [55]	$U_{mf} = \frac{2.94 \times 10^{-4} D_p^{1.7} [P_s - P_F] g}{\mu_F}$	Laminar Zone
25. Takeda [56]	$\frac{1-\epsilon}{1-\epsilon_0} = \frac{1}{1-\epsilon_0} [1 - \alpha (U_{mf}/U_t)^{0.25}]$ <p style="text-align: center;">$\alpha = 1.0 \text{ to } 1.1$</p>	Laminar Zone
26. Goroshko Rozenbaum and Todes [57]	$Re = \frac{Ar}{1400 + 5.22 \sqrt{Ar}}$	
27. Federov [58]	$Re = 0.095 Fe^{1.56}$	Fe=40 to 200
28. Hawksley [59]	$U_{mf}/U_t = \frac{\epsilon^2}{e [4.1 (1-\epsilon)(0.64+\epsilon)]}$	Laminar Zone
29. Heerden, Nobel and Van Krevlen	$G_{mf} = \frac{0.000123 D_p^2 P_F P_s g}{B \cdot \mu_F}$	$B = f(D_p)$ <p style="text-align: center;">= 0.39 to 0.78</p>

1	2	3
30. Happel [61]	$U_{mf}/U_t = \frac{3-4.5(1-\epsilon)^{1/3}+4.5}{\frac{(1-\epsilon)^{5/3}+3(1-\epsilon)^2}{3+2(1-\epsilon)^{5/3}}}$	Laminar Zone
31. Chechiotkin [62]	$U_{mf}/U_t = 0.06$	$D_p = 0.18 \text{ to } 1.5$
	$U_{mf}/U_t = 0.1$	$D_p = 2 \text{ to } 6$
32. Justat [63]	$U_{mf} = \frac{1.27 \times 10^{-3} D_p^2 (\rho_s - \rho_F) g}{\mu_F}$	Re < 10
33. Baerg, Klassen and Gishler [34]	$G_{mf} = 0.903 \times 10^3 (D_p \cdot \rho_{bd})^{1.23}$	
34. Wilhelm and Kwauk[5]	$U_{mf} \text{ from the plot of } K_{\Delta P} \text{ versus Re or } K_{\Delta F} \text{ vs Re}$	Liquid-solid systems
35. Kadimova [64]	$C_D \text{ Re}^2 = 4/3 [1 - 1.2(1-\epsilon)^{2/3}]^2 \text{ Ar}$	
36. Gupalo [65]	$\text{Re} = \text{Ar} \cdot \frac{4.8}{\epsilon} [18 + 0.61 \text{ Ar}^{0.5} \epsilon^{2.33} [[1 + (\rho_s - \rho_F)(1-\epsilon)/\rho_F]^{0.5}]^{-1}]$	-uniform fluidization
37. Karpov [66]	$\text{Re} = 0.049 [\text{Ar}(1-\epsilon)]^{0.8} [D_{pmax}/D_{peq}]^{0.48} [\rho_s/\rho_F]^{0.2}$	

1	2	3
38. Mazurov [67]	$Re = 14.5 Ar^{0.45}$	True for big particles
39. Gopichand and Rao [68]	From plot of $(P_s - P_F)/P_F \cdot Fr.$ versus U_t/U_{mf}	True both for liquid-solids and gas-solids systems
40. Leva, Grummer and Weintraub [17]	$G_{mf} = \frac{0.005 D_p^2 (P_s - P_F) P_F g_c \epsilon_{mf} \varphi_s^2}{\mu_F (1 - \epsilon_{mf})^2}$	$Re < 10$
41. Wen and Yu [18]	$\frac{D_p G_{mf}}{\mu_F} = \frac{[(33.7)^2 + 0.0408 D_p^3 P_F (P_s - P_F) g]^{1/2}}{\mu_F} - 33.7$	
	$\frac{1}{\varphi_s \cdot \epsilon_{mf}^3} = 14, \quad \frac{(1 - \epsilon_{mf})}{\epsilon_{mf}^3 \varphi_s} = 11$	
42. Narasimhan [29]	$G_{mf} = \frac{42.9 \mu_F}{D_p} [0.231 \log D_p + 1.417] [(1 - 2.212 \times 10^{-5} Re_t)^{1/2} - 1]$	$D_p = 0.001$ to 0.02 inches
43. Pillai and Raja Rao [35]	$G_{mf} = \frac{0.000701 D_p^2 \rho_F (P_s - P_F) g}{\mu_F}$	
44. Frantz [69]	$G_{mf} = 4.45 \times 10^5 \frac{D_p^2 \rho_F (P_s - P_F)}{\mu_F}$	

1

2

3

45. Ghosal and
Dutt
[70]

$$G_{mf} = \frac{0.01558 D_{peg}^2 \epsilon_{mf}^3 g \rho_F (\rho_s - \rho_F)}{\mu_F^{2.56} (1 - \epsilon_{mf})}$$

46. Subba Raju
and
Venkata
Rao [71]

$$\frac{\varphi_s D_p^3 (\rho_s - \rho_F) \rho_F g}{\epsilon_o^3 / \mu_F^2 (1 - \epsilon_o)}$$

$$\text{For } \frac{\varphi_s D_p G_{mf}}{\mu_F (1 - \epsilon_o)} \leq 50$$

$$= 250 \left[\frac{\varphi_s (D_p G_{mf})}{\mu_F (1 - \epsilon_o)} \right]$$

$$\left[\frac{\varphi_s D_p^3 (\rho_s - \rho_F) \rho_F g}{\mu_F^2} \right]$$

$$\left[\frac{\epsilon_o^3}{(1 - \epsilon_o)^2} \right]$$

$$= 19 \left[\frac{\varphi_s D_p \epsilon_{mf}}{\mu_F (1 - \epsilon_o)} \right]$$

$$\text{For } \varphi_s D_p G_{mf} \geq 50$$

47. Wester-
fried and
Cazaou
[72]

$$G_{mf} \left[\frac{2g \Delta P \cdot D_p \varphi_s}{C_D \rho_F L_s \epsilon_o (1 - \epsilon_o)} \right]^{1/2}$$

C_D vs Re
plot to be used

1	2	3
48. Saksena and Mitra [73]	$G_{mf} = 0.7 \left[\frac{D_p^{1.858} \rho_F (\rho_s - \rho_F)^{0.81}}{\mu_F^{0.905}} \right]$	
49. Rowe and Henwood [74]	$U_{mf} = 0.00081 \frac{(\rho_s - \rho_F) g D_p^2}{\mu_F}$	

The operating velocity of the fluid in a fluidizing column is normally maintained at higher values than that at minimum fluidizing condition. It is limited by the terminal velocity of the solids. Attempts have been made by various workers to identify the working velocities for the satisfactory performance of the bed. Pinchbeck and Popper [30] derived expressions to estimate U_t/U_{mf} . This ratio ranges between 10 to 90 and is considered as a criteria for the flexibility of operation in a fluidizing column. However, the range of satisfactory operation of a fluidized bed may be considerably impaired by channelling and slugging. This is specially serious with large size particles. Slugging is an extreme form of bubbling and thus it is important to understand the bubbling phenomena in deciding the type of the fluidizer.

Bubbling is one of the inherent characteristics of any gas-solid fluidized system. Considerable interest [12,75-88,90,91] has been shown in understanding the mechanism of bubble formation, its growth and rise velocity in a fluidized bed. Dotson [85] based on his study, concluded that the distribution of gas influences the bubbles in the region near the entry. Rowe [88] observed that the size of the bubble may increase rapidly soon after leaving the distributor. It is possible that the diameter of the bubble may reach that of the column resulting in slugging conditions. Davidson and Harrison [12] and Collins [89] observed that the slug flow commences when the equivalent bubble diameter is about $1/3$ to $1/2$ of bed diameter. It is, therefore, important that to avoid slugging tendencies, the distributor should be properly designed [14-16] and the bed height should be small. It was observed that the type of gas distributor may have a considerable effect upon the performance of the fluidized bed [2]. Grohse [92] and Morse et al [1] have concluded that the quality of bubbling fluidization is strongly influenced by the type of gas distributor. Groshe's conclusions may be summarized as follows:

- For less number of air inlet openings, the bed density fluctuates appreciably. It is more severe at high gas velocity where channelling may be

severe. For large number of air inlet openings, the fluctuation in the bed density is negligible at low flow rates and becomes appreciable at high flow rates. In such cases usually the bubbles are smaller and channelling is less.

- With many small air inlet orifices, contacting is uniform but large scale operation with such distributors has a serious draw back of high pressure drop.

Richardson [93], Agarwal et al [94] and other workers [95-97] have suggested different values of the grid resistance for even distribution of the gas. The grid area which is the sum of the areas of all the openings usually varies from 2-50% of the total cross sectional area of the column. Vanecek et al [41] suggest the following correlation for predicting fractional area to ensure perfect mixing as

$$S_R = 1.7 \left(\frac{U_{op}}{U_{mf}} \right)^{0.9} \dots (1.6)$$

Where S_R is the free area expressed as the percentage of the total grid or bed area and (U_{op}/U_{mf}) is the ratio of the operating to the minimum fluidizing velocity. The diameter of the openings in the grid should be such that clogging by fines is avoided during stoppage.

It is recommended that the diameter of the holes should be at least $1/10$ of the particle diameter and at the most half of the diameter of largest particle [72].

The expansion of the fluidized bed is caused by the flow of the gas through the bed which is in excess of minimum required for fluidization. It is pertinent that the bed expansion would increase with the increase in the bubble volume caused by the increased gas flow. Thus, information on bed expansion in fluidized bed is important in deciding the size of the fluidized bed equipment. Richardson and Zaki [138] have suggested the method for predicting the bed expansion of liquid fluidized bed. Lewis and Bowerman [160] have suggested expressions for predicting bed voidage based on terminal velocity for different ranges of fluid velocity. Bailey [162] has reported that the plots of e versus U on logarithm scale are not linear and the deviations increase with increase in bed height and decrease in particle size. The bed expansion of gas-solids systems can be predicted by Richardson and Zaki approach. Leva [3] has used the concept of fluidization efficiency (the fraction of total energy expended, which is useful for particle motion) for predicting the bed expansion in gas solids systems. The fluctuation ratio defined as the ratio of highest and lowest bed levels at any gas velocity has been used as a criteria for estimating

the limits of operating gas velocities in gas-solids systems. Efforts have been made to correlate the bed expansion with bubble flow by Mateson and his co-workers [98-100]. Davies and Richardson [32] correlated bed expansion in terms of bed voidage and terminal velocity.

1.2 CONTINUOUS FLUIDIZED BEDS

In the continuous fluidizer, the feed as soon as it enters the bed, gets distributed. This is because the fluidized bed is an effective solids mixer. The product leaving the bed and the material in the bed have same characteristics. This means the characteristics of the solids in a fluidizer are essentially independent of the feed condition [127]. There is a possibility of short circuiting of a part of the feed directly into the discharge immediately after entering the bed. This leads to a wide variation of residence time distribution of solids resulting in inferior product quality. To avoid this, the RTD of solids should be narrowed. This is difficult in a conventional fluidized bed. For larger particles, requiring longer contact times the residence time of solids has to be increased. Increase in residence time is achieved by increasing the hold up, which leads to deeper beds. Deep beds are however, prone to slugging.

The comparison of batch and continuous fluidized systems reveals that the data with regard to minimum fluidizing velocity, bed pressure drop, bed expansion and characteristics of slugging and channelling are similar. But due to continuous solids movement resulting in variation of RTD of solids the product quality in continuous systems is non-uniform, while batch systems give uniform product quality.

In continuous systems, the bed performance is related to the time of contact between solids and gas. Thus, the RTD of solids and gases and their holdup is of significance in designing the continuous contacting devices.

Gilliland and Mason [128], May [129], Danckwerts et al [130] and others have studied the flow pattern of gases. Namkoong et al [134] conducted dynamic response studies of RTD. Experimental results indicate that the gas flow in fluidized beds lies squarely between the two extremes of plug and backmix flow. For practical applications it is not enough to know how long the fluid element stays in the bed, but its history must be known whether it slipped through the bed as a part of a bubble or it spent most of its time percolating through the emulsion phase. For determining this, stimulus response studies have been conducted using different

models [132-136,161]. Plug flow is approached when the number of mixing stages are large [137].

The RTD of solids is an important factor in determining the quality of product. The assumption that there is complete backmixing of solid is supported by many investigators [130,138-145,155,156]. Gilliland and Mason [128] suggested that the backmixing occurred due to the circulatory motion of the solids up the centre and down the sides. According to them, at high gas rates, if slugging is prevented, the gas solids mixing is high. Mixing was found to be greater for finer particles. Similar conclusions were obtained by Danckwerts[130], Askins et al [139]. Singer et al [140] studied solids mixing characteristics by using radioisotopes. They found that by-passing of the solids was not observed when catalyst was introduced into the vessel by means of dense phase stand pipes rather than through a riser. The solids mixing phenomenon was studied by many workers[141-145] using a counter current backmixing model. In this model it is assumed that the movement of the bubble displaces solids upwards, leading to a downward movement of solids in the rest of the bed. This downward movement of the dense phase may occur at such rates as to cause the gas flow from the top of the bed to the bottom. Hence counter-current motion of the gas and solids may arise, which produces the backmixing of the gas. This model

has been more realistic than the dense phase diffusion model as claimed by Van Deemter [143]. Hovmond and Davidson [117] have introduced a slug flow model. In reality, the fluidized beds operate in the region of true bubbles and true slugs, and a better understanding is needed of the transition. Gopichand et al [146] studied the continuous fluidization and pneumatic conveyance of solids and correlations were given for finding the flow rates of solids and pressure drop and bed densities in fluidized beds.

The study of solids mixing can be carried out quite easily by following the trajectories of individual particles in the fluidized bed. Massimilla and Westwater [110] and Toomy and Johnstone [147] have used high speed cinematography to study particles trajectories. In the work of Massimilla and Westwater, particles near the wall showed pronounced alteration of fast and slow movements both upward and downward.

The beds showed more non uniformity with increased particle velocity. Kondukov et al [148] studied trajectories of tagged radioactive particles. Their results indicate that the particles move randomly in the bed, the upward motion of particles being more rapid than downward movement. They also observed that particles near the surface usually remain there for a while before

dropping into the bed. The results obtained by Rowe[149] showed that the particles followed a definite pattern of displacement caused by rising bubbles rather than following a completely random motion as is assumed normally for mixing operations. Katz and Zenz [150] have given a mathematical model to calculate the internal circulation rate. Lateral circulation rates were determined by Lochil and Sutherland [151]. Studies on solids mixing were made by Tailby and Cocquerel [152]. They studied both the cocurrent and counter-current flow of gas and solids and observed that the increase in solids feed rate increases the tendency to plug flow. Increase of air flow rate was found to be less significant and showed only a slight tendency towards perfect mixing. Their work was mainly of a qualitative nature. Yagi and Kunii [153] showed that the average residence time for a given particle size was the same in both the carry over and the overflow streams.

The concept of hold back and segregation was introduced by Danckwerts to describe the deviation from piston flow and perfect mixing. Other workers [152,154,157] have also used this representation to describe the mixing behaviour.

Particle size distribution in fluidized beds has been studied as a function of bed height by Urabe

et al [158]. It was concluded by them that the size distribution was roughly constant within the main zone of constant voidage, however, the upper falling density zone became progressively richer in fines. In addition, the main zone had less fines at high velocities indicating that fines were more rapidly eliminated at higher velocities. Chechetkin et al [159] established that there was classification of particles of the solids phase with respect to size at different heights of the bed for velocities ranging in between 1.1 to 1.3 U_{mf} . The above review indicates that while continuous fluidization is amenable to large scale operation it has the major disadvantages due to:

- i) non uniform product quality as a result of wide variation in the RTD of solids.
- ii) tendencies of slugging and bubbling in deep beds intended to provide large contact times
- iii) tendency of channelling is high in shallow beds
- iv) lack of information on behaviour of continuous beds using diplegs for feeding solids.

1.3 FLUIDIZED BEDS WITH BAFFLES

The residence time distribution of solids can be narrowed in continuous fluidized systems by introducing baffles [137,131]. From the consideration of solids-fluid contacting and solids movement in fluidized beds, baffled beds can be categorised as having the following type of baffles:

- i) Horizontal screens, tubes, rods and perforated plates
- ii) Fixed and floating packings
- iii) Solid inserts like inclined surfaces, plates, nozzles and coils.
- iv) Vertical tubes and rods.

A review of the internal baffle systems having baffles of the above types is summarised in table 1.2.

TABLE 1.2

Internal Baffle Systems cited in the
Literature [12]

Laboratory studies		Applications, large-scale studies, chemical reactions	
Reference	Aspect studied	Reference	Process or aspect studied
1	2	3	4
1. Horizontal Tubes and Rods			
Glass and Harrison (1964)	Flow patterns near obstacles	De Maria and Longfield	Gas residence time distribution
Glass (1967)	Flow patterns near obstacles	Stemerding et al (1964)	Design
Gelperin et al (1966)	Local heat transfer coefficients	Wright (1968)	Design of combustion systems
Botterill et al (1966)	Effect of obstacle on bubbles		
Cloete (1967)	Effect of obstacle on bubbles		
Morgan (1967)	Heat transfer		

Table 1.2: Contd.

1	2	3	4
2. Horizontal Screens and Perforated Plates			
Hall and Crumley (1952)	Quality of fluidiza- tion	Cox (1958)	Air drying
Massinilla and Bracale (1956)	Bed expansion, suppression of slugging	Riley (1959)	Naphthalene oxidation
Overcashier et al (1959)	Gas and solids mixing entrainment	Lewis et al(1959) Massinilla and Johnstone (1961)	Hydrogenation ethy- lene, Oxidation of ammonia
Massimilla and Westwater (1960)	Particle motion, heat transfer	Volk et al(1962)	Quality of fluidization
Baillie et al (1963)	Solids density distribution	Rowson (1963)	Adsorption of carbon disulphide
Winter et al (1953)	Gas mixing, bubble size, pressure fluctuations	Schmalfeld (1963)	Sand cracking
Wen and Chang (1967)	Heat transfer	Gelperin et al (1964)	Classification
N.J.Rao (1975)	Two stage Downcomer type fluidizer, solids downflow characteris- tics	Block (1967) Toei and Akae (1968)	Heat Transfer Design

Table 1.2: Contd.

1	2	3	4
K.M.Rao (1976) [168]	Multistage sieve plate column without downcomer solids down flow charac- teristics	Kunii and Levenspiel (1969)	Vinyl acetate monomer production (Dupont)
3. Fixed Packings			
Romero and Johnson (1962)	Quality of fluidization	McIlhinney and Osberg (1964)	Oxidation of ethylene
Sutherland et al (1963)	Bed expansion, channelling, slugging	Ishii and Osberg (1965)	Isomerization of cyclopropane
Kang and Osberg (1966)	Solids mixing	Capes and Sutherland (1966)	Ore separation
Gabor (1966)	Solids mixing and carry-over	Osberg and Tweddle (1966)	Iron ore reduction
Kato et al (1967)	Solids and gas mixing, bed expansion		
Chen and Osberg (1967)	Gas mixing		
Kang et al (1967)	Pressure fluc- tuations		

Table 1.2: Contd.

1	2	3	4
Capes and McIlhenney (1968)	Bed expansion		
Park et al (1968)	Gas mixing		
Park et al (1969)	Bubble properties		
Ziegler and Brazelton (1963)	Radial heat transfer		
4. Floating Packings			
Goikhman et al (1969)	Gas residence time distribution, bed expansion, fluctuation of bed surface		
5. Other Solid inserts			
Beck (1949)	Quality of fluidization	Betts (1963)	Manufacture of phthalie anhydride
Ohmae and Furukawa (1953)	Suppression of slugging	Murthy (1964)	Hydrogenation of crude oil under pressure

Table 1.2: Contd.

1	2	3	4
Agarwal and Davis (1966)	Bed expansion	Echigoya and Osberg (1960) Hardin (1966)	Oxidation of ethylene Drying
Grace and Harrison (1968)	Flow pattern	Boucraut and Toth (1966)	Magnetic roasting of iron ores
6. Vertical Tubes or Rods			
Sutherland (1961)	Solids mixing	Hall and Taylor (1955)	Fischer-Tropsch Synthesis
Hebden (1961)	Quality of fluidization	Volk et al (1962)	Scale-up, Hydrocol and H-iron reduction processes
Gelperin et al (1964)	Classification	Stenerding et al (1964)	Design
Golperin et al (1966)	Heat transfer	Corrigan (1953)	Oxidation of ethylene
Grace and Harrison (1968)	Flow patterns, bubble properties, bed expansion	Thompson et al (1965)	Hydrogenation of oils
Grace and Harrison (1968)	Spatial bubble distribution	Elliott et al (1966) Otero et al (1967)	Carbonization Calcination of uranyl nitrate solutions

Glass [102] studied the effect of an array of horizontal tubes on fluidization behaviour and concluded that unless the array of tubes almost fills the bed, the influence it has on the average bubble size is small. Bubble splitting by direct impingement on an immersed tube has been demonstrated by Cloete [104]. Bailie et al [106], Overcashier et al [107], Massimilla and Bracale [108] and Hall and Crumley [109] noted that in a bed containing horizontal screens, bubbles sizes tend to be smaller and fluidization appears to be smoother than in unbaffled beds. Solids mixing is observed to be impeded in presence of baffles [106,108,110]. Volk et al [111] observed that particles segregation can occur due to the impeded solids mixing and concluded that it is difficult to fluidize all bed compartments simultaneously. Bhardwaj [161] has also observed segregation of solids in beds with horizontal screen. Massimilla and Westwater have observed that introduction of baffles increases the bed density and reduces the particle velocity.

Investigations [163-167] have been carried out on the use of fixed packings and open ended screen cylinder as internals in the fluidized beds. Due to the random orientation of these packings, the fluid passing through the bed takes a tortuous path resulting in preferential flow in the bed thereby leading to severe

channelling. The bubble growth in such a fluidized bed is inhibited and hence the slugging tendencies are eliminated and bed expansion is reduced. Morgan [105] observed that usually better heat transfer is obtained by arranging the tubes vertically rather than horizontally.

Vertical baffles when placed in a fluidized bed divide the bed into a number of parallel compartments. Although these baffles promote conditions for slugging as observed by Volk, Johnson and Stotler [111], Sutherland [113] and Grace and Harrison [114], the use of these baffles is preferred in certain reactors where large residence time and reduced backmixing conditions are required. Vertical baffles in fluidized beds may be classified according to their shape and size. Volk, Johnson and Stotler tested vertical baffles of various shapes including tubes, half round sections, flat sections and tubes with fins and observed that cylindrical vertical baffles are superior to other baffles of complex geometries. Vertical rods have a number of desirable features which make them useful for large scale fluidized beds, including:

- a) Simplicity of design
- b) ease of installation and removal
- c) non interference with emptying the bed
- d) non occurrence of defluidized regions

- e) availability of additional area for heat transfer purposes.

Introduction of vertical baffles in a cylindrical fluidizing column alters the geometry of the column which in turn affects the flow pattern. The fluid velocity is zero at the baffle walls and the velocity of the fluid will be maximum at the centre of the compartments formed by the insertion of the vertical baffles.

Vertical baffles introduced in a bed may be classified in two groups viz.

- i) tubes or rods much larger in size than the bubbles formed in the bed and hence the bubbles cannot enclose the baffles; and
- ii) tubes or rods much smaller than the bubble size and hence can be enclosed by the bubbles.

Grace and Harrison [115] based on their experimental studies noted that vertical rods reduce the tendency of bubbles to coalesce obliquely and thus the development of non-uniformities of spatial bubble distribution is more gradual when thin vertical rods are employed. Botton [116]; confirmed the finding of Grace and Harrison and observed that, as a result of the lower rate of bubble coalescence caused by enclosed vertical rods, the bubbles grow in size more slowly than

they would for an unbaffled beds. Grace and Harrison further showed theoretically and experimentally that the spatial distribution of bubbles in a fluidized bed becomes non-uniform even where gas is introduced by the distributor in a perfectly uniform manner. Bubbles tend to appear more frequently and in larger sizes in the interior of the bed than near the walls. Due to the lower rate of bubble coalescence and lower velocity of bubbles, it is expected that bed height fluctuations are less and the bed densities are more.

If two surfaces are placed too close together, gas is drawn from the surrounding particulate phase into the gap between the surfaces where it rushes upwards at high velocity carrying widely dispersed particles. This causes gas-channelling in the bed. Grace and Harrison [114] proposed that at least thirty particle diameters should be maintained between all pairs of adjacent vertical surfaces in gas-fluidized beds, to avoid the channelling tendencies.

Vertical rods which are too large to be enclosed by rising bubbles tend to promote slugging. Hovmand and Davidson [117] noted that a slugging fluidized bed has certain desirable features including good gas mixing characteristics and increased gas residence times.

Vertical rods which are enclosed by rising bubbles, tend to occupy less space and offer better surfaces for heat transfer. By reducing the size of the bubbles and improving the uniformity of bubble distribution, such vertical rods lead to greater homogeneity with improved gas solids contacting. Hedden [118] observed that a fluidized bed appeared to be 'pacified' by the addition of vertical rods and the carry over of the particles was reduced.

Rowe and Stapleton [119] found that scaling up fluidized beds from first principles was difficult. Volk et al proposed a criterion of scale up based on equivalent bed diameter. Conclusion reached by Agarwal and Davis [120] is in contradiction to the Volk criterion. Using vertical plates at regular intervals they proposed that small beds be baffled in order to simulate conditions in much larger beds; whereas Volk et al proposed to add cylindrical rods to large scale beds to make their behaviour similar to that of small scale fluidized beds.

Vertical surfaces are usually added to fluidized beds in order to provide surface for heat transfer. Several workers [121-125] have studied the heat transfer between fluidized beds and immersed vertical rods. A critical review of literature reveals that, while some experimental investigations have been carried out in

vertical baffled beds with regards to solids and gas residence time, bubble formation and solids mixing, basic information required for the design of the system is apparently not available.

1.4 PROPOSED WORK

Existing information on batch fluidized bed without baffles can not be extended for the design of fluidized beds with baffles. A critical review of the available literature indicates that information available is not sufficient for the design of fluidized beds with vertical baffles. The present work has therefore, been undertaken to study the effect of vertical internal baffles in batch and continuous fluidized beds with regards to the fluidization characteristics, namely, the bed pressure drop, minimum fluidizing velocity, bed expansion behaviour, bed fluctuation, the quality of fluidization and bed hold-up and segregation of mixed size feeds.

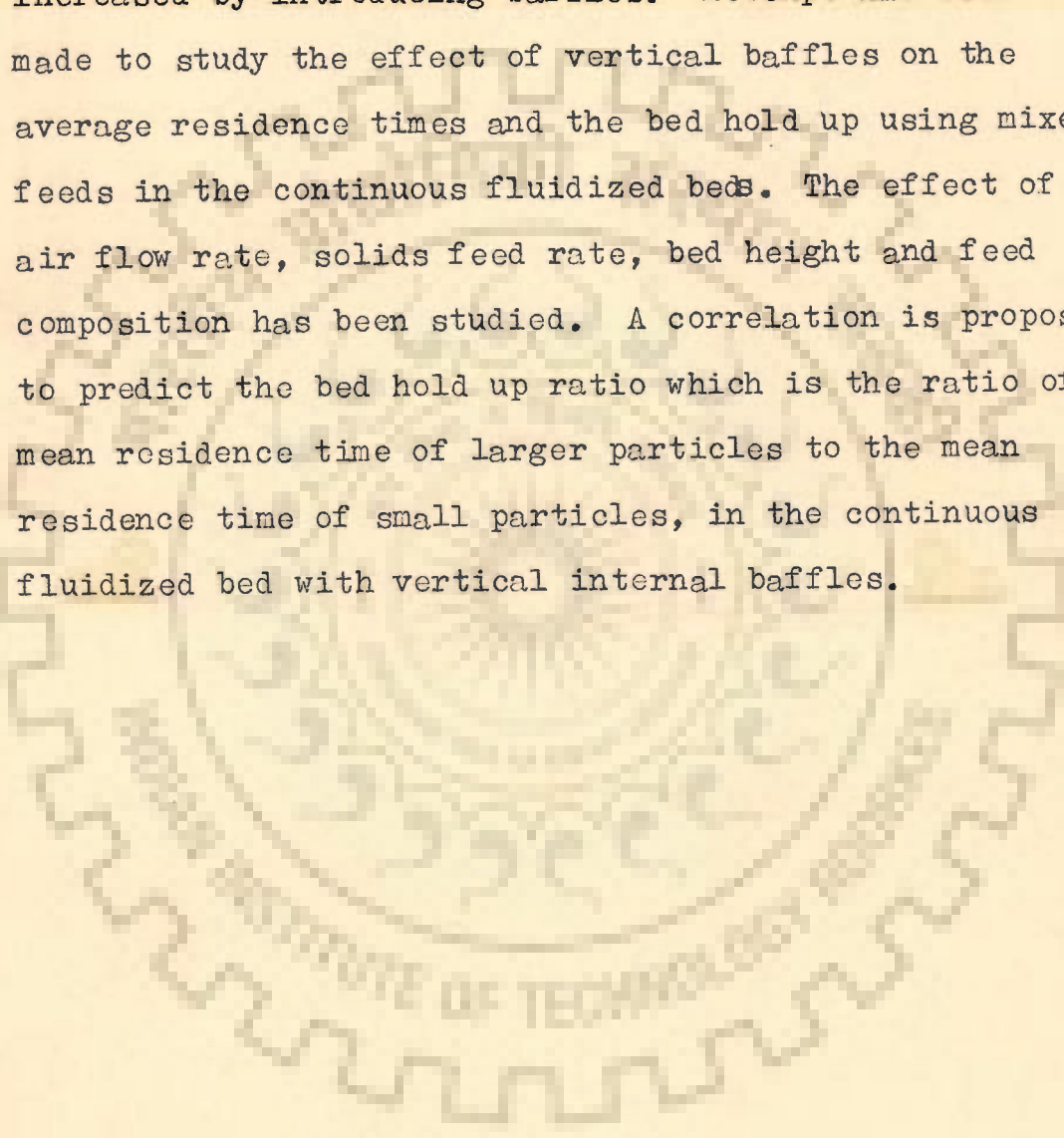
1.4.1 Batch fluidization studies have been conducted in a 70 mm perspex column provided with vertical internal baffles using air as fluidizing medium. The solids used include spherical glass beads, crushed bauxite, limestone and baryte in the size ranging from 1540 to 385 microns in close cut fractions. Bed pressure drop have been obtained for different air flow rates in fixed bed, at onset of fluidization and in the fluidized bed zones.


The minimum fluidizing velocities have been observed and compared with the predicted values using Leva's correlation. Based on the experimental data, an attempt has been made to propose correlations for predicting the minimum fluidizing velocity and pressure drop in the fluidized bed with vertical internal baffles. The bed expansion behaviour has been studied and a correlation for predicting the bed porosity at any air flow rate has been proposed. An attempt has been made to correlate the bed fluctuation ratio with air mass velocity and the performance compared with batch fluidized beds without baffles.

1.4.2 For large scale gas-solids contacting operations where continuous systems are preferred; existing information on columns without baffles cannot be extended to systems provided with vertical baffles. The effect of vertical internal baffles on continuous gas-solids fluidization has been investigated with regards to the bed pressure drop and the bed density at different air flow rates. Correlations have been proposed.

1.4.3 In the continuous systems with feeds of mixed sized particles, the mean residence time of different solid particle sizes is usually of the same order. In industrial processes, however, close cut particles are seldom used and instead, solids of mixed sizes are usually employed. Because of their equal duration of stay in

the column, the larger particles may not be fully reacted and this may result in poor quality of the product. The residence time of the particles may be increased by introducing baffles. Attempt has been made to study the effect of vertical baffles on the average residence times and the bed hold up using mixed feeds in the continuous fluidized beds. The effect of air flow rate, solids feed rate, bed height and feed composition has been studied. A correlation is proposed to predict the bed hold up ratio which is the ratio of mean residence time of larger particles to the mean residence time of small particles, in the continuous fluidized bed with vertical internal baffles.



C H A P T E R - I IA B S T R A C T

Physical and flow properties

of

solids materials used in
experiments are presented.

C H A P T E R - II

FLOW PROPERTIES OF SOLIDS

The gas-solids fluidization depends on the properties of solids and gas. The gas properties which influence the fluidization characteristics are density and viscosity. These can be estimated easily from pressure-temperature relationship or obtained from literature.

In such systems, the main properties of solids affecting fluidization are particle size, density, porosity and sphericity of the solids. For the solids in a flow system, the angle of repose is also significant. Before conducting the experimentation on fluidization, the characteristics of the solids were determined experimentally. The materials which were studied included spherical glass beads, crushed bauxite, lime stone, and baryte.

2.1 PARTICLE SIZE, D_p

The particle sizes of the materials were determined by using standard sieve analysis in B.S.sieves. In case of sharp-cut fractions the average of the openings of the sieve through which the solids passed and the sieve on which these were retained was taken as

the diameter of the particle. In case of mixed size particles, the average particle size was determined by weighted averages [4].

2.2 DENSITY, ρ_s

The density of the solids was determined by the usual methods of liquid displacement. To ensure that the results did not get affected by the wettability of the solids by a liquid, the density was determined using water and kerosene.

2.3 POROSITY, ϵ_s

The porosity of the solid material of a definite size was determined by knowing the volume of the bed and the volume of the solids. The ratio of void volume to the volume of the bed gave the porosity or void fraction of the solids bed.

To ensure that the wall effect does not influence the porosity values, cylinders of similar dimensions as used in the present experiments were employed.

2.4 SPHERICITY, ϕ_s

The sphericity of crushed materials was determined by pressure drop measurements. The pressure drop was measured for a given solids material in a fixed bed

region using air as the fluidizing medium. In the test, the gas velocity was kept in laminar zone by keeping the value of the particle Reynold's number to less than 10. The sphericity was then calculated using Ergun's fixed bed pressure drop equation (11), with voidage, pressure drop and other solid and fluid properties known.

2.5 ANGLE OF REPOSE, θ

For various material the angle of repose was determined by measuring the dimensions of the conical heap of solids formed below a perfectly circular vertical tube as shown in the Fig. 2.1.

The values of Density, porosity, sphericity and angle of repose for different materials and particle sizes as determined above are shown in table 2.1.



FIG. 2.1 MEASUREMENT OF ANGLE OF REPOSE

TABLE-2.1
PHYSICAL PROPERTIES OF SOLIDS

Sl. No.	Material	Particle size Microns	Density Kg/m^3 $\times 10^{-3}$	Porosity ϵ	Spheri- city φ_s	Angle of Repose θ Deg.
1.	Bauxite	1540	2.30	0.540	0.862	39.5
2.		977		0.530	0.880	39.0
3.		650		0.518	0.860	38.0
4.		460		0.490	0.854	37.5
5.		385		0.485	0.858	37.0
6.	Glass Beads	977	2.50	0.400	1.00	26.60
7.		650		0.390	1.00	26.00
8.		460		0.382	1.00	26.10
9.	Limestone	1540	2.74	0.575	0.594	30.5
10.		977		0.520	0.590	29.8
11.		650		0.482	0.625	29.0
12.		460		0.446	0.626	28.8
13.		385		0.432	0.600	28.5
14.	Baryte	1540	3.85	0.480	0.720	38.5
15.		977		0.480	0.695	38.0
16.		650		0.470	0.685	37.8
17.		460		0.460	0.688	37.4
18.		385		0.440	0.686	37.0

CHAPTER - IIIABSTRACT

Fluidization studies were carried out in 70 mm perspex columns using spherical glass beads, crushed bauxite, limestone and baryte in the size ranges of 1540 microns to 385 microns. The effect of vertical internal baffles on fluidization characteristics has been studied using baffles of 6 mm dia and 610 mm length. Minimum fluidizing velocity, the overall pressure drop and the bed expansion behaviour of gas-solids fluidized beds have been studied. Dimensionless correlations have been proposed for predicting the minimum fluidizing velocity, pressure drop, bed porosity and bed fluctuation ratio. The quality of fluidization was observed to be better in multibaffled fluidized beds compared to unbaffled fluidized beds. The fluctuation ratio was observed to be lower in multibaffled beds.

C H A P T E R - III

BATCH FLUIDIZATION WITH VERTICAL BAFFLES

Batch fluidized studies were conducted to investigate the effect of vertical internal baffles on fluidization characteristics viz., pressure drop, minimum fluidizing velocity, bed expansion and fluctuation behaviour in fluidized bed.

3.1 EXPERIMENTAL SET UP

The experimental unit is shown schematically in Fig. 3.1. An air line drawn from a compressor (C) passing through a M.S. surge tank (ST) was connected to the columns via an air filter (AF), pressure regulator (PR) and two rotameters (R_1, R_2). The air line of 1/2" standard size G.I. pipe was provided with G.M. globe valves (G_1 to G_9) of 1/2" standard size for air flow control and one valve (B) was provided for by-pass. Calibrated pressure gauges were mounted on the surge tank (P_1) and the pressure regulator (P_2).

The fluidizing column essentially consisted of a perspex column (K) of 70 mm I.D. and 610 mm length inserted between two special flanges (F_1, F_2). Internal baffles (IB) of 6 mm diameter having effective length of 610 mm were used. The baffles were made of stainless steel rods to ensure smooth surface. In the experiment,

the number of baffles as well as the distance between two adjacent baffles was varied. The number of baffles in the experiment were so chosen that by the insertion in the column, the cross section was divided into different compartments of nearly equal area. Photographs of the various baffle arrangements are shown in Fig. 3.4. A 3.0 mm thick aluminium grid plate (G) having 1.5 mm holes on a square pitch of 4.0 mm fitted in the flange (F_1) was used to support the bed of solids. In order that the solids may not fall in the openings and choke the holes, a 200 mesh brass wire screen (S) was put on the grid plate. The area of the opening in the grid was 10% of the empty column cross section. The column was mounted on the top of a calming section (Y) which consisted of a truncated inverted cone of mild steel having 76 mm diameter at the top and 12 mm diameter at the bottom. A cylindrical portion of 100 mm length was welded to the upper portion of the cone. The calming section had a random packing of raschig rings to provide uniform air distribution through the fluidized bed. A P V C tube of 12 mm I.D.(E) was provided near the base of the column for withdrawing the solids. Pressure tapings (PT_1, PT_2) were provided just below the grid plate and the flange (F_2) respectively. The column was supported on the base with the help of M.S. tie rods as shown in Fig. 3.2.



To compare the performance of the multibaffled column with a single baffled column, an equivalent single baffled bed (SB) was fabricated. A concentric perspex tube of 32.7 mm O.D. was placed inside the perspex column of 70 mm I.D. such that the area available for fluidization in multibaffled bed having 12 nos. baffles, and the bed having a single baffle was nearly same. The photograph of the experimental unit is shown in Fig. 3.3.

3.2 PROCEDURE

A known quantity of solids was charged into the column from the top. The solids bed was prepared for the condition of minimum consolidation as postulated by Wilhelm and Kwauk [5]. For this, the air was introduced into the column till the bed of solids was fluidized. Then the air flow was slowly stopped and the bed was allowed to settle. The height of the bed at that stage was taken as the static bed height. Subsequently the air flow rate was gradually increased and the flow rates and the corresponding pressure drop and bed heights were recorded in fixed bed, at the onset of fluidization and in fluidized bed zones. Similar data were obtained for spherical glass beads, crushed bauxite, limestone and baryte for different particle sizes.

The effect of baffle spacing obtained by changing the number of baffles and also by replacing the number of baffles with a single concentric baffle on the air

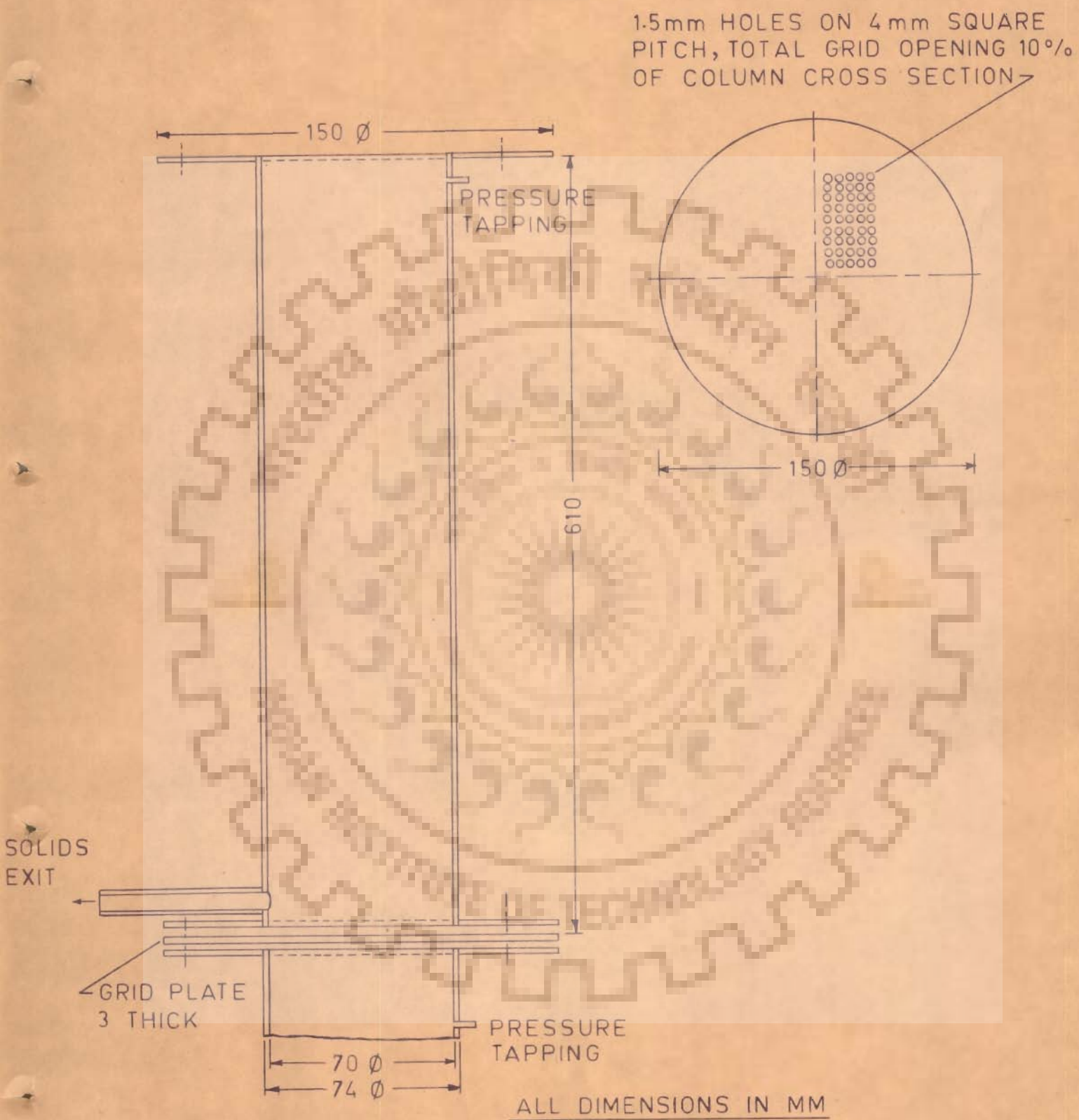


FIG. 3.2 DETAILS OF THE FLUIDIZATION COLUMN

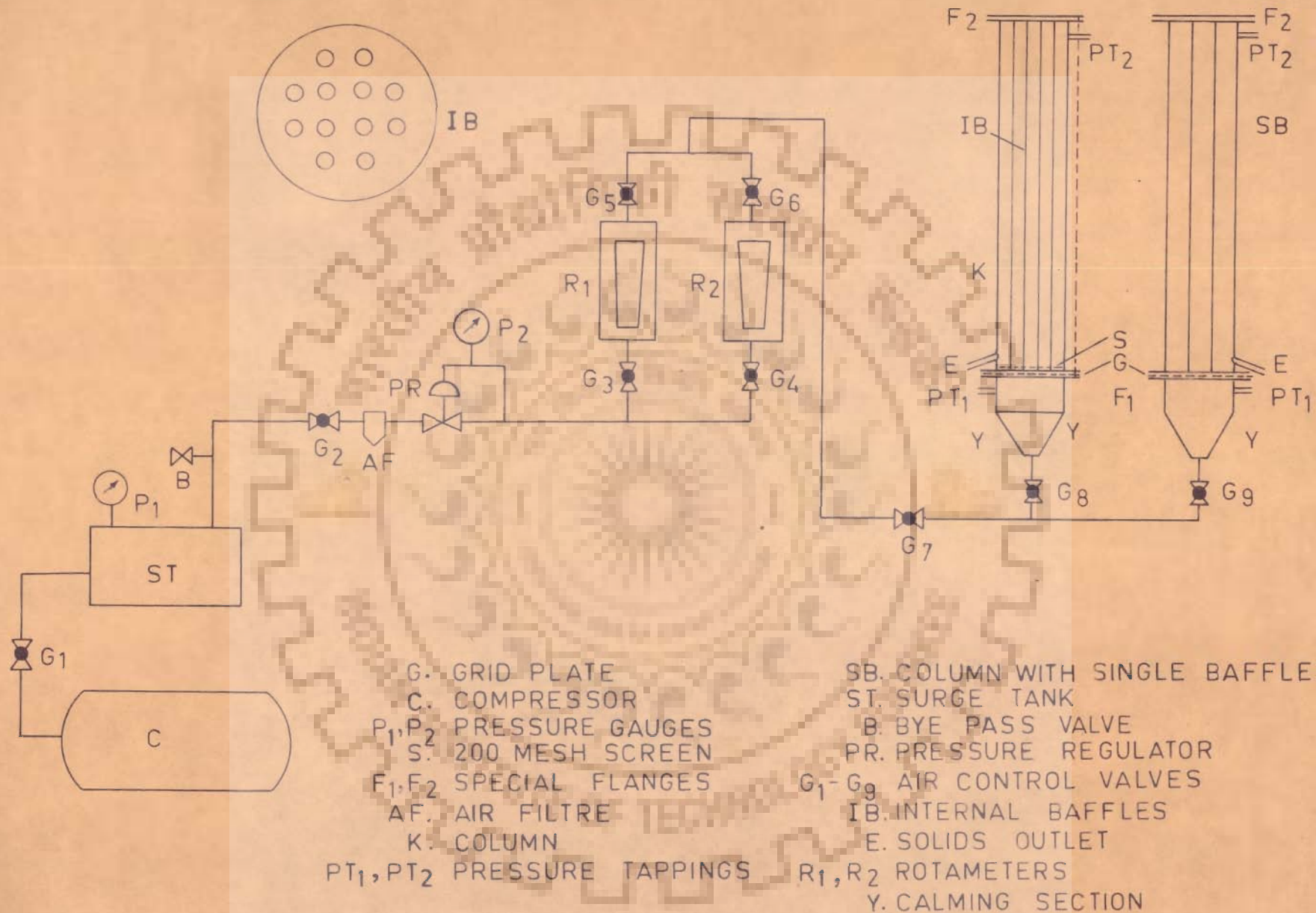
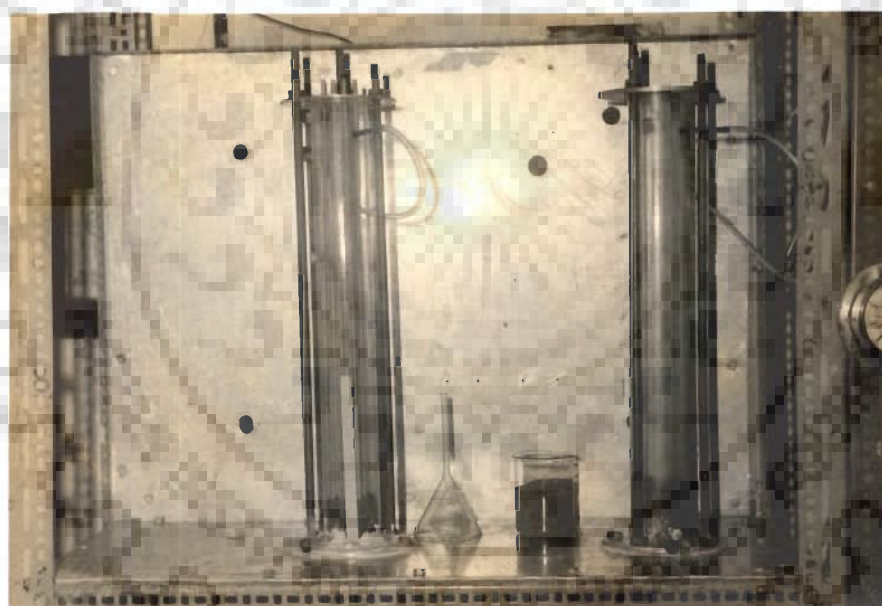


FIG. 3.1 SCHEMATIC DIAGRAM OF THE EXPERIMENTAL SETUP



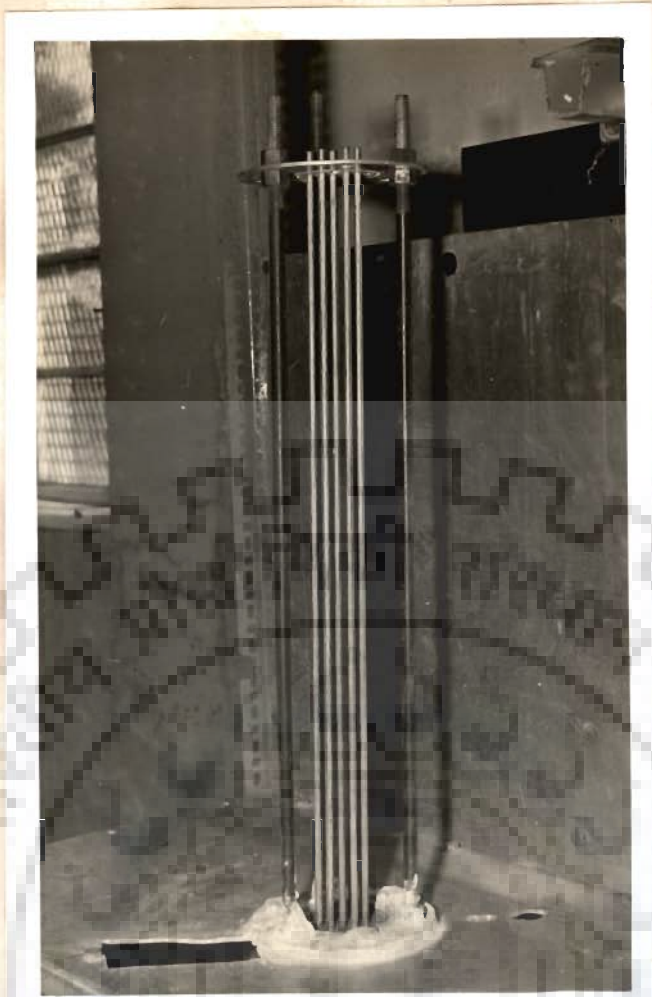
A



B

FIG.3.3 PHOTOGRAPHS SHOWING

- A. GENERAL LAYOUT OF EXPERIMENTAL SET UP FOR BATCH FLUIDIZATION STUDIES.
- B. DETAILS OF FLUIDIZING COLUMNS.



A



B

FIG.3.4 PHOTOGRAPHS SHOWING

A. BAFFLES ARRANGEMENT.

B. GRID PLATES FOR DIFFERENT BAFFLE SPACING.

mass velocity-pressure drop data in different zones of fixed bed, onset of fluidization and fluidized bed zone were studied. For comparison, similar data were obtained in different zones as mentioned above in beds without baffles. The range of experimental variables is shown in Table 3.1.

3.3 RESULTS AND DISCUSSION

Pressure drop air mass velocity data in vertical baffled fluidized bed are reported in tables 3.2 to 3.14. Similar data on beds without baffles are given in tables 3.15 to 3.19. The data pertaining to single baffle equivalent to multibaffles are tabulated in tables 3.21 to 3.26. Tables 3.27 to 3.30 show the data obtained on variation of pressure drop with air mass velocity for different baffle spacing.

3.3.1 Batch Fluidized Bed without Baffles:

Figs. 3.5 and 3.6 show the variation of pressure drop with air mass velocity in batch fluidized beds in the fixed bed, at onset of fluidization and in fluidized bed zones. It was observed from these plots that for a given particle size and solids loading, the bed pressure drop increased almost linearly with air flow rate in the fixed bed zone and once the fluidized state was attained the bed pressure drop increased very slowly. The bed

TABLE-3.1

RANGE OF EXPERIMENTAL VARIABLES

Sl. No.	Variable	Units	Range
1.	Materials	-	Bauxite, Glass beads, Limestone and Baryte
2.	Static bed porosity, ϵ	-	0.382 - 0.575
3.	Solids density, ρ_s	kg/m ³	2.30×10^3 - 3.85×10^3
4.	Solids loading, W/Δ	kg/m ²	28.4 - 71.2
5.	Air flow rate, G_f	kg/m ² .s	0 - 2.8
6.	Particle size, D_p	μm	384-1540
7.	Number of baffles	-	12, 7, 3
8.	Distance between two adjacent baffles, d_o	mm	10, 12, 16
9.	Available area for fluidization, A	m ²	3.51×10^{-3} - 3.84×10^{-3}

pressure drop was found to be much lower than the corresponding bed weight per unit area.

Minimum fluidizing velocity was observed to increase with increase in particle size and solids density. The experimental values of minimum fluidizing velocity are compared with predicted values as given by Leva's correlation [3]. The predicted values differ by less than $\pm 10\%$ of the observed values as shown in table 3.31.

Fig. 3.7 shows the bed porosity as a function of gas velocity after the onset of fluidization. The fluctuation ratio defined as the ratio of the highest to the lowest bed height as a function of reduced gas mass velocity is shown in Fig. 3.23. These observations on bed pressure drop, minimum fluidizing velocity, bed expansion and fluctuation ratio are in accordance with the earlier reported work in literature [3].

3.3.2 Batch Fluidized Beds with Vertical Internal Baffles

Figs 3.8 to 3.15 show the variation of pressure drop with air mass velocity in batch fluidized beds with 12 vertical baffles with baffle spacing of 10 mm. The bed pressure drop increased with increase in gas flow rate in fixed bed zone upto the onset of fluidization and after the onset, the bed pressure drop increased

with air flow rate at a slower rate. Though, these observations are similar to the findings in batch fluidized beds without baffles, the numerical values of pressure drop in beds with baffles were higher than the values in fluidized beds without baffles under identical operating conditions as shown in Figs. 3.16 and 3.17. The excess pressure drop may be due to the presence of additional baffles giving higher friction. The pressure coefficient values are compared with those of unbaffled beds and are shown in table 3.20.

Minimum fluidizing velocity was observed to increase with increase in particle size and solids density as shown in Fig. 3.8 to 3.11 and 3.12 to 3.13. The minimum fluidizing velocity does not seem to get affected by the bed height as shown in Figs. 3.14 and 3.15. The observed values of minimum fluidizing velocity were compared with the predicted values using Leva's correlation and the deviation was found to be as large as 40% as shown in table 3.32 and Fig. 3.18.

3.3.2.1 Bed Expansion Behaviour

The bed porosity data in beds with and without baffles are plotted in Fig. 3.7. The bed porosity in fluidized beds with vertical baffles is found to be lower than the corresponding values in beds without baffles. The bed porosity was observed to be increasing with

increase in gas velocity. The bed porosity data when plotted against particle Reynolds number on log-log scale gave linear variation as shown in Figs. 3.19 to 3.22. The bed porosity increased with increase in particle Reynolds number and for a given particle Reynolds number the bed porosity increased with decrease in particle size. The fluctuation ratios (which give a quantitative measure of the quality of fluidization) increased with increase in reduced gas mass velocity G_f/G_{mf} as shown in Fig. 3.23. The fluctuation ratios were observed to be lower in baffled beds than in beds without baffles. The plot of fluctuation ratio versus $(G_f - G_{mf})/G_{mf}$ on semilog plots, gave straight lines for beds with baffles as shown in Fig. 3.24 to 3.26. The choice of $(G_f - G_{mf})/G_{mf}$ as a controlling parameter is essentially on the basis that particle movement starts only when the gas velocity is in excess of the minimum fluidizing velocity.

3.3.2.2 Effect of Baffle Spacing

The effect of baffle spacing on fluidization characteristics was studied using 12, 7 and 3 baffles (corresponding to a baffle spacing of 10, 12 and 16 mm respectively). When the distance between two adjacent baffles was less than six particle diameters ($d_o/D_p < 6$) it was observed that the solids movement was very much restricted and the solids had a tendency to lump up and

remain as agglomerates even at higher air flow rates. This was similar to 'arching' observed in gravity flow of solids through funnels of very small throat. The fluidization was very unstable. An improvement was observed in the quality of fluidization when d_o/D_p was greater than six. Upto a value of $d_o/D_p = 10$, it was observed that the particles at the centre of the bed fluidized like a fountain indicating channelling/spouting tendencies in the bed. The rising currents of solids were observed to be shifting from one region to another over the entire bed. For baffle spacing greater than ten particle diameters, the bed behaviour was found to be smooth. Grace and Harrison [114] recommended the use of distance between two adjacent baffles not to be less than thirty particle diameters for uniform fluidization. In the present studies, the bed with 12 vertical baffles with baffle spacing of 10 mm gave uniform fluidization for particle size upto 977 microns.

The variation of bed pressure drop with air flow rate is shown in Fig. 3.27 for different baffle spacing. This is similar to the findings in beds without baffles. It was observed that the bed pressure drop was higher for beds with larger number of baffles under similar conditions of operation. The increase in the pressure drop may be due to the presence of additional baffle surface causing higher skin friction.

3.3.3 BATCH FLUIDIZED BEDS WITH SINGLE BAFFLE

The performance of multibaffled fluidized bed was compared with the fluidized bed having a single concentric baffle with spacing of 18.5 mm where the available areas for fluidization in both cases were nearly same. Figs. 3.28 to 3.30 are the plots showing the variation of pressure drop with air mass velocity in beds with single equivalent baffle. The trend of variation of pressure drop with air mass velocity is similar to the one observed in multibaffled systems. However, in the case of beds with single baffle with baffle spacing of 18.5 mm, the transition from the fixed bed to the fluidized bed is not distinctly identifiable. The visual observation of the fluidized bed revealed that the fluidization was not uniform and in certain pockets, the solids movement was fairly vigorous while it was stagnant in the other. This non uniformity persisted even at higher gas flow rates. The pressure drop in these beds was found to be of same magnitude as in beds with 12 baffles in fixed bed zone, while the corresponding values were lower in fluidized bed zones as shown in Fig. 3.31. The minimum fluidizing velocity was found to be lower in these systems than in the multibaffled fluidized beds.

The fluidized beds with vertical internal baffles differ from that of the beds without baffles due to the additional surface contributed by the baffles. Additional

surface causes the extra skin friction, leading to higher values of pressure drop. Further, the baffle walls tend to compartmentalize the bed trying to restrict the particle movement. In such smaller compartments larger bubbles can not be formed leading to more uniform fluidization, lesser bed expansion and lesser fluctuations in the expanded beds. The tendencies of slugging are also eliminated. With proper baffle spacing, channelling tendencies will also disappear.

In the case of fluidized beds with single concentric baffle, while the annular space may be sufficiently large compared to the particle size, the solids movement will still be restricted to localized zones, because of long peripheral distances and curvature effects of the column. This invariably results in non uniform fluidization in different zones of the bed.

3.3.4 Correlations

The behaviour of multibaffled fluidized beds will be significantly different from those beds without baffles. Hence an attempt has been made to propose correlations for systems with vertical internal baffles.

The correlations available for batch fluidized beds without baffles can not be extended to the systems with baffles as the presence of baffles in the beds affects the fluidization characteristics.

3.3.4.1 Minimum Fluidizing Velocity

Based on experimental data obtained, a dimensionless correlation incorporating various parameters like geometry of the column and physical properties of solids and fluid has been proposed for predicting the minimum fluidizing velocity as

$$\frac{D_p G_{mf}}{\mu_f} = 6.72 \times 10^{-2} (Ar)^{0.624} \left(\frac{D_e}{D_p}\right)^{-0.12} \left(\frac{d_o}{D_p}\right)^{-0.13} \left(\frac{L}{d_o}\right)^{0.04} \dots (3.1)$$

$Ar = g D_p^3 (\rho_s - \rho_f) / \nu_f^2 \rho_f$ is the Archimedes number which signifies the interaction of three forces, namely, the fluid resistance, the buoyant force and the gravity force.

$\frac{D_p G_{mf}}{\mu_f}$ is the Reynolds number based on particle diameter which represents the ratio of the inertial forces to viscous forces, and indicates the velocity requirements to ensure particle movement.

$\frac{D_e}{D_p}$ represents the equivalent diameter of bed to particle diameter ratio and signifies the resistance offered by the extra surface present in the bed due to the baffles, column and the fluidized particles.

$\frac{d_o}{D_p}$ represents the ratio of the gap between two baffles to particle diameter and shows the resistance for the free movement of particles in the column.

$\frac{L}{d_o}$ is the ratio of bed height to the gap between two adjacent baffles and represents the effect of compartments due to the presence of baffles.

The predicted values of the minimum fluidizing velocity from eqn. 3.1 were found to be well within $\pm 20\%$ of the experimental values as shown in Fig. 3.32.

3.3.4.2 Pressure Drop

In any fluidized bed, the total resistance to fluid flow is the sum of the pressure drops due to bed weight, the grid and the friction on the surface of the particles. In baffled fluidized beds, the pressure drop due to baffles is significant and hence the total pressure drop can be written as

$$\Delta P = \Delta P_w + \Delta P_G + \Delta P_f + \Delta P_B \quad \dots (3.2)$$

where ΔP is the total pressure drop. ΔP_w , the pressure drop due to the weight of solids will increase with increase in fluid velocity upto the onset of fluidization and thereafter it will be essentially constant and will be equal to the apparent weight of the solids

per unit area of cross section. ΔP_G , the resistance due to grid will be a function of the linear velocity of the fluid through the grid openings. ΔP_f , the pressure drop due to friction on the surface of particles will vary as the square of the fluid velocity. Both ΔP_G and ΔP_f can be evaluated based on column diameter and linear velocity as $\Delta P_G + \Delta P_f = f (Re_T)^2$. ΔP_B , the pressure drop due to friction on the surface of the baffles and the column, will be a function of equivalent diameter and linear velocity. This may be represented as $\Delta P_B = f (Re_{eq})^2$. The total pressure drop, thus will be as follows

$$\Delta P = f (W/A) + f' (Re_{eq})^2 + f'' (Re_T)^2 \quad \dots (3.3)$$

In dimensionless terms, eqn. 3.3 may be written as

$$\frac{\Delta P A}{W} = K + k_1 (Re_{eq})^2 + k_2 (Re_T)^2 \quad \dots (3.4)$$

Based on the experimental data, the values of the coefficients were evaluated as

$$K = 0.923, \quad K_1 = 3.72 \times 10^{-8}, \quad K_2 = 3.46 \times 10^{-10}$$

The correlation predicts the pressure drop within $\pm 10\%$ of the experimental values as shown in Fig. 3.33.

3.3.4.3 Bed Expansion

A dimensionless correlation for predicting the bed porosity in baffled fluidized beds has been proposed as:

$$\epsilon = 0.065 (Fr)^{-0.22} (Re_p)^{0.4} \left(\frac{d_o}{D_p}\right)^{0.69} \left(\frac{\rho_s - \rho_f}{\rho_f}\right)^{-0.11} \dots (3.5)$$

$$Fr = \frac{U_f^2}{D_p g}$$

the Froude number is the ratio of buoyancy force to the gravity force. This is the criteria to ensure that a particle is lifted freely in a fluidized bed due to buoyancy effect.

$$Re_p = \frac{D_p G_f}{\mu_f}$$

is the Reynolds number based on particle diameter and represents the ratio of the inertial forces to the viscous forces and this indicates the velocity requirement to ensure particle movement.

$$\frac{d_o}{D_p}$$

represents the ratio of the gap between two adjacent baffles to particle diameter and signifies the resistance for the free movement of particles in the column.

$$\frac{\rho_s - \rho_f}{\rho_f}$$

is the ratio of the apparent density of solids to density of fluid and represents the quality of fluidized bed.

The above correlation can be used to predict the expanded bed height for any material if the bed height at onset of fluidization is known. The values of bed porosity predicted lie within $\pm 15\%$ of the experimental values and is valid for $4 \leq Re_p \leq 175$ (Fig. 3.34).

3.3.4.4 Quality of Fluidization

The quality of fluidization in a fluidized bed is measured by the fluctuation ratio of the levels in the bed. Fluctuation ratio 'r' has been correlated as an exponential function of $(G_f - G_{mf})/G_{mf}$ as earlier done by Lewis et al [126]. This may be written as

$$r = e^{m(G_f - G_{mf})/G_{mf}} \quad \dots(3.6)$$

where m is the slope of the line on the semilog plot. The slope was observed to be a function of particle diameter and this can be evaluated from Fig. 3.35. The correlation can be used to predict the fluctuation ratio, knowing the value of m . The values of the fluctuation ratios predicted from the correlation were observed to lie within $\pm 15\%$ of the experimental values as shown in Fig. 3.36.

3.4 CONCLUSION:

The above studies in batch fluidized beds with vertical internal baffles indicate that

- slugging tendencies are eliminated
- bed expansion and bed fluctuations are reduced.
- by keeping a proper baffle spacing of not less than ten particle diameters, channelling/spouting tendencies are eliminated and uniform fluidization is achieved.
- introduction of baffles improves the quality of fluidization.
- Minimum fluidizing velocity, total pressure drop across the fluidized bed, bed expansion and fluctuations ratio, can be predicted using the proposed correlations [vide eq. 3.1, 3.4, 3.5 and 3.6].

TABLE-3.2

EXPERIMENTAL DATA

System : Air - Glass Beads
 Column Dia 70 mm
 Baffles Dia 6 mm 12 Nos. d_o 10 mm, height 610 mm
 Solids Loading per unit area $W/A = 71.2 \text{ kg/m}^2$

Run No. 101				Run No. 102			
Particle size		977 μm		Particle size		650 μm	
Static Bed Height		48 mm		Static Bed Height		45 mm	
Sl. No.	Air Flow Rate $\text{Kg/m}^2 \text{ sec}$	Pressure Drop $\text{N/m}^2 \times 10^{-2}$	Bed Height mm	Sl. No.	Air Flow Rate $\text{kg/m}^2 \text{ sec}$	Pressure Drop $\text{N/m}^2 \times 10^{-2}$	Bed Height mm
1	2	3	4	1	2	3	4
1.	0.0	0.0	48	1.	0.0	0.0	45
2.	.1028	0.59	48	2.	.1028	0.980	45
3.	.2028	1.176	48	3.	.2028	1.961	45
4.	.3055	1.765	48	4.	.3055	3.040	45
5.	.4167	2.648	48	5.	.4167	4.413	45
6.	.5139	3.334	48	6.	.5139	5.786	45
7.	.6111	4.511	48	7.	.5555*	6.472	46/45
8.	.7222	5.688	48	8.	.6111	6.570	47/45
9.	.7778*	6.668	48	9.	.7222	6.865	48/45
10.	.8194	6.865	49/48	10.	.8194	7.061	52/46
11.	.9166	7.257	50/48	11.	.9166	7.257	60/50
12.	1.028	7.551	52/49	12.	1.028	7.551	65/52
13.	1.111	7.747	55/50	13.	1.111	7.845	70/57
14.	1.222	8.041	60/53	14.	1.222	8.041	75/60
15.	1.416	8.630	70/55	15.	1.416	8.434	85/65
16.	1.639	9.218	80/60	16.	1.639	9.022	95/70

* Onset of fluidization.

Run No. 103

Particle size 460 μm

Static Bed Height 45 mm

1	2	3	4
1.	0.0	0.0	45
2.	1.028	.1176	45
3.	2.028	.3922	45
4.	3.055	.6472	45
5.	3.194*	.6472	47/45
6.	4.166	.6668	48/46
7.	5.139	.6865	52/48
8.	6.111	.7061	55/48
9.	7.222	.7257	60/50
10.	8.194	.7453	68/55
11.	9.166	.7649	75/60
12.	10.28	.7845	80/60
13.	11.11	.8041	85/65
14.	12.22	.8336	90/70
15.	14.16	.8924	100/75
16.	16.39	.9512	110/80

* Onset of fluidization.

TABLE-3.3

EXPERIMENTAL DATA

System : Air - Glass Beads

Column Dia 70 mm

Baffles 6 mm 12 Nos., do 10 mm height 610 mm

Solids loading per unit area $W/A = 56.8 \text{ kg/m}^2$

Run No. 104

Particle size 977 μm
 Static Bed Height 35 mm

Run No. 105

Particle size 650 μm
 Static Bed Height 37 mm

Sl. No.	Air Flow Rate $\text{kg/m}^2 \cdot \text{sec}$	Pressure Drop $\text{N/m}^2 \times 10^{-2}$	Bed Height mm	Sl. No.	Air Flow Rate $\text{kg/m}^2 \cdot \text{sec}$	Pressure Drop $\text{N/m}^2 \times 10^{-2}$	Bed Height mm
1	2	3	4	1	2	3	4
1.	0.0	0.0	35	1.	0.0	0.0	37
2.	.102	.49	35	2.	.102	.88	37
3.	.255	1.17	35	3.	.204	1.57	37
4.	.408	2.15	35	4.	.306	2.55	37
5.	.510	2.94	35	5.	.408	3.72	37
6.	.613	3.92	35	6.	.51	4.7	37
7.	.700	4.61	35	7.	.54*	5.0	37
8.	.715	4.90	35	8.	.613	5.29	38/37
9.	.77*	5.10	36	9.	.715	5.49	39/37
10.	.817	5.68	37/35	10.	.817	5.68	42/38
11.	.919	5.88	38/35	11.	.919	5.98	45/40
12.	1.02	6.17	40/35	12.	1.02	6.17	48/43
13.	1.12	6.47	43/36	13.	1.12	6.47	53/47
14.	1.22	6.66	46/40	14.	1.22	6.66	55/50
15.	1.43	7.25	54/40	15.	1.43	7.16	65/55
16.	1.63	7.84	60/45	16.	1.63	7.45	75/60

*Onset of fluidization.

Run No. 106

Particle size 460 μm

Static Bed Height 37 mm

	1	2	3	4
1.		0.0	0.0	37
2.		.102	1.76	37
3.		.204	3.13	37
4.		.28	4.61	37
5.		.306*	4.9	37
6.		.408	5.19	39/37
7.		.51	5.49	41/38
8.		.613	5.68	45/40
9.		.715	5.88	50/45
10.		.817	6.08	55/50
11.		.919	6.27	60/55
12.		1.02	6.47	65/60
13.		1.12	6.66	70/65
14.		1.22	6.86	75/70
15.		1.43	7.25	80/75

* Onset of fluidization.

TABLE-3.4

EXPERIMENTAL DATA

System : Air - Glass Beads

Column Dia 70 mm

Baffles 6 mm 12 Nos, d_o 10 mm

Solids Loading per unit area $W/A = 42.7 \text{ kg/m}^2$

Run No. 107
 Particle size 977 μm
 Static Bed Height 27 mm

Run No. 108
 Particle size 650 μm
 Static Bed Height 27 mm

Sl. No.	Air Flow Rate $\text{kg/m}^2 \cdot \text{sec}$	Pressure Drop $\text{N/m}^2 \times 10^{-2}$	Bed Height mm	Sl. No.	Air Flow Rate $\text{kg/m}^2 \cdot \text{sec}$	Pressure Drop $\text{N/m}^2 \times 10^{-2}$	Bed Height mm
1	2	3	4	1	2	3	4
1.	0.0	0.0	27	1.	0.0	0.0	27
2.	.102	.39	27	2.	.102	.68	27
3.	.204	.68	27	3.	.204	1.17	27
4.	.306	1.17	27	4.	.306	1.96	27
5.	.408	1.66	27	5.	.408	2.84	27
6.	.510	2.25	27	6.	.51	3.72	27
7.	.613	3.04	27	7.	.53*	3.92	27
8.	.664	3.43	27	8.	.613	4.11	27
9.	.715	3.92	27	9.	.715	4.31	29/27
10.	.766*	4.21	27	10.	.817	4.51	30/27
11.	.817	4.41	28/27	11.	.919	4.7	35/30
12.	.919	4.7	29/27	12.	1.02	4.9	40/35
13.	1.02	4.9	32/27	13.	1.12	5.1	45/38
14.	1.125	5.1	35/30	14.	1.22	5.29	50/40
15.	1.22	5.29	38/30	15.	1.43	5.88	55/45
16.	1.43	5.88	42/32				
17.	1.63	6.47	47/35				

*Onset of fluidization.

Run No. 109

Particle size 460 μm .

Static Bed Height 26 mm

	1	2	3	4
1.		0.0	0.0	26
2.		.102	1.17	26
3.		.204	2.35	26
4.		.255	3.04	26
5.		.306*	3.72	27
6.		.408	4.02	29/27
7.		.51	4.21	32/27
8.		.613	4.41	36/30
9.		.715	4.6	40/35
10.		.817	4.8	45/40
11.		.919	4.9	50/45
12.		1.02	5.1	55/45
13.		1.12	5.29	55/50
14.		1.22	5.49	60/55
15.		1.43	5.88	65/60

* Onset of fluidization.

TABLE-3.5

EXPERIMENTAL DATA

System : Air - Glass Beads

Column Dia . 70 mm

Baffles 6 mm 12 Nos., d_o 10 mm, height 610 mm

Solids Loading per unit area $W/A = 28.4 \text{ kg/m}^2$

Run No. 110

Particle size 460 μm

Static Bed Height 17 mm

Sl. No.	Air Flow Rate $\text{kg/m}^2 \cdot \text{sec}$	Pressure Drop $\text{N/m}^2 \times 10^{-2}$	Bed Height mm
1	2	3	4
1.	0.0	0.0	17
2.	.102	.98	17
3.	.204	1.76	17
4.	.255	2.15	17
5.	.306*	2.55	19/17
6.	.51	2.94	20/18
7.	.613	3.04	25/20
8.	.715	3.13	30/25
9.	.817	3.33	32/25
10.	.919	3.53	35/28
11.	1.02	3.72	38/30
12.	1.12	3.92	40/30
13.	1.22	4.11	45/32
14.	1.43	4.51	45/30

*Onset of fluidization.

TABLE-3.6

EXPERIMENTAL DATA

System : Air - Baryte

Column Dia 70 mm

Baffles 6 mm 12 Nos, d_o 10 mm

Solids Loading per unit area $W/A = 71.2 \text{ kg/m}^2$

Run No. 111				Run No. 112			
Particle size		1540 μm		Particle size		977 μm	
Static Bed Height		40 mm		Static Bed Height		40 mm	
Sl. No.	Air Flow Rate $\text{kg/m}^2 \cdot \text{sec}$	Pressure Drop $\text{N/m}^2 \times 10^{-2}$	Bed Height mm	Sl. No.	Air Flow Rate $\text{kg/m}^2 \cdot \text{sec}$	Pressure Drop $\text{N/m}^2 \times 10^{-2}$	Bed Height mm
1	2	3	4	1	2	3	4
1.	0.0	0.0	40	1.	0.0	0.0	40
2.	.1022	.19	40	2.	.1022	.19	40
3.	.204	.39	40	3.	.204	.59	40
4.	.3065	.59	40	4.	.306	.98	40
5.	.4089	.88	40	5.	.409	1.47	40
6.	.5100	.98	40	6.	.510	1.96	40
7.	.613	1.37	40	7.	.613	2.45	40
8.	.716	1.76	40	8.	.716	3.23	40
9.	.817	2.15	40	9.	.817	3.92	40
10.	.9197	2.84	40	10.	.9197	4.9	40
11.	1.025	3.53	40	11.	1.025	5.78	40
12.	1.13	4.11	40	12.	1.125	6.86	40
13.	1.226	5.0	40	13.	1.166*	7.06	42/40
14.	1.43	7.35	40	14.	1.226	7.55	45/42
15.	1.635*	8.63	42/40	15.	1.43	8.14	50/45
16.	1.839	9.31	45/40	16.	1.63	8.92	55/50
				17.	1.839	9.8	60/55

*Onset of fluidization.

Run No. 113				Run No. 114				Run No. 115			
Particle size		650 μm		Particle size		460 μm		Particle size		385 μm	
Static bed height		40 mm		Static bed height		40 mm		Static bed height		40 mm	
1	2	3	4	1	2	3	4	1	2	3	4
1.	0.0	0.0	40	1.	0.0	0.0	40	1.	0.0	0.0	40
2.	.102	.39	40	2.	.102	1.27	40	2.	.102	1.96	40
3.	.204	.98	40	3.	.204	2.35	40	3.	.204	3.92	40
4.	.306	1.76	40	4.	.306	3.92	40	4.	.306	6.08	40
5.	.409	2.74	40	5.	.409	5.49	40	5.	.36*	6.27	42/40
6.	.51	3.43	40	6.	.458	6.17	40	6.	.409	6.47	45/42
7.	.613	4.6	40	7.	.51*	6.47	42/40	7.	.51	6.67	48/45
8.	.716	5.59	40	8.	.613	6.67	45/40	8.	.613	6.86	50/48
9.	.817	6.57	40	9.	.716	6.86	50/42	9.	.716	7.06	55/48
10.	.861*	6.86	42/40	10.	.817	7.06	55/45	10.	.817	7.25	60/50
11.	.919	7.16	45/40	11.	.919	7.45	60/50	11.	.919	7.55	65/55
12.	1.025	7.45	47/42	12.	1.03	7.65	65/55	12.	1.03	7.74	70/60
13.	1.125	7.74	50/45	13.	1.125	7.84	70/60	13.	1.125	7.94	80/65
14.	1.226	8.04	55/47	14.	1.226	8.04	75/65	14.	1.226	8.14	85/70
15.	1.43	8.63	60/52	15.	1.43	8.43	80/70	15.	1.43	8.63	95/80
16.	1.63	9.22	67/55	16.	1.63	9.02	90/75				
17.	1.84	10.0	75/60								

*Onset of fluidization.

TABLE-3.7

EXPERIMENTAL DATA

System : Air - Baryte

Column Dia 70 mm

Baffles 6 mm 12 Nos. d_o 10 mm

Solids Loading per unit area $W/A = 56.8 \text{ kg/m}^2$

Run No. 116				Run No. 117			
Particle size		1540 μm		Particle size		977 μm	
Static Bed Height		27 mm		Static Bed Height		32 mm	
Sl. No.	Air Flow Rate $\text{kg/m}^2 \cdot \text{sec}$	Pressure Drop $\text{N/m}^2 \times 10^{-2}$	Bed Height mm	Sl. No.	Air Flow Rate $\text{kg/m}^2 \cdot \text{sec}$	Pressure Drop $\text{N/m}^2 \times 10^{-2}$	Bed Height mm
1	2	3	4	1	2	3	4
1.	0.0	0.0	27	1.	0.0	0.0	32
2.	.102	.196	27	2.	.102	.196	32
3.	.306	.49	27	3.	.306	.88	32
4.	.51	.88	27	4.	.51	1.57	32
5.	.715	1.47	27	5.	.715	2.64	32
6.	.919	2.25	27	6.	.919	3.92	32
7.	1.125	3.63	27	7.	1.125*	5.68	32
8.	1.43	6.08	29/27	8.	1.22	6.27	35/32
9.	1.635*	6.96	35/30	9.	1.43	6.86	35/32
10.	1.839	7.06	40/35	10.	1.63	7.74	40/35
11.	2.04	8.82	45/35	11.	1.84	8.63	50/40

*Onset of fluidization.

Run No. 118				Run No. 119				Run No. 120			
Particle size		650 μm		Particle size		460 μm		Particle size		385 μm	
Static bed height		32 mm		Static bed height		32 mm		Static bed height		33 mm	
1	2	3	4	1	2	3	4	1	2	3	4
1.	0.0	0.0	32	1.	0.0	0.0	32	1.	0.0	0.0	33
2.	.102	0.29	32	2.	0.102	0.98	32	2.	0.102	1.66	33
3.	0.306	1.37	32	3.	0.204	1.96	32	3.	0.204	2.94	33
4.	0.51	2.84	32	4.	0.306	2.94	32	4.	0.306	3.72	33
5.	0.715	4.21	32	5.	0.408	4.11	32	5.	0.35*	5.1	36/35
6.	0.817	5.1	32	6.	0.460	4.70	32	6.	0.408	5.29	37/35
7.	0.87*	5.49	35/32	7.	0.51*	5.1	32	7.	0.51	5.49	38/35
8.	0.919	5.88	36/34	8.	0.613	5.49	35/32	8.	0.613	5.68	42/37
9.	1.02	6.08	40/35	9.	0.715	5.86	40/36	9.	0.715	5.88	48/42
10.	1.12	6.47	42/36	10.	0.817	5.88	45/42	10.	0.817	6.08	53/48
11.	1.22	6.86	48/42	11.	0.919	6.08	50/45	11.	0.919	6.27	57/54
12.	1.43	7.25	54/48	12.	1.02	6.27	55/47	12.	1.02	6.47	60/55
13.	1.63	7.84	60/50	13.	1.12	6.47	60/52	13.	1.12	6.66	65/60
				14.	1.22	6.66	63/55	14.	1.22	6.86	70/60
				15.	1.43	7.06	67/55	15.	1.43	7.25	78/65
				16.	1.63	7.74	75/65				

*Onset of fluidization.

TABLE-3.8

EXPERIMENTAL DATA

System : Air - Baryte

Column Dia 70 mm

Baffles 6 mm 12 No. d_o 10 mm

Solids Loading per unit area $W/A = 42.7 \text{ kg/m}^2$

Run No. 121				Run No. 122			
Particle size		1540 μm		Particle size		977 μm	
Static Bed Height		18 mm		Static Bed Height		25 mm	
S1. No.	Air Flow Rate $\text{kg/m}^2 \cdot \text{sec}$	Pressure Drop $\text{N/m}^2 \times 10^{-2}$	Bed Height mm	S1. No.	Air Flow Rate $\text{kg/m}^2 \cdot \text{sec}$	Pressure Drop $\text{N/m}^2 \times 10^{-2}$	Bed Height mm
1	2	3	4	1	2	3	4
1.	0.0	0.0	18	1.	0.0	0.0	25
2.	.102	.196	18	2.	.102	0.196	25
3.	.306	.39	18	3.	.306	.68	25
4.	.51	.78	18	4.	.51	1.27	25
5.	.715	1.27	18	5.	.715	1.96	25
6.	.919	2.06	18	6.	.919	3.13	25
7.	1.125	3.13	18	7.	1.125	4.51	25
8.	1.22	3.72	18	8.	1.18*	4.7	25
9.	1.32	4.51	18	9.	1.22	4.9	30/25
10.	1.43	5.1	18	10.	1.43	5.49	30/25
11.	1.63*	6.08	20/18	11.	1.63	6.27	30/25
12.	1.84	6.66	25/22	12.	1.84	7.25	35/30

*Onset of fluidization.

Run No. 123				Run No. 124				Run No. 125			
Particle size		650 μm		Particle size		460 μm		Particle size		385 μm	
Static bed height		23 mm		Static bed height		24 mm		Static bed height		25 mm	
1	2	3	4	1	2	3	4	1	2	3	4
1.	0.0	0.0	23	1.	0.0	0.0	24	1.	0.0	0.0	25
2.	0.102	0.92	23	2.	0.102	0.78	24	2.	0.102	1.08	25
3.	0.306	1.17	23	3.	0.204	1.37	24	3.	0.204	2.15	25
4.	0.51	2.25	23	4.	0.306	2.25	24	4.	0.306	3.33	25
5.	0.715	3.53	23	5.	0.408	3.13	24	5.	0.35*	3.82	26/25
6.	0.817*	4.21	25/23	6.	0.460	3.72	24	6.	0.409	3.92	28/25
7.	.919	4.6	26/25	7.	0.51*	3.92	25/24	7.	0.51	4.11	30/27
8.	1.02	4.9	30/25	8.	0.613	4.11	28/25	8.	0.613	4.31	35/30
9.	1.12	5.1	30/26	9.	0.715	4.31	30/27	9.	0.715	4.51	38/34
10.	1.22	5.49	35/28	10.	0.817	4.51	35/30	10.	0.817	4.7	42/35
11.	1.43	6.08	40/30	11.	0.919	4.57	40/37	11.	0.919	4.90	45/38
12.	1.63	6.76	45/35	12.	1.02	4.9	43/40	12.	1.02	5.1	50/45
13.	1.84	7.45	50/40	13.	1.12	5.1	45/40	13.	1.12	5.29	55/50
				14.	1.22	5.29	50/45	14.	1.22	5.49	60/50
				15.	1.43	5.88	55/50	15.	1.43	6.08	70/60
				16.	1.63	6.47	60/50				

*Onset of fluidization.

TABLE-3.9

EXPERIMENTAL DATA

System : Air - Baryte
 Column Dia 70 mm
 Baffles 6 mm 12 Nos. d_o 10 mm
 Solids Loading per unit area $W/A = 28.4 \text{ kg/m}^2$

Run No. 126				Run No. 127			
Particle size		1540 μm		Particle size		977 μm	
Static Bed Height		12 mm		Static Bed Height		15 mm	
Sl. No.	Air Flow Rate $\text{kg/m}^2 \cdot \text{sec}$	Pressure Drop $\text{N/m}^2 \times 10^{-2}$	Bed Height mm	Sl. No.	Air Flow Rate $\text{kg/m}^2 \cdot \text{sec}$	Pressure Drop $\text{N/m}^2 \times 10^{-2}$	Bed Height mm
1	2	3		1	2	3	4
1.	0.0	0.0	12	1.	0.0	0.0	15
2.	.102	.098	12	2.	.102	.098	15
3.	.204	.29	12	3.	.306	.39	15
4.	.408	.49	12	4.	.51	.98	15
5.	.51	.68	12	5.	.715	1.66	15
6.	.715	.98	12	6.	.919	2.45	15
7.	.919	1.47	12	7.	1.02	3.04	15
8.	1.125	2.35	12	8.	1.12*	3.62	15
9.	1.43	3.92	12	9.	1.22	3.82	16/15
10.	1.63*	4.70	15/13	10.	1.43	4.31	20/15
11.	1.84	5.49	20/17	11.	1.63	5.1	25/20
				12.	1.84	6.08	25/20

*Onset of fluidization.

Run No. 128				Run No. 129				Run No. 130			
Particle size		650 μm		Particle size		460 μm		Particle size		385 μm	
Static bed height		15 mm		Static bed height		15 mm		Static bed height		17 mm	
1	2	3	4	1	2	3	4	1	2	3	4
1.	0.0	0.0	15	1.	0.0	0.0	15	1.	0.0	0.0	17
2.	.102	.196	15	2.	.102	.49	15	2.	.102	.78	17
3.	.204	.49	15	3.	.204	1.07	15	3.	.204	1.37	17
4.	.306	.78	15	4.	.306	1.57	15	4.	.306	2.15	17
5.	.408	1.17	15	5.	.408	2.15	15	5.	.357*	2.55	18/17
6.	.51	1.57	15	6.	.46*	2.55	15	6.	.408	2.74	20/18
7.	.613	1.96	15	7.	.51	2.74	16/15	7.	.51	2.94	20/19
8.	.715	2.55	15	8.	.613	2.94	20/15	8.	.613	3.13	22/18
9.	.817*	3.13	15	9.	.715	3.13	22/18	9.	.715	3.33	25/20
10.	.867	3.33	16/15	10.	.817	3.33	23/20	10.	.817	3.53	30/25
11.	.919	3.43	18/15	11.	.919	3.53	25/20	11.	.919	3.72	33/27
12.	1.02	3.53	20/18	12.	1.02	3.72	27/25	12.	1.02	3.82	35/30
13.	1.12	3.92	23/20	13.	1.12	3.92	30/27	13.	1.12	3.92	40/32
14.	1.22	4.11	25/22	14.	1.22	4.11	30/25	14.	1.22	4.11	45/40
15.	1.43	4.7	30/25	15.	1.43	4.51	40/30	15.	1.43	4.51	50/40
16.	1.63	5.1	35/30					16.	1.63	4.9	60/50
17.	1.84	5.78	40/35								

*Onset of fluidization.

TABLE-3.10

EXPERIMENTAL DATA

System : Air - Bauxite
 Column Dia 70 mm
 Baffles 6 mm 12 Nos d_o 10 mm
 Solids Loading per unit area $W/A = 71.2 \text{ kg/m}^2$

Run No. 131
 Particle size 1540 μm
 Static Bed Height 68 mm

Run No. 132
 Particle size 977 μm
 Static Bed Height 70 mm

Sl. No.	Air Flow Rate $\text{kg/m}^2 \cdot \text{sec}$	Pressure Drop $\text{N/m}^2 \times 10^{-2}$	Bed Height mm	Sl. No.	Air Flow Rate $\text{kg/m}^2 \cdot \text{sec}$	Pressure Drop $\text{N/m}^2 \times 10^{-2}$	Bed Height mm
1	2	3	4	1	2	3	4
1.	0.0	0.0	68	1.	0.0	0.0	70
2.	.1028	0.98	68	2.	.1028	0.392	70
3.	.2083	0.490	68	3.	.2083	0.784	70
4.	.3055	0.784	68	4.	.3055	1.471	70
5.	.3889	1.176	68	5.	.4028	2.059	70
6.	.5000	1.471	68	6.	.5000	2.746	70
7.	.7222	2.745	68	7.	.6111	4.020	70
8.	.9166	4.217	68	8.	.7222	4.707	70
9.	1.028	5.197	68	9.	.8055	5.982	72/70
10.	1.125	6.276	68	10.	.9166*	6.865	75/70
11.	1.222	6.865	68	11.	1.028	6.914	80/75
12.	1.305*	7.159	70/68	12.	1.125	6.963	85/80
13.	1.444	7.551	75/70	13.	1.222	7.061	87/82
14.	1.634	8.139	85/72	14.	1.444	7.747	92/85
15.	1.833	8.826	90/80	15.	1.639	8.336	98/88
16.	2.044	9.807	105/95				

*Onset of fluidization.

Run No. 133

Particle size 650 μm
 Static Bed Height 64 mm

Run No. 134

Particle size 460 μm
 Static Bed Height 64 mm

Run No. 133				Run No. 134			
Particle size 650 μm				Particle size 460 μm			
Static Bed Height 64 mm				Static Bed Height 64 mm			
1	2	3	4	1	2	3	4
1.	0.0	0.0	64	1.	0.0	0.0	64
2.	.1028	0.784	64	2.	.1028	2.353	64
3.	.2028	1.667	64	3.	.2028	4.511	64
4.	.3055	2.942	64	4.	.2500	5.491	64
5.	.4167	4.119	64	5.	.3055*	6.080	67/64
6.	.500	5.295	64	6.	.4167	6.276	70/65
7.	.611*	6.472	65/64	7.	.500	6.472	75/70
8.	.7222	6.527	70/65	8.	.611	6.865	80/72
9.	.8255	6.668	75/68	9.	.722	6.962	85/75
10.	.9166	6.865	80/72	10.	.8055	7.061	95/80
11.	1.028	7.061	83/78	11.	.9166	7.257	105/85
12.	1.125	7.257	85/80	12.	1.028	7.551	115/90
13.	1.222	7.551	90/85	13.	1.125	7.943	125/95
14.	1.4166	8.139	100/90	14.	1.222	8.139	130/98
15.	1.639	8.728	110/95	15.	1.416	8.336	135/100

*Onset of fluidization.

Run No. 135

Particle size 385 μm

Static Bed Height 64 mm

Sl.	Air Flow Rate $\text{kg/m}^2 \cdot \text{sec}$	Pressure Drop $\text{N/m}^2 \times 10^{-2}$	Bed Height mm
1	2	3	4
1.	0.0	0.0	64
2.	.1028	3.824	64
3.	.1944	5.688	64
4.	.2028*	5.884	65
5.	.3055	6.080	70
6.	.4167	6.374	75
7.	.500	6.668	85
8.	.6111	6.865	95
9.	.7222	7.061	105
10.	.8055	7.257	115
11.	.9166	7.355	120
12.	1.028	7.405	125
13.	1.125	7.650	135
14.	1.222	7.845	145

*Onset of fluidization.

TABLE-3.11

EXPERIMENTAL DATA

System : Air - Bauxite

Column Dia 70 mm

Baffles 6 mm 12 Nos. d_o 10 mm height 610 mm

Solids Loading per unit area $W/A = 56.8 \text{ kg/m}^2$

Run No. 136

Particle size 650 μm

Static Bed Height 50 mm

Sl No.	Air Flow Rate $\text{kg/m}^2 \cdot \text{sec}$	Pressure Drop $\text{N/m}^2 \times 10^{-2}$	Bed Height mm
1	2	3	4
1.	0.0	0.0	50
2.	.102	.58	50
3.	.204	1.27	50
4.	.306	2.05	50
5.	.408	3.13	50
6.	.51	4.31	50
7.	.613*	5.1	52/50
8.	.715	5.29	55/50
9.	.817	5.49	60/50
10.	.919	5.68	65/60
11.	1.02	5.88	68/60
12.	1.12	6.08	70/62
13.	1.22	6.27	75/65
14.	1.43	6.86	85/70
15.	1.63	7.55	95/80

*Onset of fluidization.

TABLE-3.12

EXPERIMENTAL DATA

System : Air - Bauxite

Column Dia 70 mm

Baffles 6 mm 12 Nos. d_o 10 mm height 610 mm

Solids Loading per unit area $W/A = 42.7 \text{ kg/m}^2$

Run No. 137

Particle size 650 μm

Static Bed Height 37 mm

Sl. No.	Air Flow Rate $\text{kg/m}^2 \cdot \text{sec}$	Pressure Drop $\text{N/m}^2 \times 10^{-2}$	Bed Height mm
1	2	3	4
1.	0.0	0.0	37
2.	.102	.39	37
3.	.204	.98	37
4.	.306	1.66	37
5.	.408	2.25	37
6.	.51	3.13	37
7.	.613*	3.92	40/37
8.	.715	3.92	45/38
9.	.817	4.11	45/40
10.	.919	4.31	50/45
11.	1.02	4.51	55/48
12.	1.12	4.7	60/50
13.	1.22	5.1	65/55
14.	1.43	5.49	75/65
15.	1.63	6.27	80/65

*Onset of fluidization.

TABLE -3.13

EXPERIMENTAL DATA

System : Air - Bauxite

Column Dia 70 mm

Baffles 6 mm 12 Nos. d_o 10 mm

Solids Loading per unit area $W/A = 28.4 \text{ kg/m}^2$

Run No. 138

Particle size 650 μm
 Static Bed Height 25 mm

Run No. 139

Particle size 460 μm
 Static Bed Height 23 mm

Sl. No.	Air Flow Rate $\text{kg/m}^2 \cdot \text{sec}$	Pressure Drop $\text{N/m}^2 \times 10^{-2}$	Bed Height mm	Sl. No.	Air Flow Rate $\text{kg/m}^2 \cdot \text{sec}$	Pressure Drop $\text{N/m}^2 \times 10^{-2}$	Bed Height mm
1	2	3	4	1	2	3	4
1.	0.0	0.0	25	1.	0.0	0.0	23
2.	.102	.19	25	2.	.102	1.07	23
3.	.204	.49	25	3.	.204*	1.96	27/23
4.	.306	.98	25	4.	.306	2.15	28/23
5.	.408	1.47	25	5.	.408	2.54	30/25
6.	.51	1.96	25	6.	.51	2.74	35/30
7.	.613*	2.54	27/25	7.	.613	2.94	40/32
8.	.715	2.74	30/27	8.	.715	3.13	45/37
9.	.817	2.94	35/29	9.	.817	3.23	45/40
10.	.919	3.04	36/30	10.	.919	3.43	50/42
11.	1.02	3.13	40/36	11.	1.02	3.53	60/50
12.	1.12	3.33	45/37	12.	1.12	3.72	65/50
13.	1.22	3.82	50/40	13.	1.22	3.82	70/55
14.	1.43	4.21	55/45				
15.	1.63	4.9	65/50				

*Onset of fluidization.

TABLE -3.14

EXPERIMENTAL DATA

System : Air - Limestone

Column Dia 70 mm

Baffles 6 mm 12 Nos. d_o 10 mm

Solids Loading per unit area $W/A = 71.2 \text{ kg/m}^2$

Run No. 140

Particle size 1540 μm

Static Bed Height 58 mm

Run No. 141

Particle size 977 μm

Static Bed Height 50 mm

Sl. No.	Air Flow Rate $\text{kg/m}^2 \cdot \text{sec}$	Pressure Drop $\text{N/m}^2 \times 10^{-2}$	Bed Height mm	Sl. No.	Air Flow Rate $\text{kg/m}^2 \cdot \text{sec}$	Pressure Drop $\text{N/m}^2 \times 10^{-2}$	Bed Height mm
1	2	3	4	1	2	3	4
1.	0.0	0.0	58	1.	0.0	0.0	50
2.	0.1022	.19	58	2.	.1022	.39	50
3.	.2043	.49	58	3.	.2043	.49	50
4.	.3065	.88	58	4.	.3065	1.47	50
5.	.5108	1.57	58	5.	.5100	2.74	50
6.	.7160	2.94	58	6.	.716	4.8	50
7.	.8175	3.82	58	7.	.818	5.68	50
8.	.9197	4.51	58	8.	.875	6.17	50
9.	1.110	6.57	58	9.	.9197*	6.66	51/50
10.	1.125	6.76	58	10.	1.022	6.86	53/50
11.	1.226*	7.45	60/58	11.	1.125	7.06	55/52
12.	1.430	8.14	63/60	12.	1.226	7.25	65/55
13.	1.635	8.63	67/63	13.	1.43	8.04	70/60
14.	1.805	9.02	75/65	14.	1.63	8.63	75/65

*Onset of fluidization.

Run No. 142				Run No. 143				Run No. 144			
Particle size 650 μm				Particle size 460 μm				Particle size 385 μm			
Static bed height 52 mm				Static bed height 54 mm				Static bed height 55 mm			
1	2	3	4	1	2	3	4	1	2	3	4
1.	0.0	0.0	52	1.	0.0	00.0	54	1.	0.0	0.0	45
2.	.1022	.88	52	2.	.1022	2.15	54	2.	.1022	2.74	55
3.	.2043	1.47	52	3.	.2043	2.94	54	3.	.139	3.62	55
4.	.3065	2.45	52	4.	.306	4.7	54	4.	.2045	5.0	55
5.	.408	3.43	52	5.	.361	5.88	54	5.	.278*	6.37	56
6.	.510	4.51	52	6.	.4085*	6.47	54	6.	.306	6.37	58/55
7.	.613	5.88	52	7.	.510	6.67	55	7.	.408	6.76	62/55
8.	.666*	6.37	54	8.	.613	6.67	60/55	8.	.510	6.96	70/60
9.	.716	6.67	55	9.	.716	6.96	65/58	9.	.613	7.16	75/62
10.	.817	6.86	65	10.	.817	7.16	75/60	10.	.716	7.35	80/65
11.	.9197	6.96	60/55	11.	.919	7.55	80/65	11.	.817	7.55	85/70
12.	1.022	7.06	62/58	12.	1.13	7.94	90/70	12.	.919	7.74	92/75
13.	1.13	7.35	67/60	13.	1.226	8.04	100/75	13.	1.025	7.94	100/80
14.	1.226	7.65	72/65	14.	1.43	8.43	110/80	14.	1.123	8.14	110/85
15.	1.43	8.04	85/70	15.	1.63	8.82	120/85	15.	1.226	8.33	118/90
								16.	1.388	8.63	130/95

*Onset of fluidization.

TABLE-3.15

EXPERIMENTAL DATA

System : Air - Bauxite
 Column Dia 70 mm without baffles
 Particle size = 460 μ m

Run No.201				Run No.202		
Solids loading W/A, 71.2 kg/m ²				Solids loading W/A, 42.7 kg/m ²		
Static Bed Height 65 mm						
Sl. No.	Air Flow Rate kg/m ² . sec	Pressure Drop N/m ² x10 ⁻²	Bed Height mm	Sl. No.	Air Flow Rate kg/m ² . sec	Pressure Drop N/m ² x10 ⁻²
1	2	3	4	1	2	3
1.	0.093	2.06	65	1.	0.093	1.17
2.	0.186	3.70	65	2.	0.186	2.25
3.	0.230	4.70	65	3.	0.230	3.04
4.	0.279	5.30	70/65	4.	0.279	3.13
5.	0.370	5.78	75/65	5.	0.370	3.33
6.	0.460	5.98	80/70	6.	0.460	3.62
7.	0.558	6.20	85/70	7.	0.558	3.82
8.	0.650	6.40	95/75	8.	0.650	4.02
9.	0.837	6.70	105/80	9.	0.740	4.11
10.	0.920	6.95	115/85	10.	0.920	4.6
11.	1.116	7.25	125/90	11.	1.116	4.9
12.	1.300	7.65	140/95	12.	1.30	5.1

TABLE-3.16

EXPERIMENTAL DATA

System : Air - Glass Beads
 Column Dia 70 mm without baffles
 Particle size = 460 μm

Run No. 203				Run No. 204			
Solids loading W/A, 71.2 kg/m^2				Solids loading W/A, 42.7 kg/m^2			
Static Bed Height 45 mm				Static Bed Height 27 mm			
Sl. No.	Air Flow Rate $\text{kg/m}^2 \cdot \text{sec}$	Pressure Drop $\text{N/m}^2 \times 10^{-2}$	Bed Height mm	Sl. No.	Air Flow Rate $\text{kg/m}^2 \cdot \text{sec}$	Pressure Drop $\text{N/m}^2 \times 10^{-2}$	Bed Height mm
1	2	3	4	1	2	3	4
1.	0.093	1.8	45	1.	0.093	0.88	27
2.	0.186	3.5	47/45	2.	0.186	1.66	27
3.	0.276	5.8	50/45	3.	0.279	2.64	30/27
4.	0.37	5.9	52/43	4.	0.37	2.94	35/30
5.	0.46	6.08	55/45	5.	0.46	3.13	40/32
6.	0.558	6.1	60/47	6.	0.558	3.23	45/35
7.	0.65	6.2	65/48	7.	0.65	3.43	48/37
8.	0.74	6.3	72/52	8.	0.74	3.62	50/40
9.	0.837	6.5	78/55	9.	0.837	3.82	55/40
10.	0.92	6.6	95/60	10.	0.92	4.02	60/45
11.	1.02	6.7	105/65	11.	1.023	4.21	65/50
12.	1.116	6.8	120/68	12.	1.116	4.5	70/60

TABLE-3.17

EXPERIMENTAL DATA

System : Air - Glass Beads
Column Dia 70 mm without Baffles
Solids loading W/A 71.2 kg/m²

Run No. 205

Particle size 650 μm

Static Bed Height 45 mm

Sl. No.	Air Flow Rate kg/m ² . sec	Pressure Drop N/m ² x10 ⁻²	Bed Height mm
1	2	3	4
1.	0.093	.8	45
2.	0.186	1.8	45
3.	0.279	3.1	45
4.	0.37	4.7	46/45
5.	0.46	5.8	48/45
6.	0.49	5.8	50/45
7.	0.558	5.98	55/45
8.	0.74	6.1	58/48
9.	0.837	6.2	65/50
10.	0.92	6.3	70/50
11.	1.02	6.5	78/53
12.	1.116	6.6	82/55
13.	1.30	6.9	85/60

TABLE-3.18

EXPERIMENTAL DATA

System : Air - Limestone
 Column Dia 70 mm without baffles
 Particle size 460 μ m without Baffles

Run No.206				Run No.207		
Solids loading W/A, 71.2 kg/m ²				Solids loading W/A, 42.7 kg/m ²		
Static Bed Height 55 mm				Static Bed Height 55 mm		
Sl. No.	Air Flow Rate kg/m ² . sec	Pressure Drop N/m ² x10 ⁻²	Bed Height mm	Sl. No.	Air Flow Rate kg/m ² . sec	Pressure Drop N/m ² x10 ⁻²
1	2	3	4	1	2	3
1.	0.093	1.76	55	1.	0.093	0.78
2.	0.186	3.4	55	2.	0.186	1.42
3.	0.279	5.6	58/55	3.	0.279	2.25
4.	0.37	5.9	65/55	4.	0.37	3.33
5.	0.46	5.98	70/57	5.	0.46	3.53
6.	0.558	6.1	75/62	6.	0.558	3.62
7.	0.65	6.17	85/65	7.	0.65	3.82
8.	0.74	6.2	95/68	8.	0.74	4.02
9.	0.837	6.4	100/72	9.	0.837	4.21
10.	1.023	6.8	110/75	10.	0.92	4.41
11.	1.116	6.9	120/80	11.	1.116	4.70
12.	1.30	7.15	130/85			

TABLE-3.19

EXPERIMENTAL DATA

System : Air - Baryte
 Column Dia 70 mm without baffles
 Particle size - 460 μ m

Run No. 208				Run No. 209			
Solids loading W/A, 71.2 kg/m ²		Static Bed Height 40 mm		Solids loading W/A, 42.7 kg/m ²		Static Bed Height 23 mm	
Sl. No.	Air Flow Rate kg/m ² . sec	Pressure Drop N/m ² x 10 ⁻²	Bed Height mm	Sl. No.	Air Flow Rate kg/m ² . sec	Pressure Drop N/m ² x 10 ⁻²	Bed Height mm
1	2	3	4	1	2	3	4
1.	0.093	.98	40	1.	0.093	.50	23
2.	0.186	1.8	40	2.	0.186	1.17	23
3.	0.279	3.2	40	3.	0.279	1.8	23
4.	0.37	4.9	40	4.	0.37	2.45	23
5.	0.46	5.78	42/40	5.	0.46	2.9	26/23
6.	0.558	5.9	45/40	6.	0.50	3.04	28/25
7.	0.65	6.1	52/40	7.	0.558	3.1	30/25
8.	0.74	6.2	58/42	8.	0.65	3.3	35/30
9.	0.837	6.4	65/48	9.	0.74	3.5	40/35
10.	0.92	6.6	68/50	10.	0.837	3.7	50/40
11.	1.02	6.7	75/55	11.	0.92	3.8	60/40
12.	1.116	7.0	80/65	12.	1.116	4.1	65/50
13.	1.30	7.3	95/70	13.	1.30	4.5	70/55

TABLE-3.20

COMPARISON OF PRESSURE DROP AT ONSET OF FLUIDIZATION

	Diameter of the column	70	mm			
	Particle size	460	μm			
	Baffle spacing d_0	10	mm			
	No. of Baffles	12				
Sl. No.	Material	Solids loading per unit area $W/A, \text{kg/m}^2$	Pressure drop at onset		Pressure coefficient at onset	
			$\text{N/m}^2 \times 10^{-2}$		P.A/W	
			Unbaffled	Baffled	Unbaffled	Baffled
1.	Glass beads	42.7	2.84	3.43	0.678	0.820
2.		71.2	6.08	6.47	0.870	0.926
3.	Limestone	42.7	3.33	3.82	0.795	0.910
4.		71.2	5.78	6.57	0.827	0.940
5.	Baryte	42.7	3.43	3.92	0.820	0.936
6.		71.2	5.78	6.47	0.820	0.926
7.	Bauxite	42.7	3.04	3.43	0.726	0.820
8.		71.2	5.39	6.17	0.772	0.883

TABLE-3.21

EXPERIMENTAL DATA

System - Air - Glass beads

Column diameter 70 mm

Single baffle diameter 32.7 mm

Solids loading per unit area $W/\Lambda = 71.2 \text{ kg/m}^2$

Run No. 301 Particle size 460 μm			Run No. 302 Particle size 650 μm		
Sl. No.	Air Flow Rate $\text{kg/m}^2 \cdot \text{sec}$	Pressure drop $\text{N/m}^2 \times 10^{-2}$	Sl. No.	Air Flow Rate $\text{kg/m}^2 \cdot \text{sec}$	Pressure drop $\text{N/m}^2 \times 10^{-2}$
1.	.119	2.64	1.	.119	1.07
2.	.178	3.53	2.	.238	2.15
3.	.238	4.6	3.	.47	5.0
4.	.29	5.98	4.	.52*	5.98
5.	.34*	5.78	5.	.58	6.37
6.	.41	5.98	6.	.59	6.57
7.	.59	6.37	7.	.71	6.57
8.	.83	6.76	8.	.83	6.57
9.	.95	6.96	9.	.95	6.76
10.	1.068	7.16	10.	1.06	6.96
11.	1.19	7.35	11.	1.19	7.16
12.	1.31	7.55	12.	1.3	7.35
13.	1.42	7.74	13.	1.42	7.55
14.	1.66	8.33	14.	1.66	8.23
15.	1.91	9.0	15.	1.91	8.92
			16.	2.13	9.8

* Onset of fluidization

TABLE-3.22

EXPERIMENTAL DATA

System - Air - Glass beads

Column diameter 70 mm

Single baffle diameter 32.7 mm

Solids loading per
unit area $W/\Lambda=56.8 \text{ kg/m}^2$

Run No. 303			Run No. 304		
Particle size 460 μm			Particle size 650 μm		
Sl. No.	Air Flow Rate $\text{kg/m}^2 \cdot \text{sec}$	Pressure drop $\text{N/m}^2 \times 10^{-2}$	Sl. No.	Air Flow Rate $\text{kg/m}^2 \cdot \text{sec}$	Pressure drop $\text{N/m}^2 \times 10^{-2}$
1.	0.119	2.06	1.	.119	1.07
2.	.238	3.62	2.	.238	1.86
3.	.29	4.5	3.	.35	3.04
4.	.30*	4.5	4.	.41	4.41
5.	.41	4.6	5.	.53*	4.8
6.	.47	4.9	6.	.59	4.8
7.	.59	5.1	7.	.71	5.0
8.	.71	5.29	8.	.83	5.19
9.	.83	5.39	9.	.95	5.39
10.	.95	5.58	10.	1.06	5.68
11.	1.06	5.78	11.	1.19	5.98
12.	1.19	5.98	12.	1.31	6.17
13.	1.31	6.17	13.	1.42	6.37
14.	1.42	6.37	14.	1.66	6.96
15.	1.66	6.96	15.	1.91	7.8
16.	1.91	7.55	16.	2.13	8.63

*Onset of fluidization

TABLE-3.23

EXPERIMENTAL DATA

System - Air - Glass beads
 Column diameter 70 mm
 Single baffle diameter 32.7 mm
 Solids loading per unit area $W/A = 42.7 \text{ kg/m}^2$

Run No. 305			Run No. 306		
Particle size 460 μm			Particle size 650 μm		
Sl. No.	Air Flow Rate $\text{kg/m}^2 \cdot \text{sec}$	Pressure drop $\text{N/m}^2 \times 10^{-2}$	Sl. No.	Air Flow Rate $\text{kg/m}^2 \cdot \text{sec}$	Pressure drop $\text{N/m}^2 \times 10^{-2}$
1.	0.119	1.47	1.	0.119	0.88
2.	0.238	2.25	2.	0.238	1.47
3.	0.29	2.84	3.	0.35	2.45
4.	0.35*	3.62	4.	0.47	3.43
5.	0.47	3.43	5.	0.48*	3.43
6.	0.59	3.62	6.	0.59	3.62
7.	0.71	4.02	7.	0.71	3.82
8.	0.83	4.2	8.	0.83	4.02
9.	0.95	4.4	9.	0.95	4.2
10.	1.07	4.5	10.	1.06	4.4
11.	1.19	4.7	11.	1.19	4.6
12.	1.31	4.9	12.	1.31	4.8
13.	1.42	5.1	13.	1.42	5.0
14.	1.66	5.68	14.	1.66	5.58
			15.	1.91	6.17
			16.	2.13	7.35

* Onset of fluidization

Run No.307

Particle Size 977 μm

1	2	3
1.	0.119	0.39
2.	0.23	0.78
3.	0.35	1.47
4.	0.47	1.96
5.	0.59	2.64
6.	0.71	3.43
7.	0.72*	3.62
8.	0.83	3.82
9.	0.95	4.02
10.	1.06	4.21
11.	1.19	4.4
12.	1.31	4.6
13.	1.42	4.8
14.	1.66	5.59
15.	1.91	6.37
16.	2.13	7.16

* Onset of fluidization.

TABLE -3.24

EXPERIMENTAL DATA

System - Air Limestone					
Column diameter 70 mm					
Single baffle diameter 32.7mm					
Solids loading per unit area $W/\Delta = 71.2 \text{ kg/m}^2$					
Run No.308			Run No.309		
Particle size 650 μm			Particle size 460 μm		
Sl. No.	Air Flow Rate $\text{kg/m}^2 \cdot \text{sec}$	Pressure drop $\text{N/m}^2 \times 10^{-2}$	Sl. No.	Air Flow Rate $\text{kg/m}^2 \cdot \text{sec}$	Pressure $\text{N/m}^2 \times 10^{-2}$
1	2	3	1	2	3
1.	.119	.98	1.	.119	1.86
2.	.238	1.86	2.	.238	3.33
3.	.35	3.04	3.	.35	5.39
4.	.47	4.91	4.	.42*	6.37
5.	.59	5.49	5.	.47	6.17
6.	.69*	6.3	6.	.59	6.37
7.	.71	6.3	7.	.71	6.57
8.	.83	6.3	8.	.83	6.76
9.	.95	6.66	9.	.95	6.96
10.	1.06	6.86	10.	1.06	7.15
11.	1.19	7.16	11.	1.19	7.35
12.	1.3	7.35	12.	1.31	7.55
13.	1.42	7.55	13.	1.42	7.84
14.	1.66	8.33	14.	1.66	8.33
15.	1.91	8.72			

* Onset of fluidization

TABLE -3.25

EXPERIMENTAL DATA

System - Air - Bauxite
 Column diameter 70 mm
 Single baffle diameter 32.7 mm
 Solids loading per unit area $W/\Delta = 71.2 \text{ kg/m}^2$

Run No. 312			Run No. 313		
Particle size 650 μm			Particle size 460 μm		
Sl. No.	Air Flow Rate $\text{kg/m}^2 \cdot \text{sec}$	Pressure drop $\text{N/m}^2 \times 10^{-2}$	Sl. No.	Air Flow Rate $\text{kg/m}^2 \cdot \text{sec}$	Pressure drop $\text{N/m}^2 \times 10^{-2}$
1	2	3	1	2	3
1.	.119	1.07	1.	.119	3.04
2.	.35	3.82	2.	.238	5.58
3.	.53	5.98	3.	.29*	5.78
4.	.58*	6.37	4.	.356	5.78
5.	.71	6.47	5.	.47	5.98
6.	.83	6.57	6.	.59	6.17
7.	.95	6.76	7.	.71	6.37
8.	1.06	6.96	8.	.83	6.57
9.	1.19	7.15	9.	.95	6.86
10.	1.31	7.45	10.	1.06	7.06
11.	1.42	7.74	11.	1.19	7.35
12.	1.66	8.33	12.	1.31	7.55
13.	1.91	8.72	13.	1.42	7.94

*Onset of fluidization.

TABLE -3.26

EXPERIMENTAL DATA

System - Air - Baryte

Column diameter 70 mm

Single baffle diameter 32.7 mm

Solids loading per
unit area $W/A = 71.2 \text{ kg/m}^2$

Run No. 314			Run No. 315		
Particle size 650 μm			Particle size 460 μm		
Sl. No.	Air Flow Rate $\text{kg/m}^2 \cdot \text{sec}$	Pressure drop $\text{N/m}^2 \times 10^{-2}$	Sl. No.	Air Flow Rate $\text{kg/m}^2 \cdot \text{sec}$	Pressure drop $\text{N/m}^2 \times 10^{-2}$
1	2	3	1	2	3
1.	.119	.58	1.	.119	1.47
2.	.35	2.05	2.	.238	2.74
3.	.59	3.72	3.	.356	4.31
4.	.71	4.9	4.	.476	6.08
5.	.83	6.08	5.	.53*	5.88
6.	.89*	6.47	6.	.59	5.88
7.	.95	6.47	7.	.71	6.09
8.	1.06	6.66	8.	.83	6.27
9.	1.19	6.86	9.	.95	6.47
10.	1.31	7.06	10.	1.06	6.66
11.	1.42	7.25	11.	1.19	6.86
12.	1.66	7.84	12.	1.31	7.15
13.	1.91	8.63	13.	1.42	7.45
14.	2.13	10.0	14.	1.66	8.05

*Onset of fluidization.

TABLE-3.27

EXPERIMENTAL DATA

System : Air - Baryte

Column Dia 70 mm

Particle size 460 μm

Solids Loading per unit area $W/A = 71.2 \text{ kg/m}^2$

Run No. 145

Baffle 7 Nos. 6 mm dia, $d_o = 12 \text{ mm}$

Run No. 146

Baffles 3 Nos. 6 mm dia, $d_o = 16 \text{ mm}$

Sl. No.	Air Flow Rate $\text{kg/m}^2 \cdot \text{sec}$	Pressure Drop $\text{N/m}^2 \times 10^{-2}$	Sl. No.	Air Flow Rate $\text{kg/m}^2 \cdot \text{sec}$	Pressure Drop $\text{N/m}^2 \times 10^{-2}$
1	2	3	1	2	3
1.	0.095	1.17	1.	0.095	1.07
2.	0.19	2.25	2.	0.19	2.15
3.	0.29	3.72	3.	0.29	3.72
4.	0.39	5.39	4.	0.39	5.29
5.	0.48	6.17	5.	0.43	5.88
6.	0.58	6.37	6.	0.48	6.08
7.	0.68	6.66	7.	0.58	6.37
8.	0.78	6.86	8.	0.68	6.57
9.	0.88	7.06	9.	0.78	6.76
10.	0.96	7.25	10.	0.88	6.86
11.	1.18	7.45	11.	0.96	7.06
12.	1.37	7.74	12.	1.18	7.25
13.	1.57	8.14	13.	1.37	7.45
			14.	1.57	7.84

TABLE-3.28

EXPERIMENTAL DATA

System : Air - Limestone

Column Dia. 70 mm

Particle size 460 μ m

Solids loading per unit area $W/A = 71.2 \text{ kg/m}^2$

Run No. 147

Baffle 7 Nos. 6 mm dia, $d_0 = 12 \text{ mm}$

Run No. 148

Baffles 3 Nos. 6 mm dia, $d_0 = 16 \text{ mm}$

Run No. 147			Run No. 148		
Baffle 7 Nos. 6 mm dia, $d_0 = 12 \text{ mm}$			Baffles 3 Nos. 6 mm dia, $d_0 = 16 \text{ mm}$		
Sl. No.	Air Flow Rate $\text{kg/m}^2 \cdot \text{sec}$	Pressure Drop $\text{N/m}^2 \times 10^{-2}$	Sl. No.	Air Flow Rate $\text{kg/m}^2 \cdot \text{sec}$	Pressure Drop $\text{N/m}^2 \times 10^{-2}$
1	2	3	1	2	3
1.	.095	1.86	1.	.095	1.86
2.	.19	2.64	2.	.19	2.55
3.	.29	4.21	3.	.29	4.11
4.	.39	5.58	4.	.39	5.39
5.	.48	6.37	5.	.48	6.17
6.	.58	6.47	6.	.58	6.37
7.	.68	6.66	7.	.68	6.57
8.	.78	6.76	8.	.78	6.76
9.	.88	6.96	9.	.88	6.86
10.	.96	7.16	10.	.96	6.96
11.	1.18	7.45	11.	1.18	7.16
12.	1.37	7.74	12.	1.37	7.45
13.	1.57	8.04	13.	1.57	7.84

*

TABLE-3.29

EXPERIMENTAL DATA

System : Air - Glass beads
 Column Dia. 70 mm
 Particle size 460 μ m
 Solids loading per unit area $W/A = 71.7 \text{ Kg/m}^2$

Run No. 149
 Baffles 7 Nos. 6 mm dia, d_o 12 mm

Run No. 150
 Baffles 3 Nos. 6 mm dia, d_o 16 mm

Sl. No.	Air Flow Rate $\text{kg/m}^2 \cdot \text{sec}$	Pressure Drop $\text{N/m}^2 \times 10^{-2}$	Sl. No.	Air Flow Rate $\text{kg/m}^2 \cdot \text{sec}$	Pressure Drop $\text{N/m}^2 \times 10^{-2}$
1	2	3	2	3	
1.	.095	1.86	1.	.095	1.76
2.	.19	3.72	2.	.19	3.53
3.	.29	6.08	3.	.29	5.78
4.	.39	6.47	4.	.39	6.27
5.	.48	6.66	5.	.48	6.37
6.	.58	6.98	6.	.58	6.62
7.	.68	7.16	7.	.68	6.72
8.	.78	7.35	8.	.78	6.86
9.	.88	7.65	9.	.83	7.06
10.	.96	7.65	10.	.96	7.16
11.	1.18	8.00	11.	1.18	7.35
12.	1.37	8.23	12.	1.37	7.65

TABLE-3.30

EXPERIMENTAL DATA

System : Air - Bauxite

Column Dia 70 mm

Particle size 460 μ m

Solids loading per unit area $W/A = 71.2 \text{ kg/m}^2$

Run No. 151

Run No. 152

Baffles 7 Nos 6 mm dia, d_0 12 mm

Baffles 3 Nos 6 mm dia, d_0 16 mm

Sl. No.	Air Flow Rate $\text{kg/m}^2 \cdot \text{sec}$	Pressure Drop $\text{N/m}^2 \times 10^{-2}$	Sl. No.	Air Flow Rate $\text{kg/m}^2 \cdot \text{sec}$	Pressure Drop $\text{N/m}^2 \times 10^{-2}$
1	2	3	1	2	3
1.	.095	1.07	1.	.095	1.07
2.	.19	2.15	2.	.19	2.15
3.	.29	3.72	3.	.29	3.62
4.	.39	5.29	4.	.39	5.19
5.	.48	6.17	5.	.48	6.08
6.	.58	6.47	6.	.58	6.37
7.	.68	6.66	7.	.68	6.57
8.	.78	6.86	8.	.78	6.86
9.	.88	7.06	9.	.88	6.96
10.	.96	7.25	10.	.96	7.16
11.	1.18	7.45	11.	1.18	7.35
12.	1.37	7.65	12.	1.37	7.45
13.	1.57	7.94	13.	1.57	7.65

TABLE-3.31

COMPARISON OF THEORETICAL AND EXPERIMENTAL
VALUES OF MINIMUM FLUIDIZING VELOCITIES IN
FLUIDIZED BEDS WITHOUT BAFFLES

Sl. No.	Material	$D_p, \mu\text{m}$	Minimum Fluidizing Velocity $\text{kg/n}^2.\text{s.}$	
			Theoretical*	Experimental
1	2	3	4	5
1.	Bauxite	650	0.401	0.445
2.		460	0.198	0.222
3.	Glass beads	650	0.416	0.465
4.		460	0.225	0.250
5.	Limestone	650	0.451	0.50
6.		460	0.244	0.270
7.	Baryte	460	0.339	0.377

*Values calculated using Leva's equation.

TABLE-3.32

COMPARISON OF THEORETICAL* AND EXPERIMENTAL VALUES
OF MINIMUM FLUIDIZING VELOCITIES IN BAFFLED BEDS

Sl. No.	Material	$D_p, \mu\text{m}$	Minimum Fluidizing Velocity $\text{kg/m}^2.\text{s.}$	
			Theoretical	Experimental
1	2	3	4	5
1.	Bauxite	977	0.836	0.9375
2.		650	0.401	0.625
3.		460	0.198	0.326
4.	Glass beads	650	0.416	0.562
5.		460	0.225	0.313
6.	Limestone	650	0.451	0.658
7.		460	0.244	0.426
8.	Baryte	650	0.631	0.841
9.		460	0.338	0.516

* Theoretical values of minimum fluidizing velocity are calculated using Leva's equation.

SYSTEM: AIR - GLASS BEADS

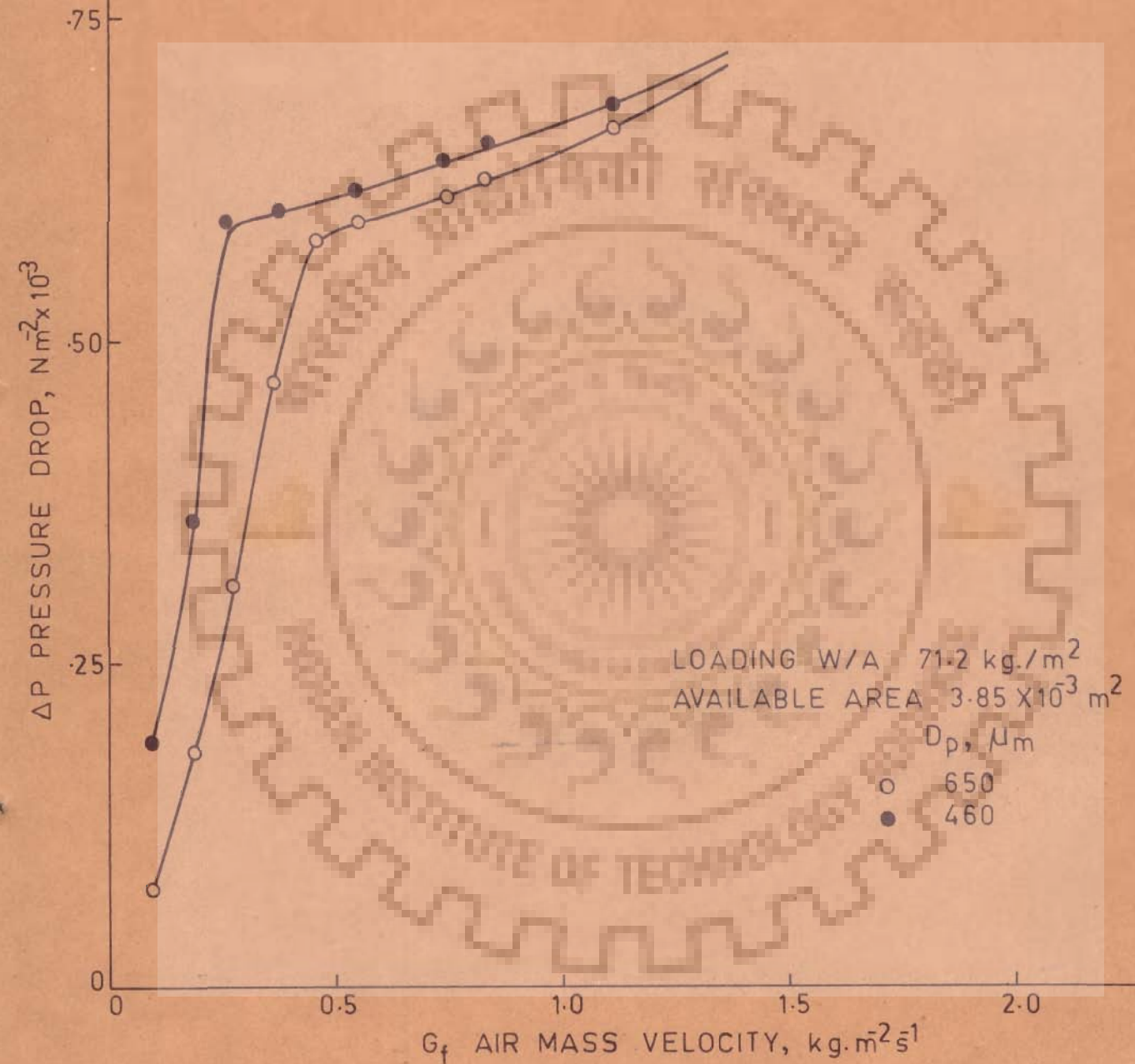


FIG. 3.5 VARIATION OF PRESSURE DROP WITH AIR MASS VELOCITY IN BATCH FLUIDIZED BED WITHOUT BAFFLES.

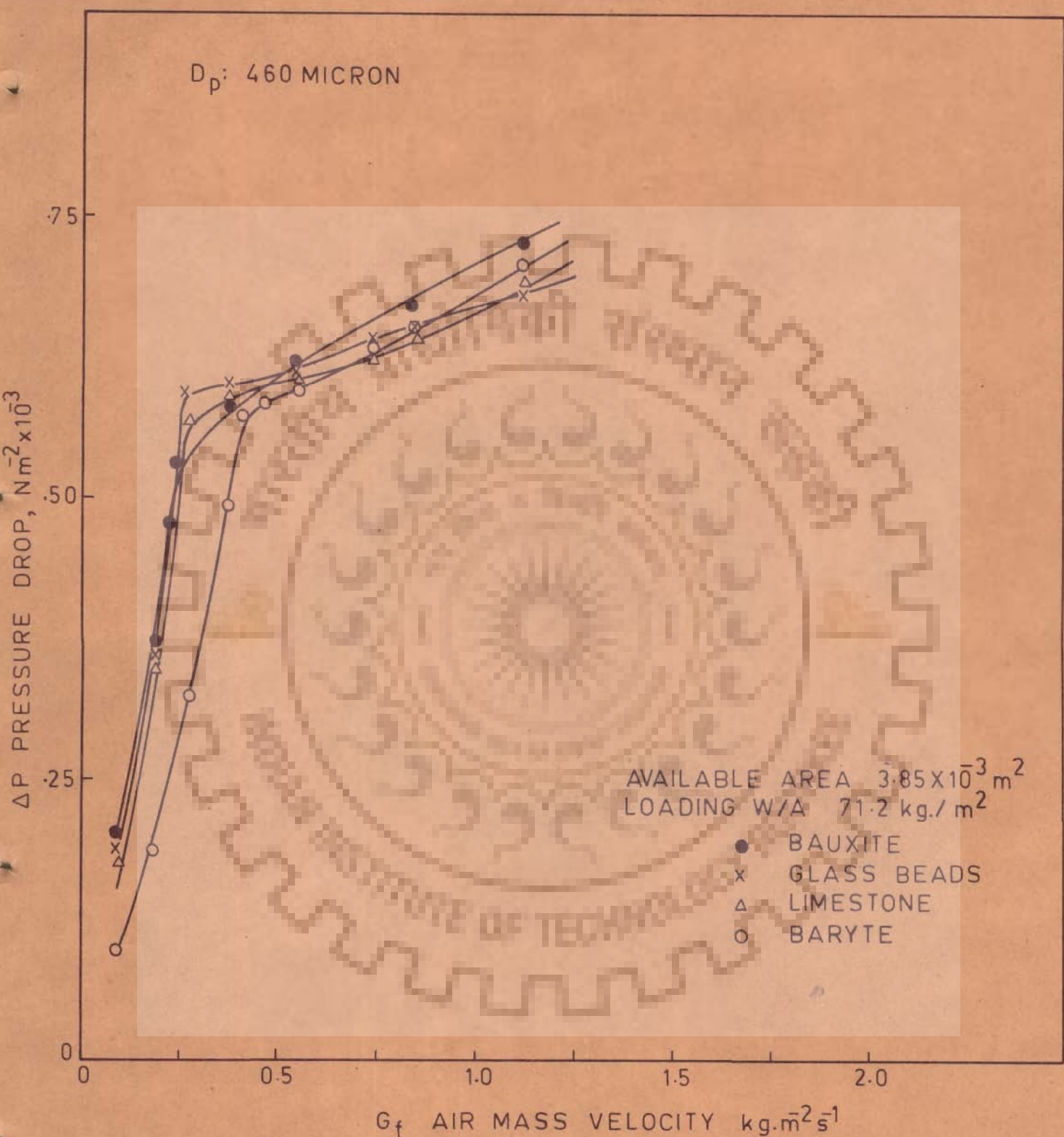


FIG. 3.6 VARIATION OF PRESSURE DROP WITH AIR MASS VELOCITY IN BATCH FLUIDIZED BED WITHOUT BAFFLES.

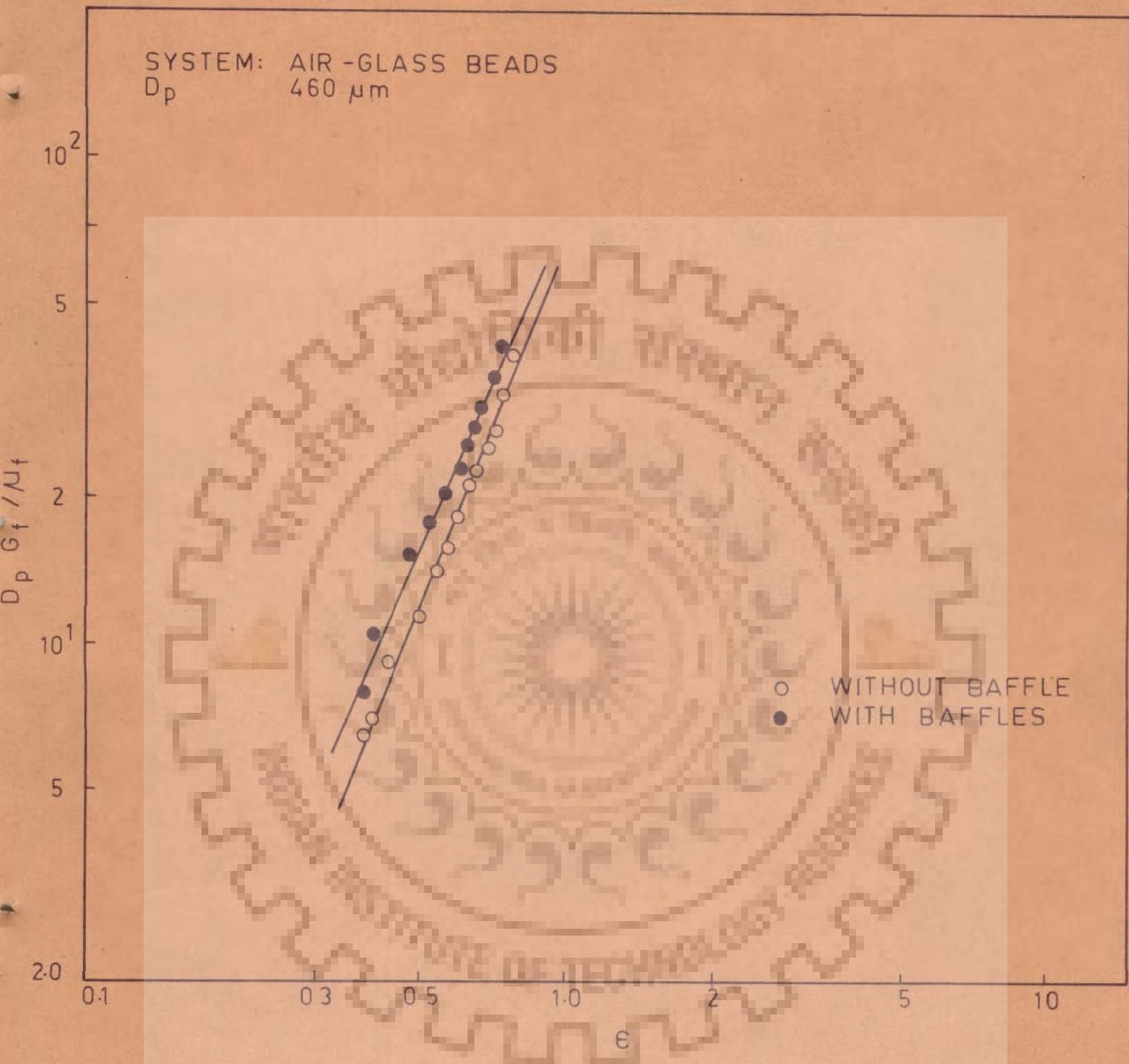


FIG. 3.7 VARIATION OF BED POROSITY WITH PARTICLE REYNOLDS NUMBER IN BATCH FLUIDIZED BEDS WITH AND WITHOUT BAFFLES.

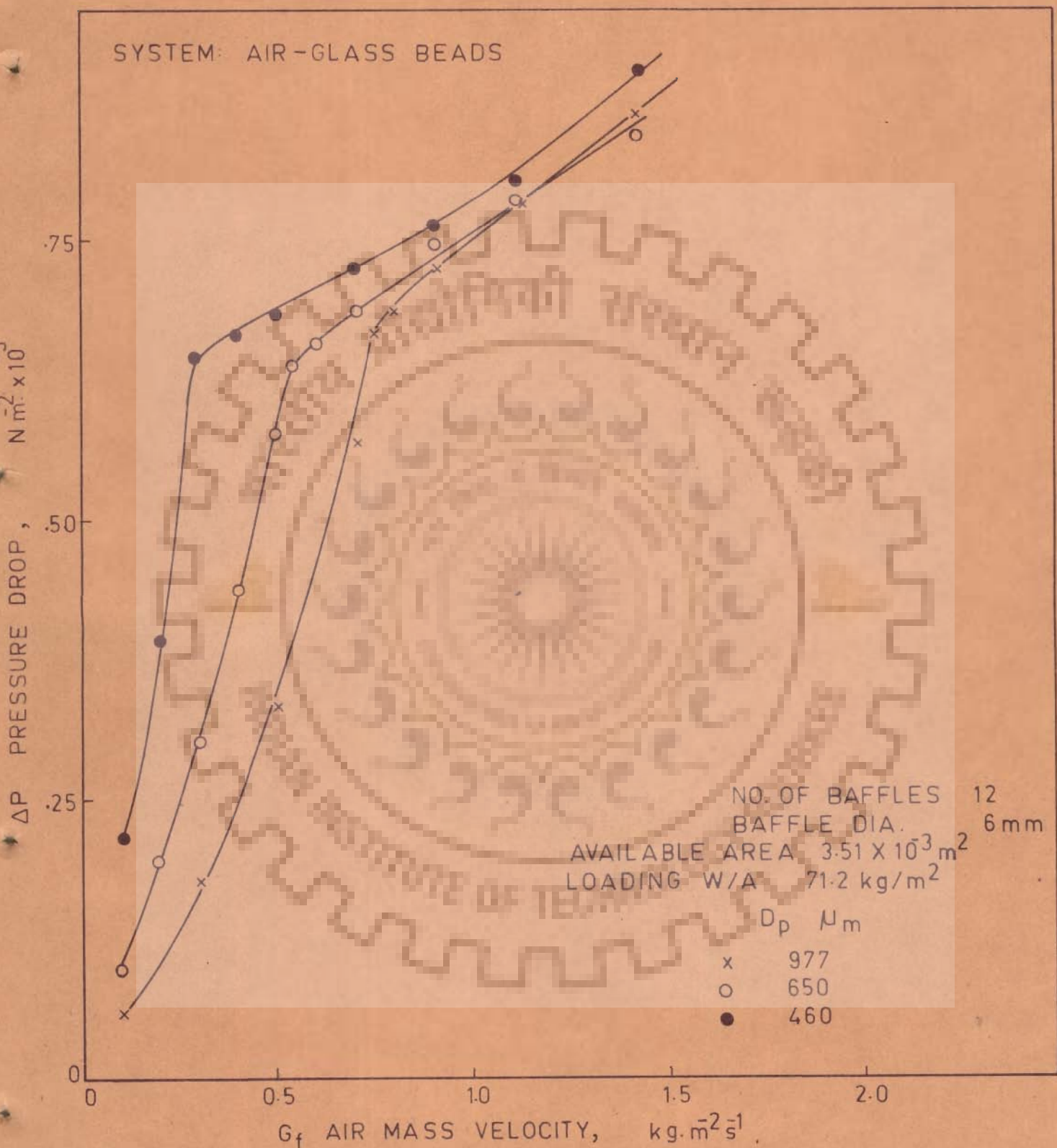


FIG. 3-8 VARIATION OF PRESSURE DROP WITH AIR MASS VELOCITY IN BATCH FLUIDIZED BED WITH VERTICAL BAFFLES.

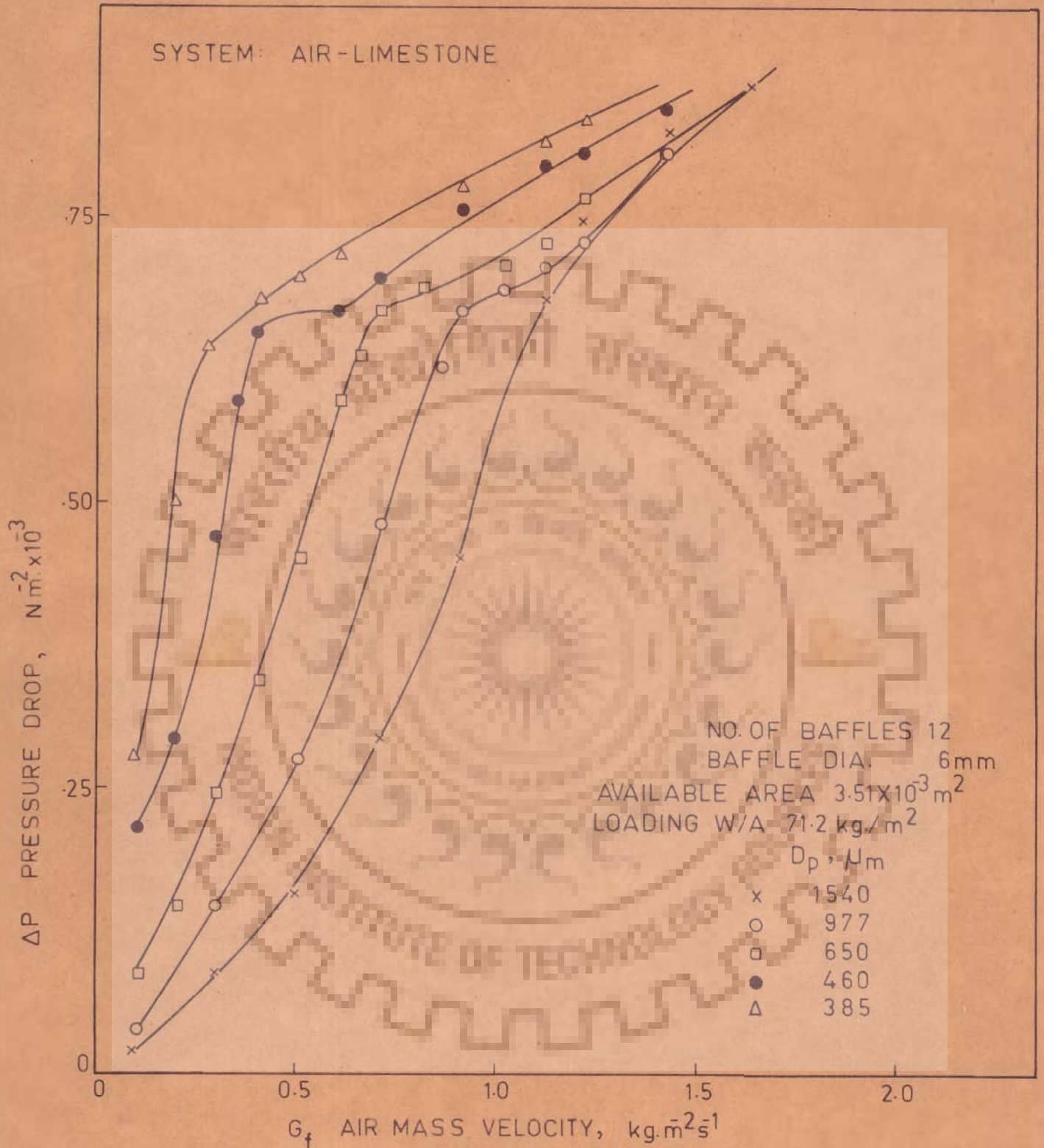


FIG. 3.9 VARIATION OF PRESSURE DROP WITH AIR MASS VELOCITY IN BATCH FLUIDIZED BED WITH VERTICAL BAFFLES.

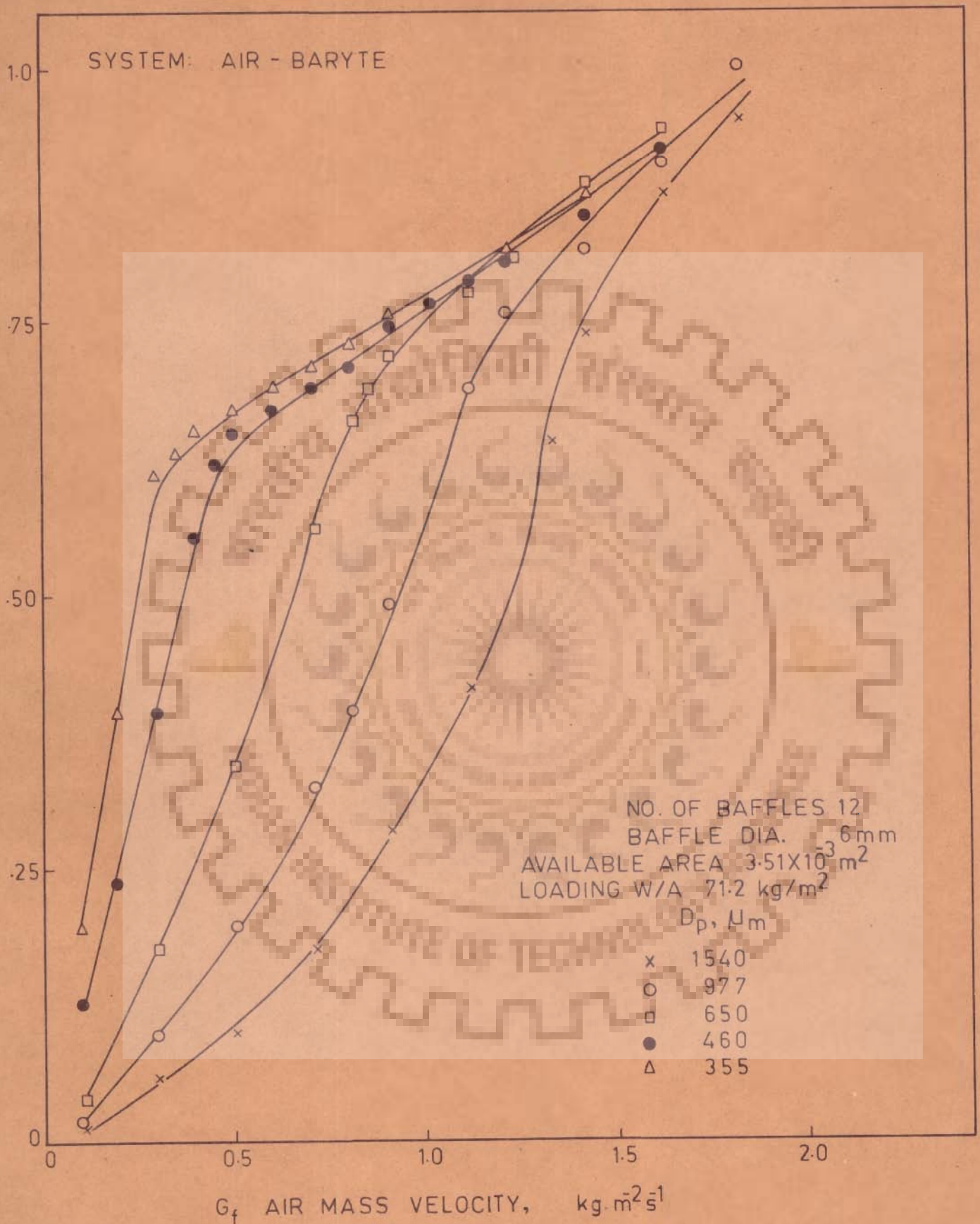


FIG. 3.10 VARIATION OF PRESSURE DROP WITH AIR MASS VELOCITY IN BATCH FLUIDIZED BED WITH VERTICAL BAFFLES.

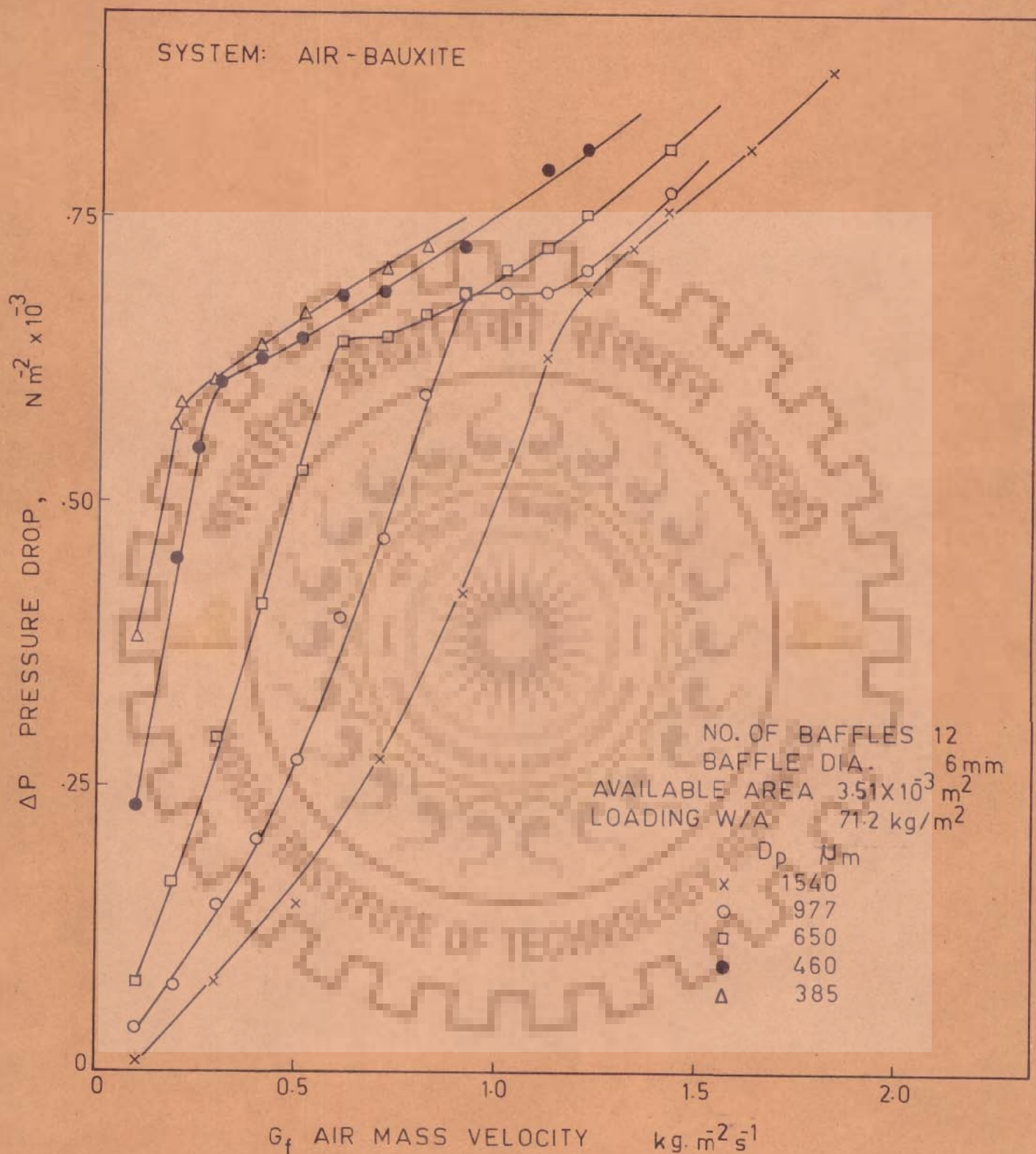


FIG. 3.11 VARIATION OF PRESSURE DROP WITH AIR MASS VELOCITY IN BATCH FLUIDIZED BED WITH VERTICAL BAFFLES.

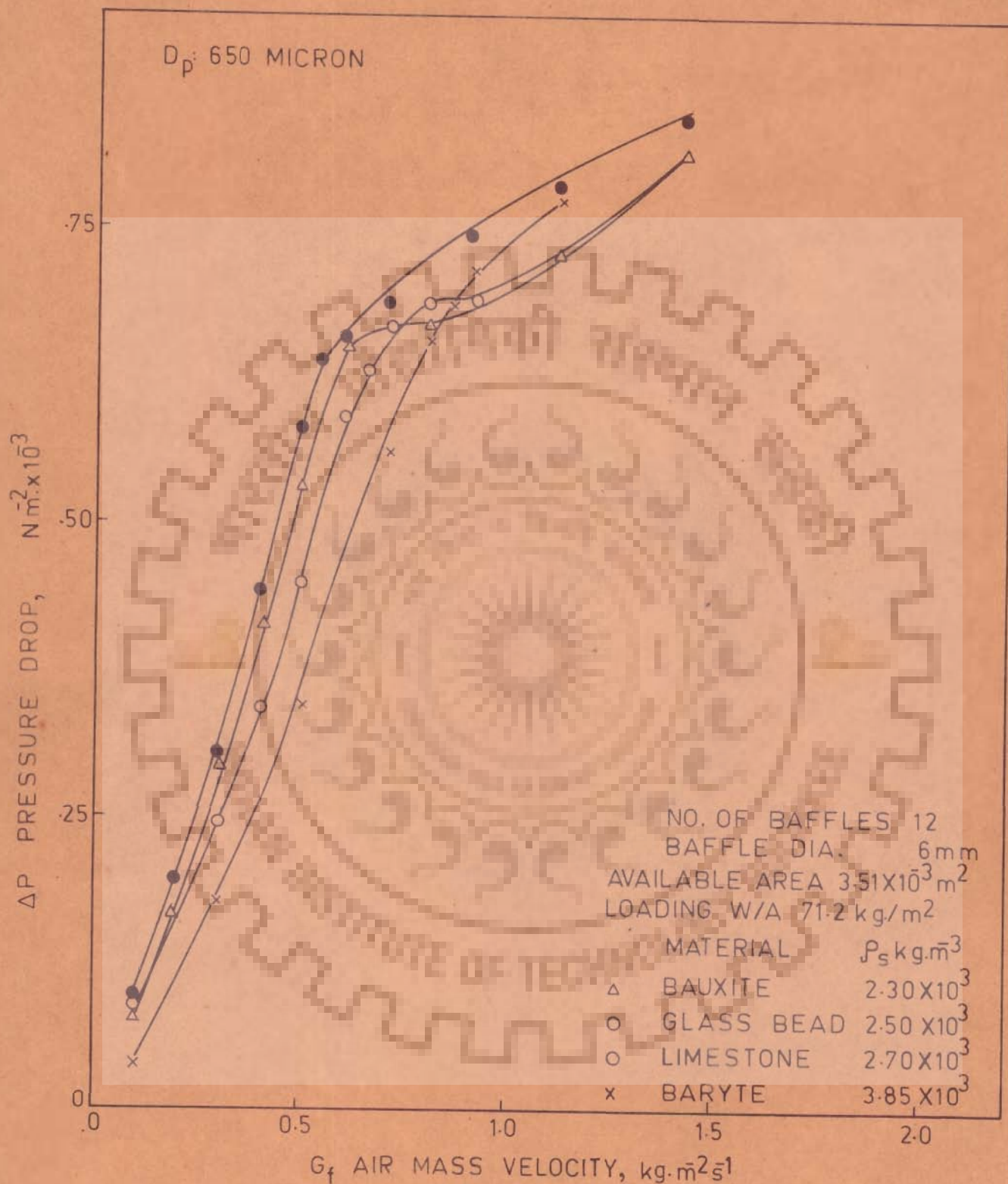


FIG. 3.12 VARIATION OF PRESSURE DROP WITH AIR MASS VELOCITY IN BATCH FLUIDIZED BED WITH VERTICAL BAFFLES.

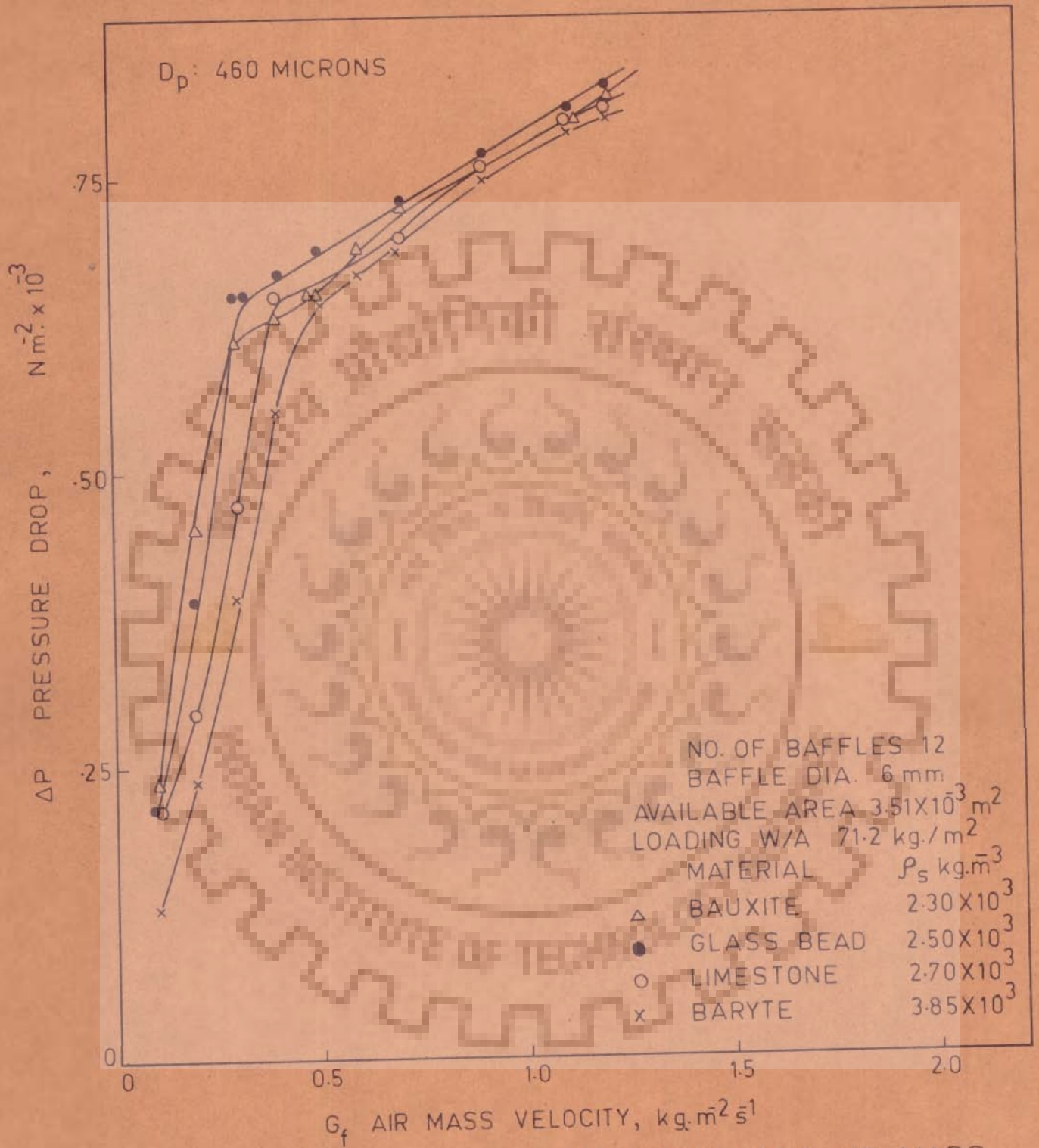


FIG.3.13 VARIATION OF PRESSURE DROP WITH AIR MASS VELOCITY IN BATCH FLUIDIZED BED WITH VERTICAL BAFFLES.

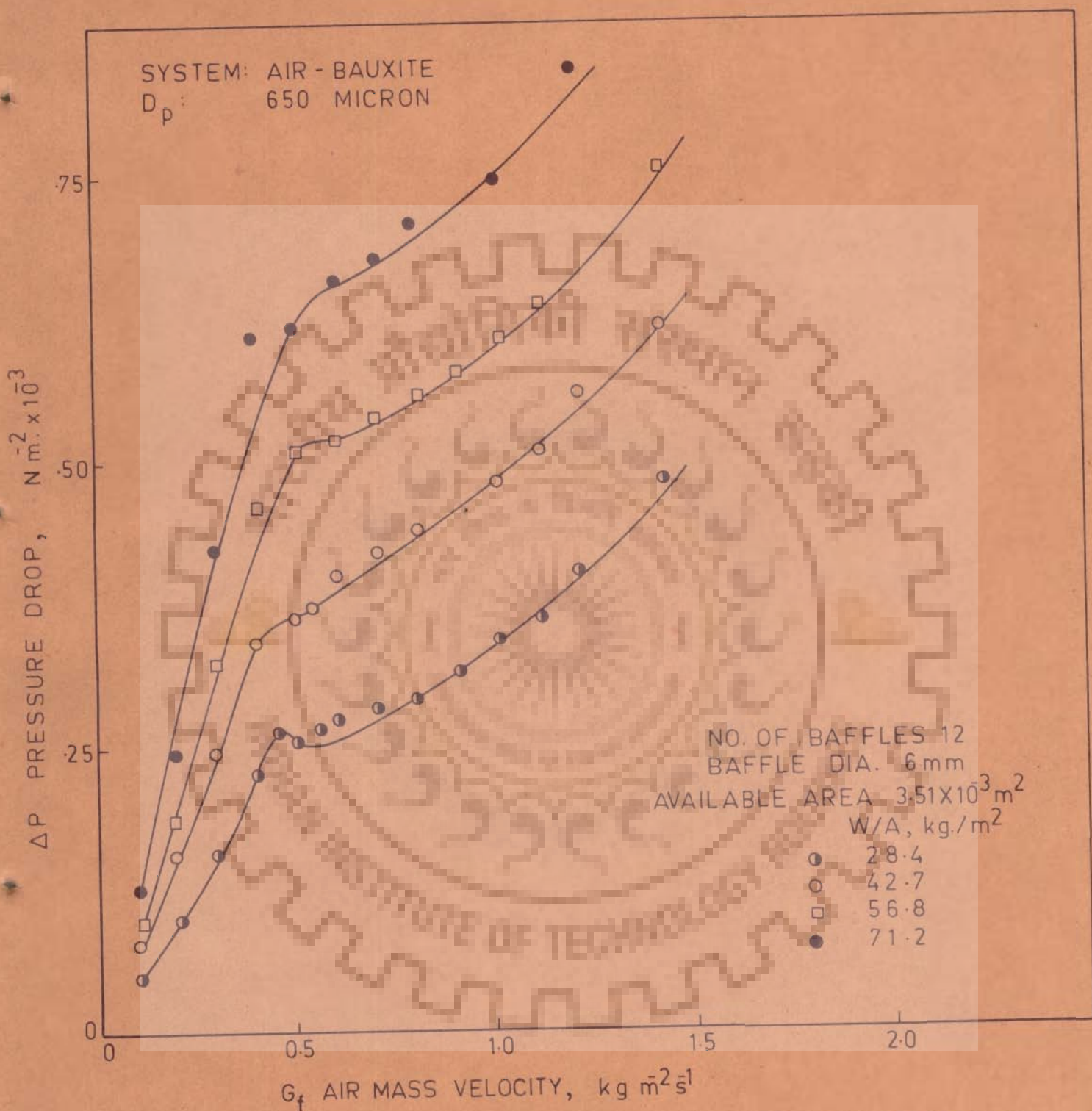


FIG.3.14 VARIATION OF PRESSURE DROP WITH AIR MASS VELOCITY IN BATCH FLUIDIZED BED WITH VERTICAL BAFFLES.

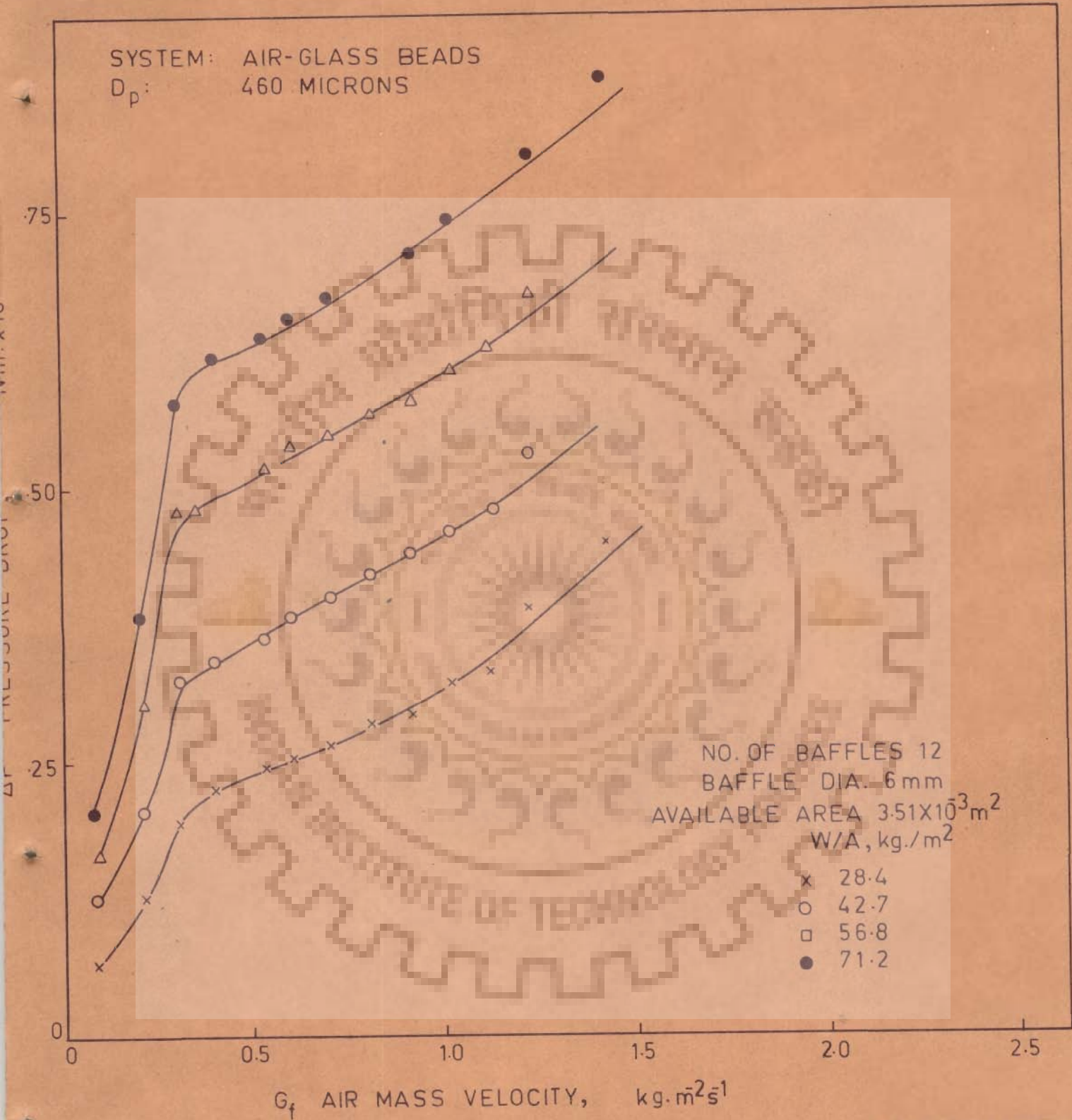


FIG. 3.15 VARIATION OF PRESSURE DROP WITH AIR MASS VELOCITY IN BATCH FLUIDIZED BED WITH VERTICAL BAFFLES.

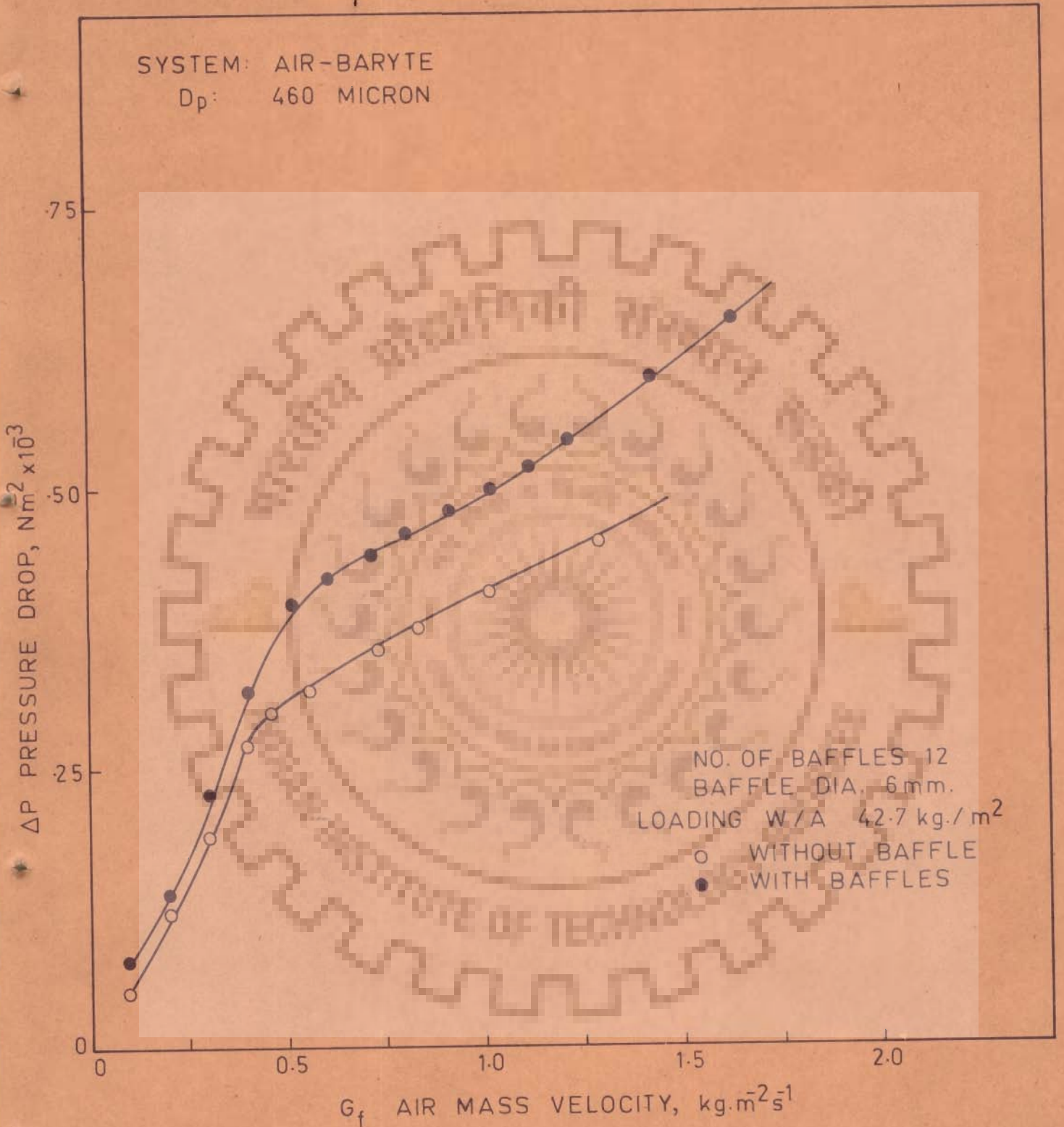


FIG. 3.16 VARIATION OF PRESSURE DROP WITH AIR MASS VELOCITY IN BATCH FLUIDIZED BEDS WITH AND WITHOUT BAFFLES.

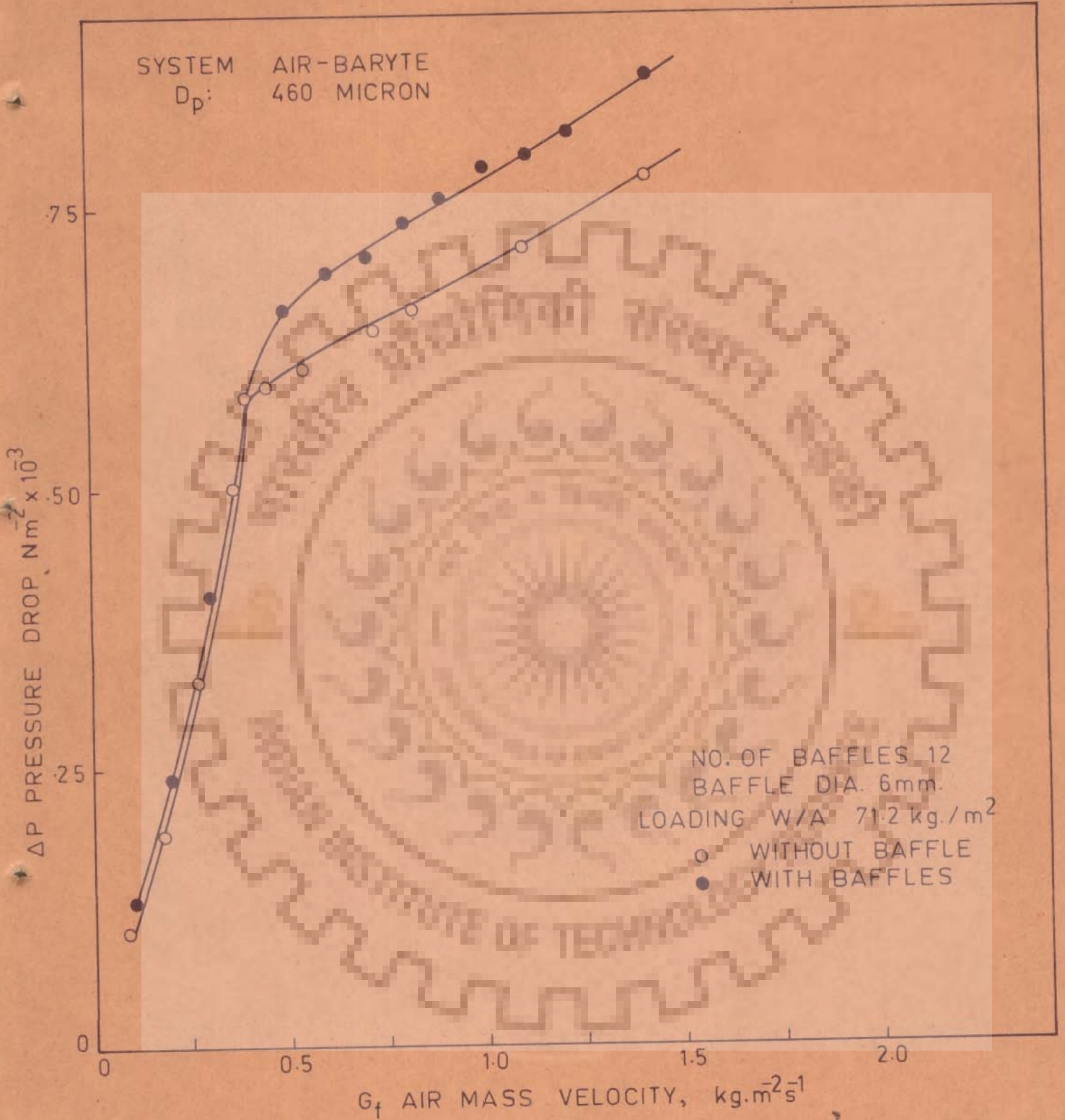


FIG 3.17 VARIATION OF PRESSURE DROP WITH AIR MASS VELOCITY IN BATCH FLUIDIZED BEDS WITH AND WITHOUT BAFFLES.

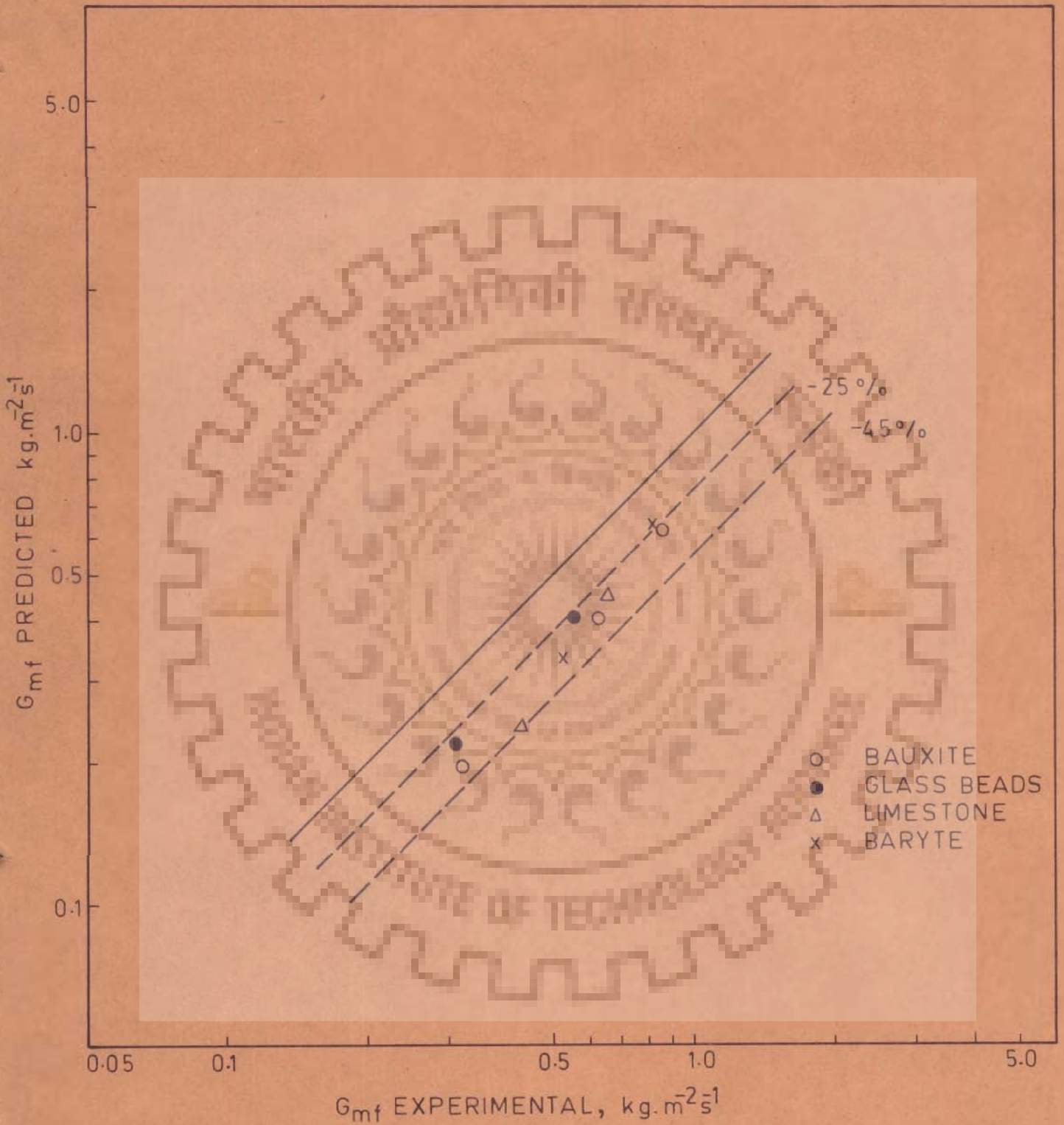


FIG. 3.18 COMPARISON OF VALUES OF MINIMUM FLUIDIZING VELOCITY OBSERVED IN BAFFLED BEDS AND PREDICTED USING LEVA'S CORRELATION.

SYSTEM: AIR + BAUXITE

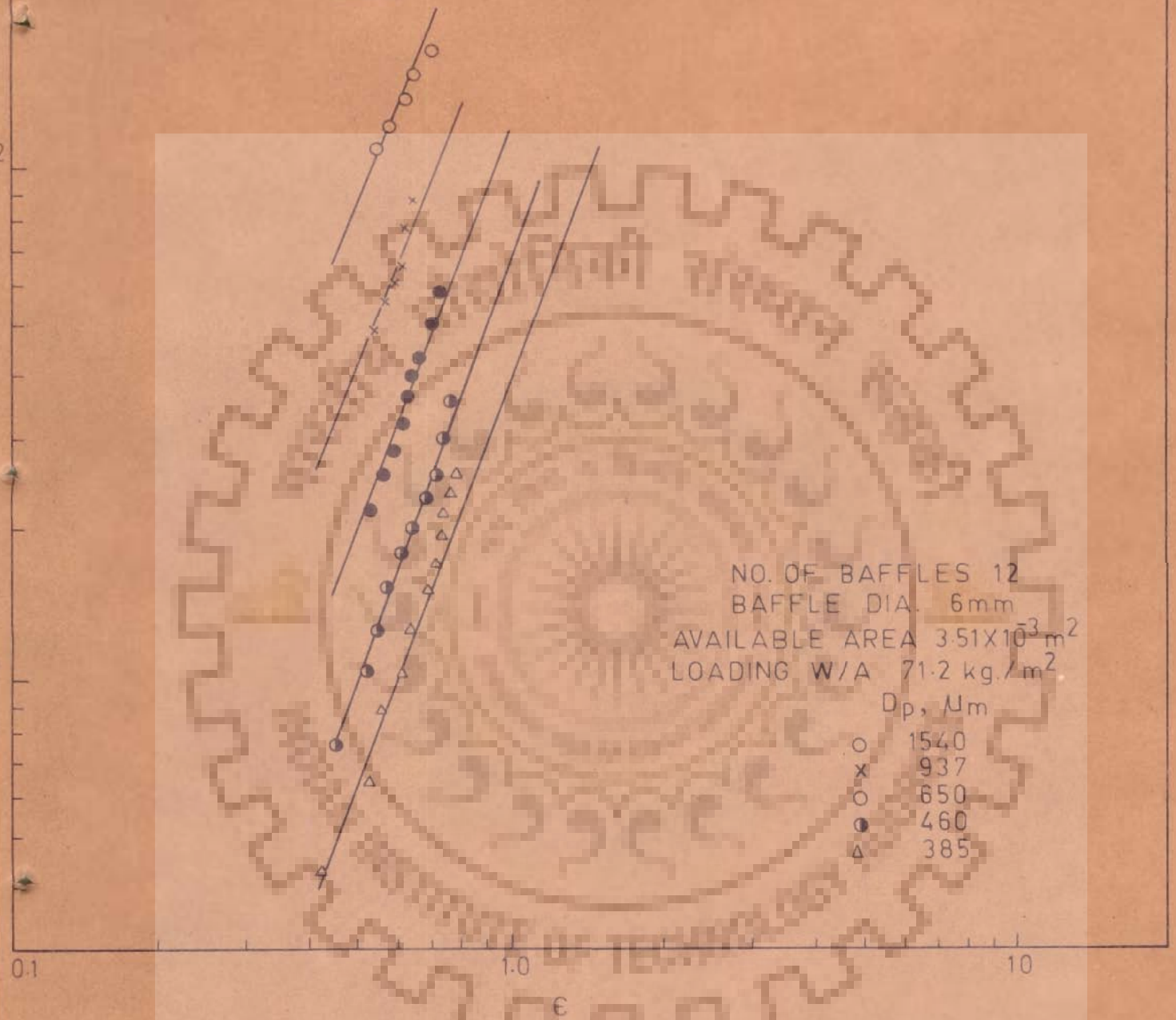


FIG. 3.19. VARIATION OF BED POROSITY WITH PARTICLE REYNOLDS NUMBER IN BATCH FLUIDIZED BED WITH VERTICAL BAFFLES.

SYSTEM: AIR - LIMESTONE

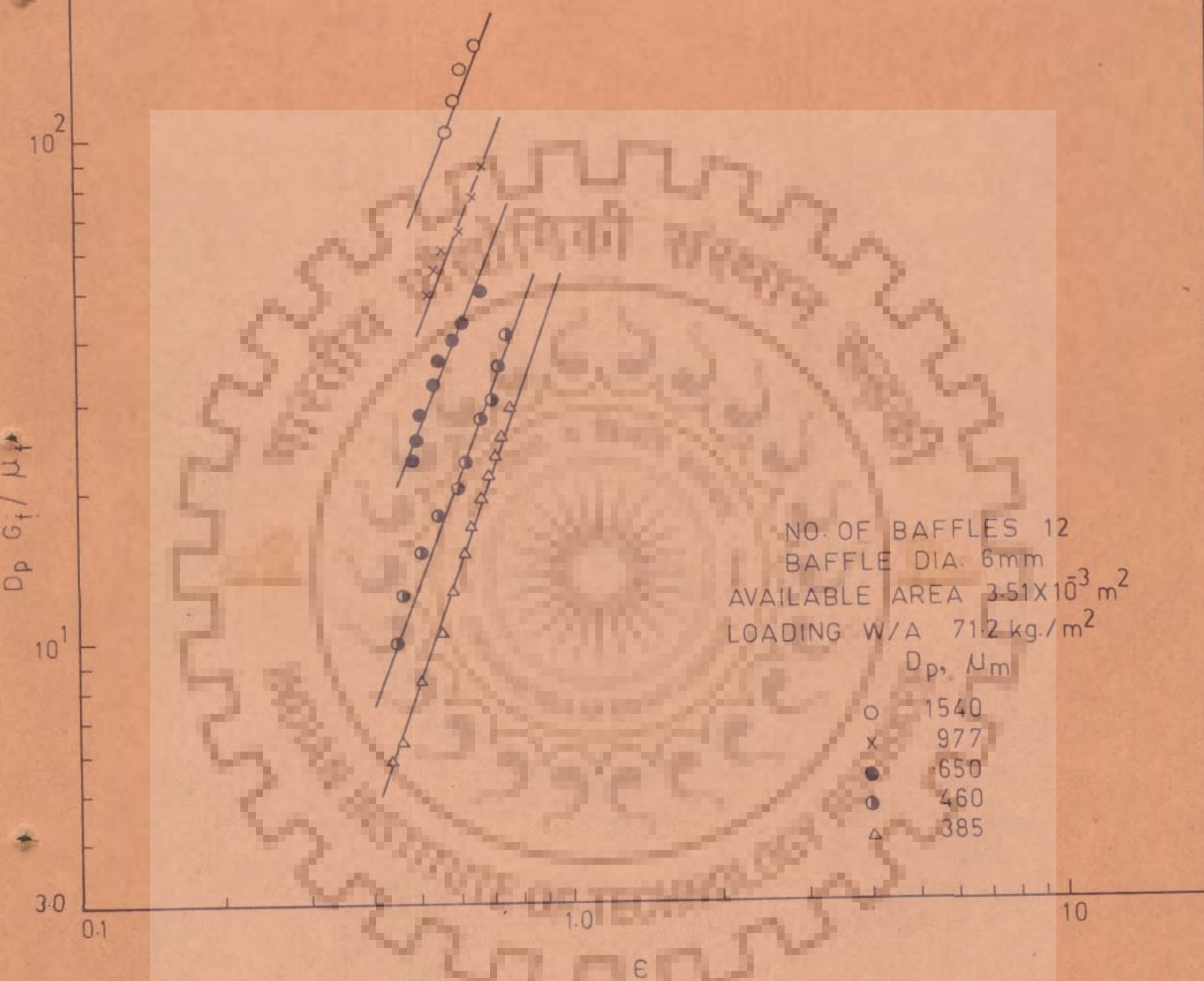


FIG. 3-20 VARIATION OF BED POROSITY WITH PARTICLE REYNOLDS NUMBER IN BATCH FLUIDIZED BED WITH VERTICAL BAFFLE

SYSTEM: AIR-BARYTE

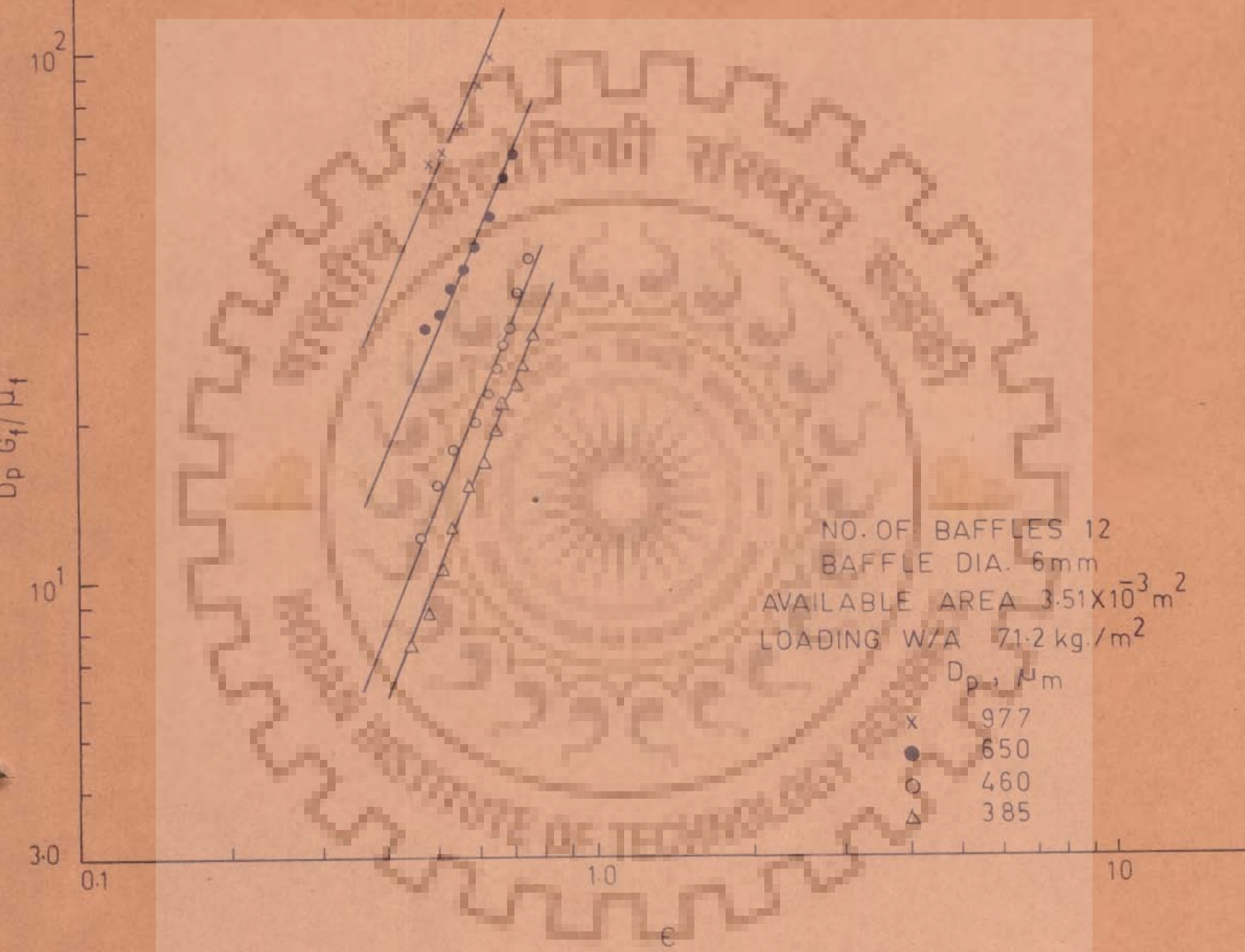


FIG. 3-21 VARIATION OF BED POROSITY WITH PARTICLE REYNOLDS NUMBER IN BATCH FLUIDIZED BED WITH VERTICAL BAFFLE

SYSTEM: AIR - GLASS BEADS

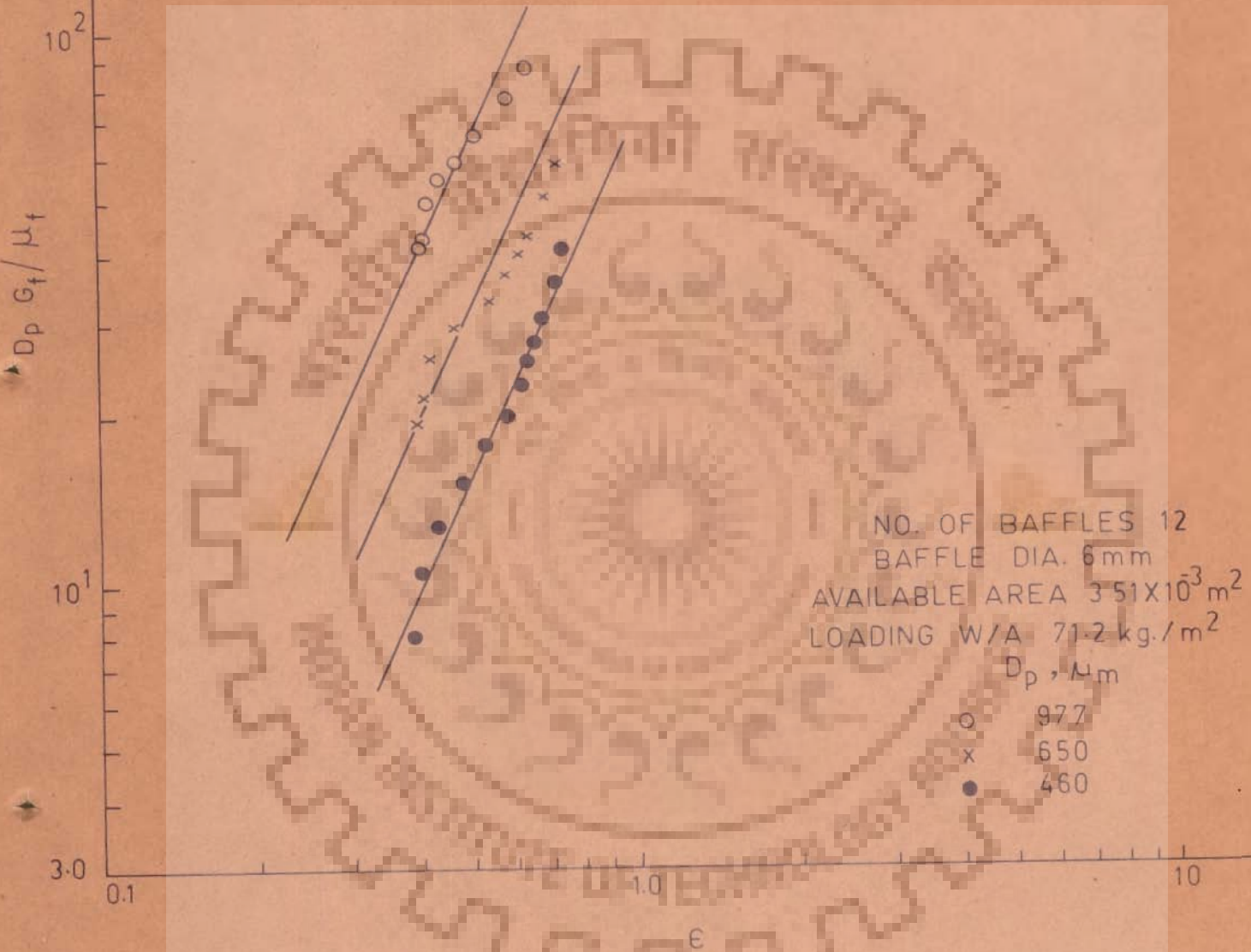


FIG. 3-22 VARIATION OF BED POROSITY WITH PARTICLE REYNOLDS NUMBER IN BATCH FLUIDIZED BED WITH VERTICAL BAFFLES

SYSTEM: AIR-GLASS BEADS
 D_p : 460 MICRONS

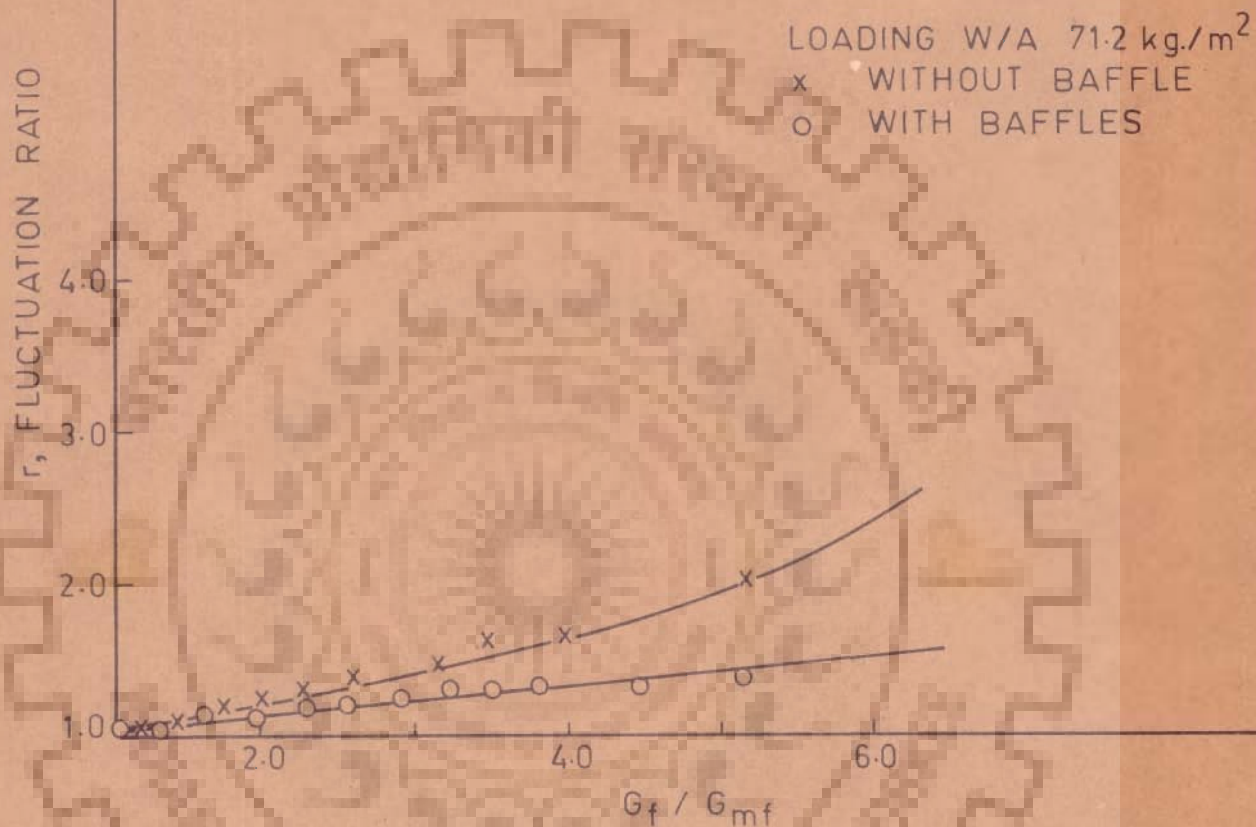


FIG. 3-23 FLUCTUATION RATIO V/S REDUCED AIR MASS VELOCITY IN BATCH FLUIDIZED BEDS WITH AND WITHOUT BAFFLES.

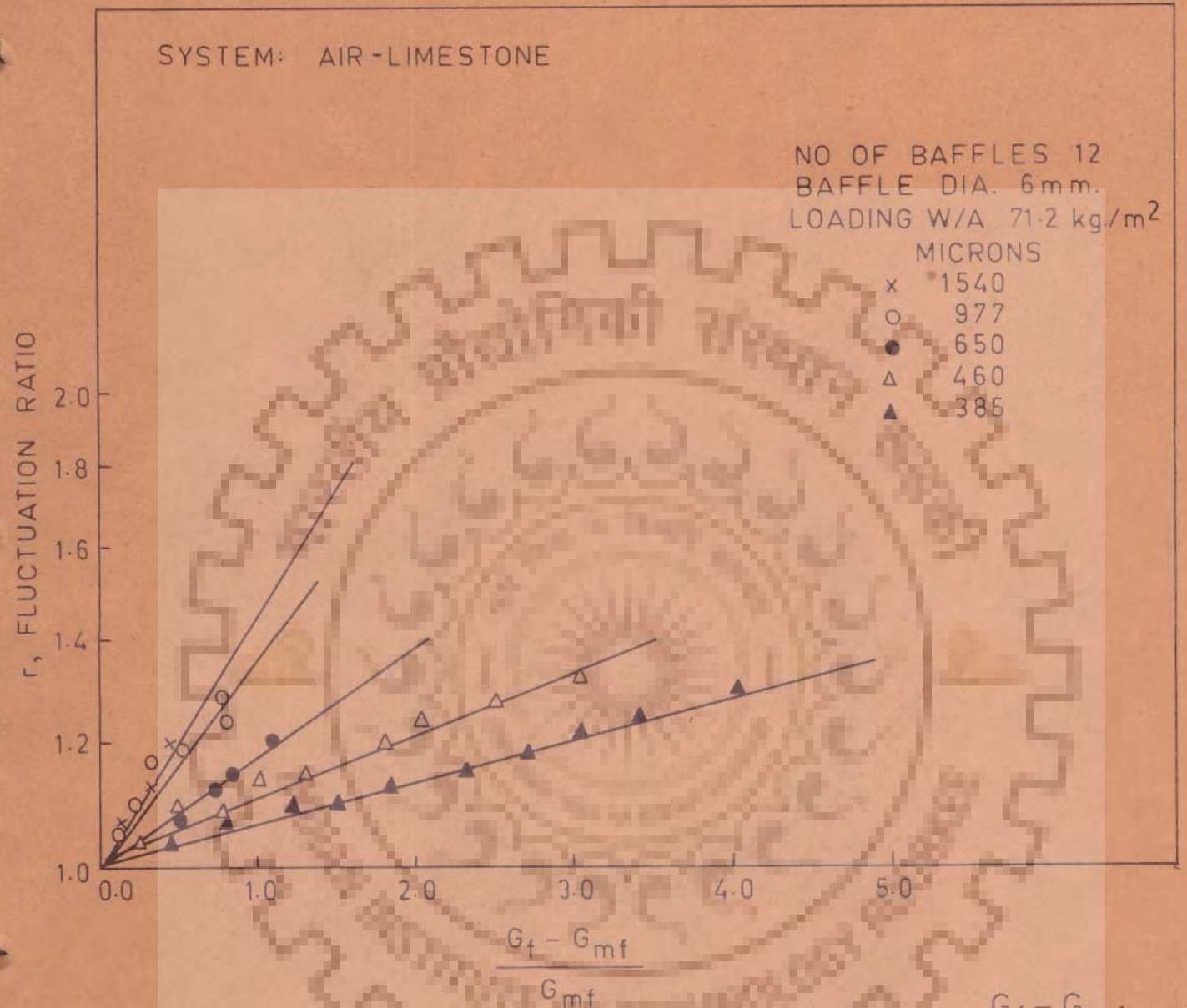


FIG. 3.24 FLUCTUATION RATIO IN RELATION WITH $\frac{G_f - G_{mf}}{G_{mf}}$ IN BATCH FLUIDIZED BED WITH VERTICAL BAFFLES.

SYSTEM: AIR-GLASS BEADS

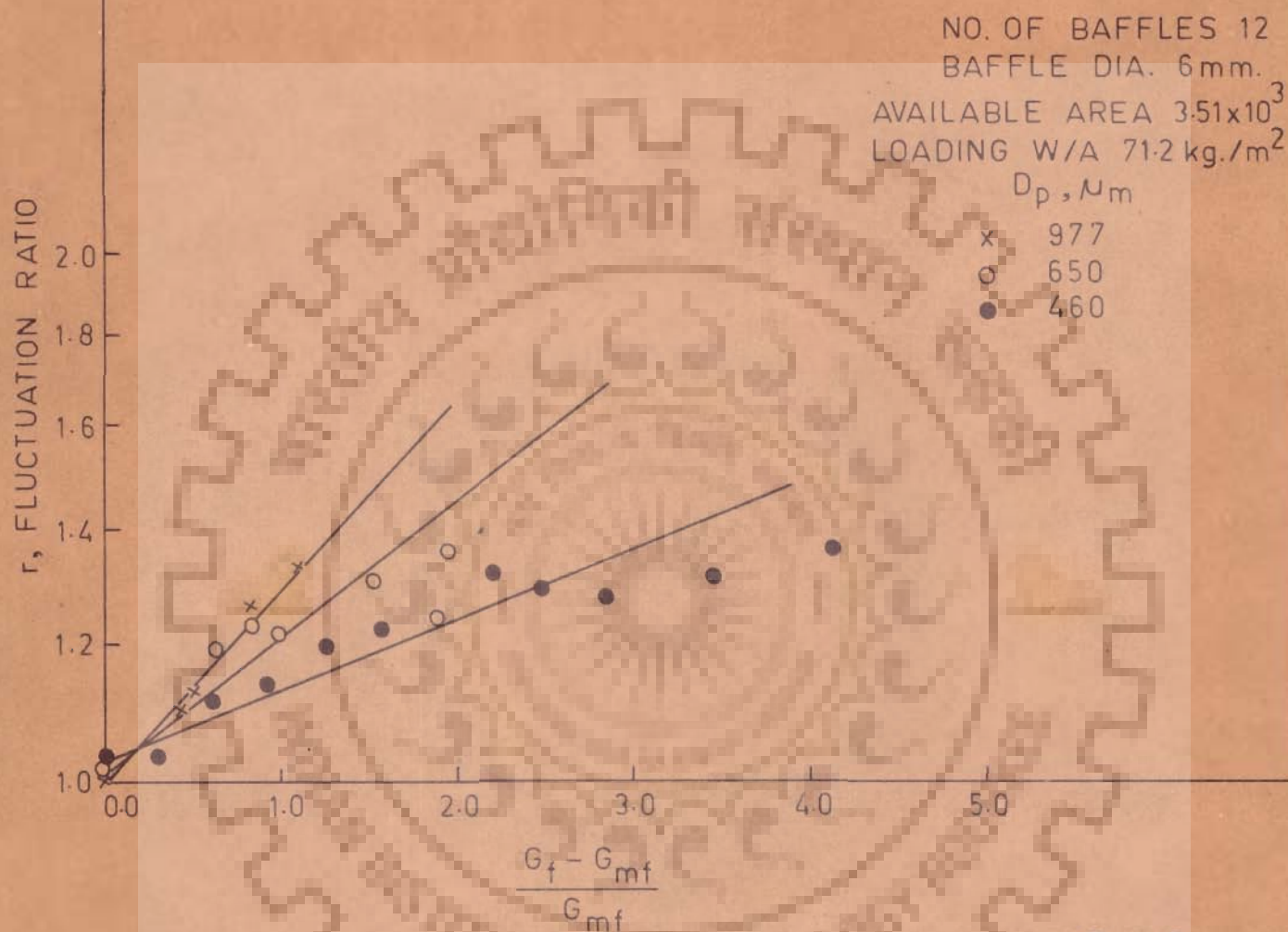


FIG. 3.25 FLUCTUATION RATIO IN RELATION WITH $\frac{G_f - G_{mf}}{G_{mf}}$ IN BATCH FLUIDIZED BED WITH VERTICAL BAFFLES.

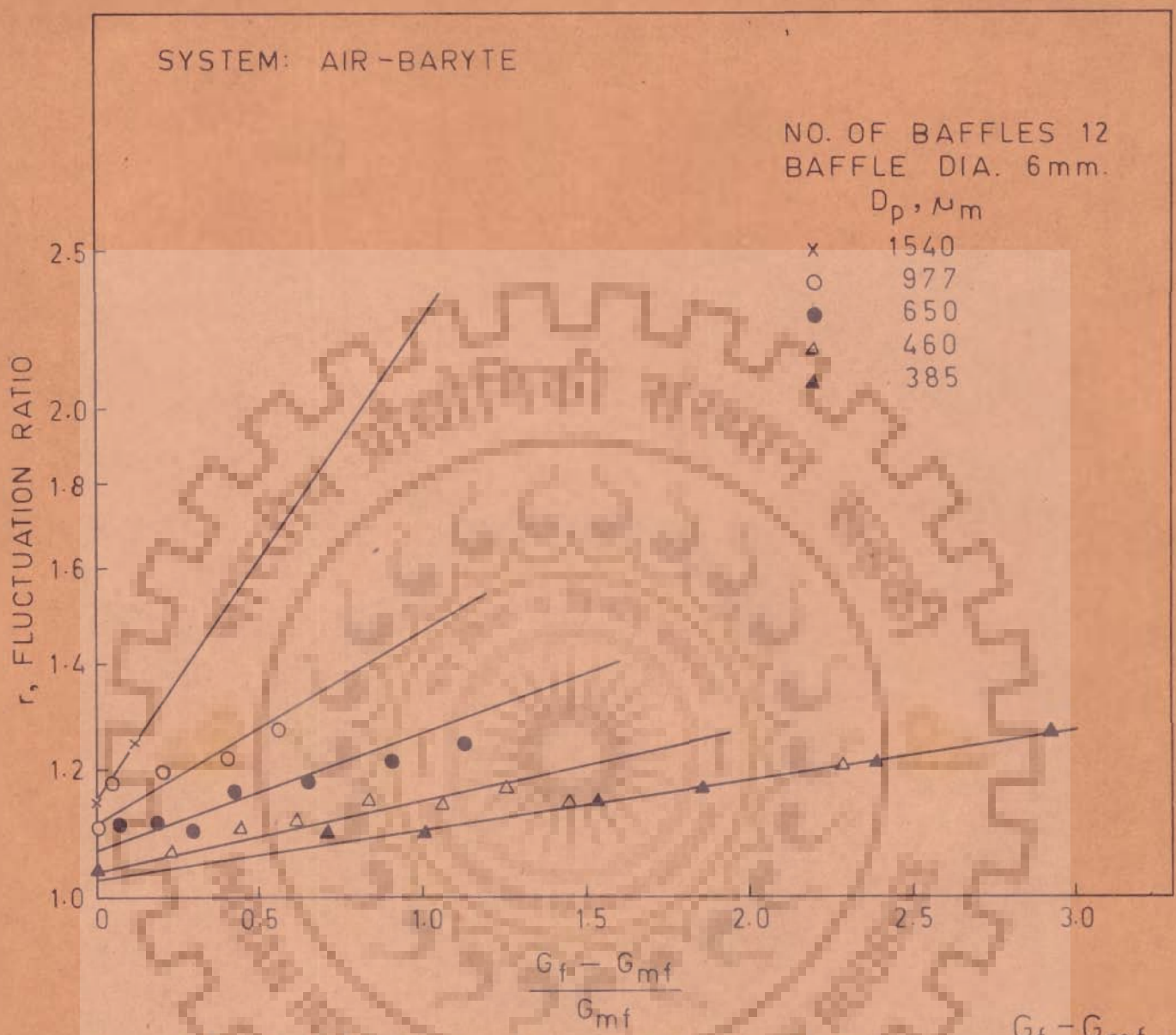


FIG. 3.26 FLUCTUATION RATIO IN RELATION WITH $\frac{G_f - G_{mf}}{G_{mf}}$ IN BATCH-FLUIDIZED BED WITH VERTICAL BAFFLES.

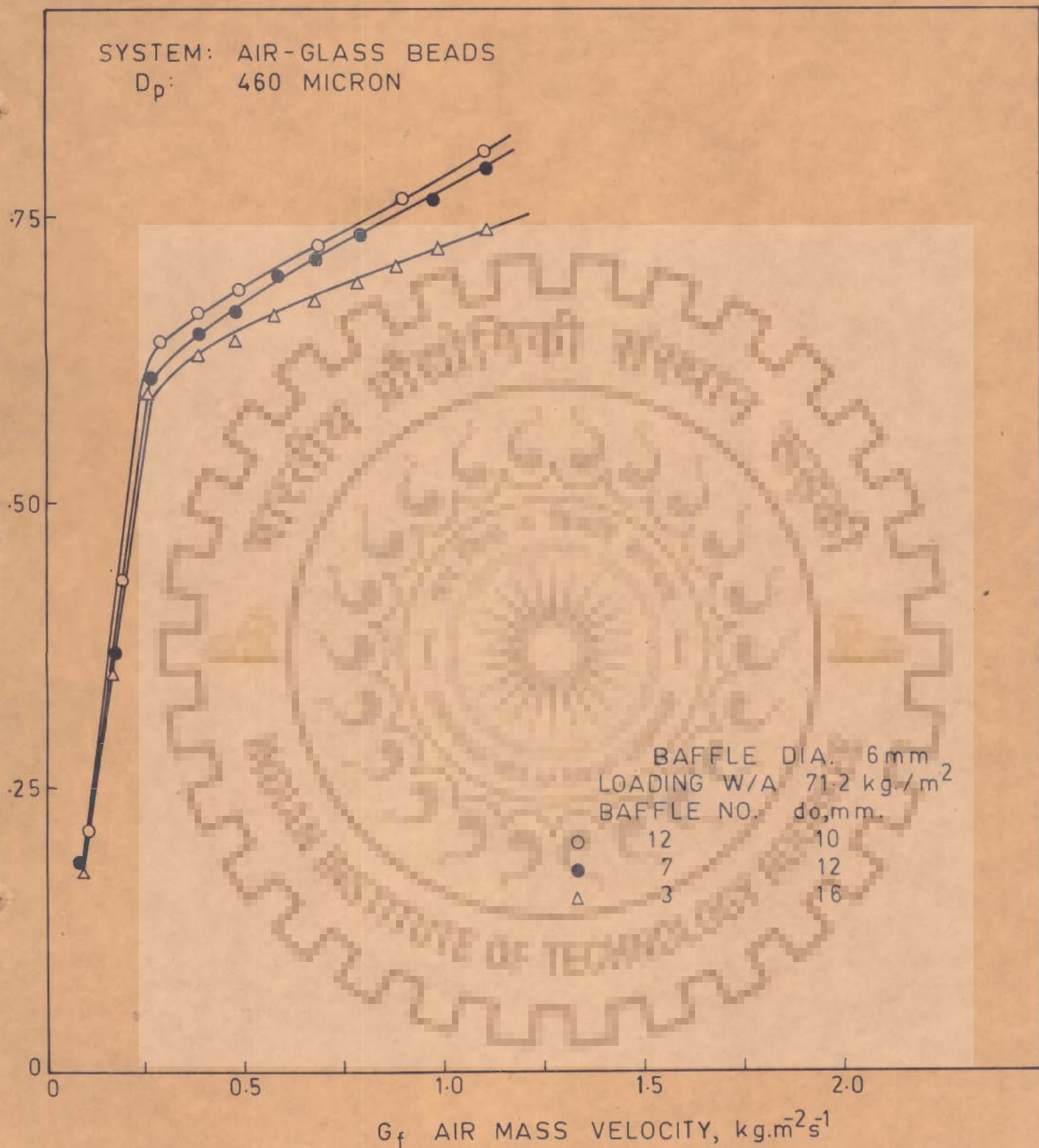


FIG. 3.27 VARIATION OF PRESSURE DROP WITH AIR MASS VELOCITY IN BATCH FLUIDIZED BED WITH VERTICAL BAFFLES.

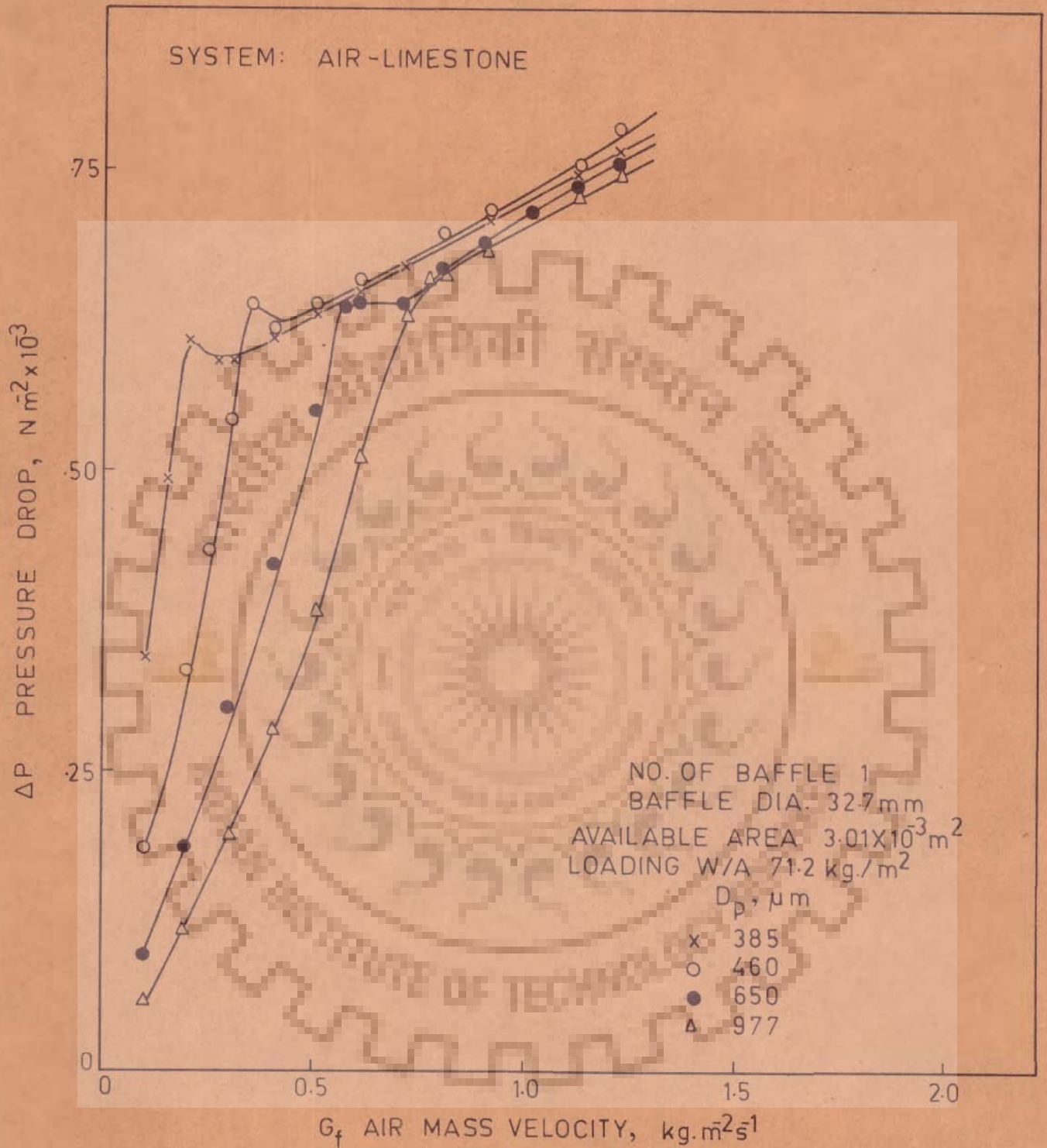


FIG. 3.28 VARIATION OF PRESSURE DROP WITH AIR MASS VELOCITY IN BATCH FLUIDIZED BED WITH SINGLE BAFFLE.

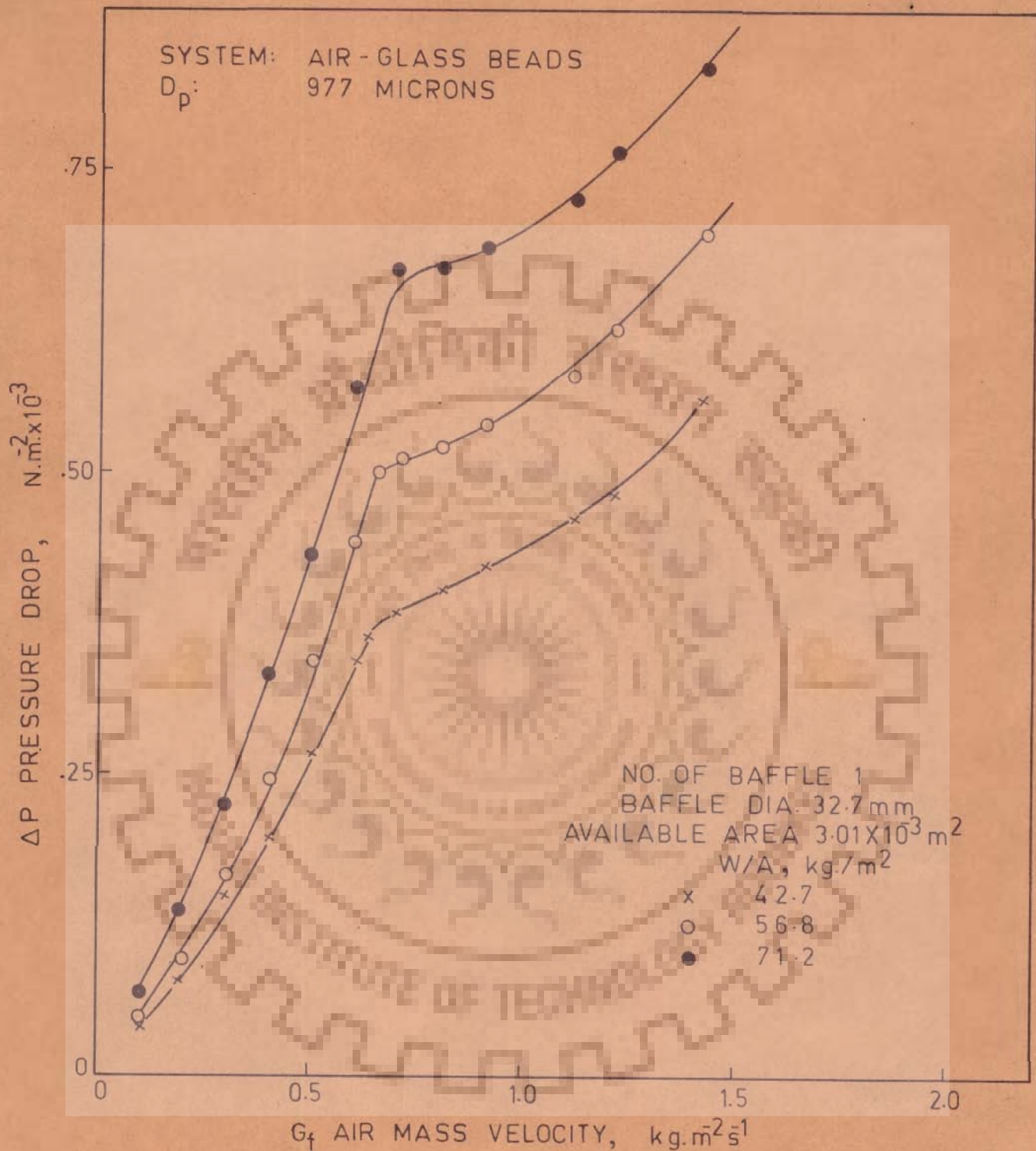


FIG. 3-29 VARIATION OF PRESSURE DROP WITH AIR MASS VELOCITY IN BATCH FLUIDIZED BED WITH SINGLE BAFFLE.

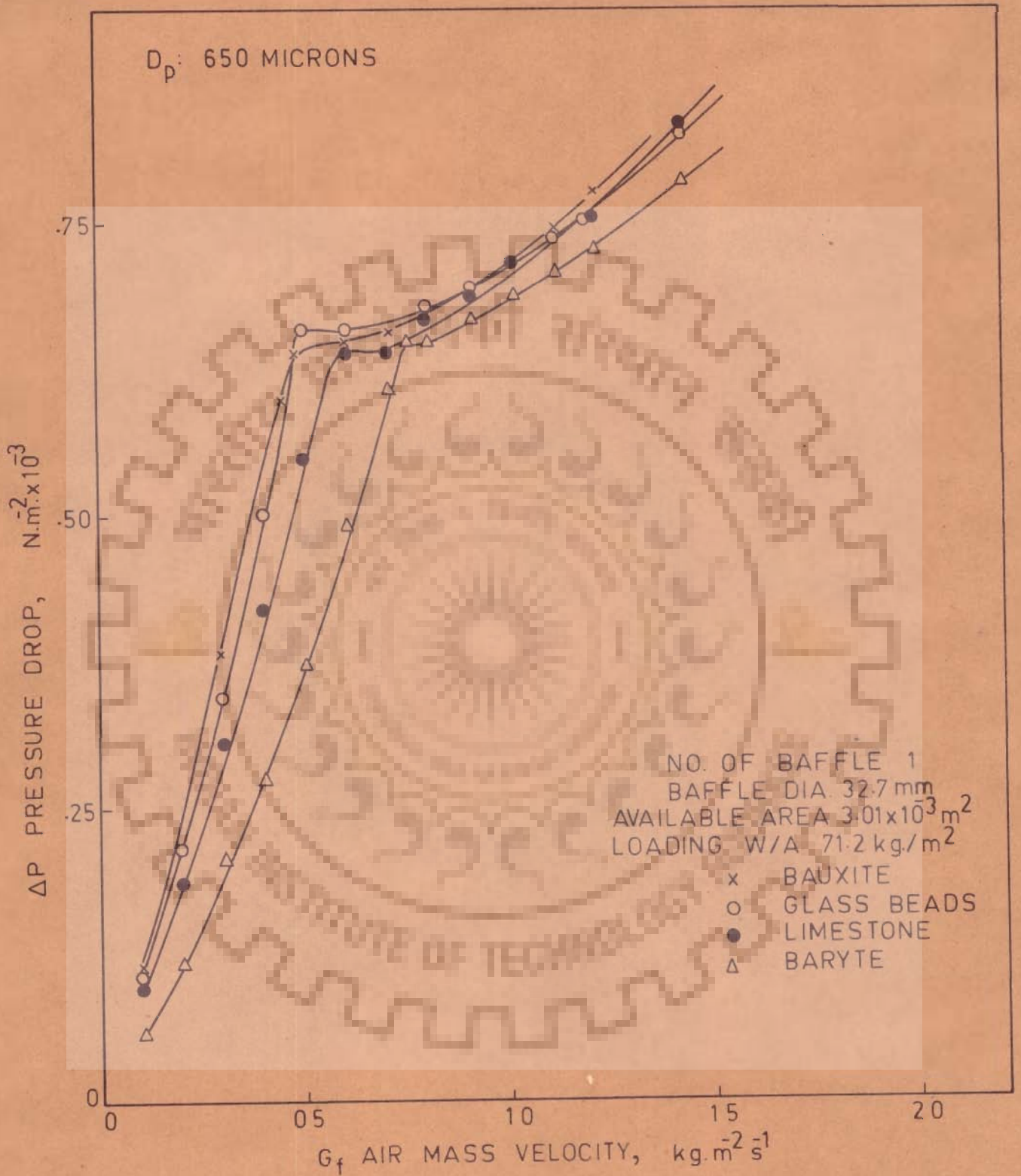


FIG.3.30 VARIATION OF PRESSURE DROP WITH AIR MASS VELOCITY IN BATCH FLUIDIZED BED WITH SINGLE BAFFLE.

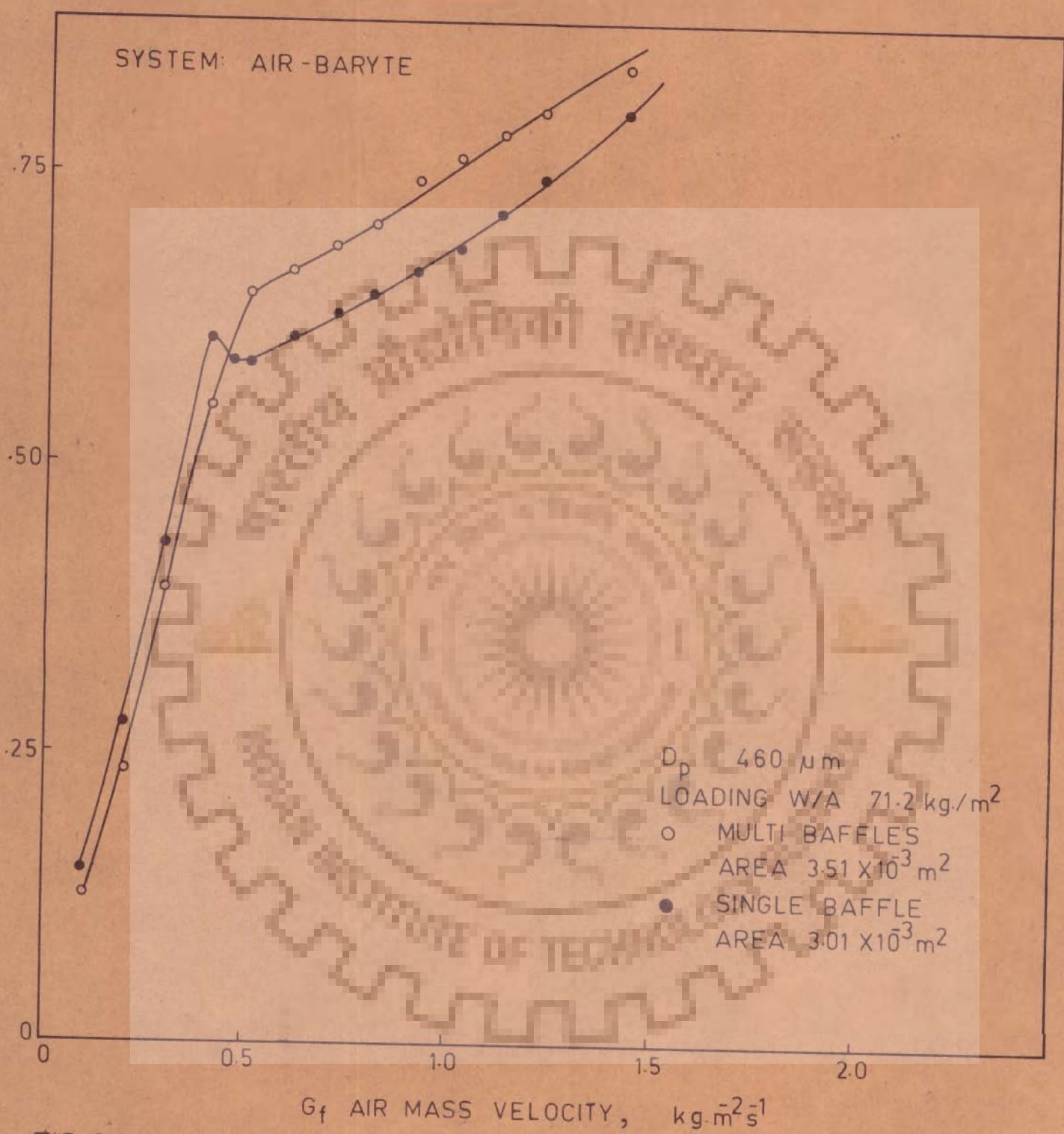


FIG. 3.31 VARIATION OF PRESSURE DROP WITH AIR MASS VELOCITY IN BATCH FLUIDIZED BEDS WITH MULTIBAFFLES AND SINGLE BAFFLES.

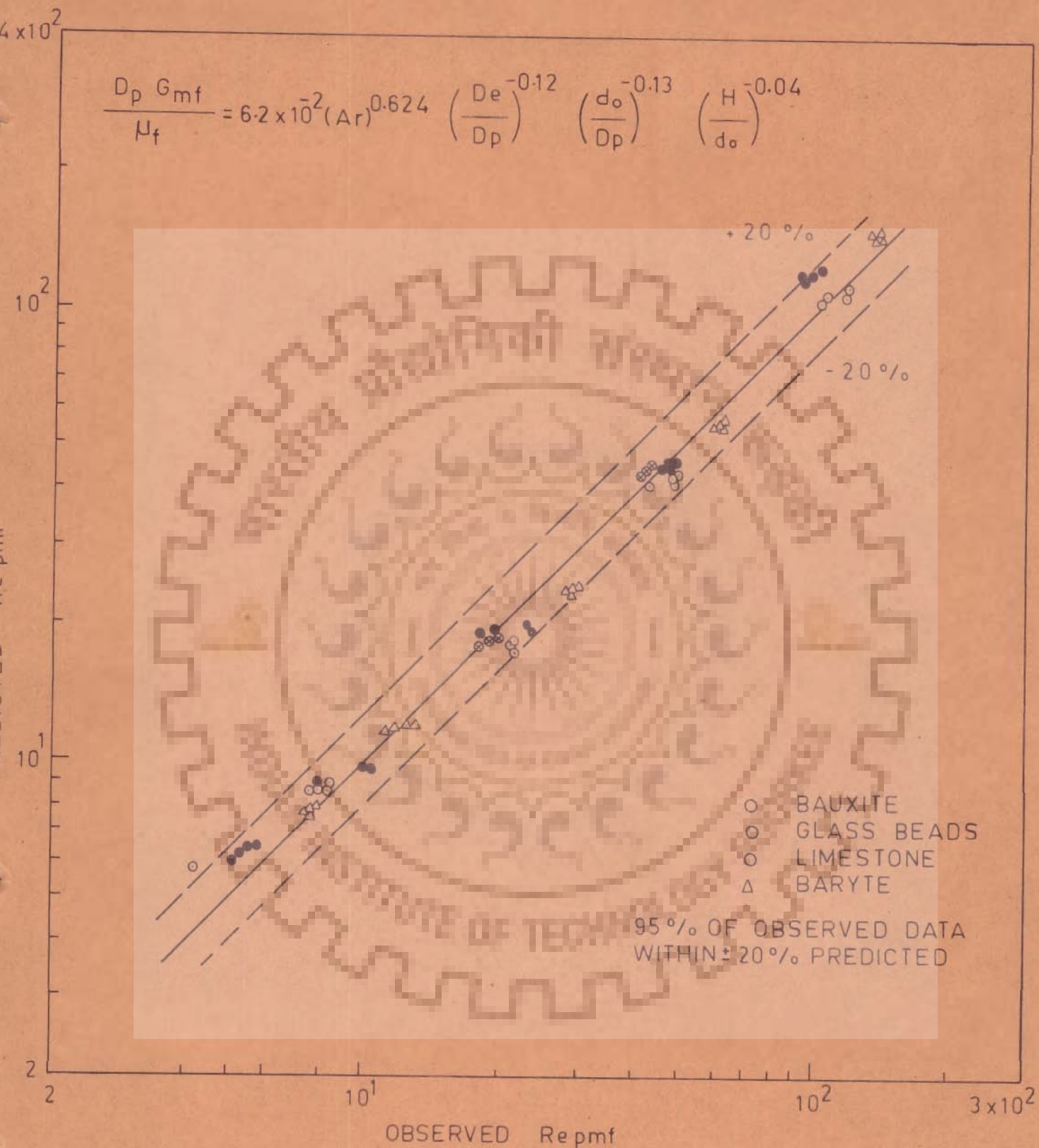


FIG. 3.32 COMPARISON OF OBSERVED AND PREDICTED VALUES OF REYNOLDS NUMBER AT ONSET OF FLUIDIZATION IN BATCH FLUIDIZED BED WITH VERTICAL BAFFLES.

$$\left(\frac{\Delta P \Delta}{W}\right) = 0.923 + K_1 (Re_{eq})^2 + K_2 (Re_T)^2$$

$$K_1 = 3.72 \times 10^{-8}$$

$$K_2 = 3.46 \times 10^{-10}$$

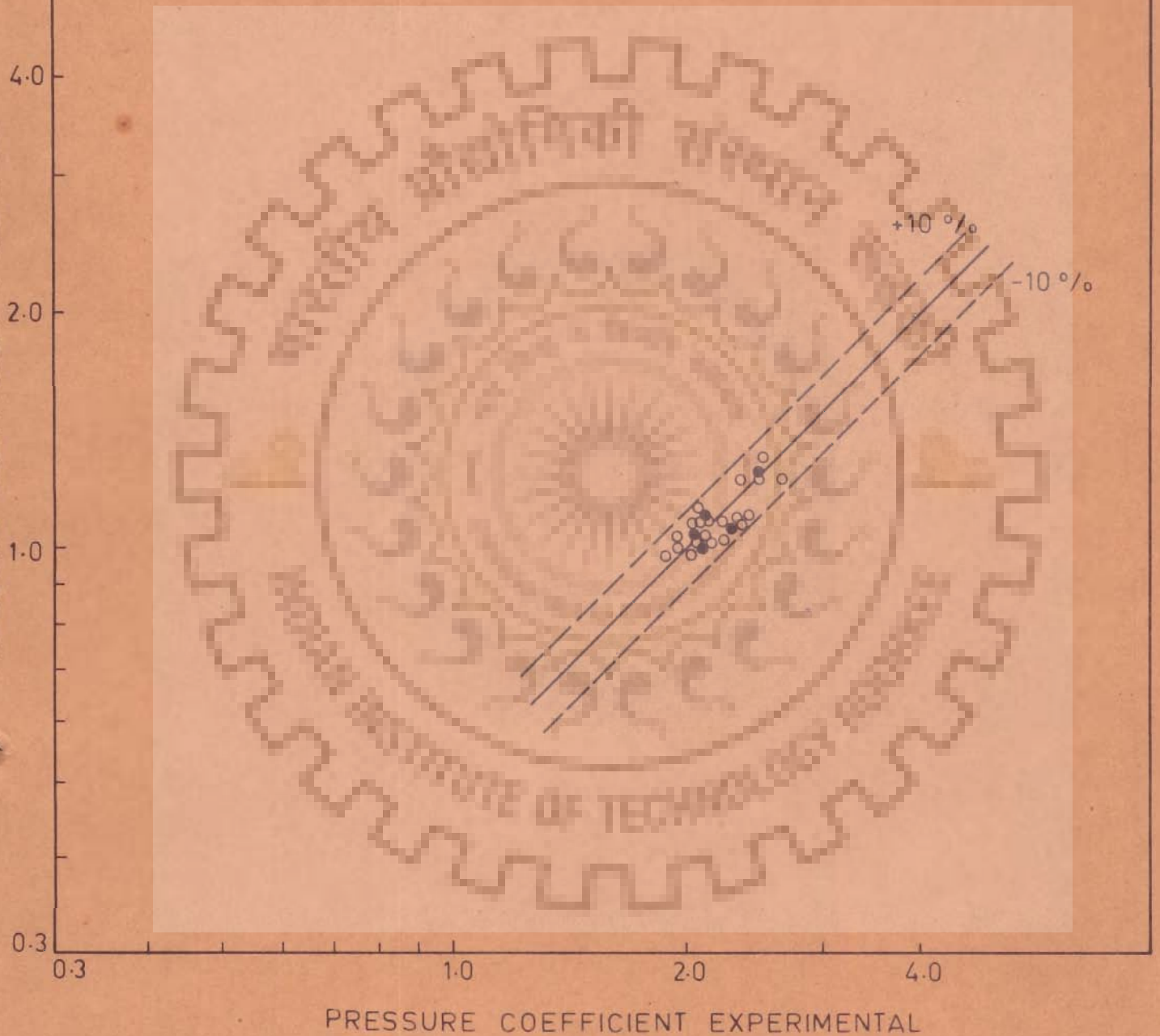


FIG. 3-33 COMPARISON OF EXPERIMENTAL AND PREDICTED VALUES OF PRESSURE COEFFICIENT IN BAFFLED BEDS AT AND BEYOND ONSET OF FLUIDIZATION.

$$\epsilon = 0.065 (Fr)^{-0.22} (Re)^{0.4} \left(\frac{d_o}{D_p}\right)^{0.69} \left(\frac{P_s - P_f}{P_f}\right)^{-0.11}$$

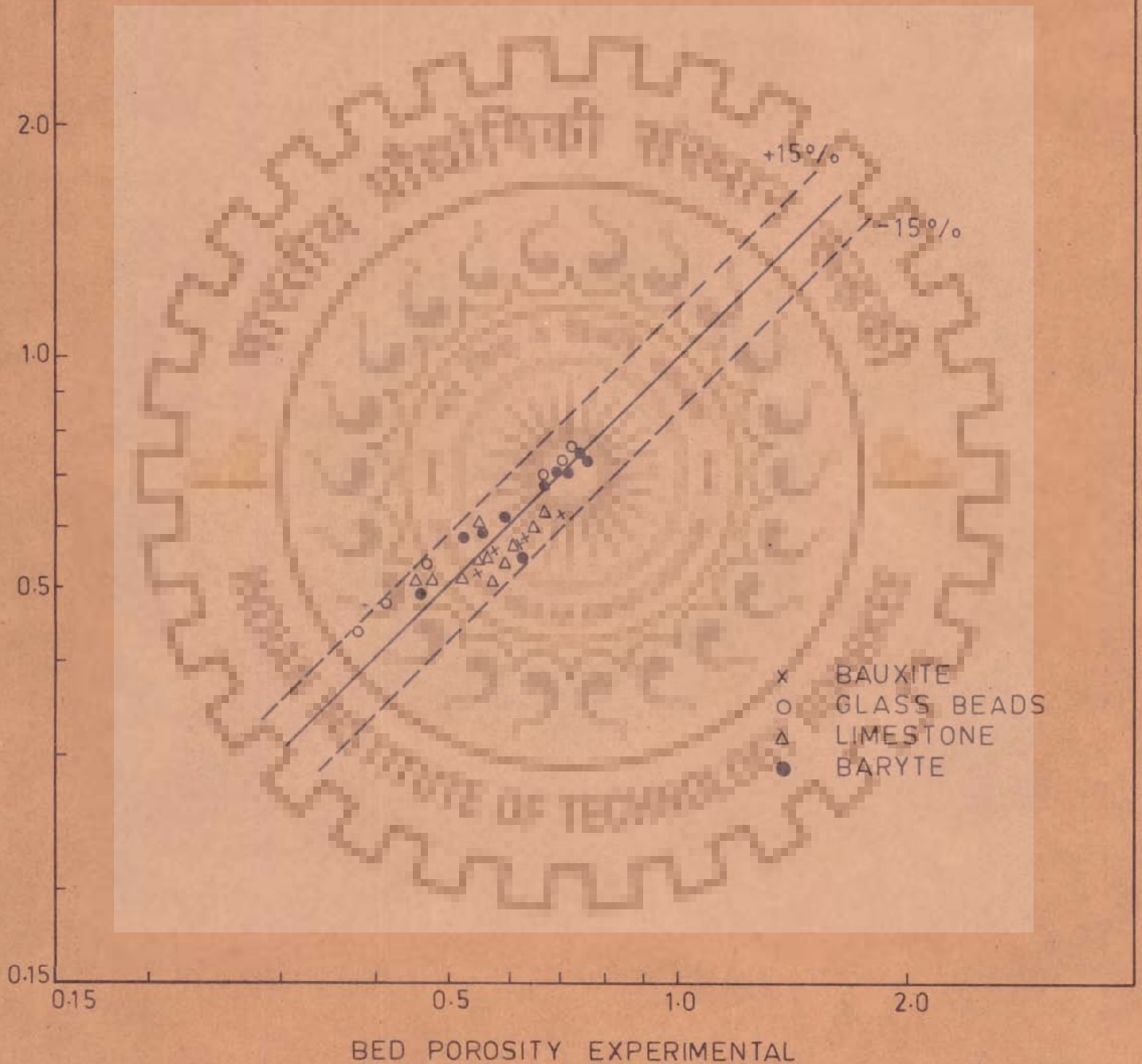


FIG. 3.34 COMPARISON OF EXPERIMENTAL AND PREDICTED VALUES OF BED POROSITY IN BATCH FLUIDIZED BED WITH VERTICAL BAFFLES.



FIG-3.35 SLOPE m AS A FUNCTION OF PARTICLE DIAMETER.

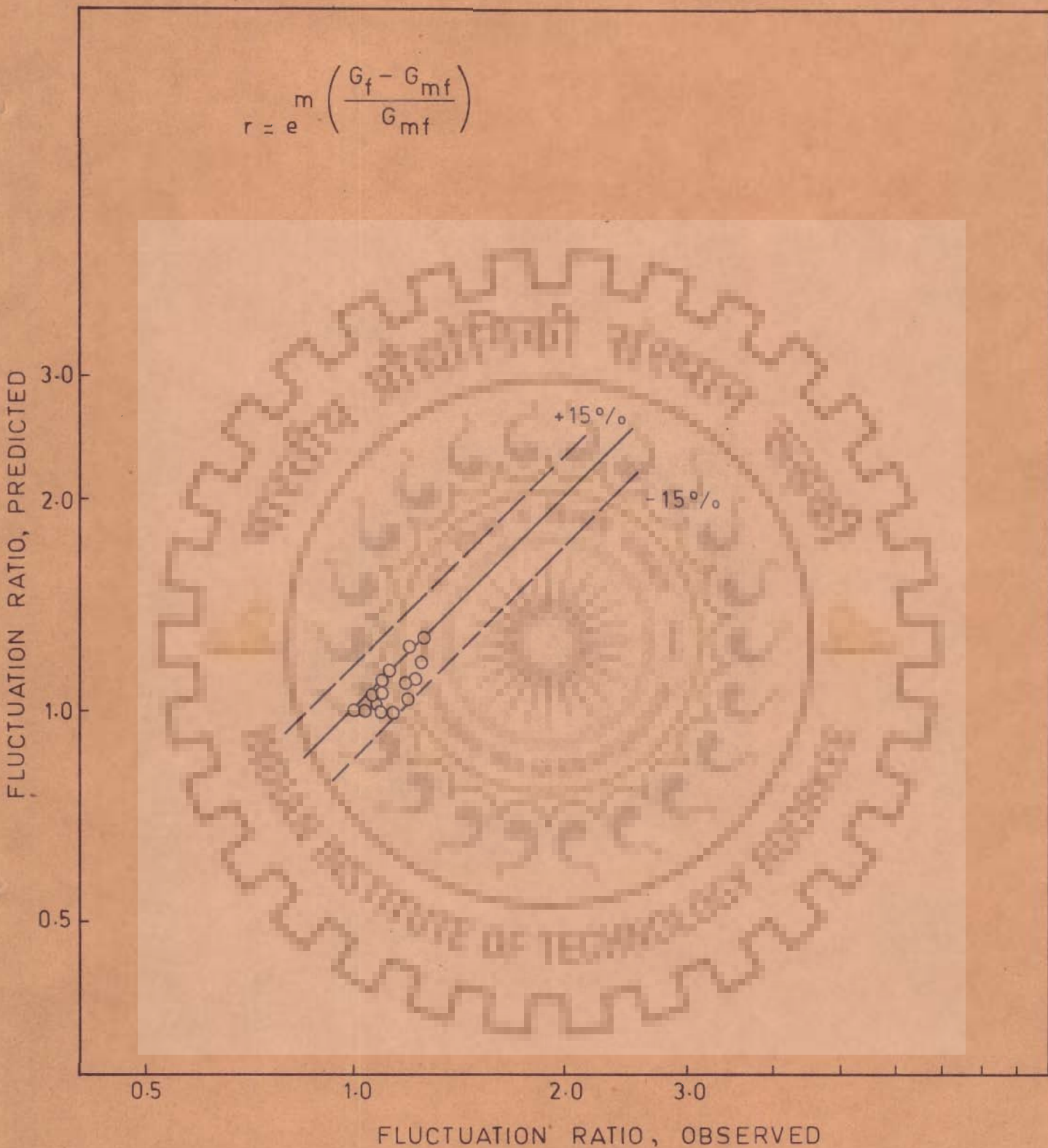


FIG. 3.36 COMPARISON OF VALUES OF FLUCTUATION RATIO OBSERVED AND PREDICTED IN BATCH FLUIDIZED BED WITH VERTICAL BAFFLES.

C H A P T E R - I VA B S T R A C T

Investigations were carried out to study the effect of vertical internal baffles on fluidization characteristic and bed expansion behaviour in continuous fluidized beds. For the same conditions of operation, pressure drop and bed density were observed to be more in continuous fluidized beds with baffles than that in the unbaffled beds. Dimensionless correlations have been proposed for predicting the pressure drop and bed density in continuous fluidized beds with vertical baffles.

C H A P T E R - I VCONTINUOUS FLUIDIZATION WITH VERTICAL BAFFLES

Fluidized beds with vertical internal baffles in continuous gas-solids operations find application in process industries. In the design of continuous fluidized bed units, a knowledge of the flow pattern of solids, pressure drop across the bed and bed densities will be required. The present investigations were conducted with an aim to study the effect of vertical baffles on bed expansion characteristics and bed pressure drop in continuous counter current gas solids fluidization.

4.1 EXPERIMENTAL SET UP

The experimental unit is shown schematically in Fig. 4.1. Air drawn from a compressor (C) was sent to the surge tank (ST). The air from the surge tank filtered through an air filter (AF) was passed through a pressure regulator (PR) which regulated the air pressure before entry to the rotameters (R_1, R_2). Two rotameters were placed in parallel for measuring the entire range of air flow during the experiments. The column used for fluidization experiments consisted essentially of a perspex column (K) of 70 mm ID and 610 mm length inserted between two special flanges. (F_1, F_2). The column was provided with internal baffles (IB) which consisted of

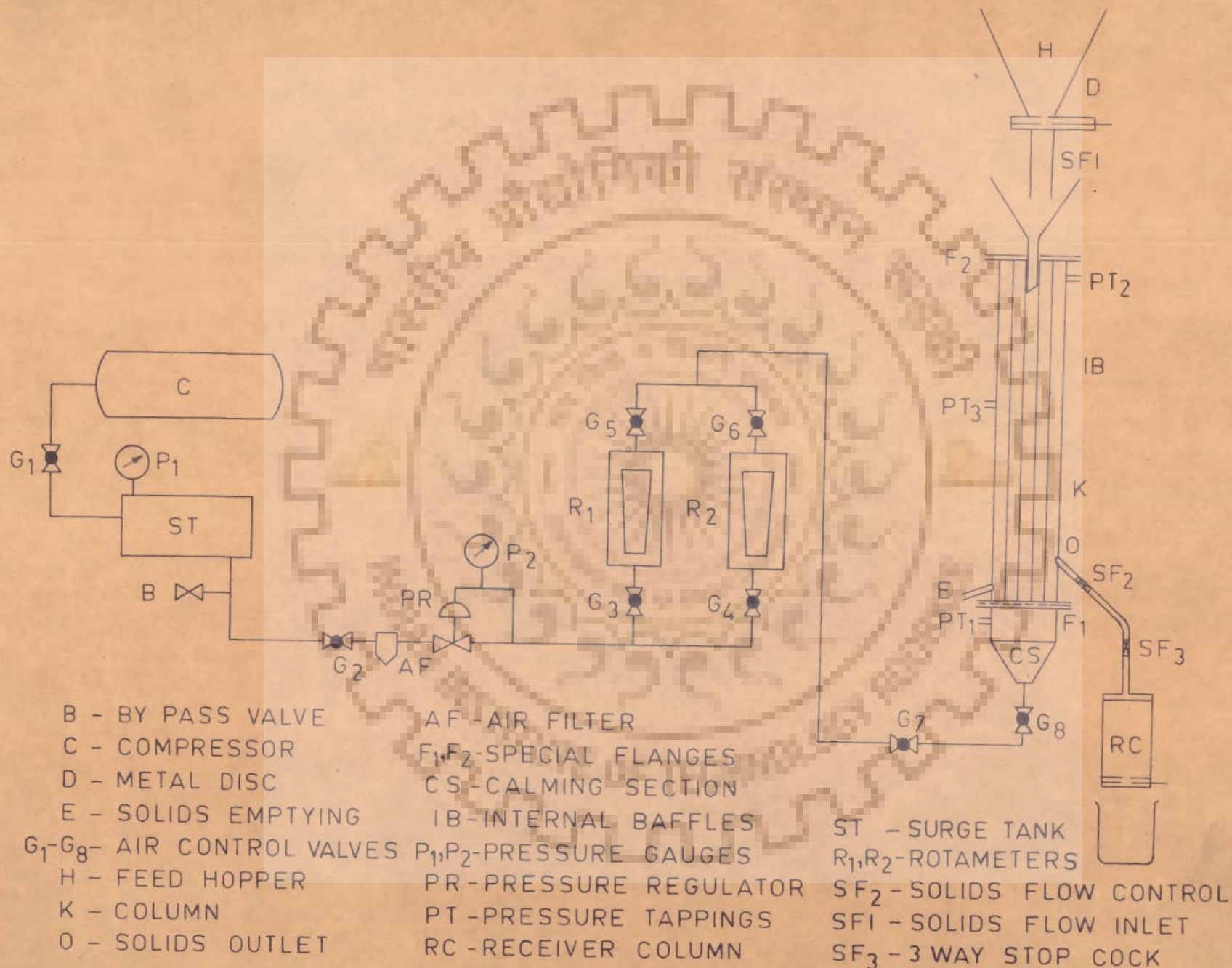


FIG. 4.1 SCHEMATIC DIAGRAM OF THE EXPERIMENTAL SET UP.

S.S. rods of 6 mm diameter and 610 mm effective length. A 3 mm thick aluminium grid plate having 1.5 mm holes on a square pitch, fitted in the flange (F_2) was used to support the bed of solids and also as air distributor. The area of the openings in the grid was 10% of the empty column cross section. The grid plate was covered with a 200 mesh brass wire screen for supporting the solids. Air was introduced in the column at the bottom through a calming section (CS) which was filled with raschig rings to provide uniform air distribution. The solids feeding was done through a M.S. feed hopper (H) and a gravity funnel mounted on the flange (F_2). Flow of solids through the hopper into the fluidizing column was regulated by a sliding disc with a slot (D) fitted between the hopper and the perspex tube leading to the gravity funnel. Different feed rates of solids were obtained by using funnels of different throat diameters.

Continuous feeding of solids was attempted by using an electric vibratory feeder with an autovariac and input voltage stabilizer. The vibratory feeder was not found satisfactory as the solids feed rates were fluctuating and hence gravity funnels were used for solids feeding.

The solids outlet (O) from the column was provided at the side near the base of the column. The discharge rate of solids from the column was regulated using a

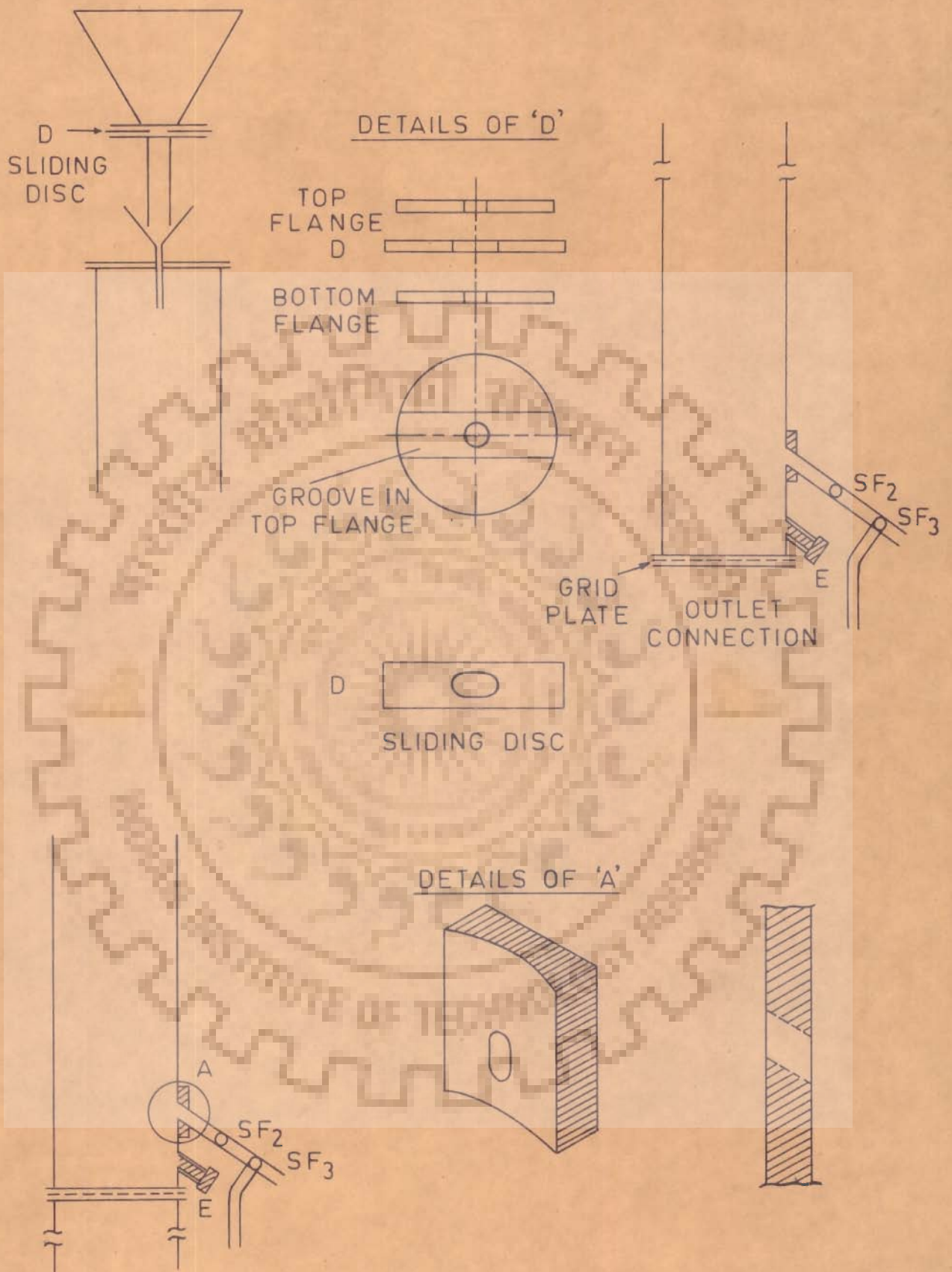


FIG. 4.2 DETAILS OF FEED INLET AND OUTLET CONNECTIONS.

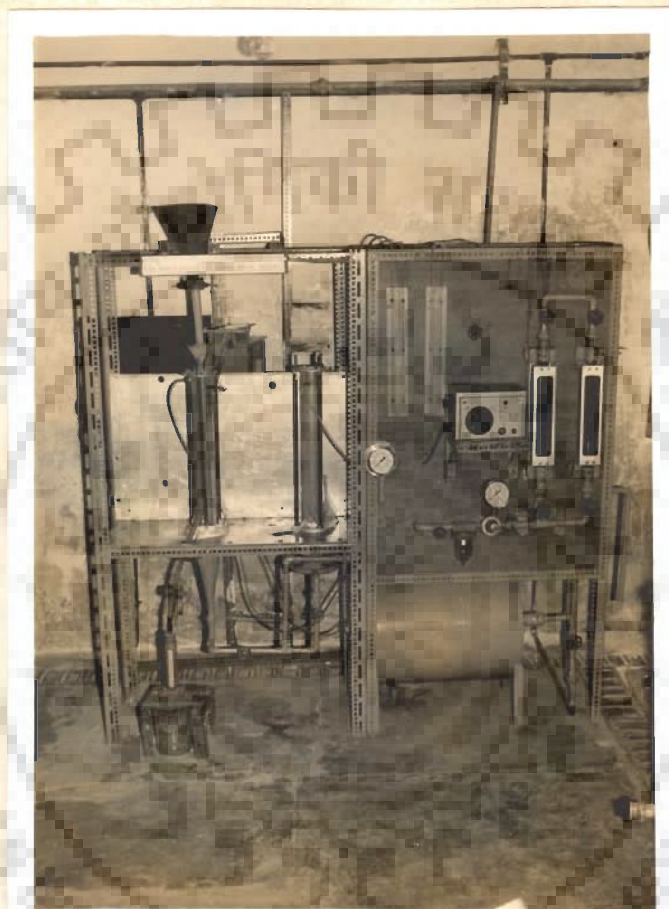


FIG. 4.3 PHOTOGRAPH SHOWING EXPERIMENTAL
SET UP OF CONTINUOUS FLUIDIZED
BED WITH VERTICAL BAFFLES.

two way and a three way stop cocks (SF_2 and SF_3) in series. Another outlet (E) was provided for emptying the column.

The details of the feed inlet and product outlet connections are given in Fig. 4.2. The photograph of the experimental unit is shown in Fig. 4.3.

4.2 PROCEDURE

Solids from the hopper were allowed to flow down into the fluidizing column through the gravity funnel of known throat diameter. The discharge rate of solids from the fluidizing column was regulated by the help of the two way stop cock (SF_2) to ensure the steady state conditions of feed and discharge rates of solids. During the operation, it was observed that solids discharge was strongly influenced by the introduction of air. At the condition of no air flow through the column the solids flow out of the column was found to be jerky and unsteady. Many a times, the solids flow used to stop due to the tendency of arching at the mouth of the discharge opening. Slight introduction of air improved the performance of the column which prevented the arch formation and enabled easy flow of solids through discharge line. Air was then introduced from the bottom of the column and the bed attained the fluidizing condition. Steady state conditions were obtained by adjusting the discharge rate of

solids corresponding to the feed rate. Steady state conditions were assumed when

- i) bed height
- ii) pressure drop across the bed and
- iii) the solids inlet and outlet rates remained constant.

Invariably the steady state reached in about 15-20 minutes time.

The column was provided with pressure tapplings PT_1 just below the grid, PT_2 just near the air outlet from the top and PT_3 at about one-third distance from the top. In the experiment, the expanded bed height (dense phase zone) was maintained between PT_3 and solids outlet location (0). The bed pressure drop was measured for different air flow rates between pressure tapplings PT_1-PT_2 and PT_1-PT_3 and these values were found to be same in all the experimental runs. For determining bed densities in the expanded bed heights the length of the column PT_1-PT_3 was considered rather than the entire length of the column from the grid to the pressure tapping PT_2 .

The bed pressure drop and bed height were noted for different air flow rates and solids feed rates. Bed density was evaluated by measuring the weight of solids in the bed for any air flow rate. This was done by

first closing the solids feed to the column by the sliding disc. The solids flow continued for sometime after this, till the feed funnel was completely discharged. The solids outlet valve was closed as soon as the last particle in the feed funnel entered the bed. The corresponding static bed heights were recorded for evaluating pressure drop per unit height of the bed. Solids in the bed were withdrawn completely through the bottom outlet (E) by air flow and were accurately weighed. This synchronization was done by very careful visual observation and manipulation. After a number of trials with the experimental set up, this operation could be done with ease and with reproducibility. For comparison, pressure drop and bed density data were obtained in continuous fluidized bed without baffles under the similar operating conditions. The range of experimental variables is given in table 4.1.

TABLE-4.1

RANGE OF EXPERIMENTAL VARIABLES

Material	Bauxite, Limestone, Glass beads and Baryte	
Density	$2.3 \times 10^3 - 3.85 \times 10^3$	kg/m ³
Particle size	385-977	micron
Solids Feed Rate	$6.9 \times 10^{-3} - 1.52 \times 10^{-2}$	kg/s
Air Flow Rate	0-2.5	kg/m ² .s

4.3 RESULTS AND DISCUSSION

The data on pressure drop for different air mass velocities and constant solids feed rate in continuous fluidized beds with baffles are given in table 4.2 to 4.9. The data for bed density - solids loading ratio are reported in table 4.10 to 4.23. Similar data were obtained in continuous fluidized beds without baffles under identical conditions for pressure drop and bed density and are given in table 4.24 to 4.27.

4.3.1 Continuous Fluidization Without Baffles

The solids down flow rate has been plotted as a function of gas flow rate in Fig. 4.4. It is observed that the solids flow rate remained almost constant throughout. At high gas velocities there was a slight decrease in solids down flow rate. The pressure drop data in continuous fluidized beds as a function of air mass velocity are shown in Fig. 4.5. Pressure drop was first observed to increase steadily and then increase at slower rate with increase in air mass velocity. This observation was similar to those made in batch fluidized bed without baffles.

4.3.2 Continuous Fluidization With Baffles

4.3.2.1 Pressure Drop

The bed pressure drop versus air mass velocity

data are plotted in Figs. 4.6 to 4.12. The bed pressure drop increased with increase in air mass velocity at a faster rate upto a certain point and thereafter the increase was slower. This observation was similar to the one seen in continuous beds without baffles. As can be seen from Figs. 4.6 and 4.7, pressure drop increases with increase in particle size for the same air flow rate. For a given material and particle size, the pressure drop increases with increase in solids feed rate as seen from Fig. 4.8 to 4.9. The pressure drop was observed to be more for the material of higher density for a given solids feed rate and particle size as shown in Figs. 4.10 to 4.12. The differences were observed to be pronounced at higher gas velocities. A comparison of the bed pressure drop is made between continuous fluidized beds with and without baffles. The plots are shown in Figs. 4.13 and 4.14 which show the variation of bed pressure drop with air mass velocity. From these plots the bed pressure drop in baffled fluidized bed was observed to be consistently higher than those observed in beds without baffles under identical conditions of operation.

4.3.2.2 Bed Density

Bed density in a fluidized bed gives information on the quality of fluidized bed and throws light on possible stable and unstable condition of the bed. It

is expected that at low air flow rates, the bed will be in dense phase conditions. The bed expansion will be nominal and bed densities will be high. At increased gas flow rates, whether bubbles are present or not, the bed expansion will be large and the bed may transform from dense phase to dilute phase. This is reflected in low values of bed densities. At very high gas flow rates indicating very low values of bed densities, the solids may even be carried over. Thus a measure of the value of bed density would indicate the stability of fluidized bed with regard to the extent of bed expansion.

Fig. 4.16 is the plot for glass beads showing the variation of bed density with the solids loading ratio (W_s/W_g) which is defined as the ratio of the mass flow rate of solids to the mass flow rate of air. It was observed that for a given solids feed rate, the lowest bed density could be obtained at high gas velocities in countercurrent operation of gas and solids. The bed density was observed to be more for small size particles. Similar observations were made for other materials also as shown in Figs. 4.17 and 4.18.

From Fig. 4.19, which is the plot showing the variation of bed density with the solids loading ratio at a given solids feed rate and particle size, it was observed that the bed density decreased with increase in

air flow rate and that the bed density was more for the material having high density.

The effect of solids feed rate on bed density was observed to be negligible.

Fig. 4.20 shows the variation of bed density with the solids loading ratio in continuous fluidized bed with vertical internal baffles compared to that in the bed without baffles. From this plot, it was observed that for any solids loading ratio, the bed density was more in fluidized bed with baffles as compared to that in the unbaffled bed. At any given gas flow rate, the bed expansion in beds with baffles is lower than that in unbaffled beds due to the restricted movement of solids. This probably may be the cause of this observation.

4.3.3 CORRELATIONS PROPOSED

4.3.3.1 Pressure Drop

The behaviour of continuous fluidized beds with baffles differs from those without baffles essentially because of the introduction of vertical surfaces. With proper baffle spacing it is expected that the solids movement is free and continuous baffled fluidized beds will have higher pressure drop than similar beds without baffles, due to additional surfaces present. In continuous systems an additional parameter which is likely

to affect the pressure drop is the solids loading ratio, R. It is expected that at higher solids loading ratio, the solids movement will be more leading to greater interaction between the solids entering the bed and the solids in fluidized state in the bed, causing thereby a higher pressure drop. Thus, any correlation predicting pressure drop in continuous fluidized beds with baffles must contain both these terms viz. Solids loading ratio and presence of baffles, besides the solids and fluid characteristics and apparatus geometry. A dimensionless correlation has been proposed for predicting the pressure drop in terms of a friction factor

$$\frac{\Delta P}{L \rho_f} = 52.5 (Fr)^{0.33} (Re_p)^{0.08} \left(\frac{D_e}{D_p}\right)^{-0.1} (R)^{0.3} \left(\frac{\rho_s - \rho_f}{\rho_f}\right)^{0.17} \dots (4.1)$$

$Fr = \left(\frac{U_f^2}{D_p \cdot g}\right)$ Froude number is the ratio of buoyancy force to the gravity force. This is a criteria to ensure that a particle is lifted freely in a fluidized bed due to buoyancy effect.

$Re_p = \left(\frac{D_p G_f}{\mu_f}\right)$ Reynolds number based on particle diameter represents the ratio of the inertial forces to the viscous forces and indicates the velocity requirements to ensure particle movement.

$\left(\frac{D_e}{D_p}\right)$ represents the ratio of the equivalent diameter of the bed to the particle diameter and signifies the resistance offered by the extra surfaces present in the bed due to the baffles, column and the fluidized particles.

$\left(\frac{P_s - P_f}{P_f}\right)$ is the ratio of the apparent density of solids to density of fluid and represents the quality of fluidized bed.

$R = \frac{W_s}{W_g}$ is the solids loading ratio and represents the condition of the bed.

The predicted values of the pressure drop in continuous fluidized beds with vertical baffles were found to lie well within $\pm 20\%$ of the experimental values, as shown in Fig. 4.15.

4.3.3.2 Bed Density

The bed density of a fluidized bed represents the weight of solids per unit volume of bed. This means all the parameters which affect the volume of the bed need to be incorporated in any correlation predicting the bed density. The volume of a fluidized bed is strongly governed by the particle movement. In vertical baffled systems the particle movement and hence the bed expansion will be affected by d_o/D_p ratio. The bed density will depend upon the solids and fluid properties and d_o/D_p

ratio. A dimensionless correlation has been proposed as

$$\frac{\rho_{bd}}{\rho_f} = 342 (Fr)^{-0.15} (Re)^{-0.008} \left(\frac{d_o}{D_p}\right)^{0.27} \left(\frac{\rho_s - \rho_f}{\rho_f}\right)^{0.11} \dots (4.2)$$

$\frac{d_o}{D_p}$ represents the ratio of the distance between two adjacent baffles to particle diameter and signifies the resistance for the free movement of particles in the column.

Bed density was plotted against linear air velocity as shown in Fig. 4.21. The slope of the line was observed to be 0.32, which is consistent with the exponent of U_f obtained from the correlation. Similarly in Fig. 4.22 was plotted

$$\frac{\rho_{bd}}{\rho_f} = 342 (Fr)^{-0.15} (Re)^{-0.008} \left(\frac{d_o}{D_p}\right)^{0.27} \left(\frac{\rho_s - \rho_f}{\rho_f}\right)^{0.11} \text{ versus } \left(\frac{d_o}{D_p}\right). \text{ The slope}$$

of the line was found to be 0.27. The exponent of $\left(\frac{d_o}{D_p}\right)$ in the correlation eqn. (4.2) also comes to 0.27.

The predicted values of bed density from the proposed correlation were found to lie within $\pm 10\%$ of the experimental values as shown in Fig. 4.23. The correlation is valid for expanded beds which are obtained at values of $G_f/G_{mf} > 1$.

4.4 CONCLUSION

Above studies indicate that

- the pressure drop in beds with vertical internal baffles is higher than that in beds without baffles under similar conditions of operations.
- bed densities are observed to be more in beds with vertical baffles as compared to that in unbaffled beds.
- correlations have been proposed for predicting the pressure drop and bed densities in continuous fluidized beds with vertical internal baffles, vide eqns. 4.1 and 4.2.

TABLE-4.2

EXPERIMENTAL DATA

System : Air - Glass Beads

Solids Feed Rate : 1.11×10^{-2} kg/s

Vertical Baffles : 6 mm dia, 12 Nos. d_o 10 mm

Sl. No.	Air Mass Velocity	Solid Flow Rate W_s	Air Flow Rate, W_g	Solids loading Ratio W_s/W_g	$\frac{\Delta P}{L}$	$\frac{N}{m^3} \times 10^{-4}$	
	kg/m ² s	kg/sx10 ²	kg/sx10 ⁴		977 μ m	650 μ m	460 μ m
1.	2	3	4	5	6	7	8
1.	.204	1.11	7.17	15.48	-	0.47	0.75
2.	.306	1.11	10.76	10.30	0.53	0.79	1.10
3.	.408	1.11	14.35	7.73	0.80	1.04	1.31
4.	.510	1.11	17.94	6.18	0.97	1.26	1.34
5.	.613	1.11	21.53	5.15	1.17	1.35	1.34
6.	.715	1.11	25.12	4.41	1.37	1.38	1.36
7.	.817	1.09	28.71	3.79	1.38	1.38	1.39
8.	.868	1.09	30.50	3.57	1.42	1.39	1.40
9.	.919	1.08	35.88	3.01	1.44	1.41	1.41
10.	1.02	1.08	43.06	2.5	1.48	1.45	1.46
11.	1.22	1.08	50.52	2.13	1.54	1.52	1.49

TABLE-4.3

EXPERIMENTAL DATA

System : Air - Baryte

Solids Feed Rate : 1.11×10^{-2} kg/s

Vertical Baffles : 6 mm dia, 12 Nos. d_o 10 mm

Sl. No.	Air Mass Velocity	Solid Flow Rate W_s	Air Flow Rate W_g	Solids loading Ratio W_s/W_g	$\frac{\Delta P}{L}$, $\frac{N}{m^3} \times 10^{-4}$				
	kg/m ² s	kg/sx10 ²	kg/sx10 ⁴		977 μ m	650 μ m	460 μ m	385 μ m	
1	2	3	4	5	6	7	7	8	9
1.	.102	1.11	3.58	31.7	-	-		0.39	0.77
2.	.204	1.11	7.17	15.48	0.37	0.52		0.80	1.00
3.	.306	1.11	10.3	10.3	0.78	0.85		1.19	1.29
4.	.408	1.11	14.35	7.73	0.90	1.1		1.41	1.46
5.	.51	1.11	17.94	6.18	1.06	1.36		1.45	1.51
6.	.613	1.10	21.53	5.11	1.31	1.45		1.48	1.58
7.	.817	1.10	28.71	3.83	1.52	1.48		1.50	1.57
8.	1.02	1.10	35.88	3.06	1.56	1.52		1.55	1.62
9.	1.22	1.09	43.06	2.53	1.62	1.56		1.57	1.70
10.	1.43	1.08	50.52	2.13	1.62	1.62		1.637	1.77

TABLE-4.4

EXPERIMENTAL DATA

System : Air - Bauxite

Solids Feed Rate : 1.11×10^{-2} kg/s

Vertical Baffles : 6 mm dia, 12 Nos. d_o 10 mm

Sl. No.	Air Mass Velocity	Solid Flow Rate W_s	Air Flow Rate W_g	Solids loading Ratio W_s/W_g	$\frac{\Delta P}{L}$	$\frac{N}{m^3} \times 10^{-4}$
	kg/m ² s	W_s kg/sx10 ²	kg/sx10 ⁴		460 μ m	650 μ m
1	2	3	4	5	6	7
1.	.102	1.11	3.58	31.7	0.362	-
2.	.204	1.11	7.17	15.48	0.735	0.45
3.	.306	1.11	10.76	10.3	1.078	0.77
4.	.408	1.11	14.35	7.73	1.29	1.01
5.	.51	1.11	17.94	6.18	1.32	1.23
6.	.613	1.10	21.53	5.11	1.33	1.32
7.	.817	1.10	28.72	3.83	1.37	1.35
8.	1.02	1.10	35.88	3.06	1.39	1.38
9.	1.22	1.09	43.06	2.53	1.44	1.41
10.	1.43	1.07	50.52	2.11	1.46	1.47

TABLE-4.5

EXPERIMENTAL DATA

System : Air - Limestone

Solids Feed Rate : 1.11×10^{-2} kg/s

Vertical Baffles : 6 mm dia, 12 Nos. d_o 10 mm

Sl. No.	Air Mass Velocity	Solid Flow Rate W_s	Air Flow Rate W_g	Solids loading Ratio W_s/W_g	$\frac{\Delta P}{L}$	$\frac{N}{m^3} \times 10^{-4}$
	kg/m ² s	W_s kg/sx10 ²	kg/sx10 ⁴		460 μ m	650 μ m
1	2	3	4	5	6	7
1.	.102	1.11	3.58	31.7	0.37	-
2.	.204	1.11	7.17	15.48	0.76	0.48
3.	.306	1.11	10.76	10.3	1.12	0.81
4.	.408	1.11	14.35	7.73	1.33	1.06
5.	.51	1.11	17.94	6.18	1.37	1.29
6.	.613	1.11	21.53	5.15	1.36	1.38
7.	.817	1.10	28.71	3.83	1.42	1.41
8.	1.02	1.10	35.88	3.39	1.44	1.44
9.	1.22	1.08	43.06	2.50	1.48	1.49
10.	1.43	1.07	50.52	2.11	1.51	1.55

TABLE-4.6

EXPERIMENTAL DATA

System : Air - Glass Beads
 Solids Feed Rate : 1.38×10^{-2} kg/s
 Particle size : 650 μ m
 Vertical Baffles : 6 mm dia, 12 Nos. d_o 10 mm

Sl. No.	Air Mass Velocity kg/m ² s	Solid Flow Rate W_s kg/s $\times 10^2$	Air Flow Rate W_g kg/s $\times 10^4$	Solids loading Ratio W_s/W_g	$\frac{\Delta P}{L}$	$\frac{N}{m^3} \times 10^{-4}$
1	2	3	4	5	6	
1.	.204	1.38	7.17	19.2		.50
2.	.306	1.38	10.76	12.8		.86
3.	.408	1.38	14.35	9.6		1.1
4.	.51	1.38	17.94	7.7		1.24
5.	.613	1.37	21.53	6.36		1.43
6.	.715	1.37	25.12	5.45		1.47
7.	.817	1.37	28.71	4.77		1.49
8.	.919	1.36	32.3	4.2		1.50
9.	1.02	1.36	35.88	3.8		1.51
10.	1.22	1.35	43.06	3.13		1.54
11.	1.43	1.35	50.52	2.67		1.60

TABLE-4.7

EXPERIMENTAL DATA

System : Air - Glass Beads
 Solids Feed Rate : 6.9×10^{-3} kg/s
 Particle size : 460 μ m
 Vertical Baffles : 6 mm dia, 12 Nos. d_o 10 mm

Sl. No.	Air Mass Velocity kg/m ² s	Solid Flow Rate W_s kg/sx10 ³	Air Flow Rate W_g kg/sx10 ⁴	Solids loading Ratio W_s/W_g	$\frac{\Delta P}{L}$, $\frac{N}{m^3} \times 10^{-4}$
1	2	3	4	5	6
1.	0.102	6.9	3.58	19.2	0.32
2.	0.204	6.9	7.17	9.6	0.64
3.	0.306	6.9	10.76	6.4	0.97
4.	0.408	6.9	14.35	4.8	1.15
5.	0.51	6.9	17.94	3.84	1.18
6.	0.613	6.9	21.53	3.2	1.19
7.	0.817	6.9	28.71	2.4	1.20
8.	1.022	6.9	35.88	1.92	1.23
9.	1.22	6.8	43.06	1.58	1.26
10.	1.43	6.8	50.52	1.34	1.30

TABLE-4.8

EXPERIMENTAL DATA

Solids Feed Rate 8.3×10^{-3} kg/s
 Particle size 650 μ m
 Baffles 6 mm dia, 12 Nos. d_o 10 mm

Sl. No.	Air Mass Velocity kg/m ² s	Solids Flow Rate, W_s kg/sx10 ³	Air Flow Rate W_g kg/sx10 ⁴	Solid Loading Ratio W_s/W_g	$\frac{\Delta P}{L}$, $\frac{N}{m^3} \times 10^{-4}$			
					Bauxite	Limestone	Glass beads	Baryte
1	2	3	4	5	6	7	8	9
1.	.204	8.3	7.17	11.5	.41	.45	.43	.47
2.	.306	8.3	10.76	7.7	.69	.75	.74	.79
3.	.408	8.3	14.35	5.78	.91	.98	.95	1.03
4.	.51	8.3	17.94	4.6	1.1	1.18	1.15	1.25
5.	.613	8.25	21.53	3.8	1.19	1.27	1.23	1.33
6.	.715	8.25	25.12	3.28	1.22	1.30	1.26	1.34
7.	.817	8.20	28.71	2.85	1.22	1.30	1.27	1.35
8.	.919	8.20	32.30	2.53	1.24	1.31	1.275	1.37
9.	1.02	8.20	35.88	2.28	1.25	1.32	1.29	1.40
10.	1.22	8.20	43.06	1.90	1.29	1.38	1.35	1.46
11.	1.43	8.19	50.52	1.62	1.34	1.44	1.40	1.51
12.	1.63	8.19	57.42	1.42	1.40	1.52	1.48	1.58

TABLE-4.9

EXPERIMENTAL DATA

Solids Feed Rate 1.52×10^{-2} kg/s
 Particle size 460 μm
 Baffles 6 mm dia, 12 Nos. d_o 10 mm

Sl. No.	Air Mass Velocity kg/m ² s	Solids Flow Rate, W_s kg/sx10 ²	Air Flow Rate W_g kg/sx10 ⁴	Solid Loading Ratio W_s/W_g	$\frac{\Delta P}{L} \cdot \frac{N}{m^3} \times 10^{-4}$			
					Bauxite	Lime stone	Glass beads	Baryte
1	2	3	4	5	6	7	8	9
1.	.102	1.52	3.58	42.4	.37	.40	.39	.42
2.	.202	1.52	7.17	21.2	.75	.81	.79	.86
3.	.306	1.52	10.76	14.12	1.13	1.24	1.17	1.32
4.	.408	1.52	14.35	10.59	1.35	1.44	1.40	1.51
5.	.510	1.52	17.94	8.47	1.38	1.47	1.43	1.54
6.	.613	1.51	21.53	7.0	1.39	1.48	1.43	1.54
7.	.817	1.51	28.71	5.26	1.43	1.53	1.49	1.59
8.	1.02	1.51	35.88	4.2	1.47	1.56	1.51	1.62
9.	1.22	1.50	43.06	3.48	1.50	1.59	1.55	1.67
10.	1.43	1.50	50.52	2.97	1.53	1.63	1.59	1.70
11.	1.63	1.50	57.42	2.6	1.57	1.68	1.62	1.75

TABLE-4.10

EXPERIMENTAL DATA

System : Air - Glass Beads
 Solids Feed Rate : 9.71×10^{-3} kg/s
 Particle size : 977 μ m
 Vertical Baffles : 6 mm dia, 12 Nos. d_o 10 mm

Sl. No.	Air Mass Velocity kg/m ² s	Solids Flow Rate, W_s kg/sx10 ³	Air Flow Rate W_g kg/sx10 ³	Solid Loading Ratio W_s/W_g	Bed Density $\frac{\text{kg}}{\text{m}^3} \times 10^{-3}$
1	2	3	4	5	6
1.	0.4087	9.58	1.43	6.7	1.26
2.	0.5109	9.55	1.79	5.33	1.17
3.	0.6131	9.51	2.15	4.42	1.11
4.	0.7153	9.49	2.51	3.78	1.05
5.	0.8175	9.46	2.86	3.30	1.0
6.	0.9197	9.45	3.23	2.92	0.975
7.	1.022	9.44	3.58	2.62	0.94
8.	1.2263	9.42	4.30	2.19	0.90
9.	1.4307	9.40	5.02	1.87	0.85

TABLE-4.11

EXPERIMENTAL DATA

System : Air - Glass Beads
 Solids Feed Rate : 9.71×10^{-3} kg/s
 Particle size : 650 μ m
 Vertical Baffles : 6 mm dia, 12 Nos. d_o 10 mm

Sl. No.	Air Mass Velocity kg/m ² s	Solids Flow Rate, W_s kg/sx10 ³	Air Flow Rate W_g kg/sx10 ³	Solids Loading Ratio W_s/W_g	Bed Density $\frac{\text{kg}}{\text{m}^3} \times 10^{-3}$
1	2	3	4	5	6
1.	0.4087	9.59	1.43	6.7	1.31
2.	0.5109	9.58	1.79	5.38	1.22
3.	0.6131	9.56	2.15	4.44	1.16
4.	0.7153	9.54	2.51	3.80	1.10
5.	0.8175	9.49	2.86	3.31	1.05
6.	0.9197	9.48	3.23	2.93	1.03
7.	1.022	9.47	3.58	2.64	0.99
8.	1.2263	9.45	4.30	2.19	0.93
9.	1.4307	9.41	5.02	1.87	0.88

TABLE-4.12

EXPERIMENTAL DATA

System : Air - Glass Beads
 Solids Feed Rate : 9.71×10^{-3} kg/s
 Particle size : 460 μm
 Vertical Baffles : 6 mm dia, 12 Nos. d_o 10 mm

Sl. No.	Air Mass Velocity $\text{kg/m}^2\text{s}$	Solid Flow Rate W_s $\text{kg/s} \times 10^3$	Air Flow Rate W_g $\text{kg/s} \times 10^3$	Solids Loading Ratio W_s/W_g	Bed Density $\frac{\text{kg}}{\text{m}^3} \times 10^{-3}$
1	2	3	4	5	6
1.	0.4087	9.6	1.43	6.7	1.38
2.	0.5109	9.55	1.79	5.33	1.29
3.	0.6131	9.50	2.15	4.42	1.22
4.	0.7153	9.46	2.51	3.77	1.16
5.	0.8175	9.41	2.86	3.29	1.09
6.	0.9197	9.37	3.23	2.90	1.04
7.	1.022	9.37	3.58	2.62	1.00
8.	1.2263	9.34	4.30	2.17	0.94
9.	1.4307	9.33	5.02	1.86	0.89

TABLE-4.13

EXPERIMENTAL DATA

System : Air - Glass Beads
 Solids Feed Rate : 1.25×10^{-2} kg/s
 Particle size : 460 μ m
 Vertical Faffles : 6 mm dia, 12 Nos. d_o 10 mm

Sl. No.	Air Mass Velocity kg/m ² s	Solid Flow Rate W_s kg/sx10 ²	Air Flow Rate W_g kg/sx10 ³	Solids Loading Ratio W_s/W_g	Bed Density $\frac{\text{kg}}{\text{m}^3} \times 10^{-3}$
1	2	3	4	5	6
1.	0.4087	1.22	1.43	8.49	1.38
2.	0.5109	1.21	1.79	6.74	1.29
3.	0.6131	1.19	2.15	5.55	1.22
4.	0.7153	1.19	2.51	4.75	1.16
5.	0.8175	1.18	2.86	4.13	1.09
6.	0.9197	1.175	3.23	3.8	1.04
7.	1.022	1.16	3.58	3.29	1.00
8.	1.2263	1.15	4.30	2.67	0.94
9.	1.4307	1.14	5.02	2.26	0.89

TABLE-4.17

EXPERIMENTAL DATA

System : Air - Baryte

Solids Feed Rate : 1.52×10^{-2} kg/s

Particle Size : 385 μ m

Vertical Baffles : 6 mm dia, 12 Nos. d_o 10 mm height 610 mm

Sl. No.	Air Mass Velocity kg/m ² s	Solid Flow Rate W_s kg/sx10 ²	Air Flow Rate W_g kg/sx10 ³	Solids Loading Ratio W_s/W_g	Bed Density $\frac{\text{kg}}{\text{m}^3} \times 10^{-3}$
1	2	3	4	5	6
1.	0.4087	1.52	1.43	10.62	1.61
2.	0.5109	1.52	1.79	8.5	1.52
3.	0.6131	1.515	2.15	7.04	1.45
4.	0.7153	1.51	2.51	6.03	1.38
5.	0.8175	1.51	2.86	5.38	1.33
6.	0.9199	1.51	3.23	4.66	1.25
7.	1.022	1.50	3.58	4.19	1.21
8.	1.2263	1.48	4.30	3.45	1.15
9.	1.4307	1.48	5.02	3.0	1.09

TABLE-4.14

EXPERIMENTAL DATA

System : Air - Baryte

Solids Feed Rate : 1.52×10^{-2} kg/s

Particle size : 977 μ m

Vertical Baffles : 6 mm dia, 12 Nos. d_o 10 mm height 610 mm

Sl. No.	Air Mass Velocity kg/m ² s	Solid Flow Rate W_s kg/sx10 ²	Air Flow Rate W_g kg/sx10 ³	Solids Loading Ratio W_s/W_g	Bed Density $\frac{\text{kg}}{\text{m}^3} \times 10^{-3}$
1	2	3	4	5	6
1.	0.5109	1.52	1.79	8.5	1.30
2.	0.6131	1.51	2.15	7.04	1.25
3.	0.7153	1.51	2.51	6.03	1.18
4.	0.8175	1.51	2.88	5.29	1.12
5.	0.9197	1.50	3.23	4.66	1.07
6.	1.022	1.50	3.58	4.19	1.03
7.	1.2263	1.49	4.30	3.46	0.99
8.	1.4307	1.49	5.02	3.96	0.94

TABLE-4.15

EXPERIMENTAL DATA

System : Air - Baryte
 Solids Feed Rate : 1.52×10^{-2} kg/s
 Particle size : 650 μm
 Vertical Baffles : 6 mm dia, 12 Nos. d_o 10 mm height 610 mm

Sl. No.	Air Mass Velocity $\text{kg/m}^2\text{s}$	Solid Flow Rate W_s $\text{kg/s} \times 10^2$	Air Flow Rate W_g $\text{kg/s} \times 10^3$	Solids Loading Ratio W_s/W_g	Bed Density $\frac{\text{kg}}{\text{m}^3} \times 10^{-3}$
1	2	3	4	5	6
1.	0.4087	1.52	1.43	10.62	1.46
2.	0.5109	1.52	1.79	8.5	1.38
3.	0.6131	1.52	2.15	7.06	1.31
4.	0.7153	1.51	2.51	6.03	1.25
5.	0.8175	1.50	2.86	5.30	1.19
6.	0.9197	1.50	3.23	4.66	1.14
7.	1.022	1.49	3.58	4.18	1.1
8.	1.2263	1.48	4.30	3.44	1.03
9.	1.4307	1.48	5.02	3.95	1.0

TABLE-4.16

EXPERIMENTAL DATA

System : Air - Baryte

Solids Feed Rate : 1.52×10^{-2} kg/s

Particle Size : 460 μ m

Vertical Baffles : 6 mm dia, 12 Nos. d_o 10 mm height 610 mm

Sl. No.	Air Mass Velocity kg/m ² s	Solid Flow Rate W_s kg/sx10 ²	Air Flow Rate W_g kg/sx10 ³	Solids Loading Ratio W_s/W_g	Bed Density $\frac{\text{kg}}{\text{m}^3} \times 10^{-3}$
1	2	3	4	5	6
1.	0.4087	1.52	1.43	10.62	1.57
2.	0.5109	1.52	1.79	8.5	1.43
3.	0.6131	1.51	2.15	7.04	1.38
4.	0.7153	1.51	2.51	6.03	1.32
5.	0.8175	1.51	2.87	5.30	1.25
6.	0.9197	1.50	3.23	4.66	1.20
7.	1.022	1.50	3.58	4.19	1.16
8.	1.2263	1.48	4.30	3.45	1.11
9.	1.4307	1.48	5.02	2.95	10.3

TABLE-4.18

EXPERIMENTAL DATA

System : Air - Baryte
 Solids Feed Rate : 1.25×10^{-2} kg/s
 Particle Size : 460 μ m
 Vertical Baffles : 6 mm dia, 12 Nos. d_o 10 mm height 610 mm

Sl. No.	Air Mass Velocity kg/m ² s	Solid Flow Rate W_s kg/sx10 ²	Air Flow Rate W_g kg/sx10 ³	Solids Loading Ratio W_s/W_g	Bed Density $\frac{\text{kg}}{\text{m}^3} \times 10^{-3}$
1	2	3	4	5	6
1.	0.4087	1.22	1.43	8.50	1.57
2.	0.5109	1.22	1.79	6.80	1.43
3.	0.6131	1.21	2.15	5.55	1.38
4.	0.7153	1.20	2.51	4.75	1.32
5.	0.8175	1.20	2.86	4.18	1.25
6.	0.7197	1.20	3.23	3.80	1.20
7.	1.022	1.19	3.58	3.23	1.16
8.	1.2263	1.19	4.30	2.67	1.11
9.	1.4307	1.17	5.02	2.25	1.03

TABLE-4.19

EXPERIMENTAL DATA

System : Air - Bauxite
 Solids Feed Rate : 1.25×10^{-2} kg/s
 Particle Size : 460 μ m
 Vertical Baffles : 6 mm dia, 12 Nos. d_o 10 mm height 610 mm

Sl. No.	Air Mass Velocity kg/m ² s	Solid Flow Rate W_s kg/sx10 ²	Air Flow Rate W_g kg/sx10 ³	Solids Loading Ratio W_s/W_g	Bed Density $\frac{\text{kg}}{\text{m}^3} \times 10^{-3}$
1	2	3	4	5	6
1.	0.4087	1.21	1.43	8.45	1.31
2.	0.5109	1.21	1.79	6.75	1.225
3.	0.6131	1.19	2.15	5.55	1.14
4.	0.7153	1.19	2.51	4.75	1.09
5.	0.8175	1.185	2.87	4.13	1.03
6.	0.9197	1.185	3.23	3.7	0.98
7.	1.022	1.16	3.58	3.23	0.94
8.	1.2263	1.15	4.30	2.67	0.89
9.	1.4307	1.14	5.02	2.26	0.83

TABLE-4.20

EXPERIMENTAL DATA

System : Air - Limestone
 Solids Feed Rate : 7.4×10^{-3} kg/s
 Particle Size : 460 μ m
 Vertical Baffles : 6 mm dia, 12 Nos. d_o 10 mm height 610 mm

Sl. No.	Air Mass Velocity $\text{kg/m}^2\text{s}$	Solid Flow Rate W_s $\text{kg/s} \times 10^3$	Air Flow Rate W_g $\text{kg/s} \times 10^3$	Solids Loading Ratio W_s/W_g	Bed Density $\frac{\text{kg}}{\text{m}^3} \times 10^{-3}$
1.	2	3	4	5	6
1.	0.4087	7.4	1.43	5.17	1.45
2.	0.5109	7.4	1.79	4.13	1.36
3.	0.6131	7.39	2.15	3.43	1.28
4.	0.7153	7.36	2.51	2.93	1.21
5.	0.8175	7.33	2.87	2.55	1.15
6.	0.9197	7.33	3.23	2.27	1.09
7.	1.022	7.31	3.58	2.04	1.06
8.	1.2263	7.29	4.30	1.69	1.00
9.	1.4307	7.26	5.02	1.44	0.93

TABLE-4.21

EXPERIMENTAL DATA

System : Air - Limestone
 Solids Feed Rate : 7.4×10^{-3} kg/s
 Particle Size : 385 μ m
 Vertical Baffles : 6 mm dia, 12 Nos. d_o 10 mm height 610 mm

Sl. No.	Air Mass Velocity kg/m ² s	Solid Flow Rate W_s kg/sx10 ³	Air Flow Rate W_g kg/sx10 ³	Solids Loading Ratio W_s/W_g	Bed Density $\frac{\text{kg}}{\text{m}^3} \times 10^{-3}$
1	2	3	4	5	6
1.	0.4087	7.4	1.43	5.17	1.50
2.	0.5109	7.4	1.79	4.13	1.38
3.	0.6131	7.39	2.15	3.43	1.31
4.	0.7153	7.36	2.51	2.93	1.23
5.	0.8175	7.33	2.86	2.55	1.16
6.	0.9197	7.33	3.23	2.27	1.10
7.	1.022	7.31	3.58	2.04	1.07
8.	1.2263	7.29	4.30	1.69	1.01
9.	1.4307	7.27	5.02	1.44	0.97

TABLE-4.22

EXPERIMENTAL DATA

System : Air - Limestone

Solids Feed Rate : 1.25×10^{-2} kg/s

Particle Size : 460 μ m

Vertical Baffles : 6 mm dia, 12 Nos. d_o 10 mm height 610 mm

S1. No.	Air Mass Velocity kg/m ² s	Solid Flow Rate W_s kg/sx10 ²	Air Flow Rate W_g kg/sx10 ³	Solids Loading Ratio W_s/W_g	Bed Density $\frac{\text{kg}}{\text{m}^3} \times 10^{-3}$
1	2	3	4	5	6
1.	0.4087	1.22	1.43	8.49	1.45
2.	0.5109	1.21	1.79	6.75	1.36
3.	0.6131	1.20	2.15	5.58	1.28
4.	0.7153	1.19	2.51	4.75	1.21
5.	0.8175	1.18	2.86	4.13	1.15
6.	0.9197	1.18	3.23	3.7	1.09
7.	1.022	1.16	3.58	3.23	1.06
8.	1.2263	1.15	4.30	2.67	1.0
9.	1.4307	1.14	5.02	2.25	0.93

TABLE-4.23

EXPERIMENTAL DATA

System : Air - Bauxite
 Solids Feed Rate : 9.72×10^{-3} kg/s
 Particle Size : 460 μ m
 Vertical Baffles : 6 mm dia, 12 Nos., d_o 10 mm height 610 mm

Sl. No.	Air Mass Velocity kg/m ² s	Solid Flow Rate W_s kg/sx10 ³	Air Flow Rate W_g kg/sx10 ³	Solids Loading W_s/W_g	Bed Density $\frac{\text{kg}}{\text{m}^3} \times 10^{-3}$
1	2	3	4	5	6
1.	0.4087	9.62	1.43	6.70	1.31
2.	0.5109	9.55	1.79	5.33	1.225
3.	0.6131	9.51	2.15	4.42	1.14
4.	0.7153	9.47	2.51	3.77	1.09
5.	0.8175	9.43	2.86	3.29	1.03
6.	0.9197	9.43	3.23	2.9	0.99
7.	1.022	9.39	3.58	2.62	0.94
8.	1.2263	9.35	4.30	2.17	0.89
9.	1.4307	9.35	5.02	1.86	0.83

TABLE-4.24

EXPERIMENTAL DATA

System : Air - Glass Beads
 Solids Feed Rate : 6.9×10^{-3} kg/s
 Particle Size : 460 μ m
 Without Baffles :

Sl. No.	Air Mass Velocity kg/m ² s	Solid Flow Rate W _s kg/sx10 ³	Air Flow Rate W _g kg/sx10 ⁴	Solids Loading W _s /W _g	Δ P/L $\frac{N}{m^3} \times 10^{-4}$	Bed Density $\frac{kg}{m^3} \times 10^{-3}$
1	2	3	4	5	6	7
1.	0.093	6.9	3.58	9.2	0.29	-
2.	0.186	6.9	7.17	9.6	0.60	-
3.	0.279	6.9	10.3	6.4	0.93	-
4.	0.37	6.9	14.35	4.8	1.07	1.30
5.	0.46	6.9	17.94	3.84	1.08	1.22
6.	0.558	6.9	21.53	3.20	1.09	1.14
7.	0.74	6.9	28.71	2.40	1.11	1.04
8.	0.92	6.9	35.88	1.92	1.13	.94
9.	1.116	6.8	43.06	1.58	1.16	.89
10.	1.30	6.8	50.52	1.34	1.22	.83

TABLE-4.25

EXPERIMENTAL DATA

System : Air - Limestone
 Solids Feed Rate : 1.11×10^{-2} kg/s
 Particle Size : 650 μm
 Without Baffles :

Sl. No.	Air Mass Velocity $\text{kg/m}^2\text{s}$	Solid Flow Rate W_s $\text{kg/s} \times 10^2$	Air Flow Rate W_g $\text{kg/s} \times 10^4$	Solids Loading W_s/W_g	$\Delta P/L$ $\frac{\text{N}}{\text{m}^3} \times 10^{-4}$	Bed Density $\frac{\text{kg}}{\text{m}^3} \times 10^{-3}$
1	2	3	4	5	6	7
1.	0.186	1.11	7.17	15.48	0.45	-
2.	0.279	1.11	10.76	10.3	0.78	-
3.	0.37	1.11	14.35	7.73	1.02	-
4.	0.46	1.11	17.94	6.18	1.22	1.20
5.	0.558	1.11	21.53	5.15	1.31	1.14
6.	0.65	1.10	25.12	4.37	1.32	1.08
7.	0.74	1.10	28.71	3.83	1.35	1.0
8.	0.92	1.09	35.88	3.03	1.39	.94
9.	1.116	1.09	43.06	2.53	1.41	.90
10.	1.30	1.08	50.52	2.13	1.48	.86

TABLE-4.26

System : Air - Baryte
 Solids Feed Rate : 8.3×10^{-3} kg/sec
 Particle Size : 650 μ m
 Without Baffles :

Sl. No.	Air Mass Velocity kg/m ² s	Solids Flow Rate W_s kg/s $\times 10^3$	Air Flow Rate W_g kg/s $\times 10^4$	Solids Loading W_s/W_g	Δ P/L $\frac{N}{m^3} \times 10^{-4}$	Bed Density $\frac{kg}{m^3} \times 10^{-3}$
1	2	3	4	5	6	7
1.	0.186	8.3	7.17	1.5	.45	-
2.	0.279	8.3	10.76	7.7	.77	-
3.	0.37	8.3	14.35	5.78	1.0	1.4
4.	0.46	8.3	17.94	4.60	1.09	1.30
5.	0.558	8.25	21.53	3.80	1.25	1.24
6.	0.74	8.25	28.71	3.28	1.24	1.12
7.	0.92	8.20	35.88	2.85	1.35	1.03
8.	1.116	8.20	43.06	2.53	1.4	.98
9.	1.30	8.20	50.52	2.28	1.44	.92

TABLE-4.27

EXPERIMENTAL DATA

System : Air - Bauxite
 Solids Feed Rate : 1.52×10^{-2} kg/s
 Particle Size : 460 μ m
 Without Baffles

Sl. No.	Air Mass Velocity kg/m ² s	Solid Flow Rate W _s kg/sx10 ²	Air Flow Rate kg/sx10 ⁴	Solids Loading Ratio W _s /W _g	Δ P/L $\frac{N}{m^3} \times 10^4$	Bed Density $\frac{kg}{m^3} \times 10^{-3}$
1	2	3	4	5	6	7
1.	0.093	1.52	3.58	42.4	.35	-
2.	0.186	1.52	7.17	21.2	.43	-
3.	0.279	1.52	10.3	14.12	1.1	-
4.	0.37	1.52	14.35	10.59	1.32	1.26
5.	0.46	1.52	17.94	8.47	1.35	1.17
6.	0.558	1.51	21.53	7.0	1.37	1.09
7.	0.74	1.51	28.71	5.26	1.4	.95
8.	0.92	1.51	35.88	4.20	1.44	.87
9.	1.116	1.50	43.06	3.48	1.46	.80
10.	1.30	1.50	50.52	2.97	1.50	.74

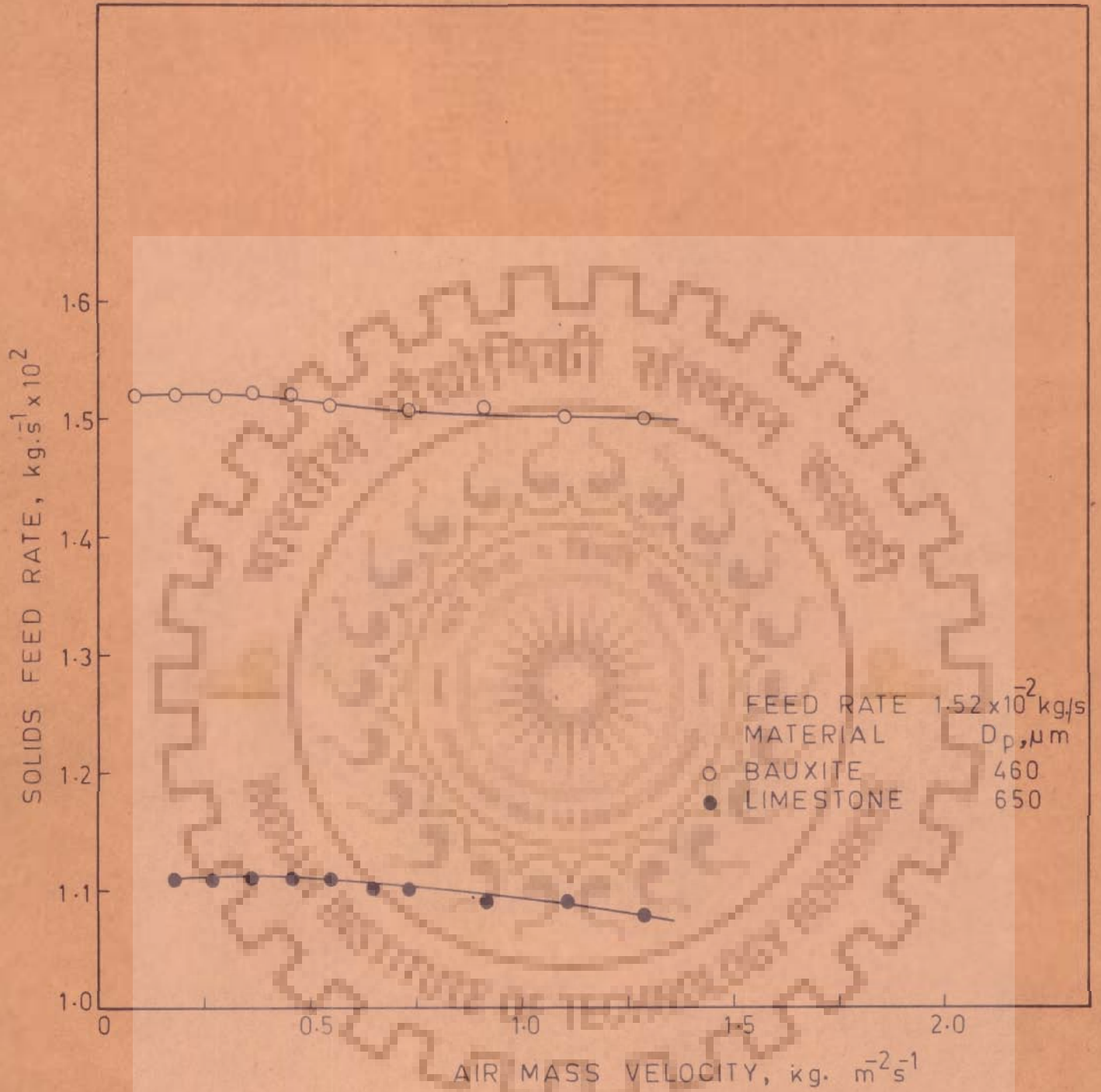


FIG. 4.4 EFFECT OF AIR FLOW RATE ON SOLIDS DOWN-FLOW RATE IN CONTINUOUS FLUIDIZED BEDS WITHOUT BAFFLES.

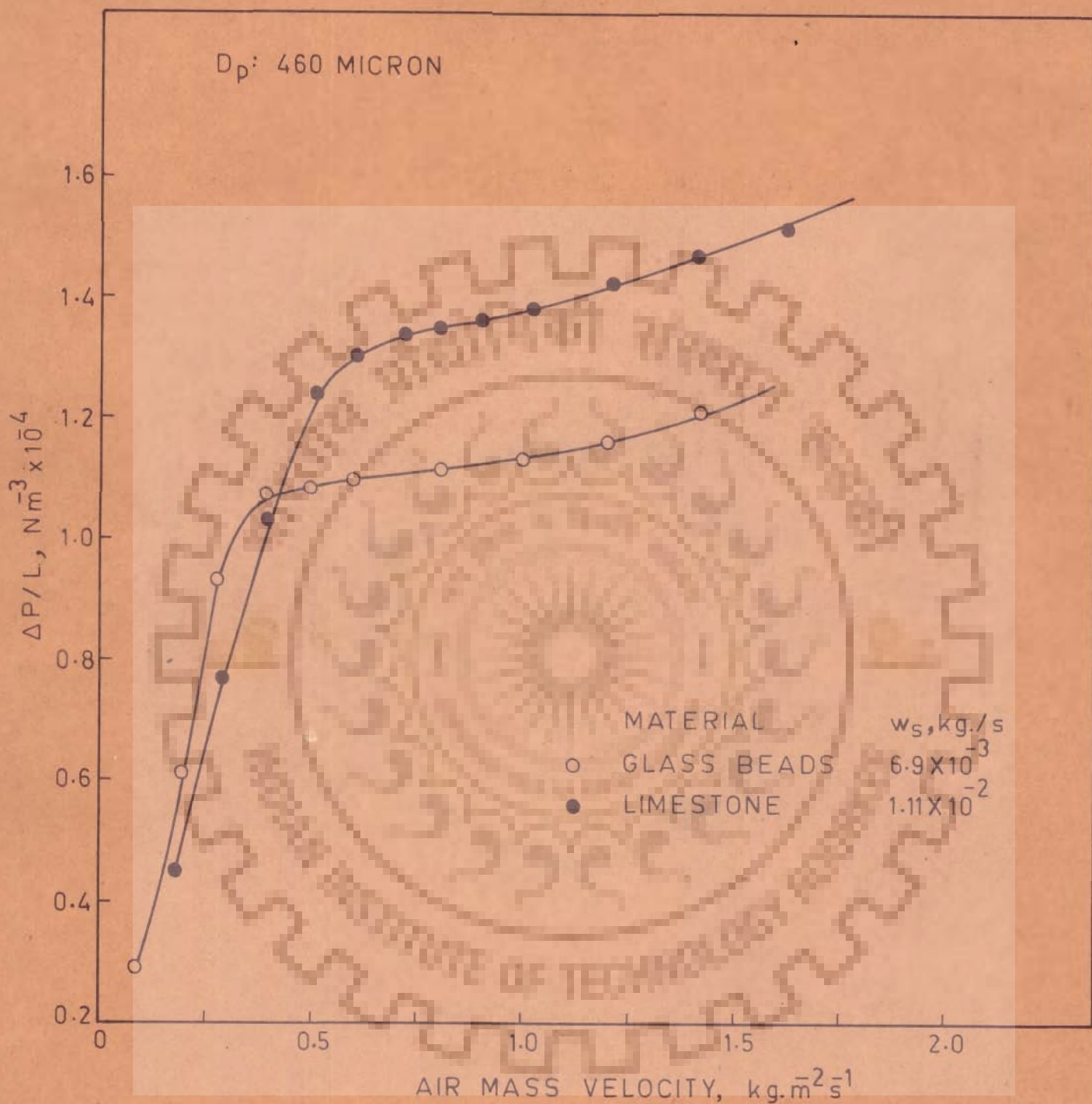


FIG. 4.5 VARIATION OF PRESSURE DROP WITH AIR MASS VELOCITY IN CONTINUOUS FLUIDIZED BED WITHOUT BAFFLES.

SYSTEM: AIR-GLASS BEADS

BAFFLE DIA. 6mm

NO. OF BAFFLES 12

d_o 10mm
 w_s 1.11×10^{-2} kg./s

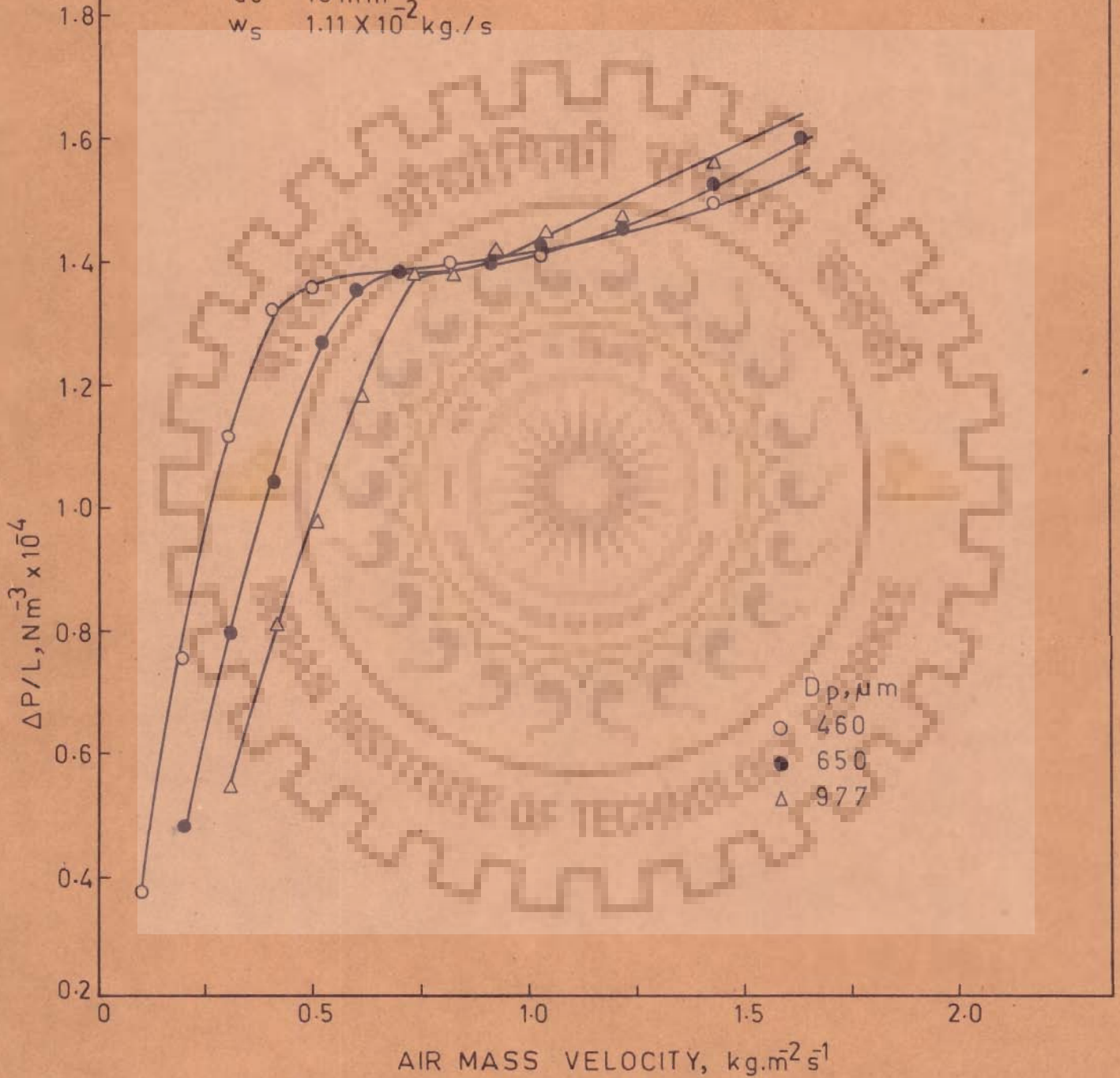


FIG. 4.6 VARIATION OF $\Delta P/L$ WITH AIR MASS VELOCITY IN CONTINUOUS FLUIDIZED BEDS WITH VERTICAL BAFFLES.

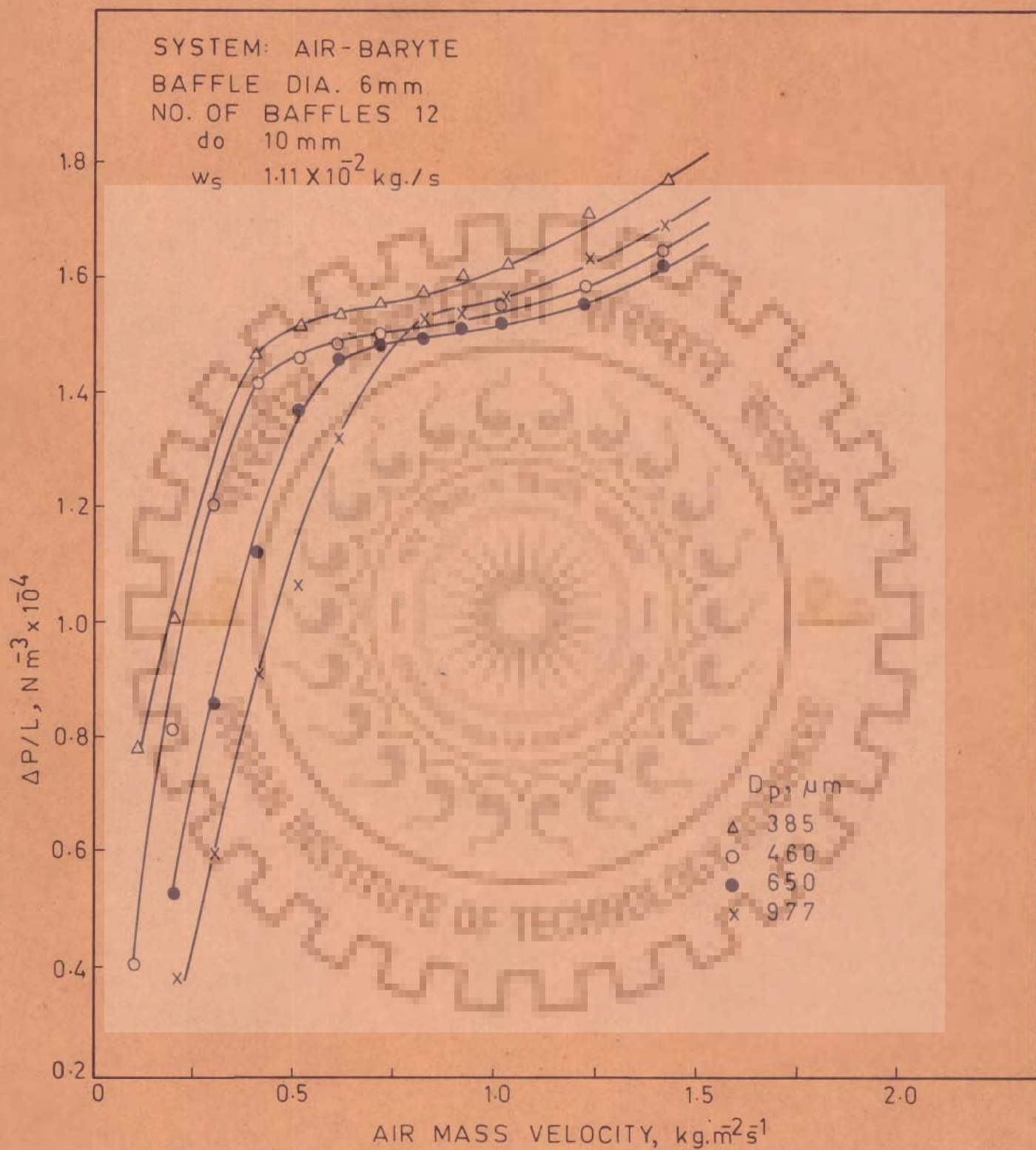


FIG. 4.7 VARIATION OF $\Delta P/L$ WITH AIR MASS VELOCITY IN CONTINUOUS FLUIDIZED BEDS WITH VERTICAL BAFFLE

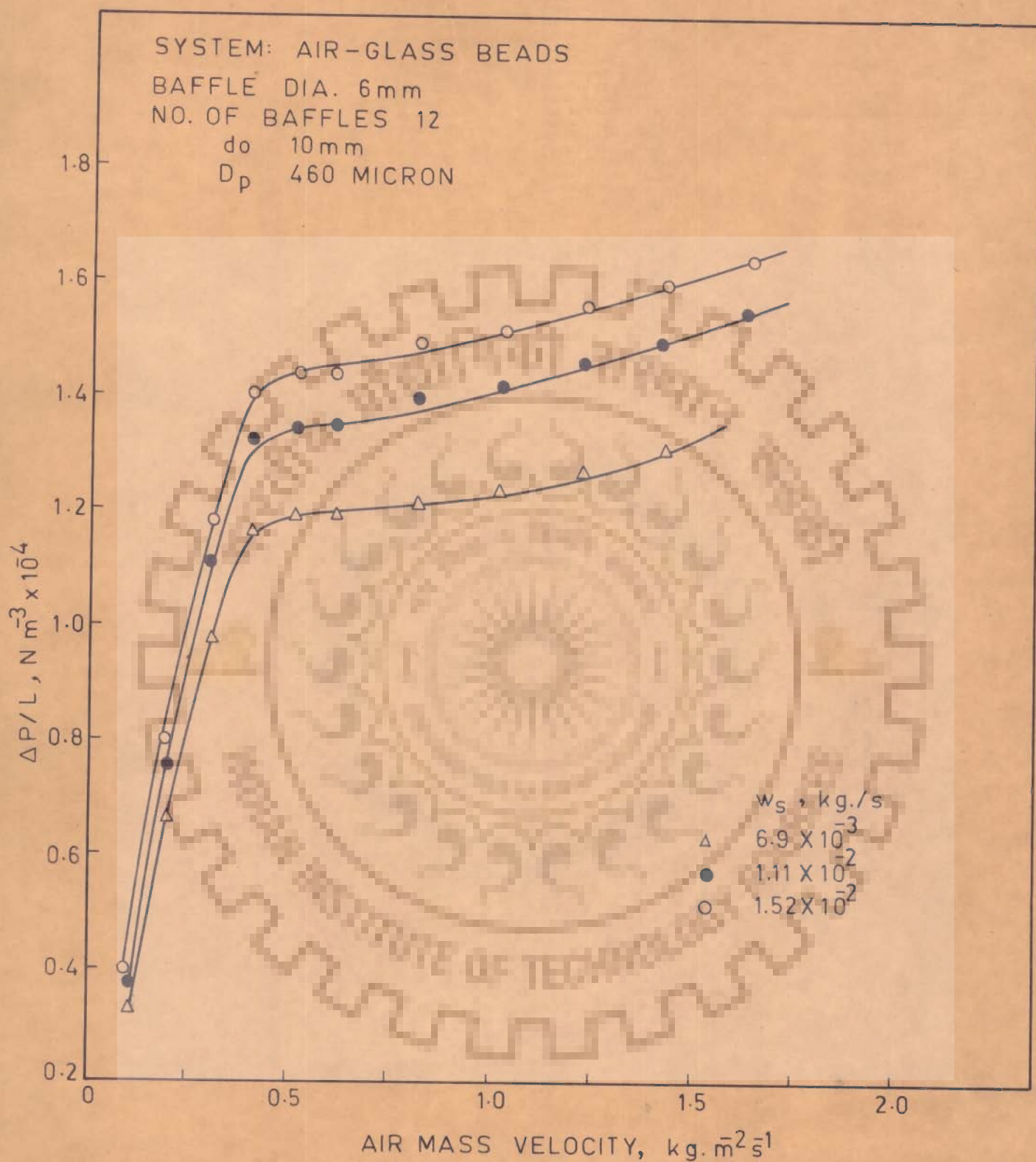


FIG 4.8 VARIATION OF $\Delta P/L$ WITH AIR MASS VELOCITY IN CONTINUOUS FLUIDIZED BEDS WITH VERTICAL BAFFLES.

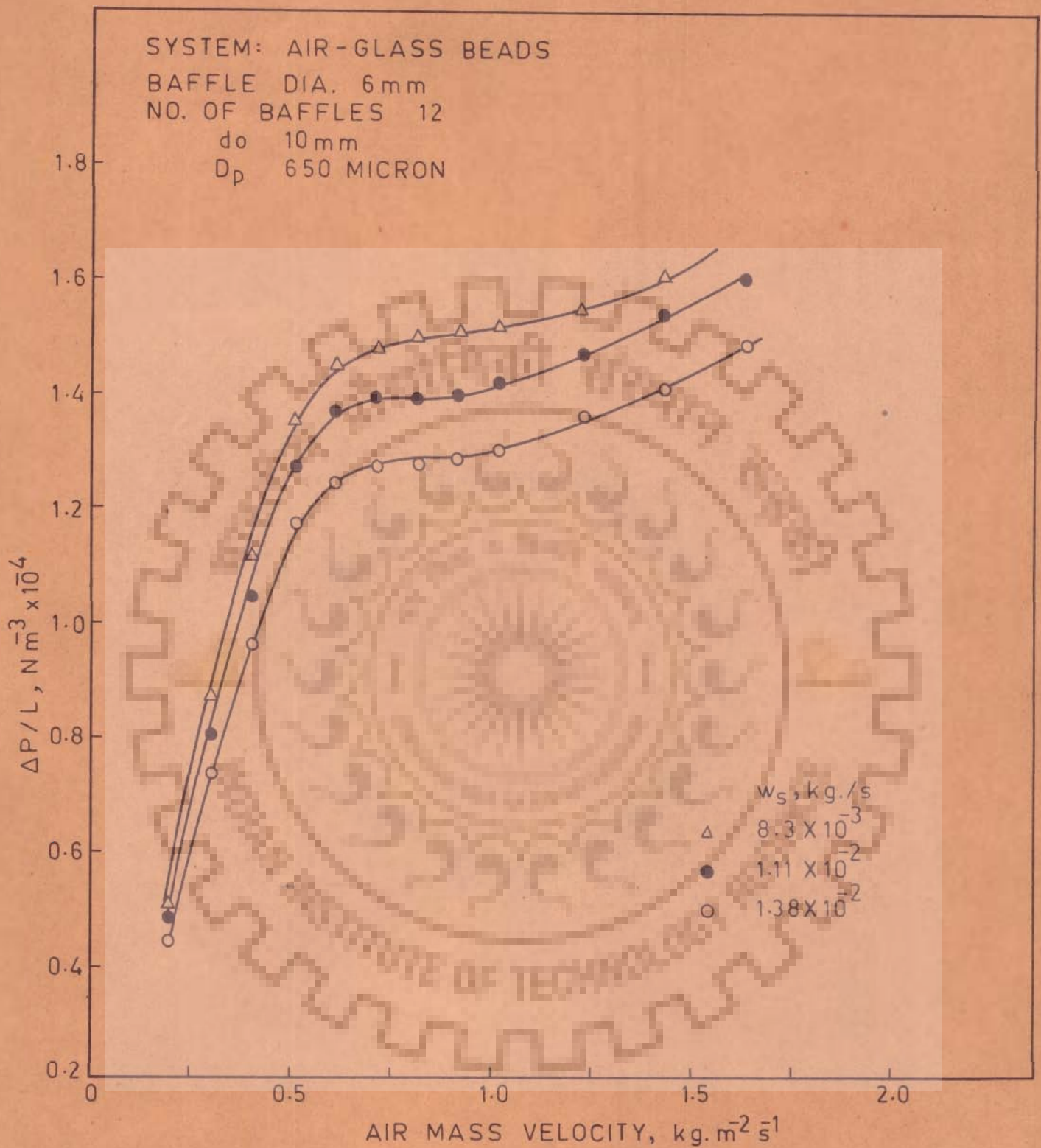


FIG. 4.9 VARIATION OF $\Delta P/L$ WITH AIR MASS VELOCITY IN CONTINUOUS FLUIDIZED BEDS WITH VERTICAL BAFFLES.

BAFFLE DIA. 6mm
 NO. OF BAFFLES 12
 D_p 650 MICRON
 w_s 8.3×10^{-3} kg./s

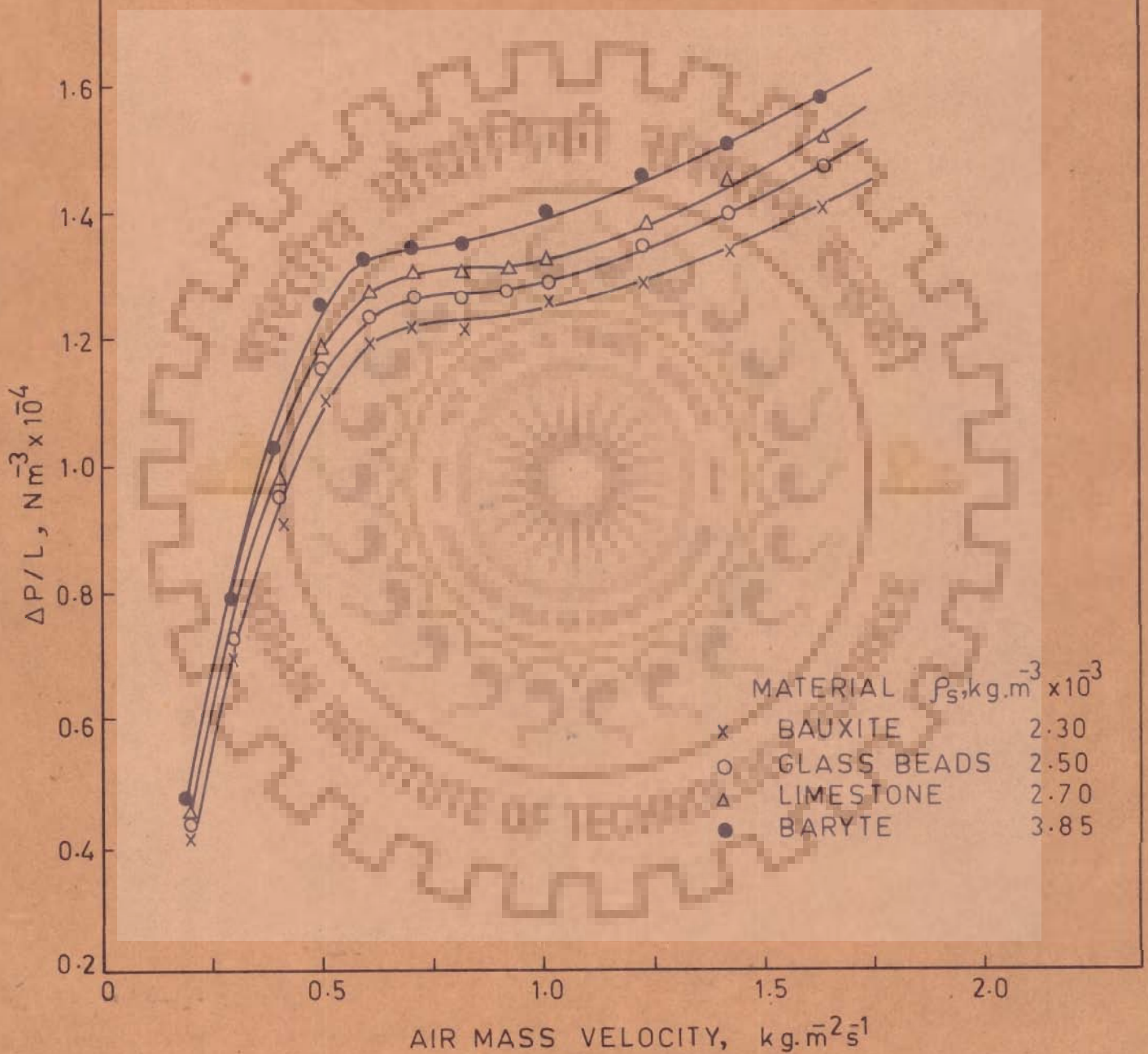


FIG. 4.10 VARIATION OF $\Delta P/L$ WITH AIR MASS VELOCITY IN CONTINUOUS FLUIDIZED BEDS WITH VERTICAL BAFFLES.

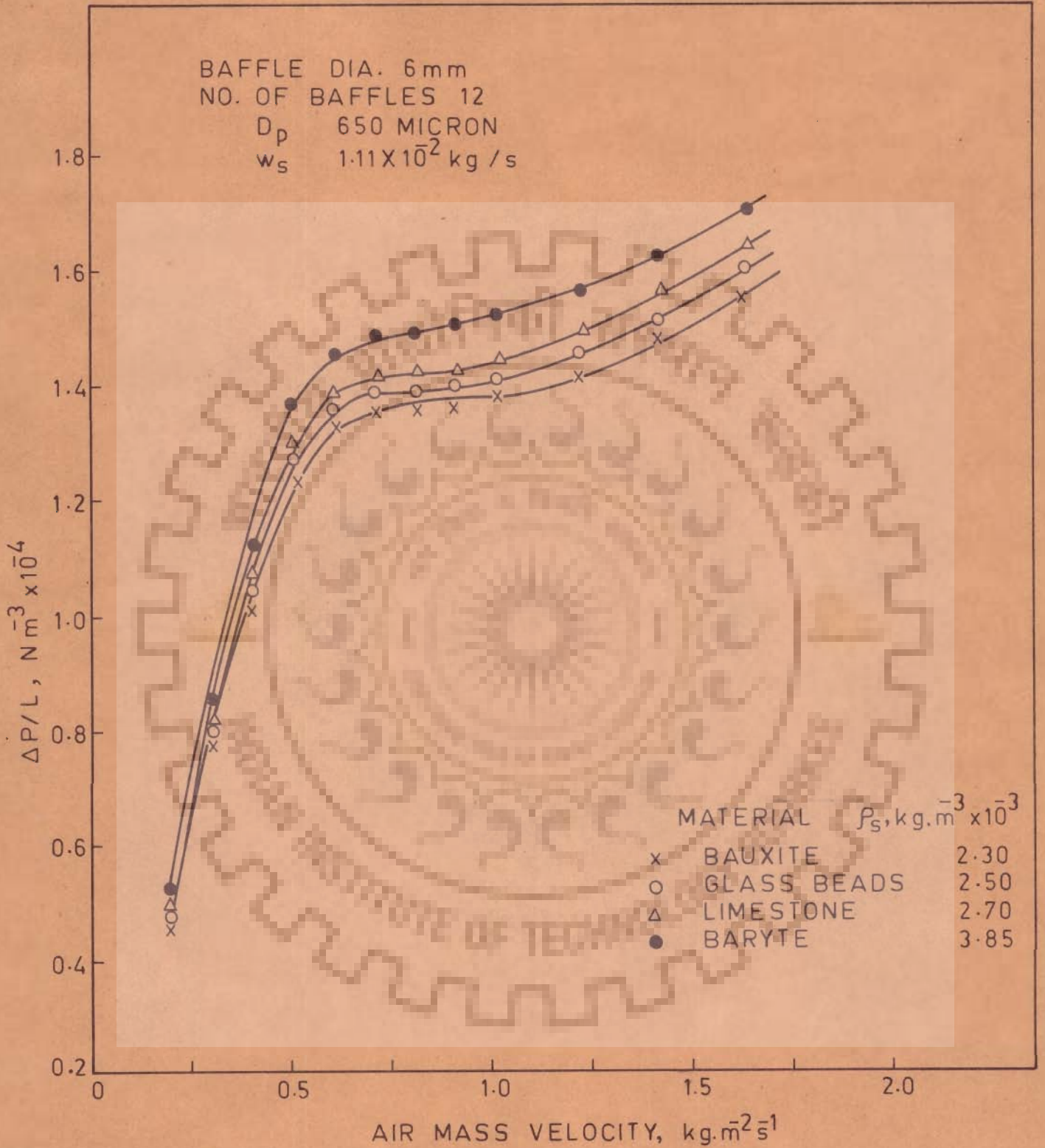


FIG. 4.11 VARIATION OF $\Delta P/L$ WITH AIR MASS VELOCITY IN CONTINUOUS FLUIDIZED BEDS WITH VERTICAL BAFFLES.

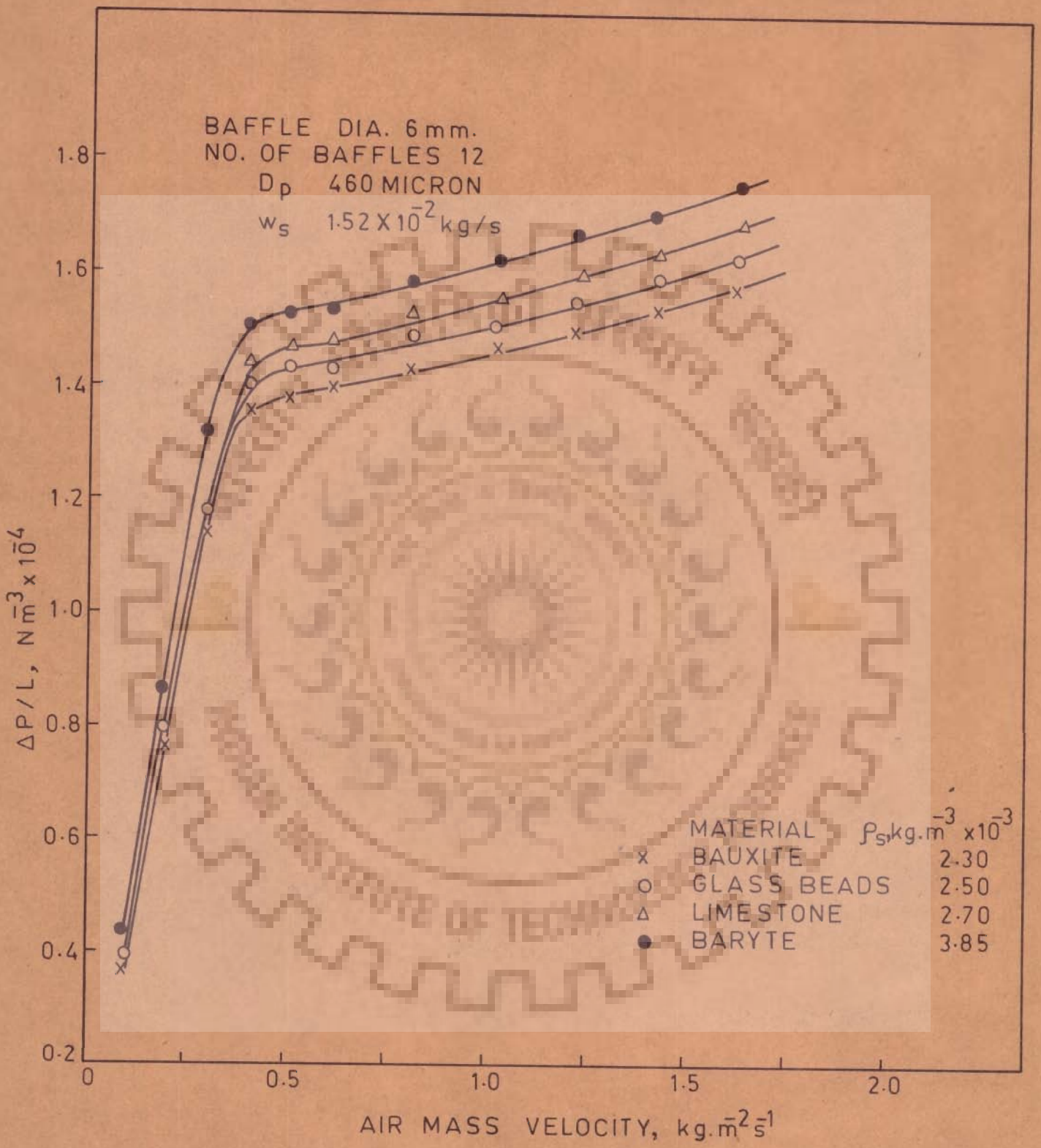


FIG. 4.12 VARIATION OF $\Delta P/L$ WITH AIR MASS VELOCITY IN CONTINUOUS FLUIDIZED BEDS WITH VERTICAL BAFFLES.

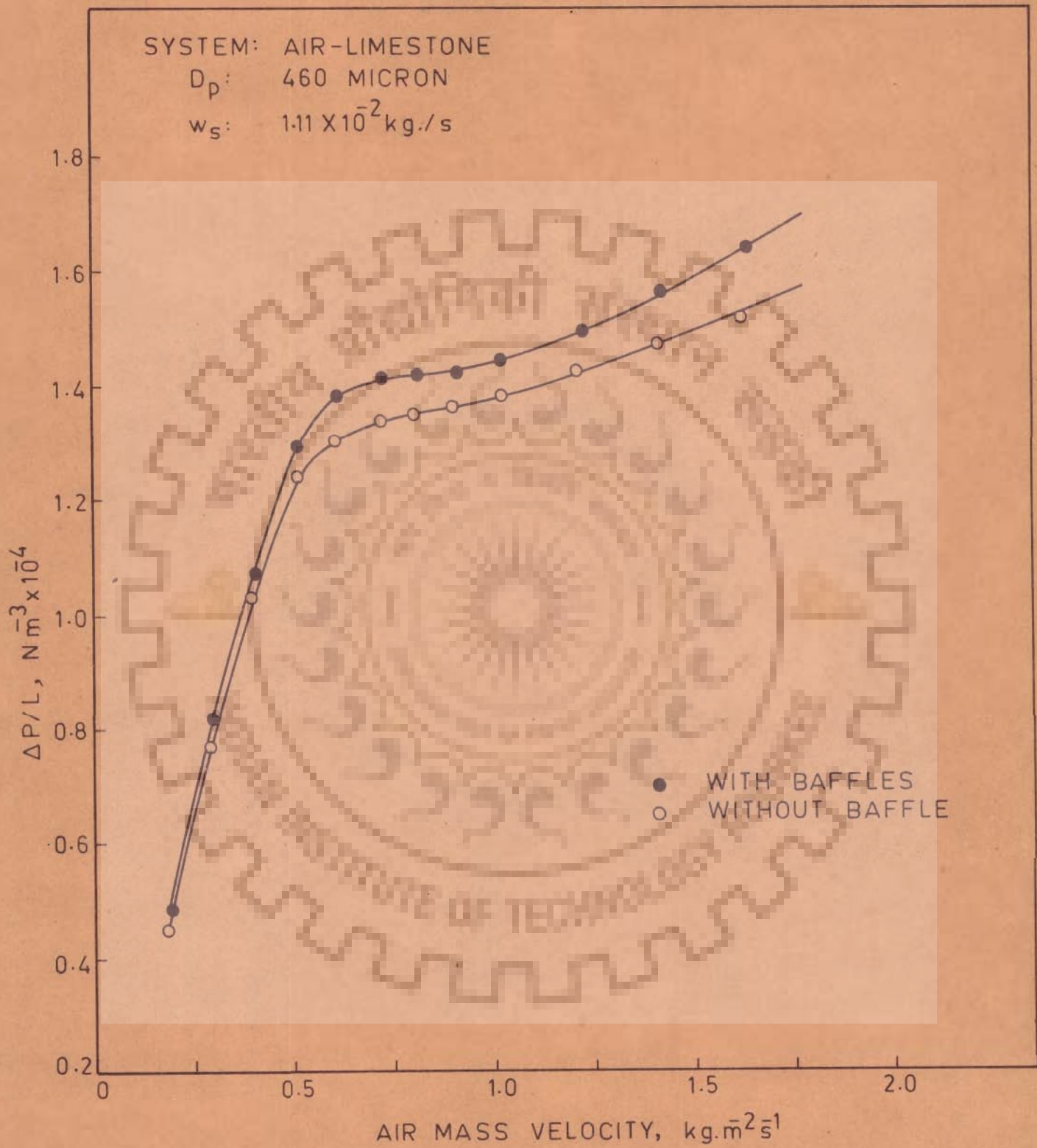


FIG. 4.13 VARIATION OF $\Delta P/L$ WITH AIR MASS VELOCITY IN BEDS WITH AND WITHOUT VERTICAL BAFFLES.

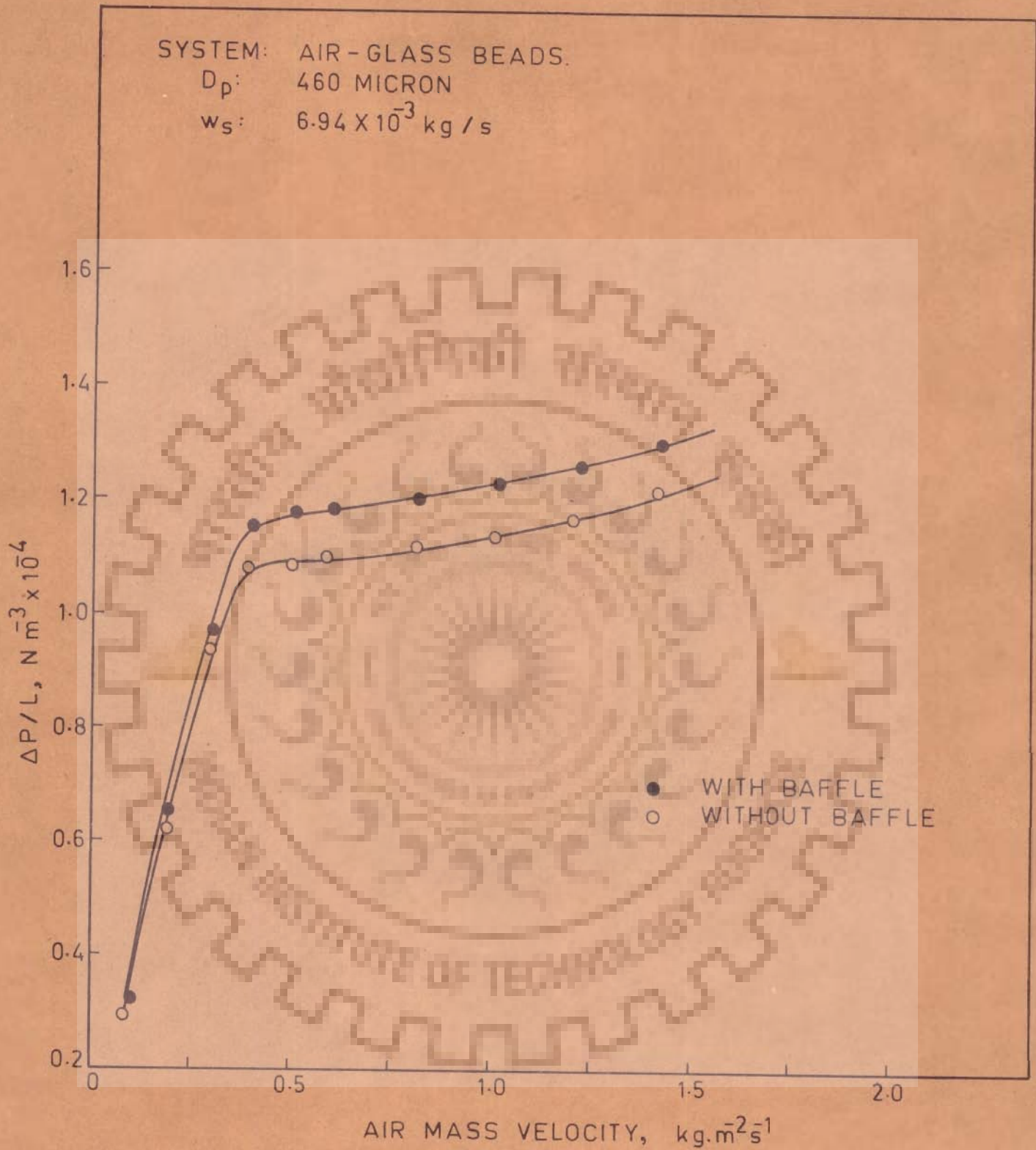


FIG. 4.14 VARIATION OF $\Delta P/L$ WITH AIR MASS VELOCITY IN BEDS WITH AND WITHOUT VERTICAL BAFFLES.

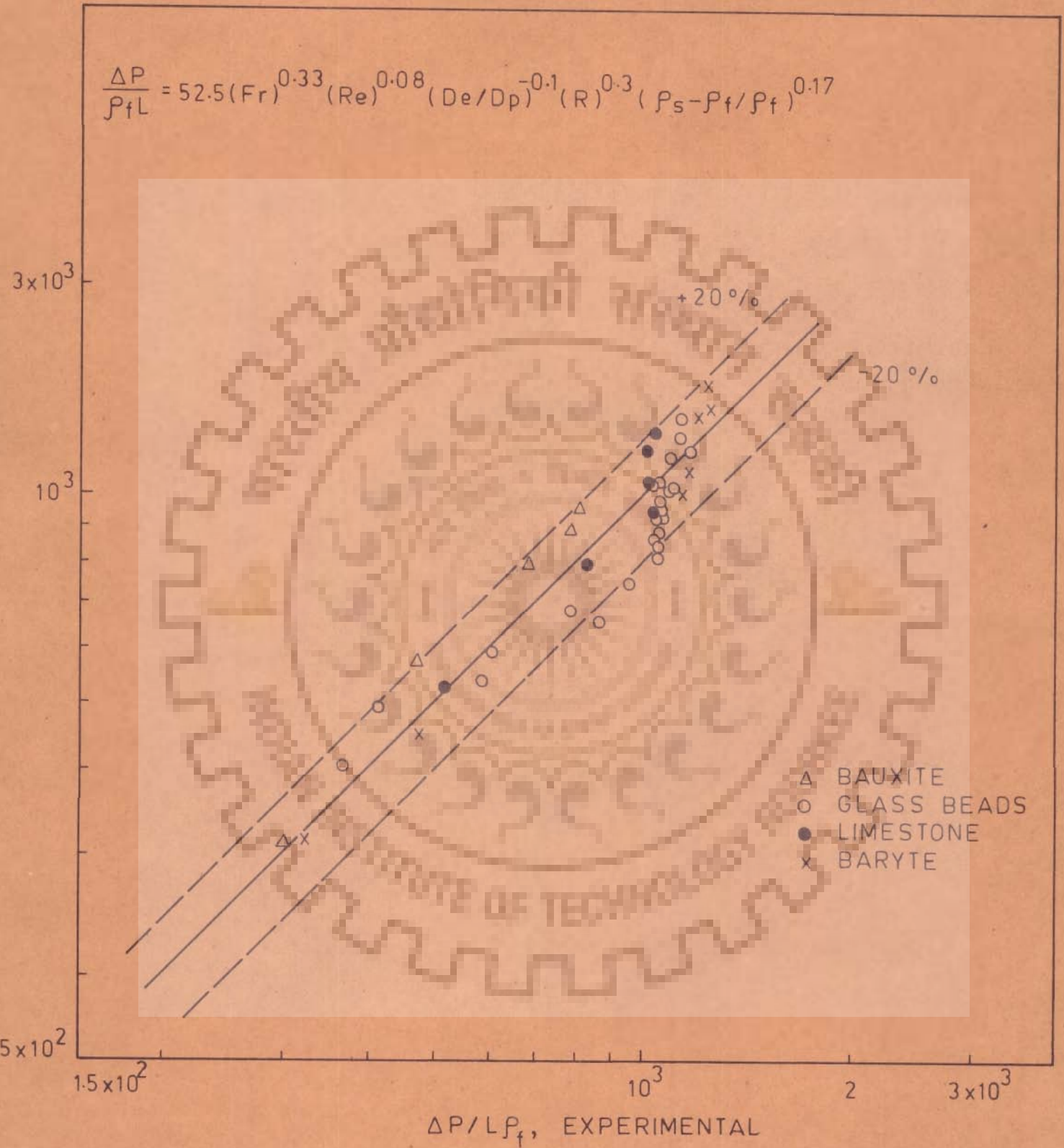


FIG. 4.15 COMPARISON OF VALUES OF $\Delta P / L \rho_f$ EXPERIMENTAL AND PREDICTED IN CONTINUOUS FLUIDIZED BEDS WITH VERTICAL BAFFLES.

SYSTEM: AIR-GLASS BEADS

BAFFLE DIA. 6mm

NO OF BAFFLES 12

d_o 10mm⁻²

w_s 1.52×10^{-2} kg./s

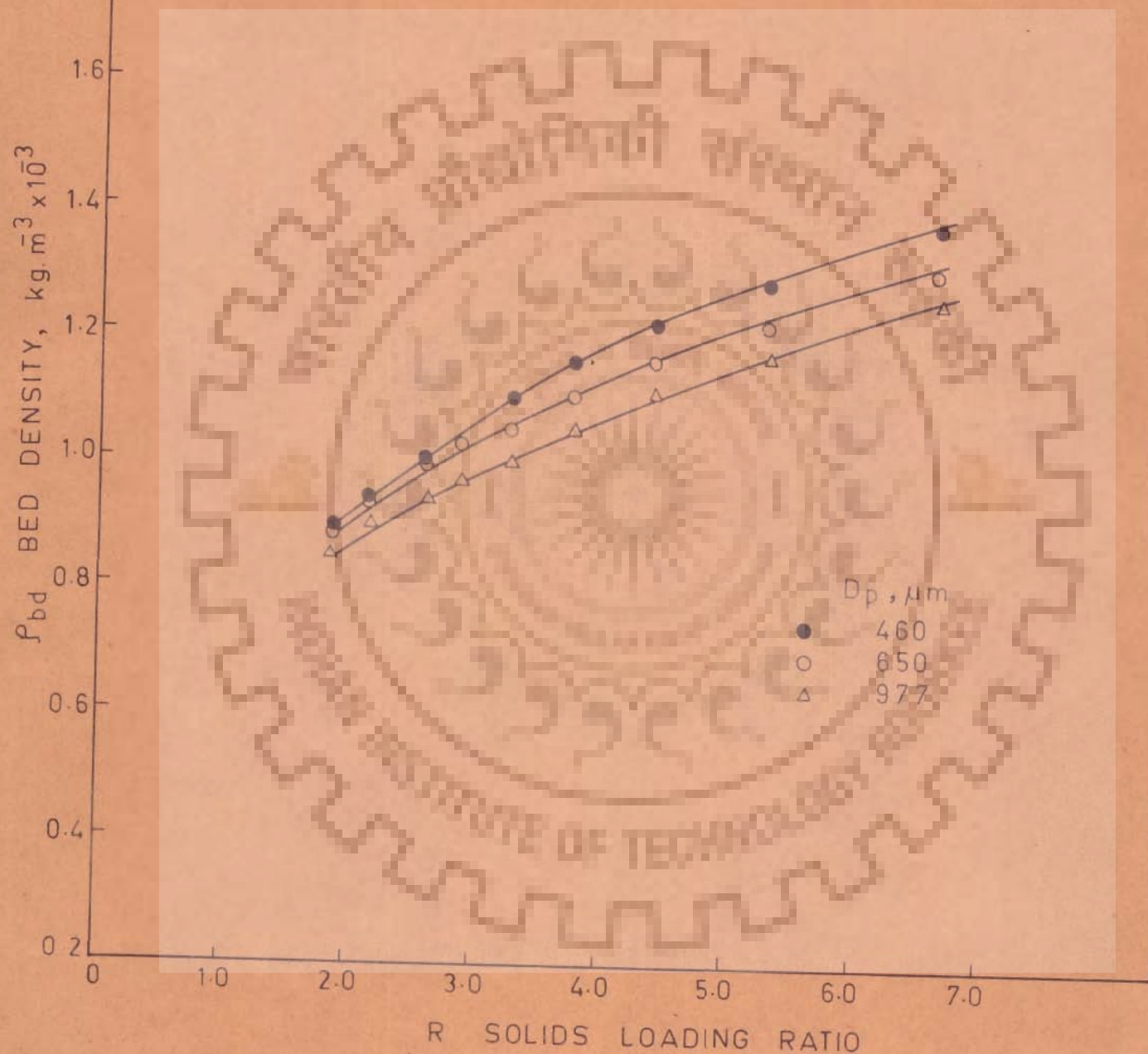


FIG. 4.16 VARIATION OF BED DENSITY WITH SOLIDS LOADING RATIO IN CONTINUOUS FLUIDIZED BEDS WITH BAFFLES.

SYSTEM: AIR-BARYTE
BAFFLE DIA. 6mm
NO. OF BAFFLES 12
do 10 mm
 $w_s 1.52 \times 10^{-2} \text{ kg/s}$

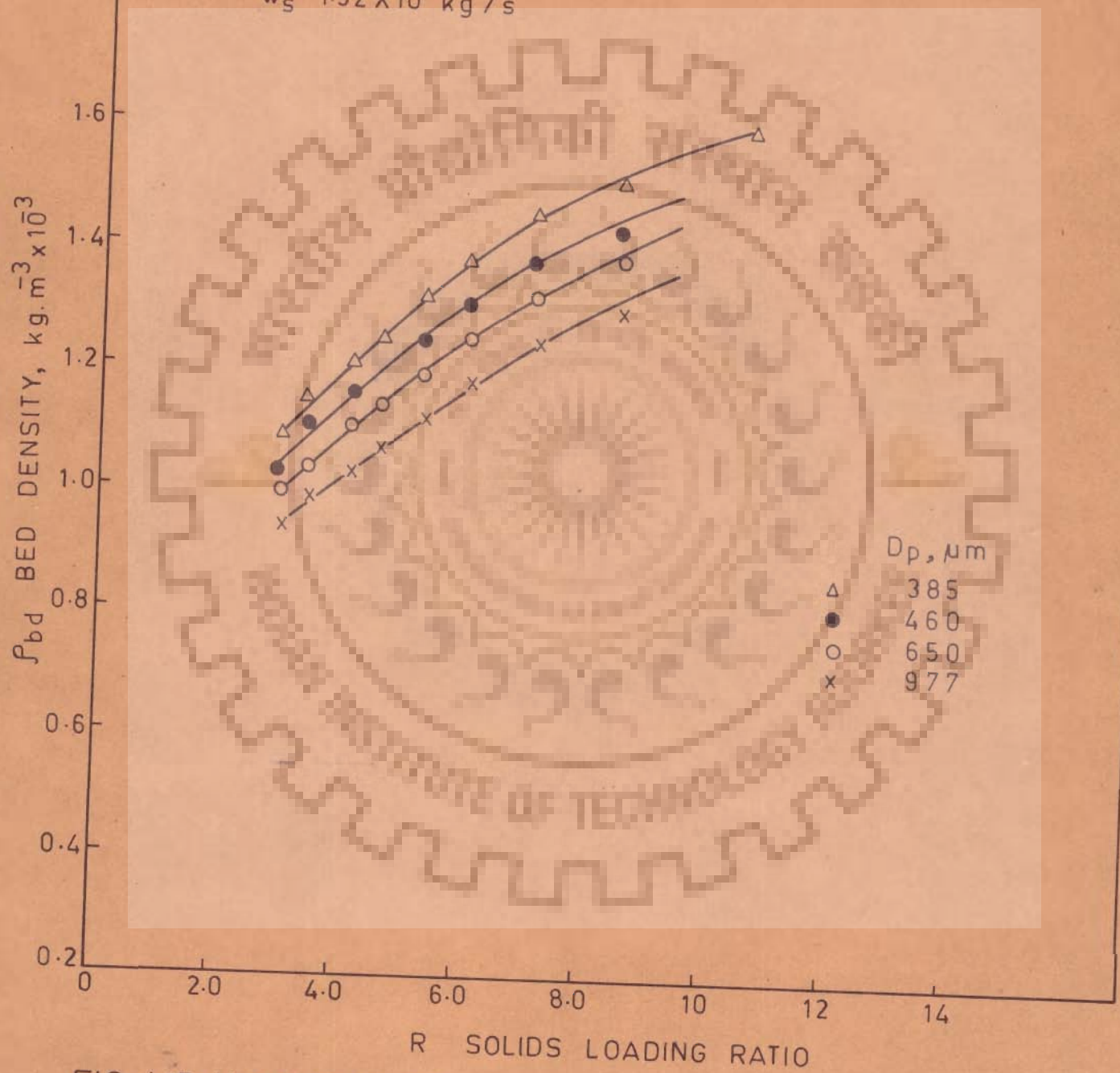


FIG. 4.17 VARIATION OF BED DENSITY WITH SOLIDS LOADING RATIO IN CONTINUOUS FLUIDIZED BEDS WITH BAFFLES.

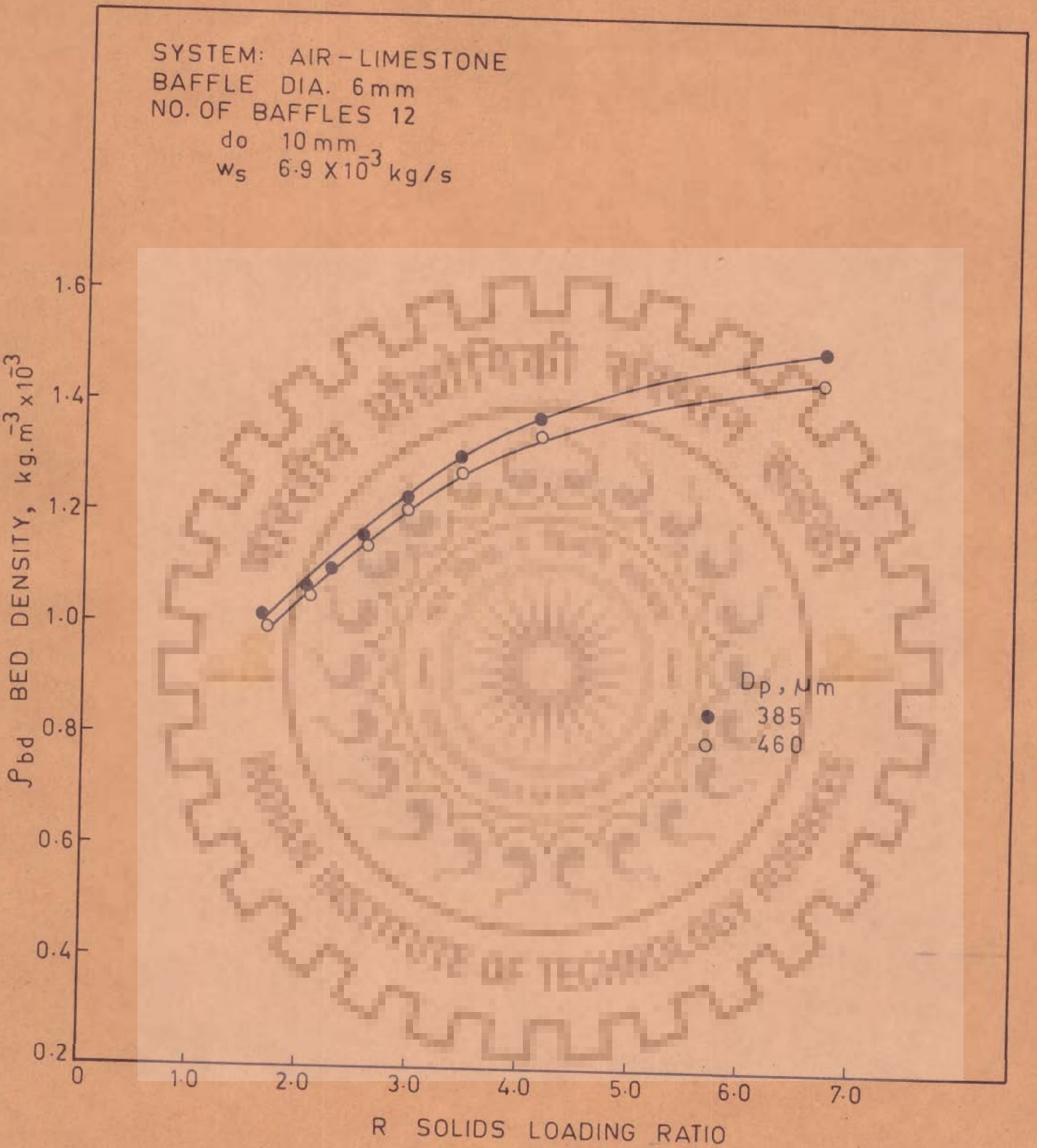


FIG. 4.18 VARIATION OF BED DENSITY WITH SOLIDS LOADING RATIO IN CONTINUOUS FLUIDIZED BEDS WITH BAFFLES.

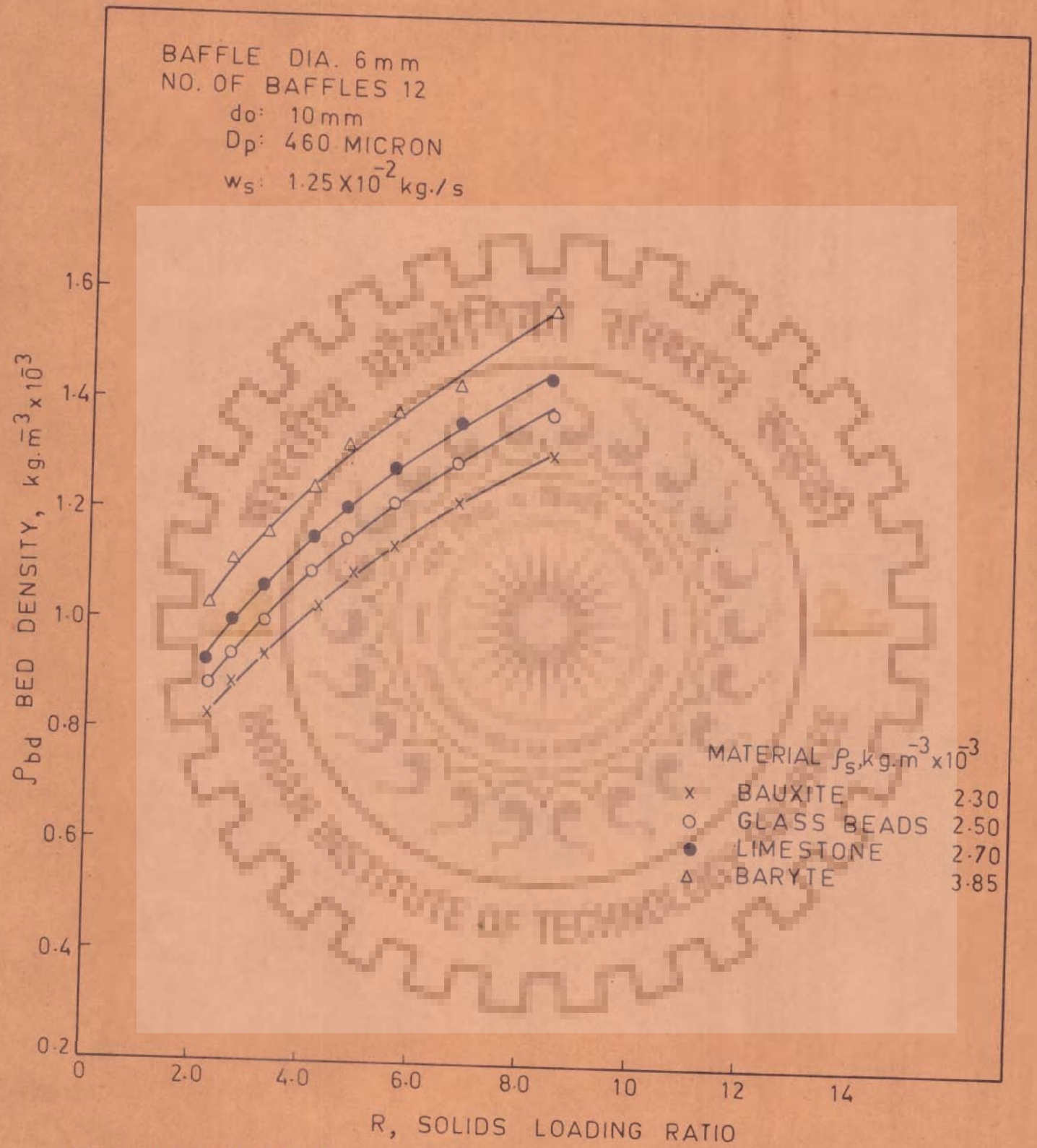


FIG. 4.19 VARIATION OF BED DENSITY WITH SOLIDS LOADING RATIO IN CONTINUOUS FLUIDIZED BEDS WITH BAFFLES.

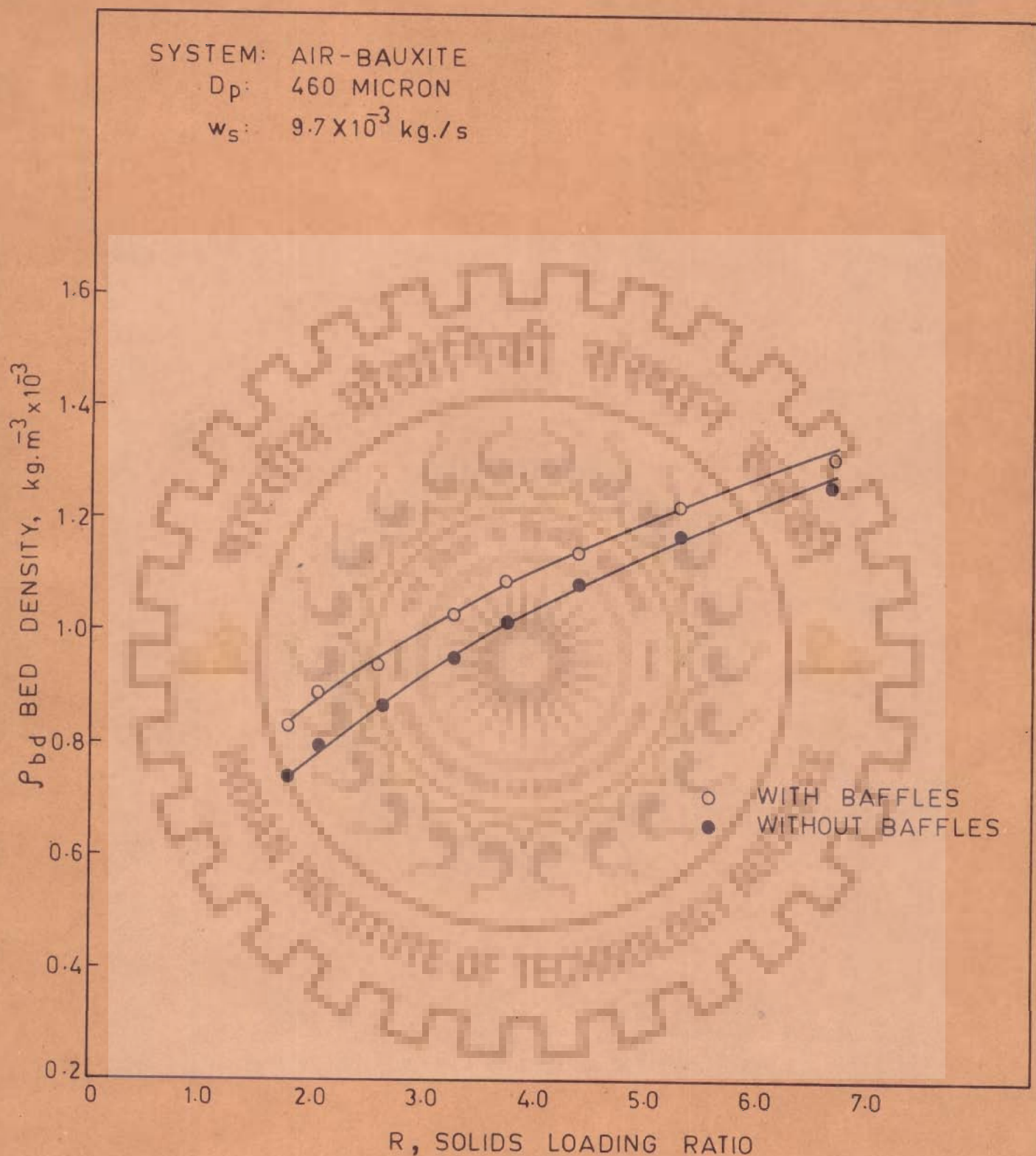


FIG. 4.20 VARIATION OF BED DENSITY WITH SOLIDS LOADING RATIO IN CONTINUOUS FLUIDIZED BEDS WITH AND WITHOUT BAFFLES.

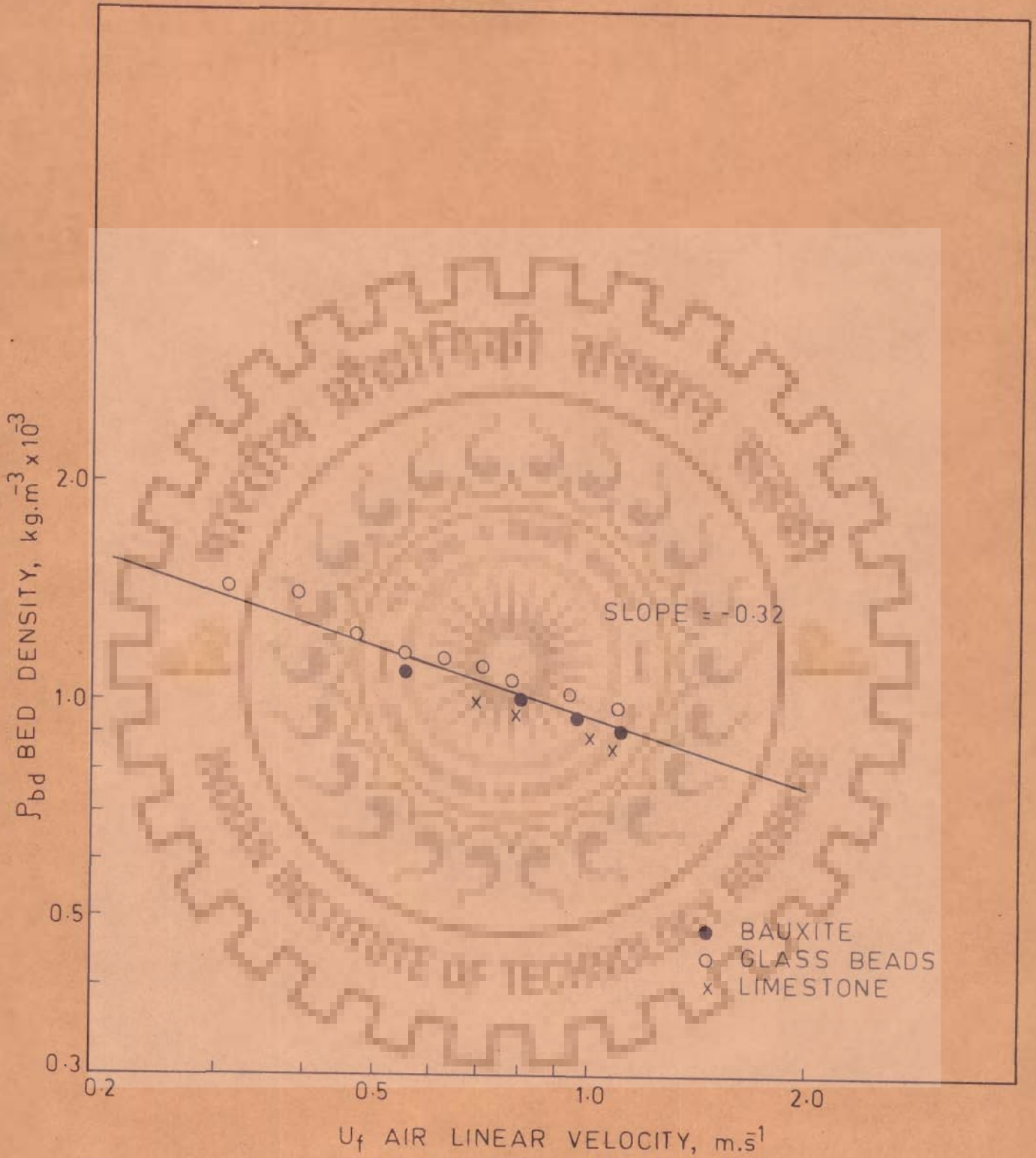


FIG. 4.21 VARIATION OF BED DENSITY WITH AIR LINEAR VELOCITY.

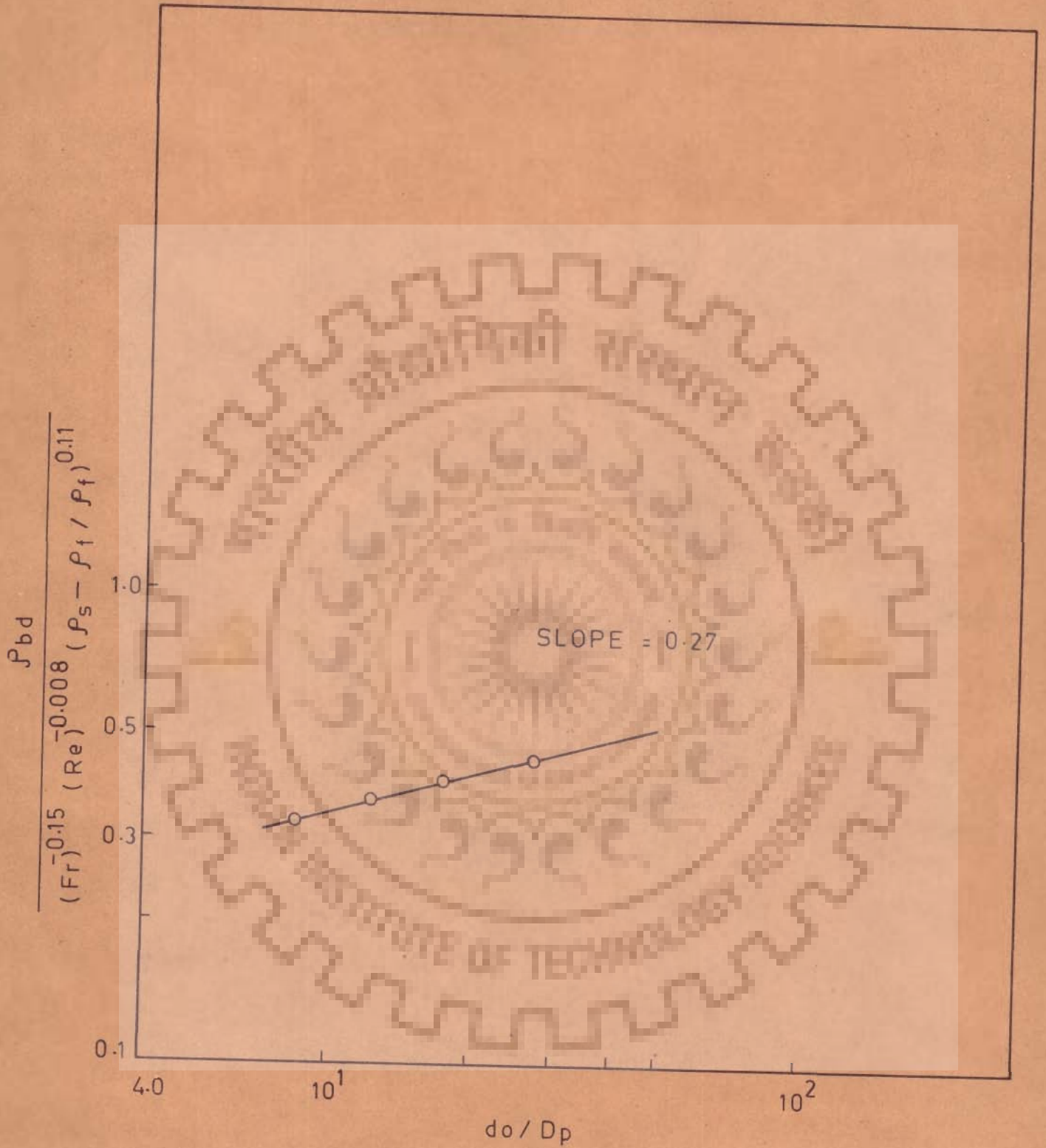


FIG. 4.22 EFFECT OF d_o / D_p ON BED DENSITY

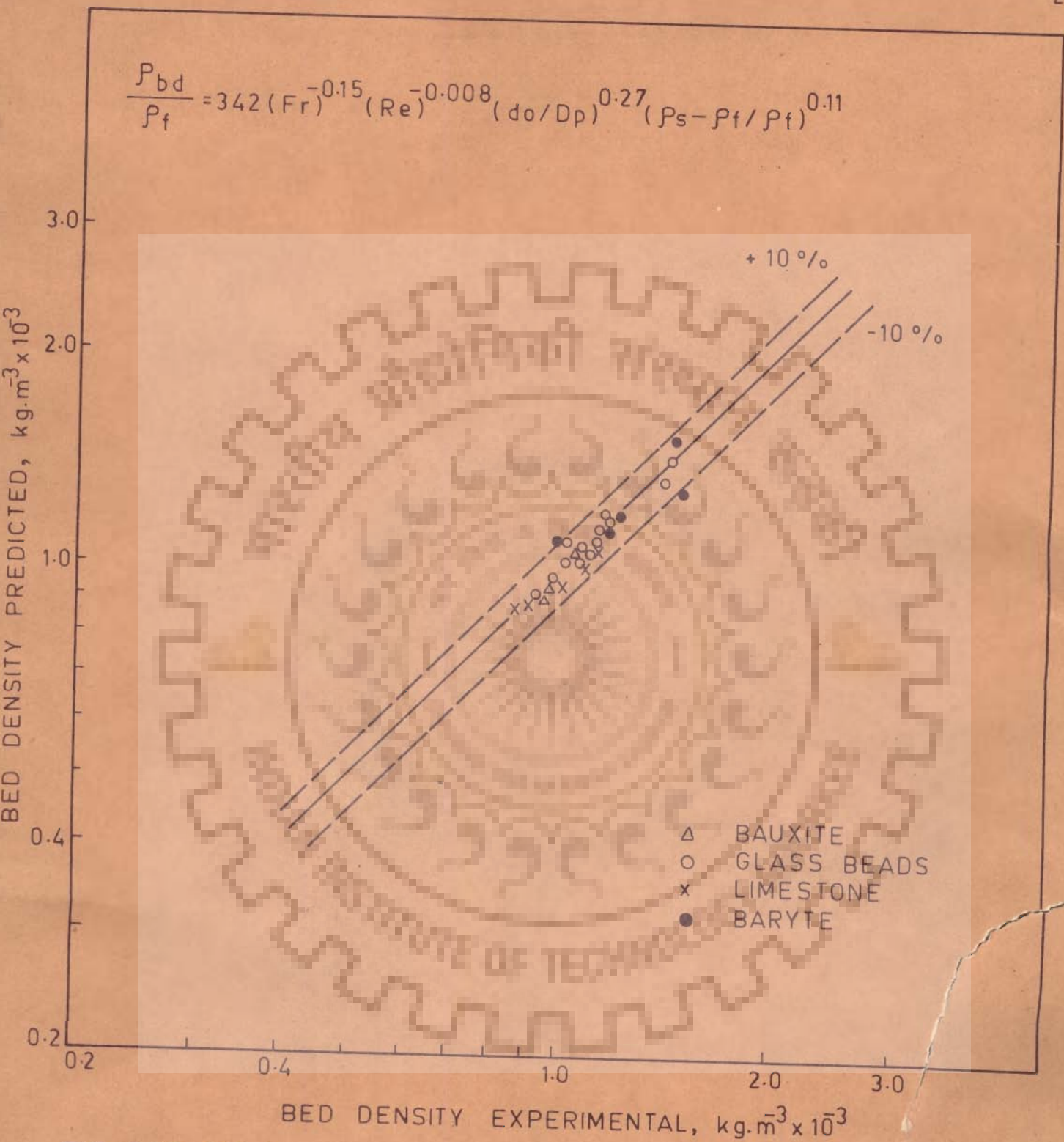


FIG. 4.23 COMPARISON OF VALUES OF BED DENSITY OBSERVED AND PREDICTED IN CONTINUOUS FLUIDIZED BEDS WITH BAFFLES.

C H A P T E R - VA B S T R A C T

Effect of vertical internal baffles on bed hold up of mixed size particles has been studied in countercurrent continuous gas-solids fluidization. A dimensionless correlation has been proposed for predicting the bed hold-up ratio as a function of reduced gas velocity (U_f/U_{mf}) and dimensionless time parameter (τ_B).

CHAPTER - VHOLD-UP STUDIES IN CONTINUOUS FLUIDIZATION
WITH VERTICAL BAFFLES

In continuous fluidized bed reactors, the quality of product will depend upon the RTD of the solids. The determination of RTD of solids is complicated and time consuming. In practice average residence times and the bed hold ups are evaluated for any system, which give sufficient information on the performance of the reactor. In mixed feeds, a better quality product can be achieved if the reactors provide an inherent mechanism which will ensure a longer stay time for the larger particles, compared to smaller particles. In fluidized beds provided with internal baffles, it is expected that larger particles with small d_o/D_p ratios will have a tendency of less free movement and longer stay times in the bed. However, when mixed size feeds are used, the average values of bed hold up do not give enough information for predicting the reactor performance. In the present experimental investigations an attempt has been made to evaluate the average stay times of larger and smaller particles when mixed feeds are used.

5.1 EXPERIMENTAL SET-UP

The schematic flow diagram of the experimental unit is shown in Fig. 5.1. This essentially consisted of a

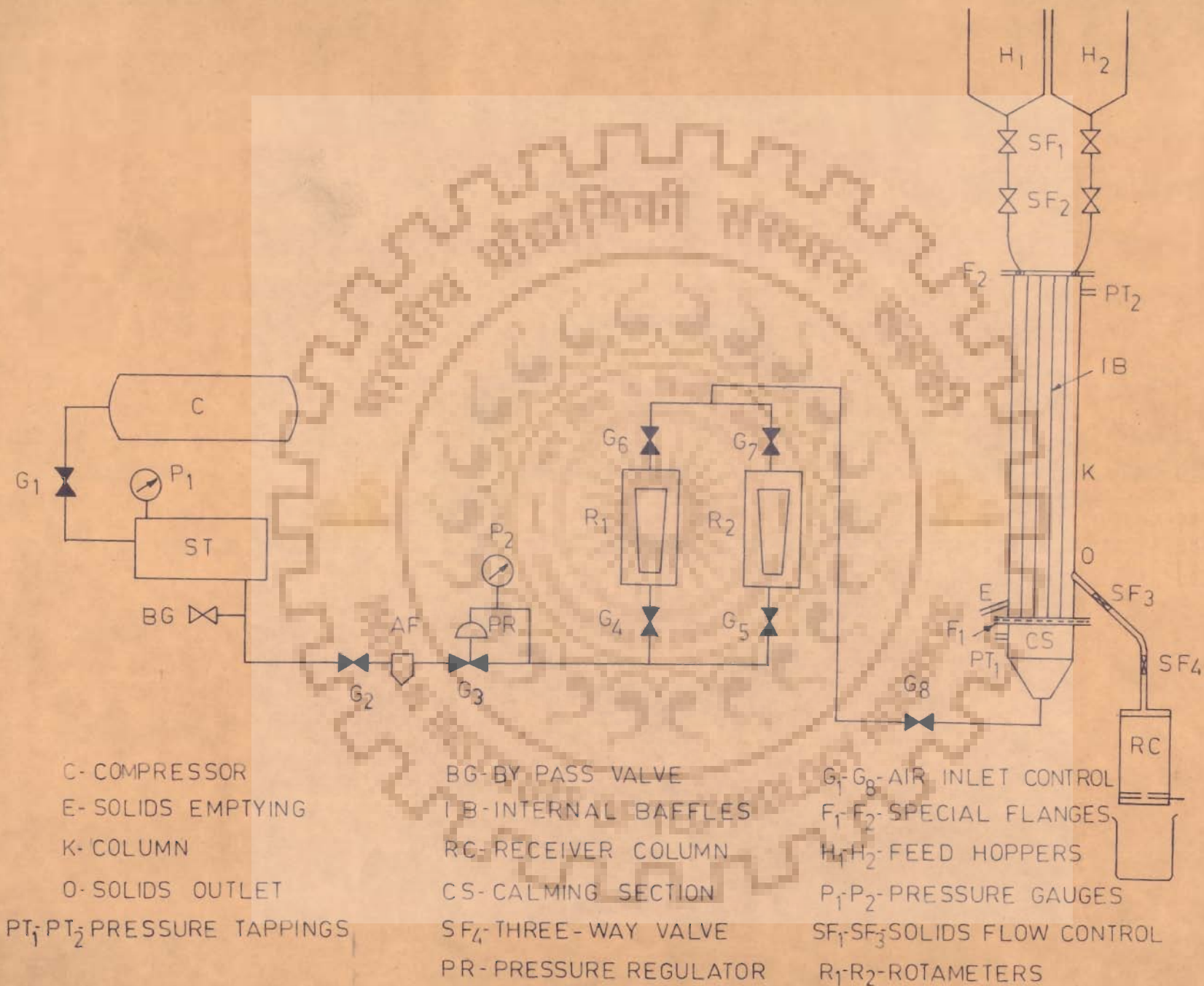


FIG. 5.1 SCHEMATIC DIAGRAM OF EXPERIMENTAL SET UP

perspex column (K) 70 mm I.D. and 610 mm length placed between two special flanges (F_1, F_2) 12 baffles (IB) of 6 mm diameter and 610 mm effective length made of stainless steel rod, were inserted in the column as internal baffles. A grid plate made of 3 mm thick aluminium sheet having 1.5 mm holes drilled on a square pitch of 4 mm was fitted in the special flange (F_1). The area of the openings in the grid was 10% of the empty column cross section. The grid plate, covered with a 200 mesh brass wire screen, was used as air distributor and to support the solids. Air drawn from the compressor (C) and regulated through pressure regulator (PR) was introduced into the column at the bottom through a calming section (CS) which was filled with porcelain raschig rings to provide uniform air distribution through the bed. The solids were fed into the column from the hoppers (H_1, H_2). The solids feed rates were controlled by two stop cocks (SF_1, SF_2). The solids discharge rate from the column was controlled by a 2-way and a 3-way stop cocks (SF_3, SF_4). The solids leaving the column were collected in a receiver (RC). The samples of solids leaving the column were collected through a 3-way stop cock (SF_4). The photograph of general layout of the experimental unit is shown in Fig. 5.2. Photographs of the solids feeding and discharge and sampling systems are shown in Figs. 5.3 and 5.4.

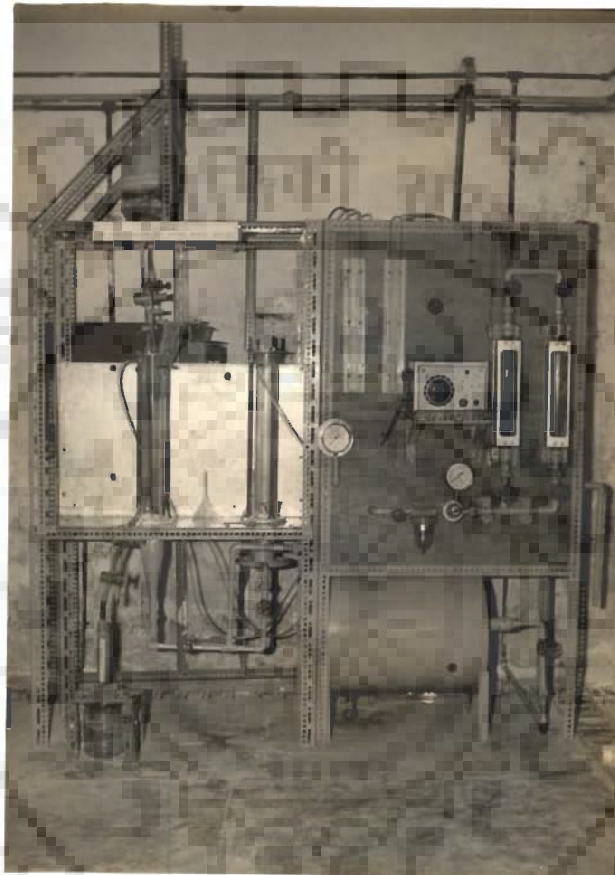


FIG. 5.2 PHOTOGRAPH SHOWING EXPERIMENTAL
SET UP FOR HOLD-UP STUDIES IN
CONTINUOUS BEDS WITH VERTICAL
BAFFLES.

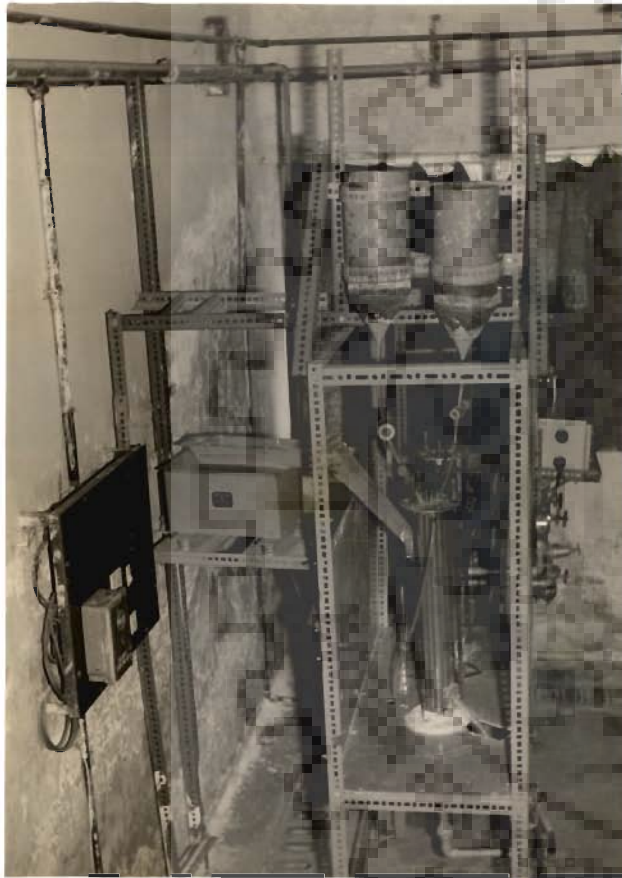


FIG.5.3 PHOTOGRAPH SHOWING SOLIDS FEEDING ARRANGEMENT.



FIG.5.4 PHOTOGRAPH SHOWING SOLIDS DISCHARGE AND SAMPLING ARRANGEMENT.

5.2 PROCEDURE

Solids were fed to the fluidizing column from the feed hoppers (H_1 and H_2). The solids feed rate from the hopper to the column was adjusted by using stop cock (SF_1). The discharge rate of solids was regulated with the help of a stop cock (SF_3). Air was then introduced from the bottom of the column and the bed attained the fluidizing conditions. Steady state conditions were obtained by adjusting the discharge rate of solids same as that of the feed rate. Steady state conditions were assumed when

- i) bed height
- ii) pressure drop across the bed and
- iii) the solids inlet and outlet rates remained constant.

The steady state, invariably, reached in about 15-20 minutes time.

Since the hold up studies were conducted using feeds of mixed sizes, it was essential to check the solids compositions in bed and discharge streams. The composition of the outgoing stream was determined by sieve analysis of the samples withdrawn through the 3-way stop cock (SF_4), when the composition of the discharged solids remained steady and matched with feed composition, stop cocks (SF_2 and SF_3) were simultaneously closed to arrest the material in the bed. The solids remained in the bed, give the bed hold up. The composition of the solids in

the bed was determined by withdrawing the material from the column through discharge outlet (E) and by performing sieve analysis. For getting data on bed and feed composition at different air flow rates, it was necessary to maintain the bed hold-up constant. After solids were discharged for measuring the bed hold up at a given air flow rate, fresh solids were charged through the feed hopper into the column by opening the stop cock (SF_2). The discharge valve (SF_3) was adjusted in such a way that the bed height was same as the value taken in the earlier run and by minor adjustment of the discharge valve steady state conditions were obtained. With practice it was possible to make this adjustment in such a manner that the bed hold up at different air flow rates remained almost constant.

The observations were made on bed and discharge compositions at different air flow rates for different feed compositions and different bed hold ups.

The range of experimental variables is shown in table 5.1.

TABLE-5.1RANGE OF EXPERIMENTAL VARIABLES

Material	Glass Beads
Density	2.5×10^3 kg/m ³
Particle size	D _{p1} 460 micron
	D _{p2} 650 micron
Bed Hold up	0.425 - 0.800 kg
Solids Feed Rate	2×10^{-3} - 4.2×10^{-3} kg/s
Air Flow Rate	0 - 2 kg/m ² .s
Solid Feed Composition (W_{DP1}/W_{DP2})	1:2, 1:1, 2:1

5.3 RESULTS AND DISCUSSIONS

Data obtained in continuous fluidized beds with baffles for constant bed hold up and different compositions of mixed sized particles, with regard to feed, bed and discharge streams are reported in tables 5.2 to 5.10. Data were obtained without baffles under similar conditions of operations as mentioned above and are given in tables 5.11 to 5.14.

In order to ensure that the data obtained at different air flow rates for a given feed composition and solids feed rate are at constant bed hold up

conditions, the quantity of material present in the bed under steady state conditions is evaluated and the data are shown in Figs. 5.5 and 5.6. As can be seen from the graphs the total bed hold up during the experimental runs at different air velocities for a given feed composition has been nearly constant. The maximum deviation from the average values has been $\pm 3\%$. In the experiments, it was possible to have any average bed hold up value for different feed rates of solids and at different air velocities. The present experimental data have been taken corresponding to different average hold up values in each case of with and without baffles for a given feed compositions, feed rates and air flow rates. However, on analysis of the hold up material, it was found that the hold up values for each particle size varied with gas flow rate for a given feed composition. The bed hold up for large size particles increased with air flow rate while that of the smaller particles decreased with air flow rates, indicating change in bed composition with air flow rates.

The mean residence times \bar{t}_1 and \bar{t}_2 for two different particles D_{p1} and D_{p2} in continuous fluidized beds with mixed feeds, may be defined as

$$\bar{t}_1 = \frac{W_1}{w_1} , \quad \bar{t}_2 = \frac{W_2}{w_2}$$

where W_1 and W_2 are the individual hold ups of each

particle size and w_1 and w_2 are the individual feed rates of the solids of each sizes when mixed feeds of particle size D_{p1} and D_{p2} are used. The suffix 1 is for small size particles and 2 for large size particles. The mean residence time for any particle size will be affected if the hold up fraction of that particular size changes. In order to analyse the data with regard to the individual bed hold up of a given size, a term hold up ratio is defined as,

$$H(2,1) = \frac{\bar{t}_2}{\bar{t}_1} = \frac{W_2}{W_1} \cdot \frac{w_1}{w_2} .$$

The bed hold up ratio gives a dimensionless measure of the retention times of different particles in the bed. This will be affected by the feed rates of different sized particles as well as the hold ups of these particles. If the feed rates of two different sized particles are same, the hold up ratio will give the ratio of the individual hold up of different sizes. In other cases, the bed hold up ratio is a product of the ratio of the hold up of larger to smaller particles in the bed W_2/W_1 and the ratio of the feed rates of smaller to larger particles w_1/w_2 .

5.3.1 Hold up ratio without Baffles

Fig. 5.7 shows the variation of bed hold up ratio with air mass velocity for a constant feed composition

of 1:1 with bed hold up as the parameter. It was observed that the bed hold up ratio increased with increase in air flow rate upto a value (G_f/G_{mf} ranging between 1.8-2.0) beyond which the hold up ratio remained steady or the rate of increase was negligible. Similar trend was observed for other feed composition also as shown in Fig. 5.8.

Fig. 5.9 is the plot at constant bed hold up, showing the variation of bed hold up ratio with air mass velocity with feed composition as the parameter. It was observed that the hold up ratio first increased with increase in air mass velocity upto a value of G_f/G_{mf} ranging between 1.8-2.0, beyond which the rate of increase slowed down. It is also observed that for a constant air mass velocity, the bed hold up ratio was less for the beds having greater proportion of larger size particles.

5.3.2 Hold-Up Ratio with Vertical Baffles

Fig. 5.10 shows the variation of bed hold up ratio with air mass velocity for constant bed hold up with feed composition as parameter. It was observed that unlike in the case of beds without baffles, the bed hold up ratio increased steadily with increase in air flow rate. It was also observed that the bed hold up ratios were lower for the beds having greater proportion of large size particles in the solids feed for a given bed hold up

and air flow rate. This observation is in accordance with that made in fluidized beds without baffles. Similar trends were observed for other bed hold ups with feed compositions as parameter as shown in Figs. 5.11 and 5.12.

Fig. 5.13 shows at constant solids feed composition, the variation of bed hold up ratio with air mass velocity with bed hold up as parameter. Bed hold up ratio was observed to increase with increase in air flow rate. The bed hold up ratios were observed to be more for large bed hold up.

Figs. 5.14 and 5.15 show the comparison of the variation of bed hold up ratio with air mass velocity with feed composition as parameter in beds with and without baffles. It was observed from these plots that the bed hold up ratio increased steadily with increase in air mass velocity in beds with baffles, whereas in beds without baffles, the bed hold up ratio increased with increase in air mass velocity in the range of G_f/G_{mf} between 1.8-2.0, beyond which it remained steady.

5.3.3 Mechanism of Particle Movement in continuous Fluidized Beds with Mixed Feeds.

In a continuous fluidized bed, there is a velocity profile for the gas which is nearly flat at the centre and decreases towards the wall of the column. This

results in greater particle movement at the centre of the bed and normally particles near the wall tend to stagnate. Thus at any velocity higher than the minimum fluidizing velocity for uniform sized particles, there will only be pockets of stagnation near the periphery and zones of violent particle movement near the centre. The area of stagnant zone decreases with increase in air velocity.

When mixed sized feeds are used, at any given air velocity, while the linear velocity profile is same as mentioned above, the tendency of larger particles having lower values of G_f/G_{mf} at any gas flow rate will be, to remain less mobile than smaller particles. This invariably leads to greater movement of small particles throughout in the bed than the larger particles. Even in the periphery where the linear velocity of gas is much lower, smaller particles will exhibit greater random motion. Thus at air velocities, when bed is by and large uniform, at the point of solids discharge from the column, the smaller particles will have greater tendency to go out of the discharge opening than the larger particles. This will result in continuous depletion of smaller size particles in the bed giving higher bed hold up ratios.

When the gas velocity is sufficiently high, the beds will indicate bubbling tendencies. As the bubbles of gas rise upward in the fluidizer, its size grows rapidly and solid particles are carried upward. The bubbles break near the top surface and particles carried by the bubbles are thrown out. The movement of the bubbles continuously displaces solids upwards, leading to downward movement of solids in the rest of the bed. As the bubbles move up, the wake behind it sucks in solids from the surroundings and carry it along with the bubbles. In the bubbling beds, the downward movement of solids is expected to be slower than the upward movement of the solids caused by the bubble rise. Kondukov et al [148] observed that the particles near the wall of the column usually remain there for a while before dropping into the bed. Because of the bubbling tendency in mixed sized beds, the smaller particles are preferentially picked up by the wake of the bubble and are kept in continuous motion. Any particle in the bed has two forces working on it.

- i) the suction from the wake behind the bubble trying to carry the particles upward
- ii) the random motion of particles trying to push the particle out through the discharge.

Both larger and smaller particles have fairly turbulent motion even near the wall, giving them equal chance to

get out of the bed through the discharge in proportion to their concentrations. The suction force behind the wake, on the other hand, is greater for the smaller particles than in the larger particles due to difference in the masses of each of the individual particles. As a result of these two, the smaller particles have a tendency to stay longer in the bed than larger ones resulting in a slower rate of rise in the bed hold up ratio. This trend becomes more pronounced in slugging beds which occur at high velocities or in deep beds. Bhardwaj [161] and Chechetkin et al [159] have reported decreasing values of bed hold up ratio with increase in air flow rates. This might be in slugging zones.

In continuous fluidized beds with vertical internal baffles, the presence of baffles alters the linear velocity profile significantly from the one observed in beds without baffles. The presence of large number of baffles leads to formation of large number of compartments with linear velocity almost reaching zero value near each baffle surface and near the wall of the column. Unlike in beds without baffles localized stagnant pocket near the periphery are not observed in these beds. Because of comparatively greater movement of smaller particles than the larger ones at any air velocity, smaller particles have a greater chance of moving out through the discharge. Thus it is expected that at lower velocities bed hold up

ratios are higher in beds with baffles than without baffles under similar conditions of operation.

At higher velocities the tendencies of bubbling are reduced as larger bubbles can not be formed due to the presence of baffles. This results in a more uniform bed with lesser segregation of coarser particles towards the wall as compared to the fine particles. This results in a continuous rise in bed hold up ratio with air velocity. The same trend will continue even at high velocities as tendency of slugging are not present.

5.3.4 CORRELATION

In baffled fluidized beds the solids movement at any gas flow rate is affected by two factors, viz.

- i) d_o/D_p ratio indicating free movement of particles
and
- ii) reduced gas velocity U_f/U_{mf} , indicating the driving force for the random motion.

For any particle size, large values of d_o/D_p and U_f/U_{mf} will mean greater movement and hence easier removal from the bed. Thus, it is expected that at any given U_f and d_o , larger particles will have lower values of d_o/D_p and U_f/U_{mf} compared to smaller particles.

5.3.4.1 Correlation Proposed

In baffled beds, the solids composition in the bed will depend upon U_f/U_{mf} , bed hold up W and d_o/D_p . The gas contact time in fluidized bed is defined by Levenspiel [132] as

$$T_G = V_s/V_f \quad \dots (5.1)$$

where V_s is the volume of solids in the bed and V_f is the volumetric flow rate of gas.

The average time spent by the solids in the bed (τ_s) can be expressed in terms of total bed hold up (W) and solids feed rate (w_s) as

$$\tau_s = W/w_s \quad \dots (5.2)$$

The ratio of τ_s/T_G from eqns. 5.1 and 5.2 is termed τ_B , dimensionless time parameter. The bed hold up ratio

$$H(2,1) = f [\tau_B, U_f/U_{mf}, d_o/D_p] \quad \dots (5.3)$$

where U_f/U_{mf} is reduced air velocity for baffled beds. While estimating U_{mf} values, the effect of d_o/D_p is considered and hence d_o/D_p need not be taken separately. Since the feed and bed have got different solids compositions, their calculated average particle diameter will be different. Based on average particle diameter corresponding to the bed composition, U_{mf} has been computed using eqn. 3.1, proposed earlier for minimum fluidizing

velocity in batch fluidized beds with vertical baffles.

When the values of bed hold up ratio for different feed compositions are plotted against U_f/U_{mf} as shown in Fig. 5.16, it is observed that the points for different feed compositions at a constant bed hold up, merge on single line, whereas a plot of hold up ratio versus air mass velocity (Fig. 5.11) gives different curves for different feed compositions. Therefore, the use of U_f/U_{mf} is more reasonable as it lowers down the effect of changes of feed composition. U_{mf} values for different feed composition were found to be different giving different values of (U_f/U_{mf}) . It was therefore, not advisable to use regression analysis without graphical interpolation. In Fig. 5.17, values of $H(2,1)$ were plotted as a function of τ_B on log-log graph paper. Two zones are seen in this plot similar to Fig. 5.14. The transition occurs at air flow rates U_f/U_{mf} in the range of 1.5-1.7. In industrial processes the air flow rates of the order of 1.5 to 1.7 U_{mf} are insignificant. Therefore, only the slope of the higher air flow was determined using least square best fit method, which comes to 0.1. Using this value $H(2,1)/\tau_B^{0.1}$ was plotted as a function of U_f/U_{mf} as shown in Fig. 5.18. This gives a correlation

of the type

$$\frac{H(2.1)}{\tau_B^{0.1}} = f (U_f/U_{mf}) \quad \dots (5.4)$$

Based on the above analysis, the following correlation has been proposed as

$$\frac{H(2.1)}{\tau_B^{0.1}} = 0.44 (U_f/U_{mf})^{0.26} \quad \dots (5.5)$$

The values predicted using the above correlation were found to lie within $\pm 7\%$ of the experimental values as shown in Fig. 5.19.

5.4 CONCLUSION

The above hold up studies indicate that

- hold up of larger particles increases with increase in air flow rate as compared to the smaller particles in beds with vertical internal baffles.
- hold up ratio increases steadily with increase in air flow rate in beds with vertical baffles unlike in the beds without baffles where the hold up ratio first increases and at higher air flow rates it becomes steady.
- hold up ratio can be predicted from the correlation proposed (eqn. 5.5).

TABLE-5.2

MATERIAL: SPHERICAL GLASS BEADS

Solid Feed = 6.6×10^{-4} kg/s of 460 μ m and 1.32×10^{-3} kg/s of 650 μ m
 Solids Feed Rate = 19.8×10^{-4} kg/s
 Vertical Baffles = 6 mm dia, 12 Nos. d_o 10 mm
 Avg. Bed Hold Up = 0.483 kg
 Avg. Static Bed Height = 80.0 mm

G_f kg/m ² s	W_2/W_1	Avg. D_p mm	τ_s s.	T_G s	τ_B	U_f/U_{mf}	H(2,1)
1	2	3	4	5	6	7	8
0.357	308/166	0.580	237.0	0.195	1215.38	0.848	0.928
0.510	315/164	0.585	239.5	0.138	1735.5	1.2105	0.96
0.715	321/159	0.587	240.0	0.0987	2431.6	1.695	1.009
0.817	325/156	0.588	240.5	0.0865	2780.3	1.950	1.04
1.020	333/152	0.590	242.4	0.0698	3472.7	2.430	1.095
1.220	342/149	0.592	245.4	0.0589	4166.4	2.980	1.147
1.430	355/139	0.596	246.6	0.0508	4854.3	3.410	1.277

TABLE-5.3

MATERIAL SPHERICAL GLASS BEADS

Solid Feed = 6.6×10^{-4} kg/s of 460 μ m and 1.32×10^{-3} kg/s of 650 μ m
 Solid Feed Rate = 19.8×10^{-4} kg/s
 Vertical Baffles = 6 mm dia, 12 Nos., d_o 10 mm,
 Avg. Bed Hold Up = 0.606 kg
 Avg. Static Bed Height = 120 mm

G_f kg/m ² s	W_2/W_1	Avg. D_p mm	τ_s s	τ_G s	τ_B	U_f/U_{mf}	H(2,1)
1	2	3	4	5	6	7	8
0.357	403/202	0.586	302.4	0.2487	1215.87	0.847	0.99
0.510	406/199	0.587	302.4	0.1743	1735.0	1.20	1.02
0.715	412/194	0.589	303.0	0.1246	2430.5	1.69	1.06
0.817	417/192	0.590	304.8	0.1097	2777.7	1.94	1.086
1.020	424/186	0.591	303.0	0.0872	3472.2	2.42	1.14
1.430	440/166	0.598	307.3	0.0632	4861.1	3.39	1.33

TABLE-5.5

MATERIAL: SPHERICAL GLASS BEADS

Solid Feed = 1.32×10^{-3} kg/s each of 460 μm and 650 μm
 Solids Feed Rate = 2.64×10^{-3} kg/s
 Vertical Baffles 6 mm dia. 12 Nos. d_o 10 mm,
 Avg. Bed Hold up = 0.435 kg
 Avg. Static Bed Height = 80.0 mm

G_f kg/m ² s	W_2/W_1	Avg. D_p mm	τ_s s	T_G s	τ_B	U_f/U_{mf}	H(2,1)
1	2	3	4	5	6	7	8
0.357	212/221	0.553	162.0	0.1781	909.6	0.90	0.96
0.510	214/218	0.554	162.0	0.1244	1302.2	1.27	0.98
0.715	223/216	0.556	168.0	0.0903	1860.4	1.755	1.03
0.817	227/211	0.558	163.8	0.0788	2078.6	2.09	1.07
1.020	230/208	0.559	164.0	0.0630	2603.1	2.55	1.10
1.220	238/200	0.563	164.0	0.0525	3123.8	3.10	1.19
1.430	246/184	0.568	161.0	0.0442	3642.5	3.64	1.337

TABLE-5.4

MATERIAL: SPHERICAL GLASS BEADS

Solid Feed = 6.6×10^{-4} kg/s of 460 μ m and 1.32×10^{-3} kg/s of 650 μ m
 Solids Feed Rate = 19.8×10^{-4} kg/s
 Vertical Baffles 6 mm dia, 12 Nos. d_o 10 mm
 Avg. Bed Hold Up = 0.795 kg
 Avg. Static Bed Height = 150.0 mm

G_f kg/m ² s	W_2/W_1	Avg. D_p mm	τ_s s	T_G s	τ_B	U_f/U_{mf}	H(2,1)
1	2	3	4	5	6	7	8
0.357	536/268	0.5866	402.0	0.3307	1215.6	0.845	1.00
0.510	538/261	0.588	399.5	0.2304	1733.9	1.19	1.03
0.715	540/248	0.590	393.6	0.1620	2429.6	1.68	1.088
0.817	551/244	0.591	397.2	0.1430	2777.6	1.92	1.13
1.020	557/237	0.593	396.0	0.1144	3461.5	2.40	1.16
1.220	569/226	0.595	395.4	0.0953	4149.0	2.85	1.259
1.430	580/210	0.5995	394.8	0.0812	4862.0	3.34	1.350

TABLE-5.6

MATERIAL: SPHERICAL GLASS BEADS

Solid Feed = 1.32×10^{-3} kg/s each of 460 μm and 650 μm
 Solids Feed Rate = 2.64×10^{-3} kg/s
 Vertical Baffles 6 mm dia, 12 Nos. d_o 10 mm
 Avg. Bed Hold Up = 0.645 kg
 Avg. Static Bed Height = 120.0mm

G_f kg/m ² s	W_2/W_1	Avg. D_p mm	τ_s s	τ_G s	τ_B	U_f/U_{mf}	H(2,1)
1	2	3	4	5	6	7	8
0.357	327/319	0.556	241.8	0.2652	911.5	0.88	1.02
0.510	331/316	0.557	242.4	0.1860	1302.8	1.26	1.047
0.715	340/309	0.559	243.0	0.1332	1823.1	1.75	1.10
0.817	345/299	0.561	241.2	0.1157	2083.3	2.00	1.15
1.020	351/292	0.563	241.08	0.0925	2604.7	2.52	1.20
1.220	359/280	0.566	239.4	0.0766	3125.0	3.03	1.28
1.430	378/270	0.570	243.0	0.0666	3645.9	3.54	1.40

TABLE-5.7

MATERIAL: SPHERICAL GLASS BEADS

Solid Feed = 1.32×10^{-3} kg/s each of 460 μm and 650 μm
 Solids Feed Rate = 2.64×10^{-3} kg/s
 Vertical Baffles 6 mm dia, 12 Nos. d_o 10 mm
 Avg. Bed Hold Up = 0.766 kg
 Avg. Static Bed Height = 150.0 mm

G_f kg/m ² s	W_2/W_1	Avg. D_p mm	τ_s s	T_G s	τ_B	U_f/U_{mf}	H(2,1)
1	2	3	4	5	6	7	8
0.357	403/384	0.557	294.6	0.3237	910.1	0.87	1.05
0.510	409/373	0.559	292.8	0.2252	1300.1	1.255	1.09
0.715	418/358	0.562	291.0	0.1596	1823.3	1.74	1.16
0.817	422/349	0.564	288.6	0.1387	2080.7	1.98	1.21
1.020	431/329	0.567	285.0	0.1094	2605.1	2.47	1.31
1.220	439/310	0.571	280.8	0.0898	3126.9	3.00	1.41
1.430	452/290	0.575	278.4	0.0763	3648.7	3.40	1.49

TABLE-5.8

MATERIAL: SPHERICAL GLASS BEADS

Solid Feed = 2.76×10^{-3} kg/s of 460 μm and 1.38×10^{-3} kg/s of 650 μm
 Solids Feed Rate = 4.14×10^{-3} kg/s
 Vertical Baffles 6 mm dia, 12 Nos. J_0 10 mm
 Avg. Bed Hold Up = 0.446 kg
 Avg. Static Bed Height = 80.0 mm

G_f kg/m ² s	W_2/W_1	Avg. D_p mm	τ_s s	T_G s	τ_B	U_f/U_{mf}	H(2,1)
1	2	3	4	5	6	7	8
0.357	143/314	0.519	109.2	0.1880	580.8	0.95	0.965
0.510	147/311	0.520	109.8	0.1319	832.4	1.40	1.00
0.715	149/297	0.523	106.8	0.0917	1164.6	1.90	1.065
0.817	153/289	0.525	106.08	0.0795	1334.3	2.19	1.12
1.020	159/281	0.528	105.6	0.0633	1668.2	2.80	1.20
1.220	165/272	0.531	104.5	0.0524	1994.2	3.30	1.29
1.430	175/265	0.535	105.6	0.0452	2336.2	3.82	1.40

TABLE-5.9

MATERIAL: SPHERICAL GLASS BEADS

Solid Feed = 2.76×10^{-3} kg/s of 460 μm and 1.38×10^{-3} kg/s of 650 μm
 Solids Feed Rate = 4.14×10^{-3} kg/s
 Vertical Baffles 6 mm dia, 12 Nos. d_o 10 mm
 Avg. Bed Hold Up = 0.646 kg
 Avg. Static Bed Height = 120.0 mm

G_f kg/m ² s	W_2/W_1	Avg. D_p mm	τ_s s	T_G s	τ_B	U_f/U_{mf}	H(2,1)
1	2	3	4	5	6	7	8
0.357	212/440	0.521	156.0	0.2674	533.3	0.94	1.03
0.510	219/430	0.524	155.4	0.1864	833.3	1.35	1.085
0.715	226/424	0.526	156.0	0.1337	1166.6	1.89	1.13
0.817	230/414	0.527	154.2	0.1156	1333.3	2.16	1.18
1.020	236/402	0.530	153.0	0.0918	1666.6	2.70	1.25
1.220	249/395	0.533	154.2	0.0771	1999.9	3.23	1.34
1.430	262/382	0.537	154.2	0.0660	2333.3	3.78	1.46

TABLE-5.10

MATERIAL : SPHERICAL GLASS BEADS

Solid Feed = 2.76×10^{-3} kg/s of 460 μ m and 1.38×10^{-3} kg/s of 650 μ m
 Solids Feed Rate = 4.14×10^{-3} kg/s
 Vertical Baffles 6 mm dia 12 Nos. d_o 10 mm
 Avg. Bed Hold Up = 0.784 kg
 Avg. Static Bed Height = 180.0 mm

G_f kg/m ² s	W_2/W_1	Avg. D_p mm	τ_s s	T_G	τ_B s	U_f/U_{mf}	H(2,1)
1	2	3	4	5	6	7	8
0.357	262/518	0.523	187.2	0.3208	583.5	0.93	1.065
0.510	272/512	0.526	187.8	0.2257	832.0	1.30	1.12
0.715	283/503	0.528	188.4	0.1616	1165.8	1.80	1.19
0.817	298/492	0.531	189.6	0.1421	1334.2	2.05	1.28
1.020	310/488	0.533	191.4	0.1149	1665.8	2.60	1.35
1.220	318/472	0.536	189.6	0.0948	2000.0	3.15	1.435
1.430	325/432	0.541	181.8	0.0776	2342.7	3.65	1.530

TABLE-5.11

MATERIAL: SPHERICAL GLASS BEADS

Solids Feed = 1.32×10^{-3} kg/s each of 460 μm and 650 μm
 Solids Feed Rate = 2.64×10^{-3} kg/s
 Avg. Bed Hold Up = 0.800 kg without baffles
 Avg. Static Bed Height = 150.0 mm

Sl. No.	Air Mass Velocity kg/m ² s	Solids Fraction		Hold Up Ratio H(2,1)
		650 μm	460 μm	
1	2	3	4	5
1.	0.204	385	418	0.92
2.	0.357	398	402	0.99
3.	0.510	404	391	1.03
4.	0.715	412	379	1.09
5.	0.817	424	374	1.13
6.	1.02	432	366	1.18
7.	1.22	438	362	1.21
8.	1.43	441	367	1.20

TABLE-5.12

MATERIAL: SPHERICAL GLASS BEADS

Solids Feed = 1.32×10^{-3} kg/s each of 460 μm and 650 μm
 Solids Feed Rate = 2.64×10^{-3} kg/s
 Avg. Bed Hold Up = 0.644 kg without baffles
 Avg. Static Bed Height = 120.0 mm

Sl. No.	Air Mass Velocity kg/m ² s	Solids Fraction kg x 10 ³		Hold Up Ratio H(2,1)
		650 μm	460 μm	
1	2	3	4	5
1.	0.204	305	335	0.91
2.	0.357	317	327	0.97
3.	0.510	322	322	1.00
4.	0.715	334	317	1.05
5.	0.817	340	309	1.10
6.	1.02	346	298	1.16
7.	1.22	352	292	1.20
8.	1.43	355	290	1.22

TABLE-5.13

MATERIAL: SPHERICAL GLASS BEADS

Solids Feed = 6.6×10^{-4} kg/s of 460 μm and 1.32×10^{-3} kg/s of 650 μm
 Solids Feed Rate = 19.8×10^{-4} kg/s
 Avg. Bed Hold Up = 0.460 kg without baffles
 Avg. Static Bed Height = 80 mm

Sl. No.	Air Mass Velocity kg/m ² s	Solids Fraction kg x 10 ³		Hold Up Ratio H(2,1)
		650 μm	460 μm	
1	2	3	4	5
1.	0.357	298	163	0.91
2.	0.510	300	160	0.93
3.	0.715	301	160	0.94
4.	0.817	306	154	0.99
5.	1.02	313	146	1.07
6.	1.22	318	142	1.12
7.	1.43	322	137	1.17

TABLE-5.14

MATERIAL: SPHERICAL GLASS BEADS

Solid Feed = 6.6×10^{-4} kg/s of 460 μm and 1.32×10^{-3} kg/s of 650 μm
 Solids Feed Rate = 19.8×10^{-4} kg/s
 Avg. Bed Hold Up = 0.660 kg without baffles
 Avg. Static Bed Height = 120.0 mm

Sl. No.	Air Mass Velocity kg/m ² s	Solids Fraction kg x 10 ³		Hold Up Ratio H(2,1)
		650 μm	460 μm	
1	2	3	4	5
1.	0.357	430	232	0.925
2.	0.510	437	228	0.950
3.	0.715	442	225	0.980
4.	0.817	447	220	1.015
5.	1.02	452	208	1.085
6.	1.22	460	198	1.160
7.	1.43	465	193	1.205

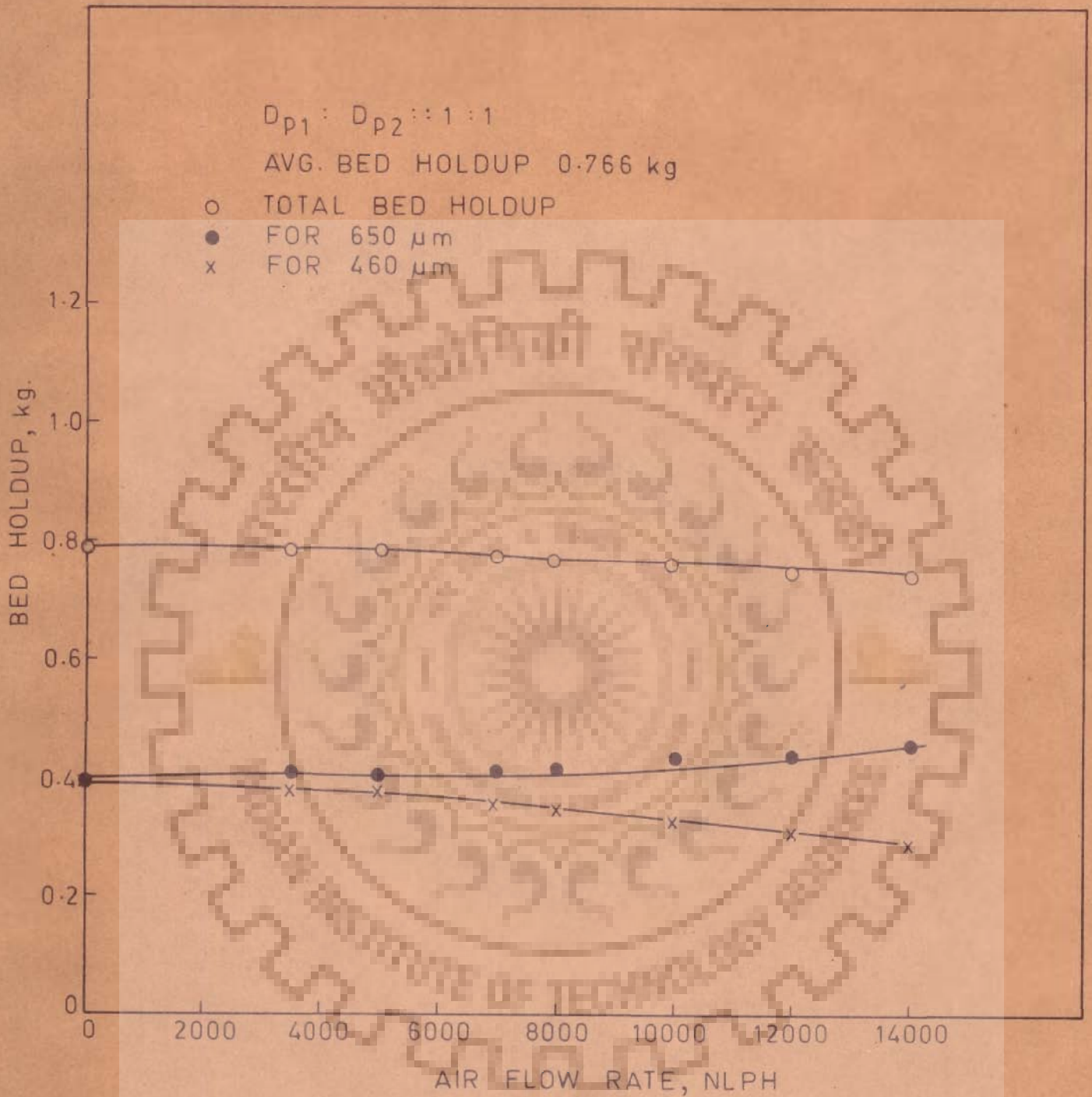


FIG. 5.5 TYPICAL PLOT SHOWING THE CONTROLLED BED HOLDUP VALUES AT DIFFERENT AIR FLOW RATES.

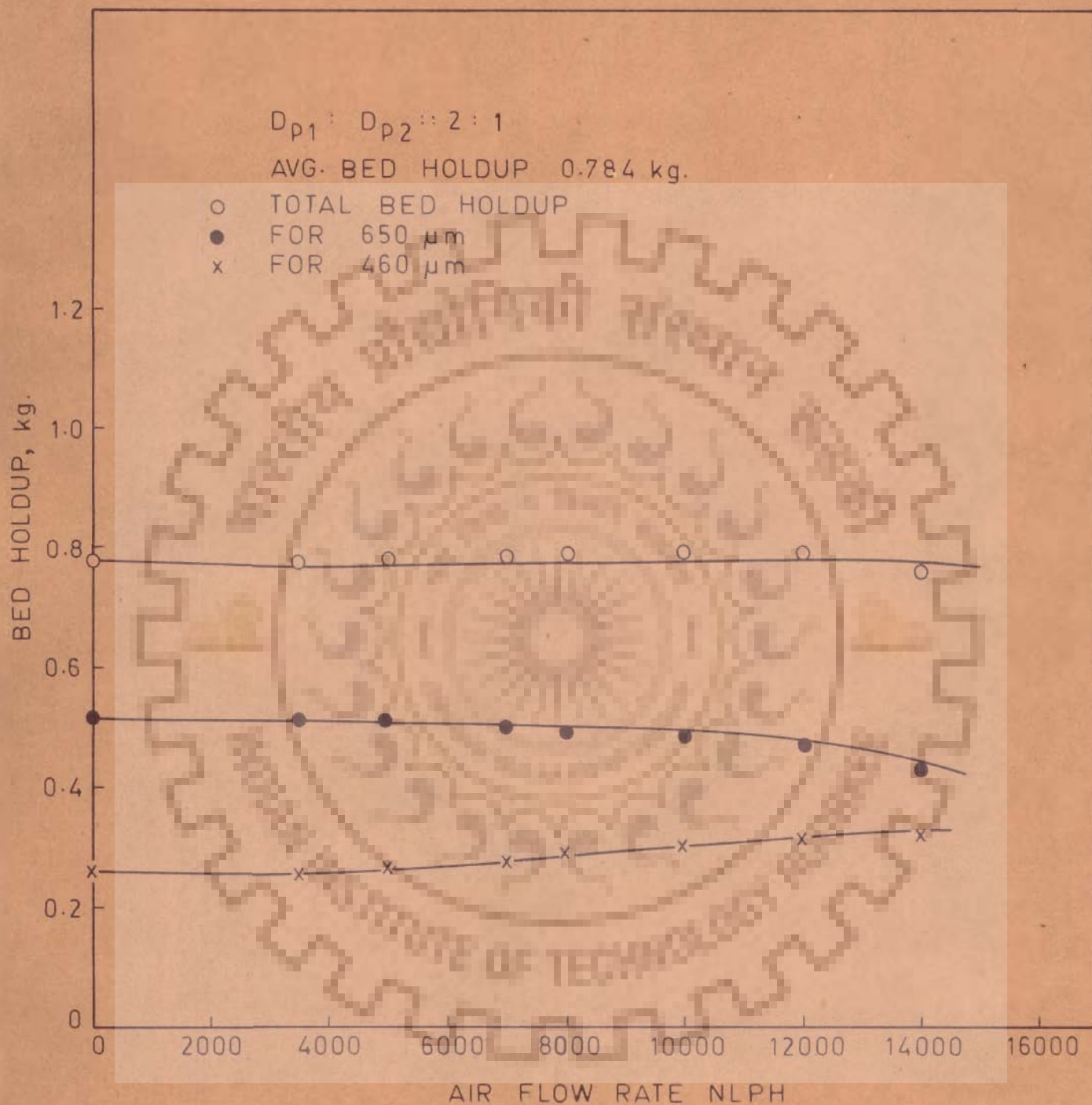


FIG. 5.6 TYPICAL PLOT SHOWING THE CONTROLLED BED HOLDUP VALUES AT DIFFERENT AIR FLOW RATES.

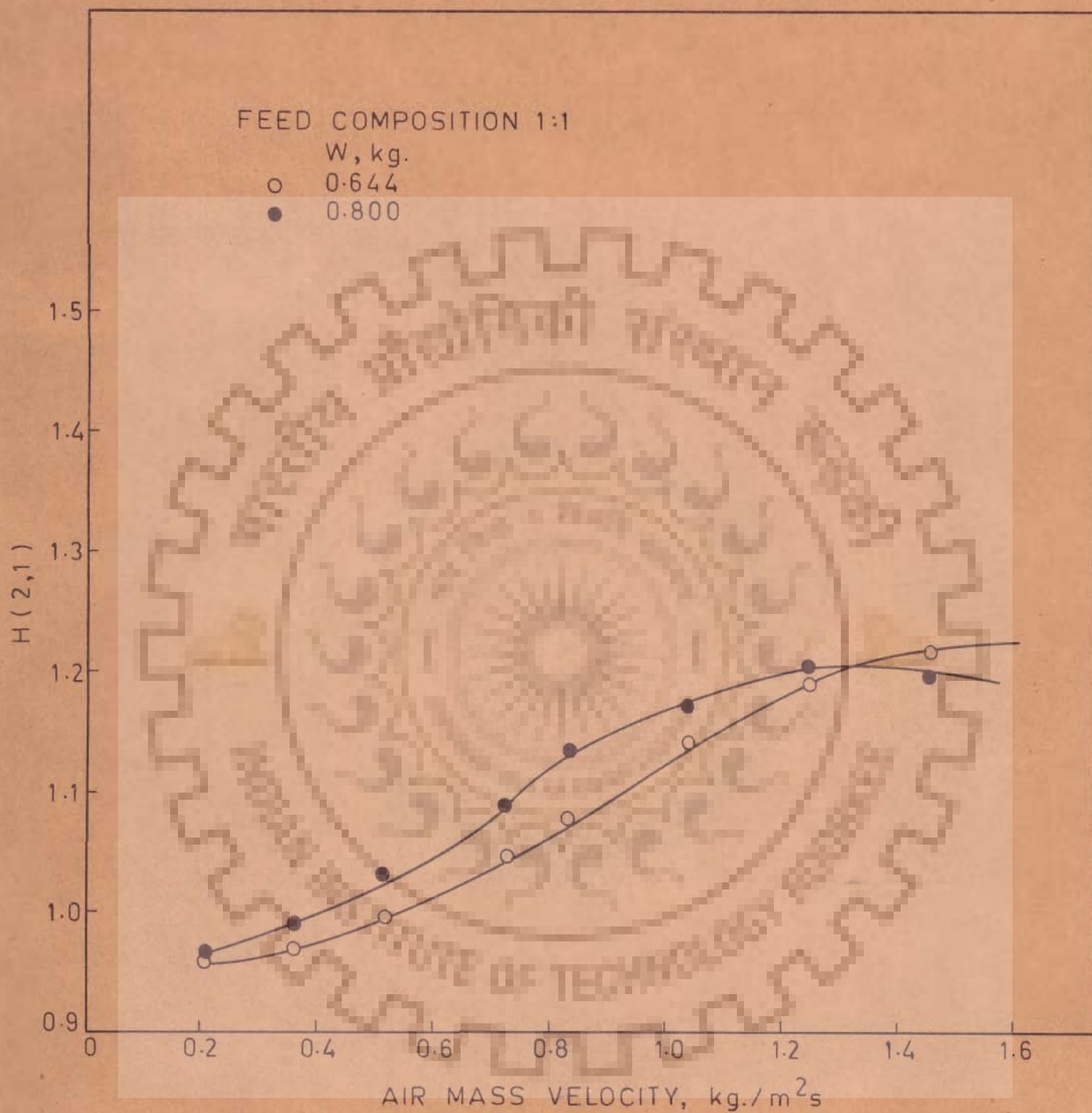


FIG. 5.7 VARIATION OF HOLDUP RATIO WITH AIR MASS VELOCITY IN CONTINUOUS FLUIDIZED BEDS WITHOUT BAFFLES.

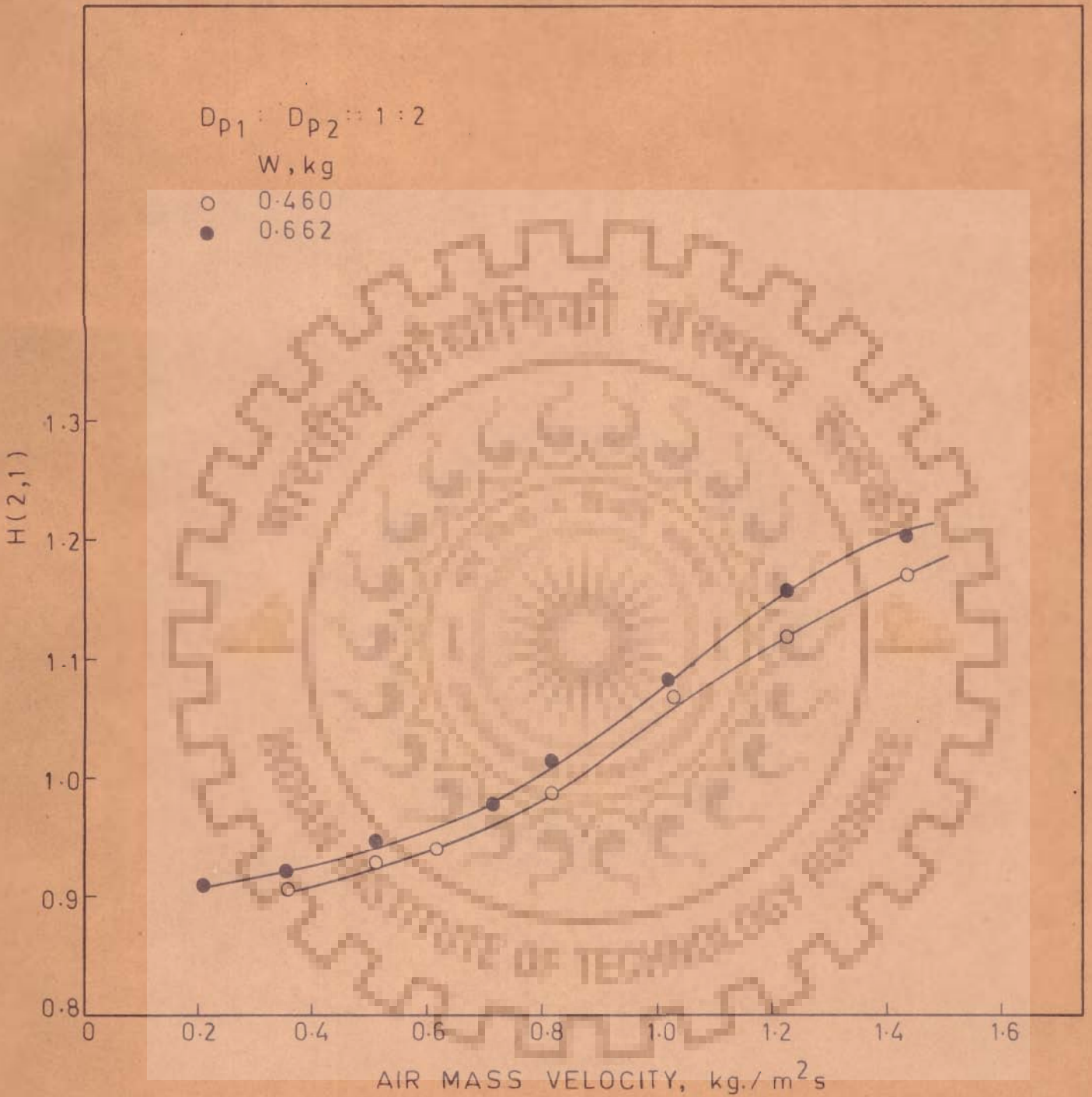


FIG. 5.8 VARIATION OF HOLDUP RATIO WITH AIR MASS VELOCITY IN CONTINUOUS FLUIDIZED BEDS WITHOUT BAFFLES.

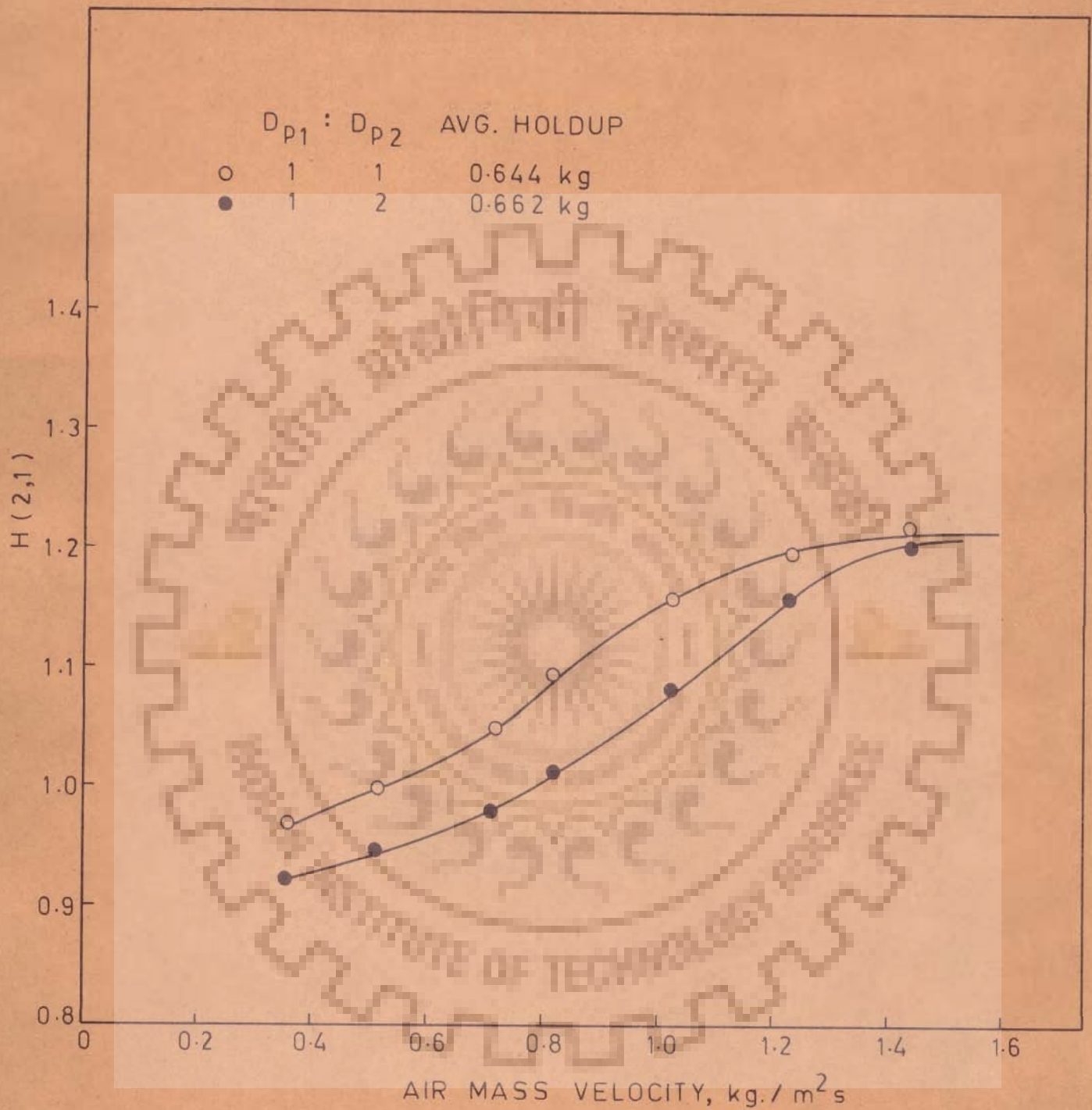


FIG. 5.9 VARIATION OF HOLDUP RATIO WITH AIR MASS VELOCITY IN CONTINUOUS FLUIDIZED BED WITHOUT BAFFLES.

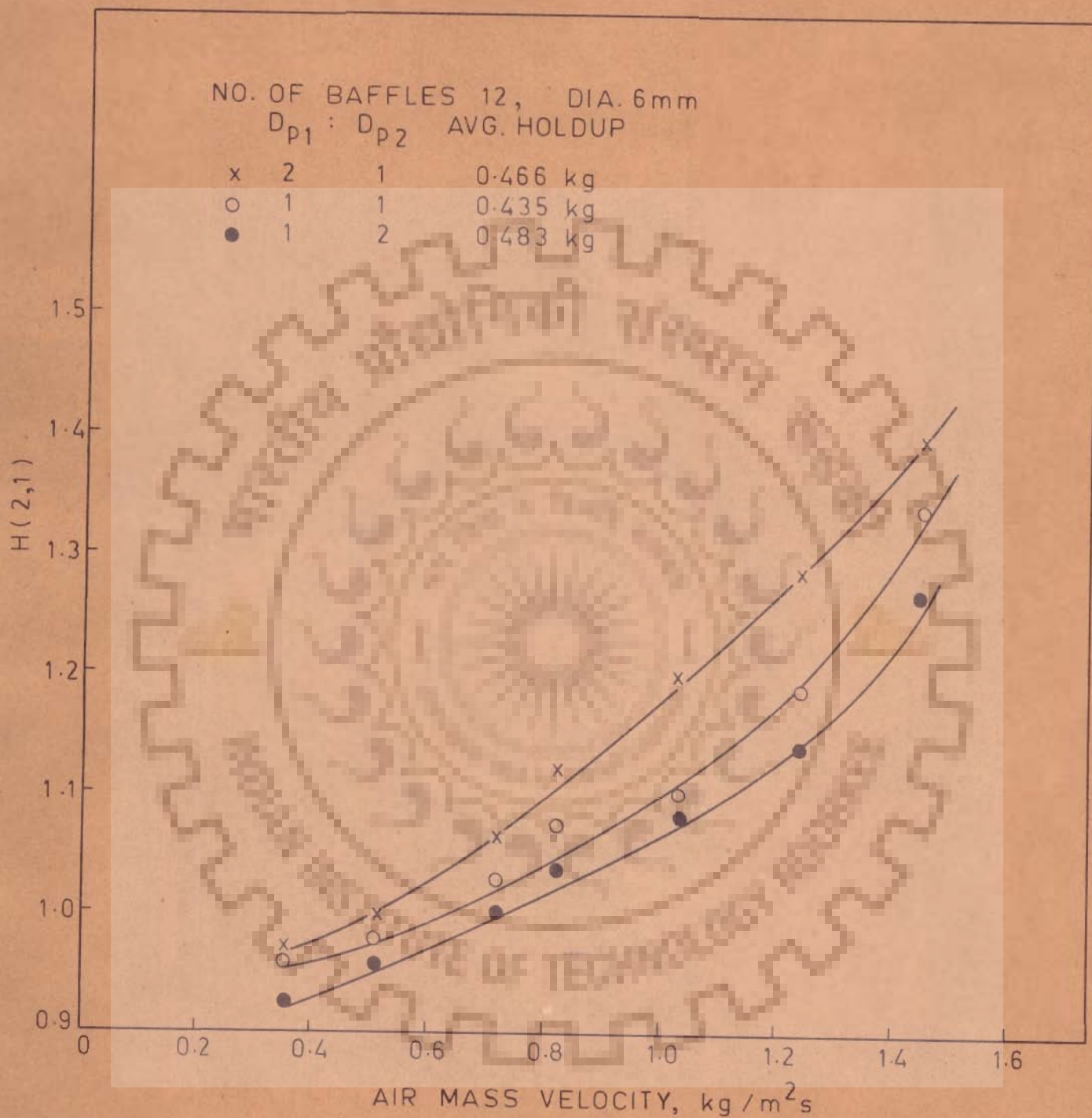


FIG. 5.10 VARIATION OF HOLDUP RATIO WITH AIR MASS VELOCITY IN CONTINUOUS FLUIDIZED BEDS WITH VERTICAL BAFFLES.

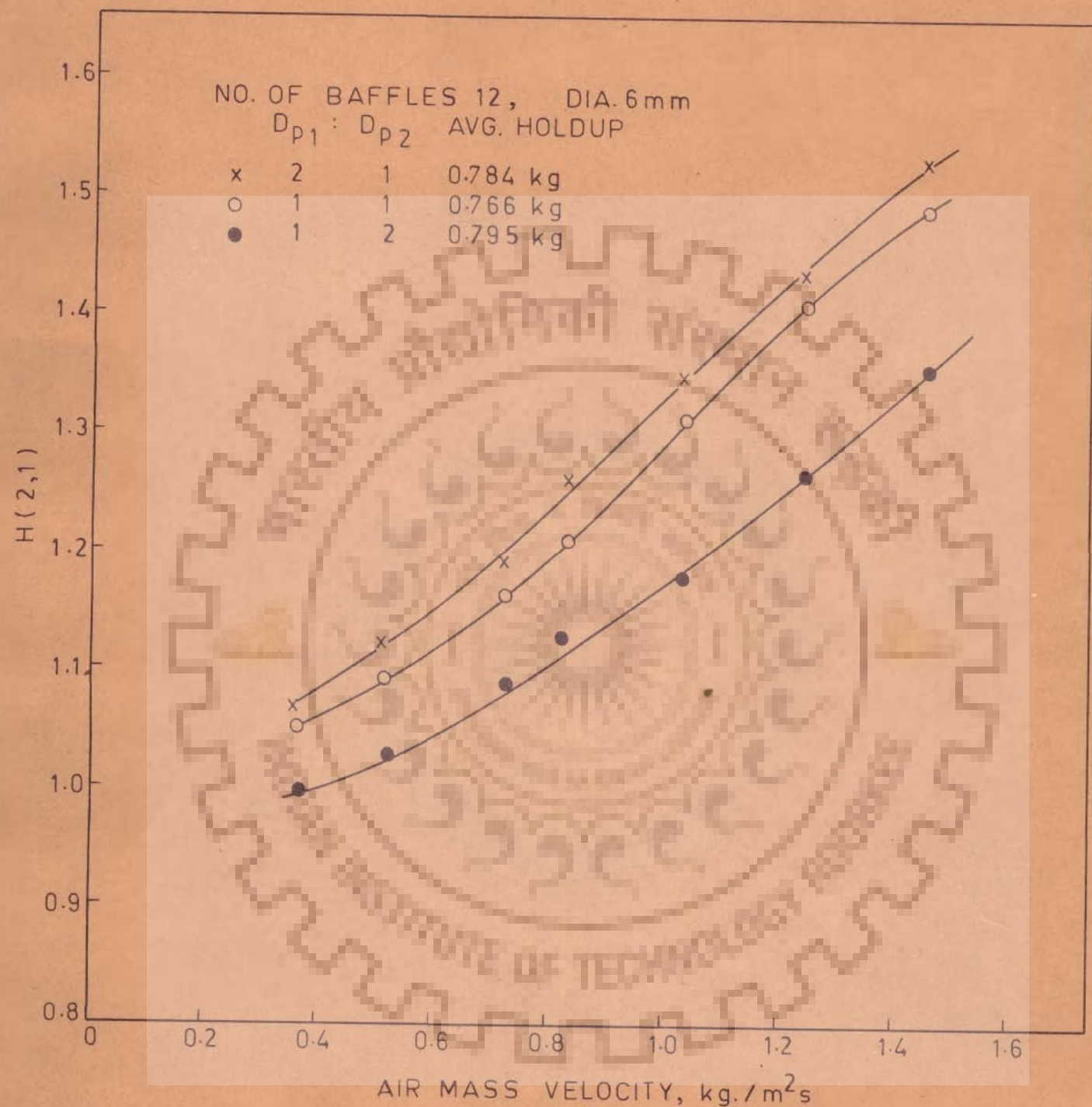


FIG. 5.12 VARIATION OF HOLDUP RATIO WITH AIR MASS VELOCITY IN CONTINUOUS FLUIDIZED BEDS WITH VERTICAL BAFFLES.

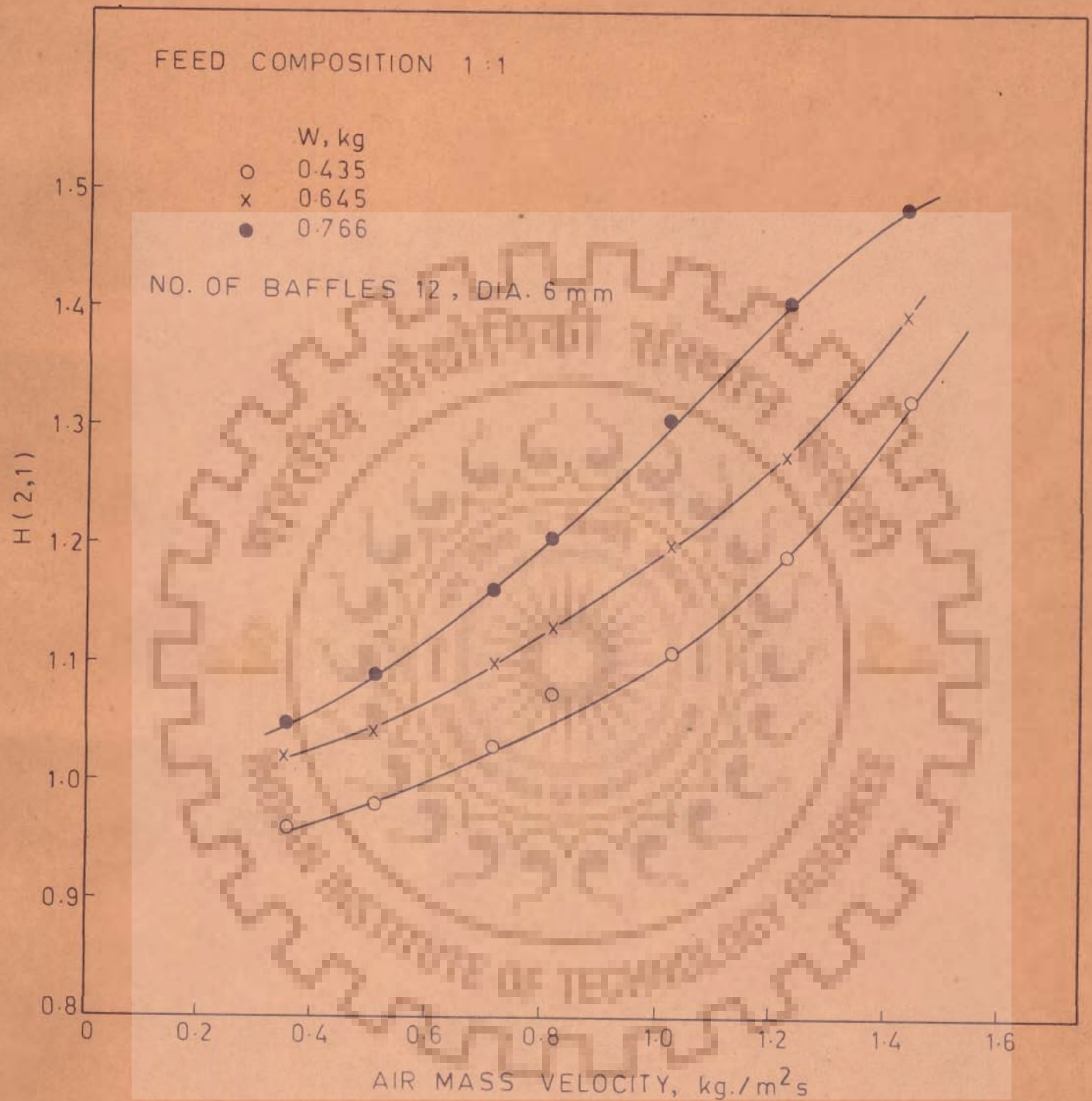


FIG. 5.13 VARIATION OF HOLDUP RATIO WITH AIR MASS VELOCITY IN CONTINUOUS FLUIDIZED BEDS WITH VERTICAL BAFFLES.

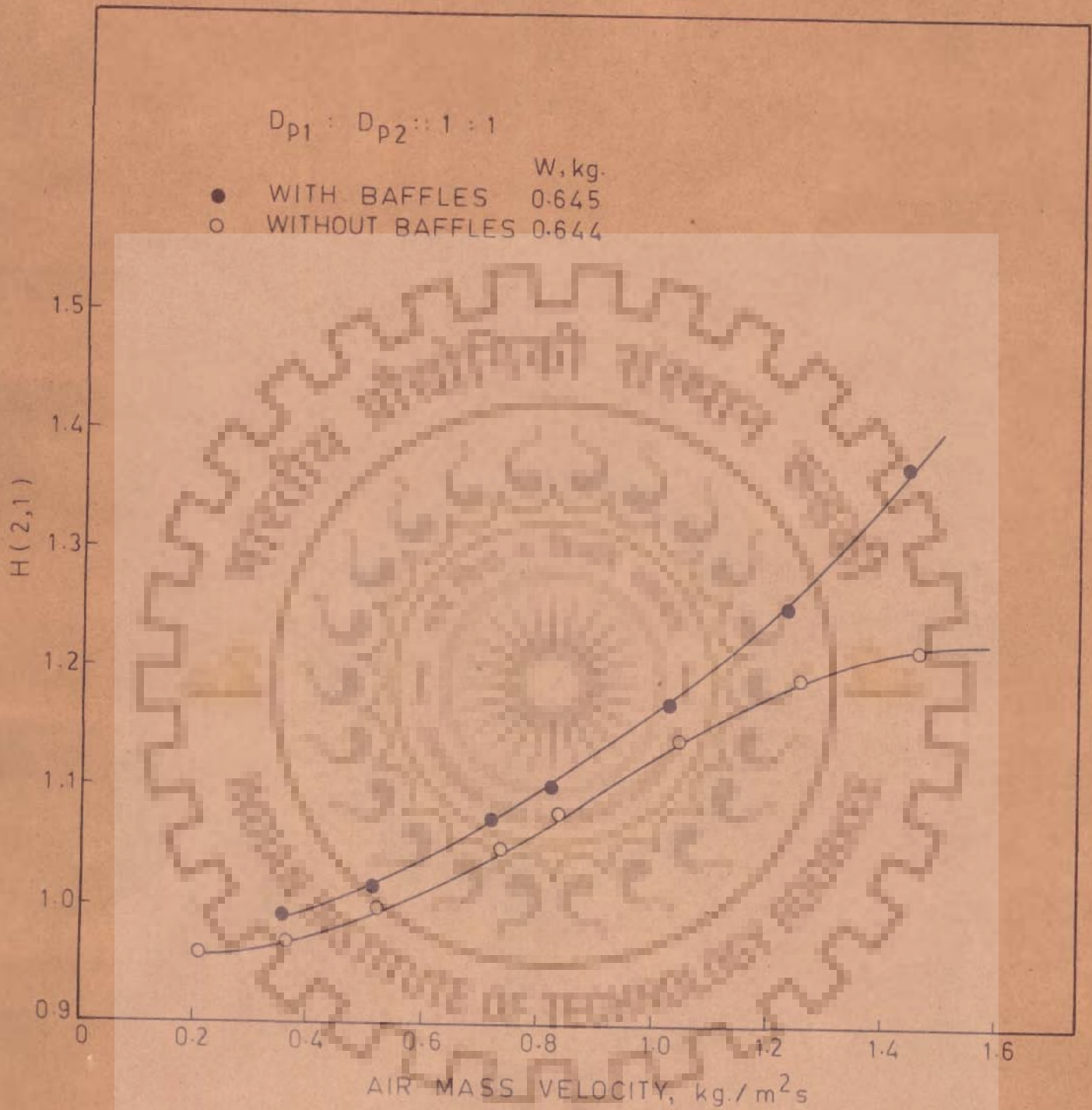


FIG. 5.14 VARIATION OF HOLDUP RATIO WITH AIR MASS VELOCITY IN CONUOUS FLUIDIZED BEDS WITH AND WITHOUT VERTICAL BAFFLES.

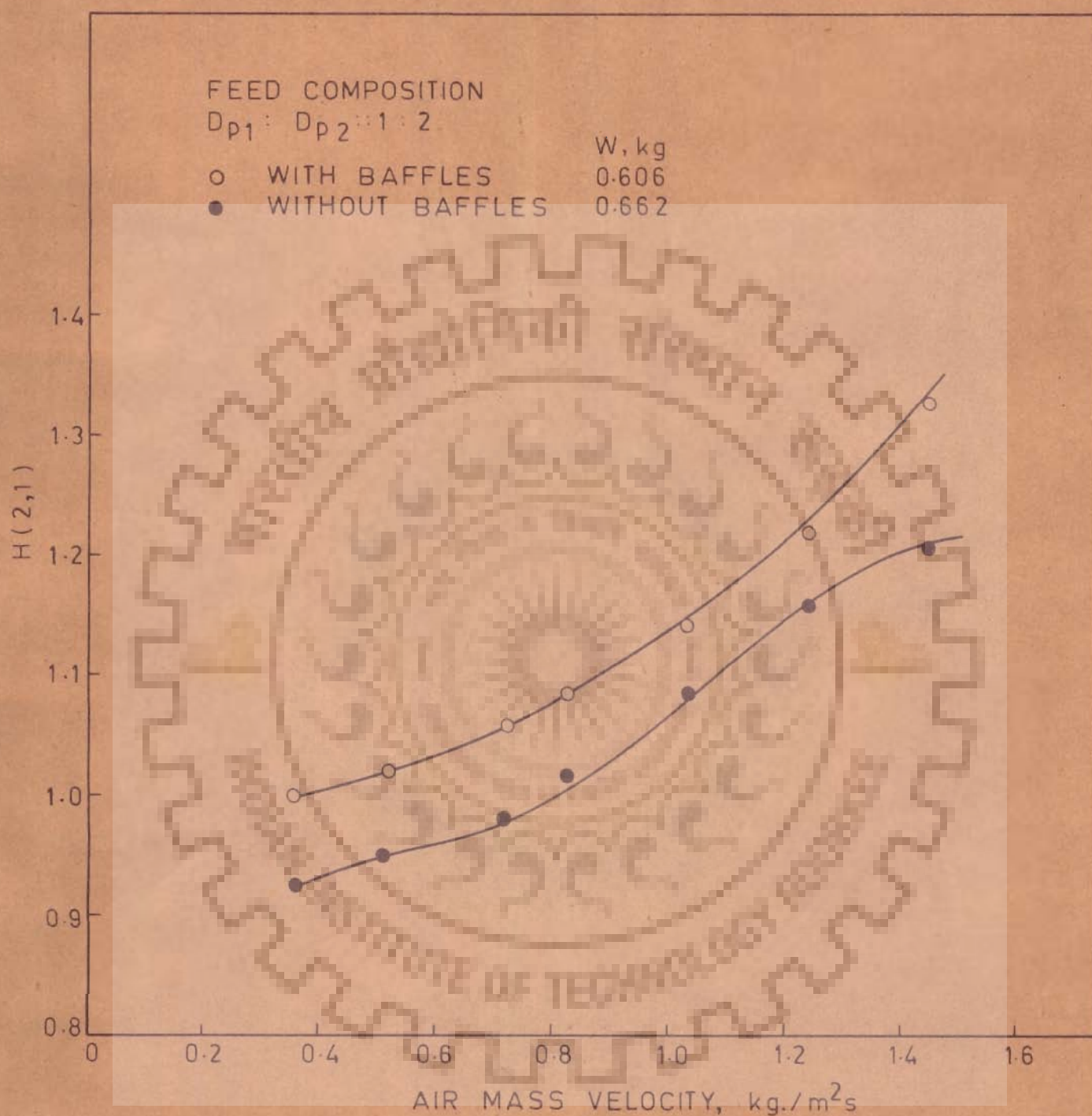


FIG. 5.15 VARIATION OF HOLDUP RATIO WITH AIR MASS VELOCITY IN CONTINUOUS FLUIDIZED BEDS WITH AND WITHOUT VERTICAL BAFFLES.

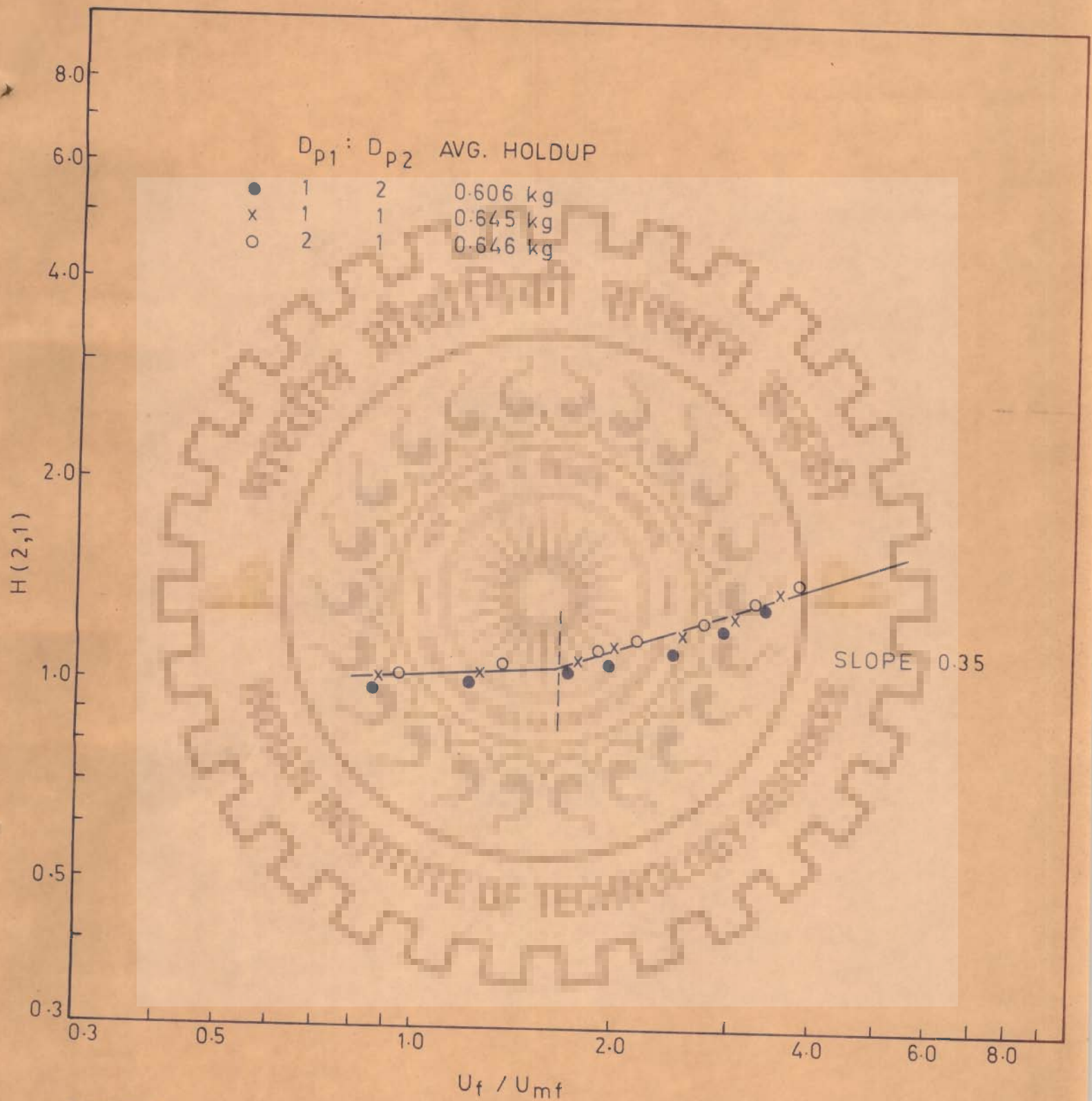


FIG. 5.16 EFFECT OF REPLACING AIR MASS VELOCITY BY U_f/U_{mf} ON HOLD-UP RATIO.

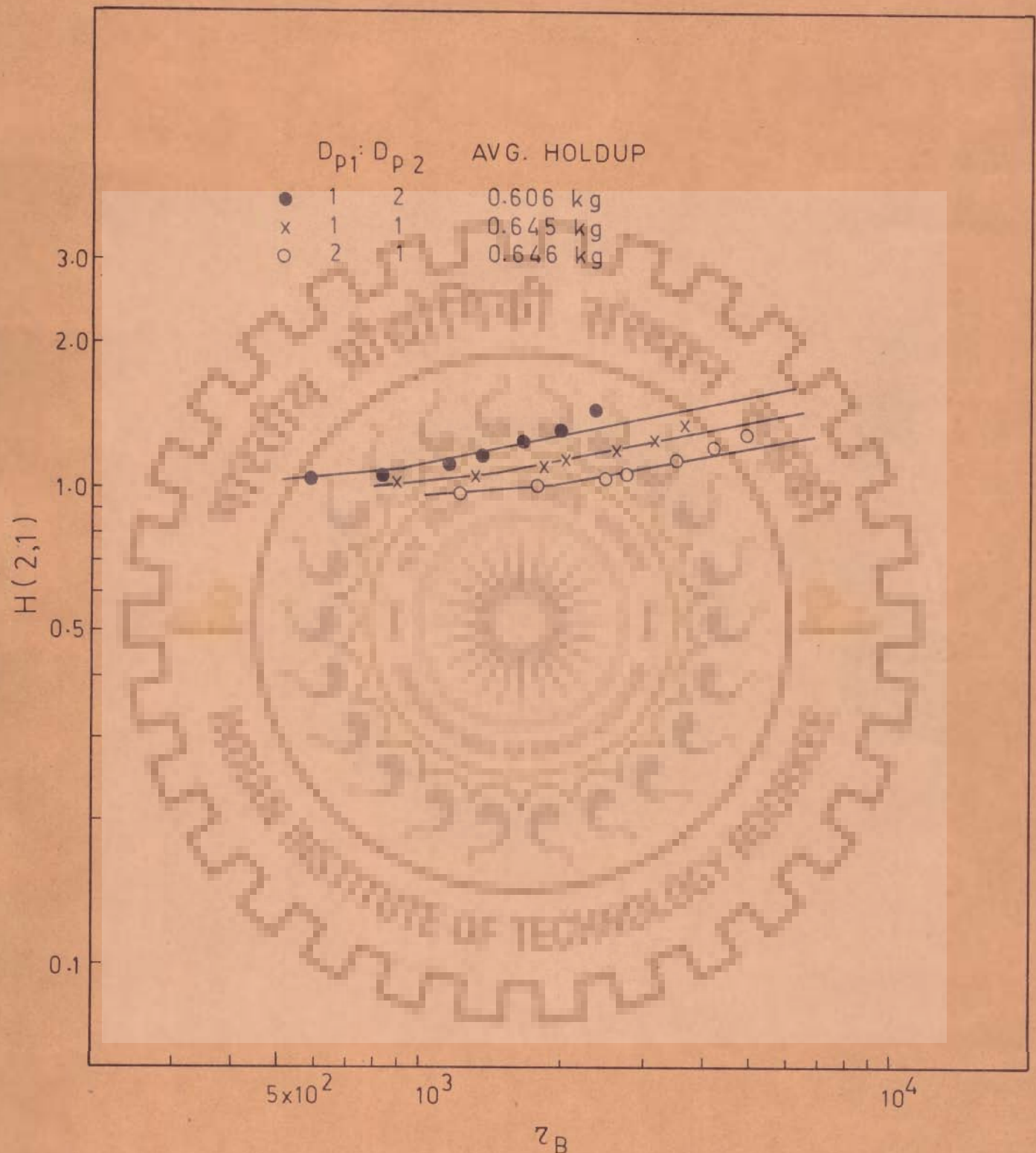


FIG. 5.17 CORRELATING $H(2,1)$ WITH z_B

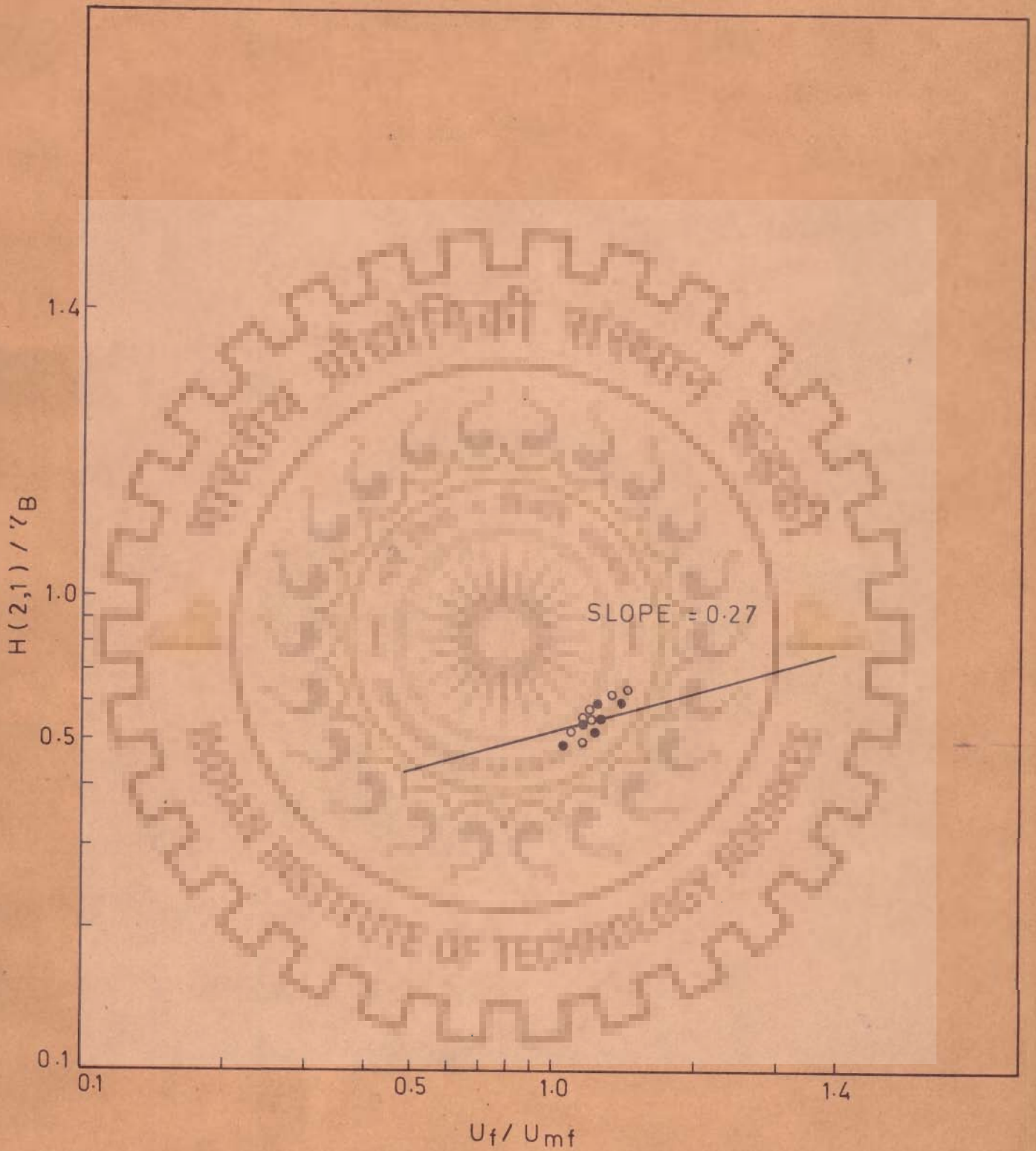


FIG. 5.18 CORRELATION OF $H(2,1)$ AND z_B .

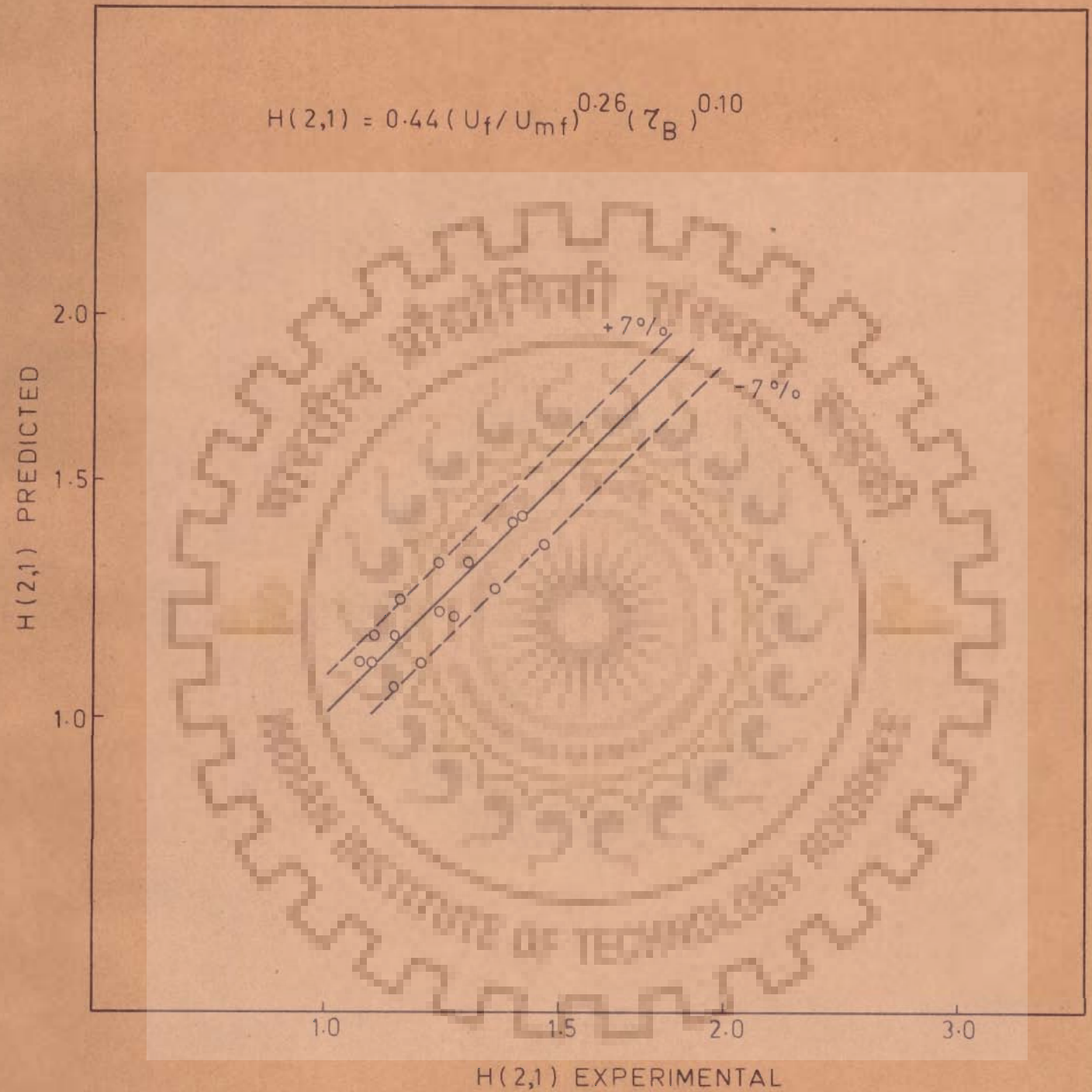
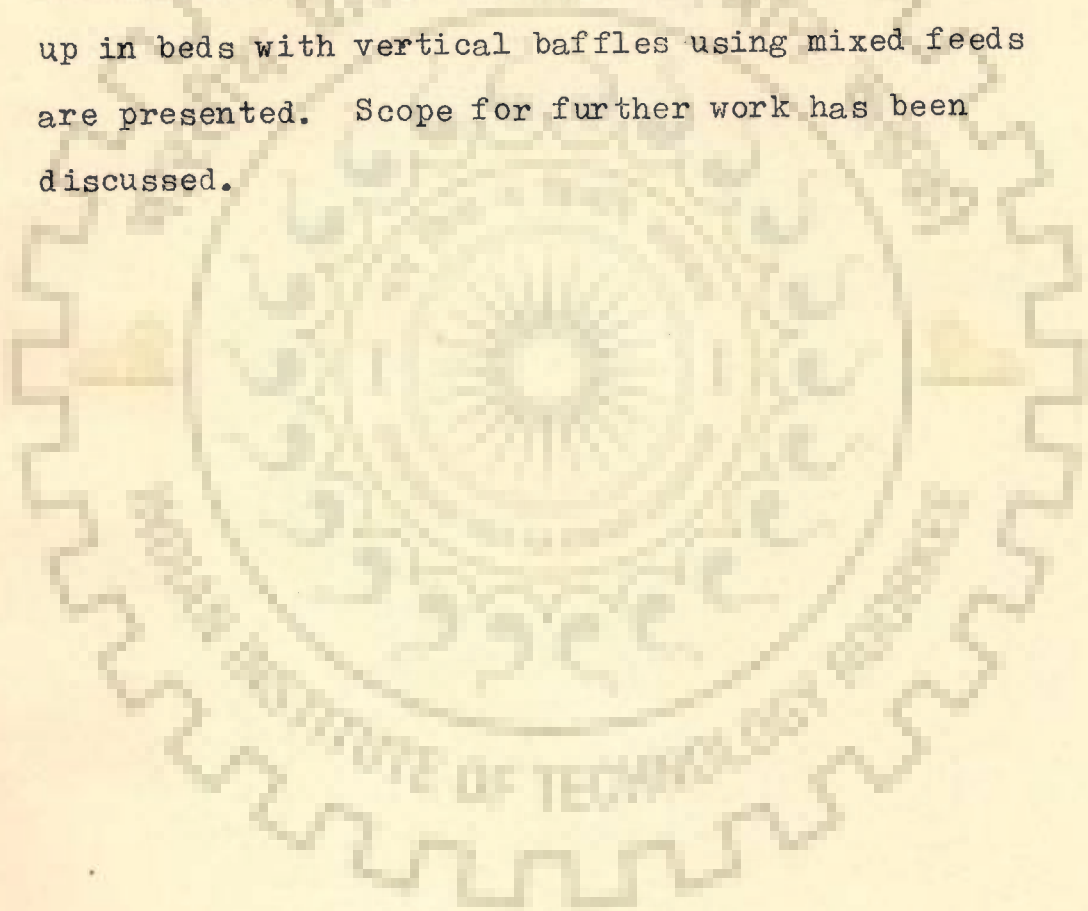


FIG. 5.19 COMPARISON OF VALUES OF HOLD-UP RATIO PREDICTED AND OBSERVED IN CONTINUOUS FLUIDIZED BEDS WITH VERTICAL BAFFLES.

C H A P T E R - V IA B S T R A C T

Conclusions based on the present studies on batch fluidized beds with vertical baffles, continuous fluidized beds with vertical baffles and hold up in beds with vertical baffles using mixed feeds are presented. Scope for further work has been discussed.



C H A P T E R - V I

CONCLUSIONS AND RECOMMENDATIONS

The present studies include the effect of vertical internal baffles on gas-solids fluidization in batch and continuous systems. The presence of vertical internal baffles improve the quality of fluidization by reducing the slugging tendencies in batch fluidized beds. In continuous systems, the bed density is increased for sharp cuts and hold up ratio is increased for mixed sized feeds.

6.1 Batch Fluidized Beds with Vertical Internal Baffles

Batch fluidization studies have been conducted in fluidized beds with vertical internal baffles numbering 12, 7 and 3 respectively. The variation in bed pressure drop with air mass velocity in fixed bed zone, at the onset of fluidization and in fluidized bed zone is observed to be in accordance with the earlier reported works on fluidized beds without baffles. Pressure drop in fluidized beds with vertical baffles is observed to be more than that of unbaffled beds. This increase in pressure drop is caused by the extra skin friction due to the baffles. The correlation given by eqn. 3.4 can be used for predicting the overall pressure drop across the bed at and beyond onset of fluidization.

A minimum distance of six particle diameters between two adjacent baffles or between baffles and the wall of the column will have to be maintained for the movement of particles to occur. Below this ratio the particles are interlocked due to arching and no fluidization occurs even at velocities beyond the minimum fluidizing velocities. When the interbaffle distance of ten particles diameter is maintained normal fluidization results.

The presence of vertical internal baffles hinders the particle movement even when the interbaffle distance is greater than ten particle diameters and upto 28 particle diameters. The minimum fluidizing velocities required will be higher as additional energy will be required to unlock and initiate free movement of the particles.

Eqn. 3.1 has been proposed to predict the minimum fluidizing velocity in batch fluidized beds incorporating the factors due to particle properties, geometry of the bed and baffle and fluid characteristics.

The bed expansion and fluctuation ratio will be lower in beds with vertical internal baffles as bubbling is reduced because of the presence of vertical baffles. Eqn. 3.5 and 3.6 have been proposed for predicting the bed porosity and fluctuation ratio.

6.2 Continuous Fluidized Beds with Vertical Internal Baffles

The effect of vertical baffles on continuous gas solids fluidization has been studied with regard to bed pressure drop and bed density. Introduction of vertical internal baffles in the bed will increase the pressure drop both due to the additional baffle surface and the friction due to restricted particle movement.

The presence of vertical baffles also increases the bed density due to lower bed expansion and increased pressure drop.

Eqns. 4.1 and 4.2 have been proposed to predict the bed pressure drop and bed density for sharp cuts respectively in continuous fluidized beds with vertical baffles.

6.3 Hold-up Studies in Continuous Systems with Mixed Sized Feeds

In continuous fluidized beds without baffles using mixed feeds, the G_f/G_{mf} values will be higher for smaller particles than for larger ones, resulting in a greater mobility for smaller particles. At lower values of G_f/G_{mf} smaller particles will be continuously moving up the centre and down the walls of the column giving a higher concentration of fines near the periphery. Greater mobility and higher concentration of smaller

particles near the walls and location of solids discharge at the periphery results in a preferential removal of fines giving increased bed hold up ratio with gas flow rate.

At higher gas flow rates bubbling will become predominant. Each gas bubble will carry behind a wake of solids. As the bubble moves up, the solids are sucked into the wake. The smaller particles will be carried with the bubbles at a faster rate than the larger ones giving increased concentration of fines at the centre than the periphery of the column. As a result larger particles will have a greater tendency to move out of the peripheral discharge opening. This results in a slower rate of increase in the bed hold up ratio with increase in gas velocity. At higher gas flow rate, when severe bubbling condition is present the hold up ratios are even likely to fall down.

Hence the bed hold up ratio in beds without baffles will first increase with increase in gas flow rate reaching a peak value after which the hold up ratio will decrease. The transition occurs at G_f/G_{mf} ranging between 1.8 to 2.0.

The introduction of vertical internal baffles leads to formation of large number of compartments in the beds giving uniform bed composition. Smaller particles with large d_o/D_p ratio have greater movement than the larger

ones having low d_o/D_p values at any air velocity. The smaller particles have a greater chance of moving out through the discharge. Thus the bed hold up ratios increase with increasing air flow rate. At higher velocities of air the bubbling tendencies are reduced by the presence of baffles. The smaller particles will continue to be removed from the bed at a faster rate compared to larger particles. Thus the bed hold up ratio increases steadily with increase in air flow rate. The same trend continues even at high velocities as slugging tendency is not present in beds with vertical internal baffles. This is an improvement in the bed performance with baffles compared to that of bed without baffles. Eqn. 5.5 has been proposed for predicting the bed hold up ratio in the beds with vertical internal baffles.

6.4 Scope for Further Work

Further work is necessary in the following areas in order that the data can be conveniently scaled up for use in large size units:

- Effect of baffle characteristics, diplegs and column size.
- Effect of location of solids outlet in continuous systems on solids downflow characteristics and bed hold up ratios.
- Studies on individual RTD of particles for systems having mixed sized feeds.

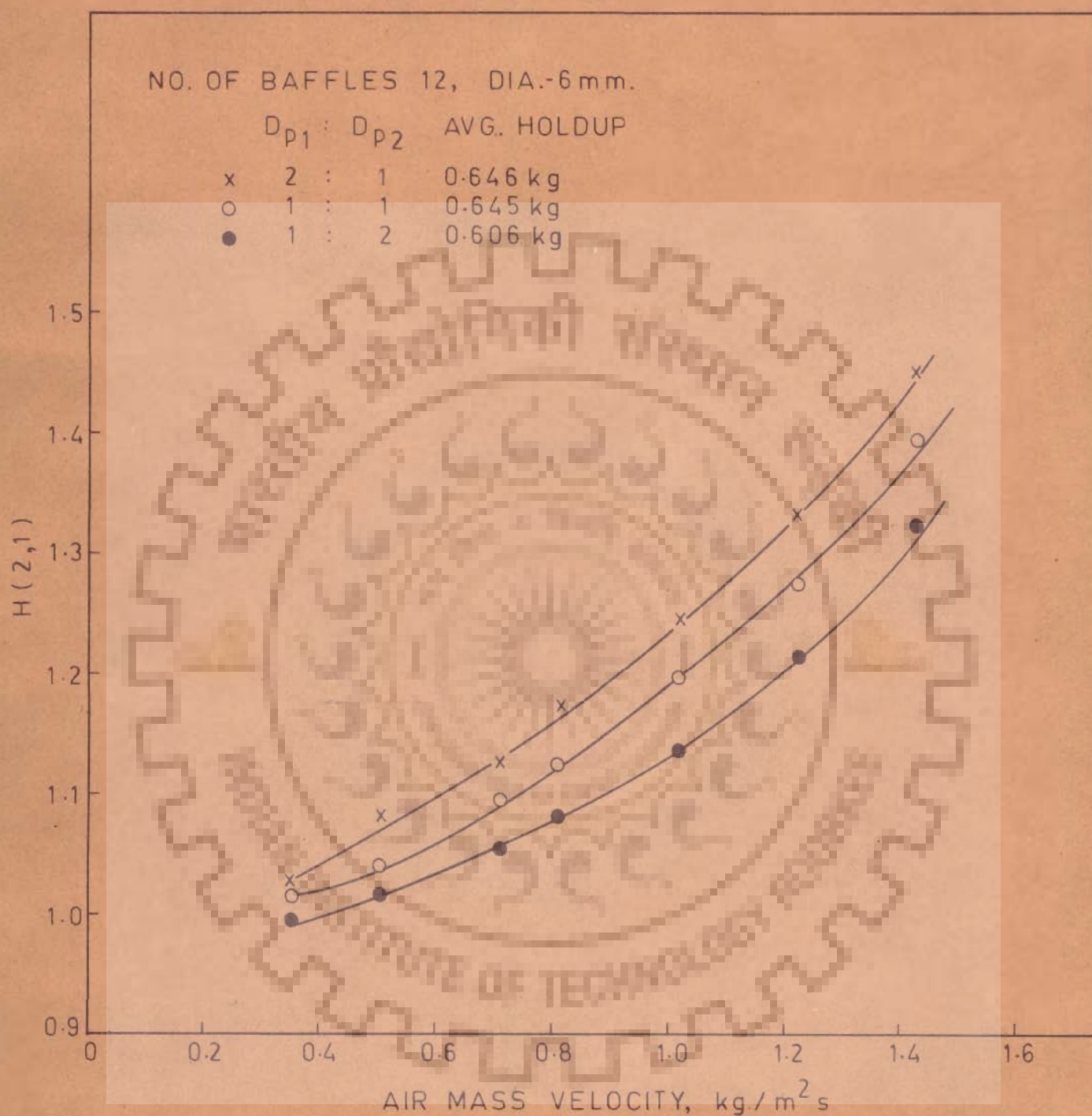


FIG. 5.11 VARIATION OF HOLDUP RATIO WITH AIR MASS VELOCITY IN CONTINUOUS FLUIDIZED BEDS WITH VERTICAL BAFFLES.



APPENDICES

```

C   PH D THESIS  YOGESH CHANDRA
C   PROGRAM WAS EXECUTED AT THE COMPUTER CENTRE AT SERC ROORKEE
C   DIMENSIONA(15,15),X(15,100),XB(15),CO(15),Y(100),ER(100)
2  READ1,N,M,IM
1  FORMAT(3I5)

C
C   N IS NO. OF VARIABLES  M IS NO. OF DATA POINTS
C   IM =1 INDICATES RELATIONSHIP OF TYPE  $Y=A*(X**B)*(Z**C)$ 
C   IM=2 RELATION IS  $Y=A+B*X+C*Z$ 
C   READING OF DATA POINTS
C
3  FORMAT(6E12.5)
   DO5 J=1,M
   READ3,(X(I,J),I=1,N)
5  CONTINUE
C   IF IM=1 GO TO 10 , IF IM=2 GO TO 20
   IF(IM-1)10,10,20
10  DO15 I=1,N
   DO 15 J=1,M
15  X(I,J)=LOGF(X(I,J))
20  AM=M
   DO 50I=1,N
   SUM=0.0
   DO 40 J=1,M
   SUM=SUM+X(I,J)
40  CONTINUE
   XB(I)=SUM/AM
50  CONTINUE
   PUNCH 55
55  FORMAT( 5X, 11HMEAN VALUES//)
   PUNCH 3,(XB(I),I=1,N)
   DO 60 I=1,N
   DO 60 J=1,M
60  X(I,J)=X(I,J)-XB(I)
   N1=N-1
   DO 65 I=1,N1
   DO 65 K=I,N
   A(I,K) =0.0
   DO 65 J=1,M
   A(I,K) =A(I,K)+X(I,J)*X(K,J)
65  CONTINUE
   DO 70 I=2,N1
   I1=I-1
   DO 70 J=1,I1
70  A(I,J) =A(J,I)
   PUNCH 71
71  FORMAT( 5X, 24HCoefficient OF EQUATIONS//)
   DO 80 I=1,N1
   PUNCH 3,(A(I,J),J=1,N)
80  CONTINUE

```

```

CALL SIMEQ(A,N1,CO)
COI1 =XB(N)
DO 82 K=1,N1
COI1 =COI1-CO(K)*XB(K)
82 CONTINUE
IF(IM-1)83,83,84
83 COI =EXPF(COI1)
GO TO 85
85 PUNCH 86
84 COI= COI1
86 FORMAT (5X,22HCONSTANTS OF RELATION//)
PUNCH 87 ,COI
87 FORMAT (5X,2HA=,E12.5)
PUNCH 88,(CO(K),K=1,N1)
88 FORMAT (2X,5HB(I)=,6E12.5)
DO 90 K=1,N
DO 90 J=1,M
90 X(K,J) =X(K,J)+XB(K)
DO 100 J=1,M
Y(J)=Y(J)+CO(K)*X(K,J)
100 CONTINUE
IF(IM-1)105,105,120
105 DO 115 J=1,M
DO 110 I=1,N
110 X(I,J)=EXPF(X(I,J))
Y(J)=EXPF(Y(J))
115 CONTINUE
120 DO 130 I=1,M
ER(I) =(Y(I)-X(N,I))*100./X(N,I)
130 CONTINUE
PUNCH 131
131 FORMAT (5X,12HF;NAL RESULT//)
PUNCH 132
132 FORMAT ( 40H*****1H*,
139H*****//)
PUNCH 133
133 FORMAT(4X,2HX1,10X,2HX2,10X,2HX3,10X,2HX4,10X,2HX5,10X,2HX6)
PUNCH 132
DO 140 J=1,M
PUNCH3,(X(I,J),I=1,N),Y(J),ER(J)
140 CONTINUE
PUNCH 132
GO TO 2
STOP
END

```

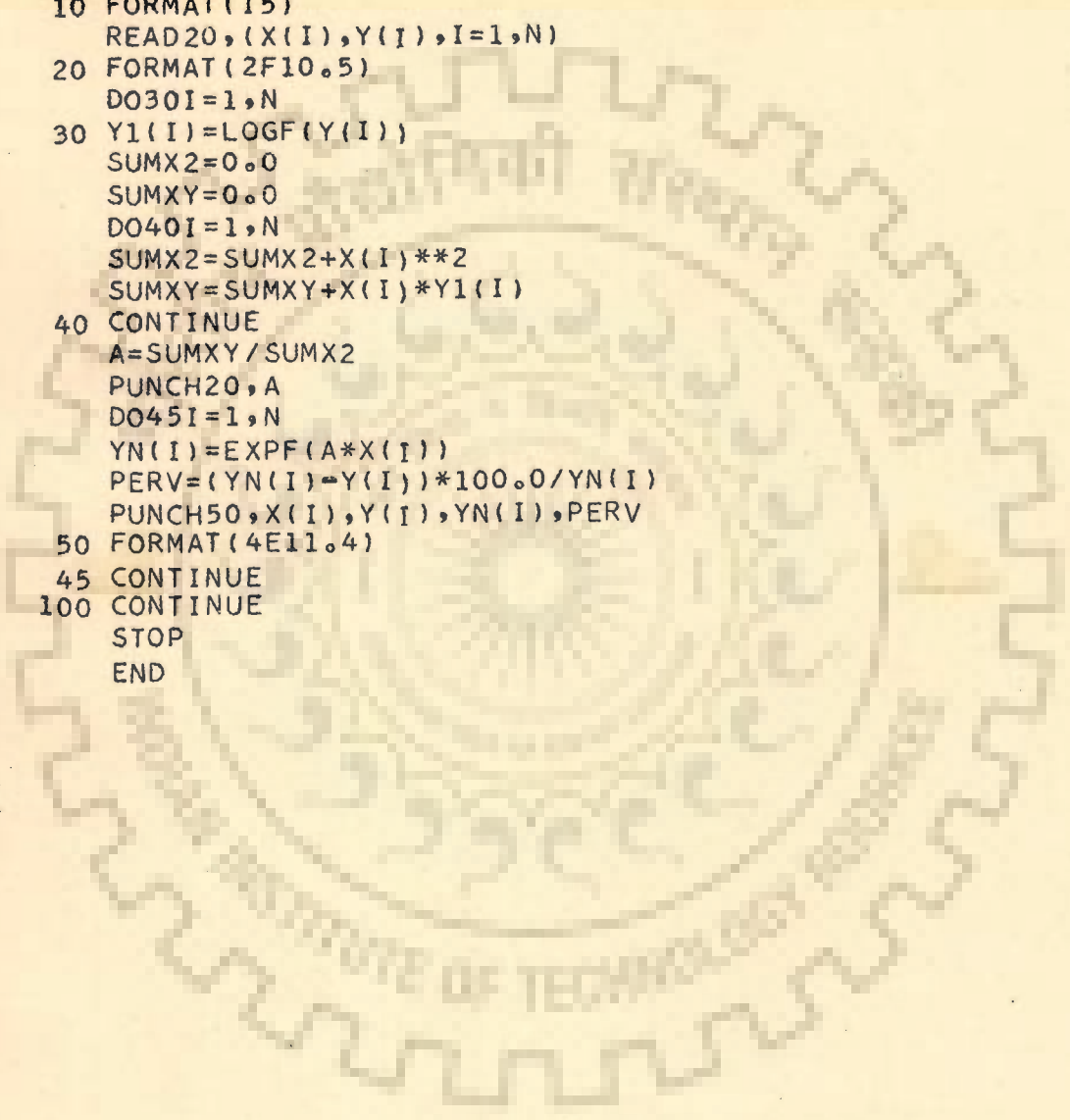


```

SUBROUTINE SIMEQ(A,N,X)
DIMENSION A(15,15),U1(15,15),U(15,15),X(15)
M=N+1
DO20IT=1,N
JT=1
1 IF(JT-1)3,3,2
2 J=IT+1
I=IT
GO TO 4
3 I=IT
J=IT
4 U(I,J)=A(I,J)
IF(IT-1)7,7,5
5 M1=IT-1
DO6K=1TM1
6 U(I,J)=U(I,J)-U(I,K)*U(K,J)
7 IF(JT-1)8,8,10
8 I=I+1
IF(I-N)4,4,9
9 JT=2
GO TO 1
10 U(I,J)=U(I,J)/U(I,T)
J=J+1
IF(J-M)4,4,20
20 CONTINUE
DO30 I=1,N
DO30 J=1,M
IF(I-J)25,27,27
25 U1(I,J)=U(I,J)
GO TO 30
27 U1(I,J)=0.0
30 CONTINUE
DO 35J=1,N
35 X(J)=0.0
N1=N
40 I=N1
X(I)=U1(I,M)
DO45 J=1,N
45 X(I)=X(I)-U1(I,J)*X(J)
N1=N1-1
IF(N1-1)47,40,40
47 RETURN
END

```

```
C CURVE FITTING PH D THESIS YOGESH CHANDRA
C PROGRAM WAS EXECUTED AT THE COMPUTER CENTRE AT SERC ROORKEE
  DIMENSIONY(100),X(100),Y1(100),YN(100)
  READ10,MP
  DO 100IP=1,MP
  READ10,N
10  FORMAT(I5)
  READ20,(X(I),Y(I),I=1,N)
20  FORMAT(2F10.5)
  DO30I=1,N
30  Y1(I)=LOGF(Y(I))
  SUMX2=0.0
  SUMXY=0.0
  DO40I=1,N
  SUMX2=SUMX2+X(I)**2
  SUMXY=SUMXY+X(I)*Y1(I)
40  CONTINUE
  A=SUMXY/SUMX2
  PUNCH20,A
  DO45I=1,N
  YN(I)=EXPF(A*X(I))
  PERV=(YN(I)-Y(I))*100.0/YN(I)
  PUNCH50,X(I),Y(I),YN(I),PERV
50  FORMAT(4E11.4)
45  CONTINUE
100 CONTINUE
  STOP
  END
```



REFERENCES

1. Morse, R.D. and Ballou, C.O., Chem. Engg. Prog. 47, 199 (1951).
2. Shuster, W.W. and Gomezplata, A., A.I.Ch.E. Jl. 6, 454 (1960).
3. Leva, M., 'Fluidization' McGraw Hill Book Co. Ny (1959).
4. Kunii, D. and Levenspiel, O, 'Fluidization Engineering', John Wiley and Sons NY (1969).
5. Wilhelm, R.H. and Kwauk, M, Chem. Eng. Prog. 44, 201 (1944).
6. Romero, J.B. and Johnson, L.N., Chem. Engg. Prog. Symp. Ser. No. 38, 58, 28 (1962).
7. Blake, F.C., Tr. Am. Instn. Chem. Engr. 14, 415 (1922) as cited in Ref. (3).
8. Burke, S.P., and Plummer. W.B., Ind. Eng. Chem. 20, 1196 (1928) as cited in Ref. (3).
9. Chilton, T.H. and Colburn, A.P. ibid, 23, 8, 913 as cited in Ref. (3).
10. Carman, P.C., Tr. Inst. Chem. Eng. (British) 15, 150 Part I (1937) as cited in Ref. (3).
11. Ergun, S., Chem. Eng. Prog. 48, 89 (1952).
12. Davidson, J.F. and Harrison, D., 'Fluidization' Academic Press London (1971).

13. Adler, H.L. and Happel, J, Chem.Eng. Prog. Symp. Ser. No. 38, 58, 98 (1962).
14. Hiby, J.W., Chem. Ingr. Tech. 36, 2228 (1964) as cited in Ref. (12).
15. Petrie, J.C. and Black, D.E. Chem. Eng. Prog. Symp. Ser. No. 67, 62, 64 (1966).
16. Whitehead, A.B., and Dent, D.C.. Proceedings of the International Symposium on 'Fluidization' Netherland University Press, Amsterdam (1967) as cited in Ref. (12).
17. Leva, M, Grummer, M. and Weintraub, M., Chem.Eng. Prog. 44, 511 (1948).
18. Wen, C.Y. and Yu, Y.N., Chem.Eng. Prog. Symp. Ser. No. 62, 62, 100 (1966).
19. Miller, C.O. and Logwinuk, A.K.. Ind Eng. Chem. 43, 122 (1951).
20. Van Heerden, C., Nobel, A.P.P. and Vankrevelen, D.W., Can. Jl. Res. 28, 282 (1950).
21. Johnson, E., Intn. Gas Eng. Publication Vol. 1, No. 378, 179 (1949-50).
22. Akopian, I.A. and Kastkin. A.G., Khim Prom.No. 2 (1955).
23. Bena, J., Ilavsky, J. and Kassaczky, E., Chem. Prumysl No.10, 285 (1960) as cited in Ref (41).
24. Beilin, M.I., Khimiya, i. Tekhnol. Topl. i.Masel Vol. 6, No.4,19 (1961) as cited in Ref. (40).

25. Erkova, L.N. and Smirnov, N.I., Tr. Leningrads Tekhn.Inta. in Lensoveta No. 45 (1958).
26. Winterstien, G. and Rose, K., Chem. Tech. Vol. 13, No.2 (1961) as cited in Ref. (39).
27. Goddard, K.E. and Richardson, J.F., Chem. Eng. Sci. 24, 363 (1969).
28. Beranek, J. and Sokol D., Fluidni Technika, (1961) as cited in Ref. (41).
29. Narasimhan, G., A.I.Ch.E. Jl. 11, 550 (1965).
30. Pinohbeck, P.H. and Popper. F., Chem.Eng. Sci. 6, 57 (1956).
31. Bourgois, P. and Grenier, P., Can. Jl. Chem. Eng. 46, 325 (1968).
32. Davies, L. and Richardson, J.F., Tr. Instn. Chem. Engrs. 44, 293 (1966).
33. Frantz, J.F., Chem. Eng. Prog. Symp. Ser. No.62, 62, 2137 (1966).
34. Baerg, A., Klassen, J. and Gishler, P.E., Can. Jl. Res. 28, 287 (1950).
35. Pillai, B.C. and Raja Rao, M., Indian Jl. Tech. 9, 77 (1971).
36. Balakrishnan, D. and Raja Rao, M., Chem. Proc. and Eng. 5, 6, 17 (1971).
37. Motamedi, M. and Jameson, G.J., Chem.Eng. Sci.23, 791 (1968).

38. Murthy, V.S. and Raja Rao, M; Seminar on Recent Developments in Chemical Engineering held at I.I.T. Bombay (1971).
39. Sen Gupta, P. and Rao, M.N., Indian Chem.Eng. Vol XIII, No. 1, Che 11, January (1971).
40. Zabrodsky, S.S., 'Hydrodynamics and Heat Transfer in Fluidized bed' Translation Editor F.A.Zenz M.I.T. Press, Cambridge Mass.(1966).
41. Vanecek, D., Markavart, M. and Drobhlav, R; 'Fluidized Bed Drying' Translation Editor J.Landau, Leonard Hill, London (1966).
42. Aliev, V.S., Indyukov, N.M., and Rustamov, M.I.Khim. I. Tekhnol Topl i. Masel Vol. 4, No.8; 65 (1959).
43. Ginzburg, A.S., and Rezhikov, V.A., Inzh. Fiz. Zh. Akad. Nauk Belorussk, S.S.R. Vol. 5, No. 8, 40 (1962).
44. Graf, E., Ph.D. Thesis, 'Eidgenossische Technische Hochschule Zurich (1955).
45. Grishim, M.A., Inzh-Fiz Zhurn. 3, No.3, 40 (1960).
46. Dementiev, V.M. Teploenergetika, 6, No. 1, 50 (1959).
47. Zabrodsky, S.S., Tr. In-ta Energetika Akad. Nauk B S S R No.3 (1957).
48. Boguslavskii, N.M. and Melik - Akhnazarov, T. Kh., GOSINTI, Moscow (1960).

49. Leva, M., Weintraub, M., Grummer, M., Pollichik, M. and Storch, H. U.S. Bur. Mines. Bull. No. 504 (1951).
50. Leva, M., Shirai, T., and Wen, C. Genie. Chim 75, No.2, 33 (1956).
51. Loeffler, A. and Ruth, B., A.I.Ch.E. Jl., 15, 3, 310 (1959) as cited in Ref. (39).
52. Petrov, V.N., Tr. Mosk In-ta. Neftekhim i, Gazovoi Promyshlennosti No.28, 102 (1960).
53. Rowe, P.N., Tr.Instn. Chem.Engrs., 39, No.3, 175 (1961).
54. Smirnov, A.M., Shor Nauch. Trnd. Quib, Indrst. Inst. No.8, 3, (1959) as cited in Ref. (39).
55. Straneo, P. and Cappi, E. Chim. e. Ind. 43, No.12, 1393 (1961) as cited in Ref. (39).
56. Takeda, K., Bull. Jamagata. Univ. 4, No.2, 273 (1959) as cited in Ref. (39).
57. Goroshko, V.D., Rozenbaum, R.B. and Todes, O.M., Izvestiya Vuzov Neft' i Gaz., No.1, 125 (1958).
58. Federov, I.M., Theo. Res. Proc. Sush. Gose. energoiz Dat. (1955) as cited in Ref. (39).
59. Hawskley, P.G.W., 'Some Aspects of Fluid Flow' Edward Arnold London (1951) as cited in Ref. (39).
60. Heerden, C.Van., Nobel, A.P.P. and Krevlen, D.W.V., Chem. Engg. Sci, 1, 37 (1951).

61. Happel, J., A.I.Ch.E. Jl., 4, 2, 197 (1958).
62. Checkiotkin, A.V., Nauch, Dok, Vish, Skol-Khimia. Technol. 2, 406 (1959) as cited in Ref. (39).
63. Justat, A., Katauza Zawiesinowa i Zapomniany Patent Polski, Pwzem. Chem. 28, 16, (1949) as cited in Ref. (39).
64. Kadimova, K.S., Neft Khoz No.3, 24 (1953) as cited in Ref. (39).
65. Gupalo, U.P., Inz. Physik Jl. 511, No.196 (1962) as cited in Ref. (39).
66. Karpov, A. T. Izv Mvo. USSR Ser, Energetica 8, 71 (1962).
67. Mazurov, D.I., Inz. Physik Jl. Vol. 5, No. 13 (1962) as cited in Ref. (39).
68. Gopichand, T. and Rao, M.N., Tr. Ind. Inst. Chem. Engr. Vol. VII, 35 (1958-59).
69. Frantz, J.F., Chem. Eng. 60, No.19, 161 Sept. 17 (1962).
70. Ghoshal, S.K. and Dutt, D.K., Ind. Chem.Engg. (Trans) VIII, 3, 58 (1966).
71. Subbaraju, K. and Venkata Rao, C., Ind. Jl. Tech. 2, No.7, 222 (1964).
72. Westerfried, F. and Cazacu, C., Stud. Siceret. Energet. 10, No.1, (1960) as cited in Ref. (39).
73. Saksena, R.K. and Mitra, C.R., Indian Chem.Engr., Vol. XIV, No.3, 35, July-Sept (1972).

74. Rowe, P.N. and Henwood, G.A., *Tran. Instn. Chem. Engr. (London)* 39, 43 (1961).
75. Kunii, D. and Levenspiel, O., *Ind. Eng. Chem. Funda.* 7, 446 (1968).
76. Yasui, G. and Johnson, L.N., *A.I.Ch.E. Jl.* 4, 445 (1958).
77. Davidson, J.F., Paul, R.C., Smith, M.J.S. and Duxbury, H.A., *Tr. Instn. Chem. Engr. (London)* 37, T-323 (1959).
78. Harrison, D. and Leung, L.S., *Tr. Instn. Chem. Engr. (London)* 40, T-146 (1962).
79. ~~Lockett~~, Davidson, J.F. and Harrison, D., *Chem. Eng. Sci.*, 22, 1059 (1967).
80. Rowe, P.N. and Patridge, B.A., *Tr. Instn. Chem. Engr. (London)* 43, T-157 (1965).
81. Toei, R., Matsuno, R., Sumitani, T. and Mori, M., *Int. Chem. Eng.* 8, 351 (1968).
82. Davies, R.M. and Taylor, G.I., *Proc. Roy. Soc.* 375 (1950) as cited in Ref. (12).
83. Davidson, J.F. and Harrison, D. 'Fluidized Particles' Cambridge Univ. Press N.Y. (1963).
84. Rice, W.J. and Wilhelm, R.H., *A.I.Ch.E. Jl.* 4, No. 4, 423 (1958).
85. Dotson, J.M., *A.I.Ch.E. Jl.* 5, No. 2, 169 (1959).
86. Murray, J.D., *Jl. Fluid Mech.* 21, Part 3, 465 (1965).

87. Grace, J.R., and Harrison, D., Tr. Instn. Chem. Engr. (London) 39, 175 (1961).
88. Rowe, P.N., Ibid. 39, 18, 175 (1961).
89. Collins, R., Chem. Eng. Sci., 20, 851 (1965).
90. Morooka, S., Tajuna, K. and Miyanchi, T., Int. Chem.Eng. 12, 1., 168 Jan. (1972).
91. Miwa, K., Mori, S., Kato, T. and Muchi. I., ibid., 12, 1, 187, Jan. (1972).
92. Groshe, E., A.I.Ch.E. Jl. No.1, 358 (1955).
93. Richardson, J.F. and Zaki, W.N., Tr. Inst. Chem. Engrs (London) 32, 35 (1954).
94. Agarwal, J.C., Davis, W.L. and King, D.T., Chem. Eng. Prog. 58, 85, Nov. (1962) as cited in Ref. (4).
95. Ruzamov, I.M., Manshilin, V.V., Terakhov, N. I. and Babaev, V.V. Int. Chem.Eng. 12, 1, 187, Jan. (1972).
96. Milonov, V.M., Int. Chem. Eng. 12, 3, 473, July (1972).
97. Murtazin, K. Kh., Maksimenko, M.Z., Sunyaev, Z.I., Sudovikov, A.D. and Glushchenko, I.F., Int. Chem. Eng. 12, 2, 335, April (1972).
98. Matesen, J.M., Chem.Eng. Prog. Symp. Ser-66, 101, 47 (1970).
99. Matesen, J.M., Hovmond, S., and Davidson, J.F., Chem.Eng. Sci 24, 1743 (1969).

100. Matesen, J.M. and Tarmy, B.L., Am. Inst. Chem. Engrs. Meeting Tampa, Florida, May (1968).
101. Glass, D.H. and Harrison, D., Chem. Eng. Sci. 19, 1001 (1964).
102. Glass, D.H., Ph.D. Dissertation Univ. of Cambridge as cited in Ref. (12).
103. Wace, P.F. and Burnett, S.J., Tr. Instn. Chem. Engr. 39, 168 (1961).
104. Cloets, F. L. D., Proceed. Intntnl. Symp. on Fluidization pp 305-307, Netherland Univ. Press (Amesterdam) (1967).
105. Morgan, C., Ph.D. Dissertation, Univ. of Cambridge as cited in Ref. (12).
106. Bailie, R.C., Chung, D.S. and Fon, L.T., Ind. Eng. Chem. Fund 2, 245 (1963).
107. Overcashier, R.H., Todd, D.B. and Olney, R.B. A.I.Ch.E.J. 5, 54 (1959).
108. Massimilla, L. and Bracale, S. Ricerca, Sci. 26, 487 (1956).
109. Hall, C.C. and Crumley, P.J., Appl. Chem. 2, S-47 (1952).
110. Massimilla, L. and Westwater, J.W. A.I.Ch.E.J. 6, 134 (1960).
111. Volk, W., Johnson, C.A. and Stotler, H.H., Chem. Eng. Prog. 58, 44 (1962).
112. Lewis, W.K., Gilliland, E.R. and Glass, W. A.I.Ch.E.J. 5, 419 (1959).

113. Sutherland, K.S., Trans. Instn. Chem. Eng. 39, 188 (1961).
114. Grace, J.R. and Harrison, D. Proceedings I.Chem. E-VTG/VDI (Joint meeting, Brighton) as cited in Ref. (12).
115. Grace, J.R. and Harrison, D., Tripartite Chem. Eng. Conference Session 32, Montreal as cited in Ref.(12).
116. Botton, R.J., Chem.Engg. Prog. Symp. Ser. 66, 8 (1970).
117. Hovmand, S. and Davidson, J.F. Trans. Instn. Chem.Eng. 46, 190 (1968).
118. Hebden, D., Trans. Instn. Chem.Eng. 39, 224 (1961).
119. Rowe, P.N. and Stapleton, W.M., *ibid* p. 181.
120. Agarwal, J.C. and Davis, W.L., Chem.Eng. Prog. Symp Ser. 62, 101 (1966).
121. Miller, C.O. and Logwinuk, A.K., Ind. Eng.Chem. 43, 1220 (1951).
122. Vreedenbarg, H.A., Chem.Eng. Sci. 11, 274 (1960).
123. Baskakov, A.P. and Berg, B.V., Inzh-Fiz. Zh. 10, 738 (1966), as cited in Ref. (12).
124. Gelperin, N.I., Kruglikov, V.J. and Ainshtein, V.G. Khim Prom 42, 34 (1966) as cited in Ref. (12).
125. Genetti, W.E. and Knudsen, J.G., Tripartite Chem.Eng. Conference, Int. Chem.Eng. London as cited in Ref. (12).

126. Lewis, W.K., Gilliland, E.R. and Bauer, W.C.;
Ind. Eng.Chem 41, 104 (1949).
127. Quinn, M.F. Ind.Eng. Chem. Vol. 55 (7) 18-25
(1963).
128. Gilliland, E.R. and Mason, Ind.Eng. Chem. 45,
1177 (1953).
129. May, W.G., Chem.Eng. Prog. 55, 12, 49-56 (1959).
130. Danckwerts, P.V., Jenkins, J.W. and Place, G.,
Chem. Eng. Sci. 3, 26-35 (1954).
131. Nankoong, S. and Sasaki, M., Int.Chem.Eng. 6,4,
668 (1966).
132. Levenspiel, O., Chemical Reaction Engg. John
Wiley and Sons, New York (1962).
133. Levenspiel, O. and Bischoff, K.B., Advances in
Chemical Engg. Vol. 4, 95 Academic Press
New York (1963).
134. Dayan, J., Ph.D.Thesis, Illinois Institute of
Technology Chicago (1967) as cited in
Ref. (4).
135. Yoshida, K. and Kunii, D., J1. Chem.Engg.Japan 1,
11 (1968).
136. Fitzgerald, T., Ph.D.Thesis, Illinois Institute
of Technology Chicago, as cited in Ref.(4).
137. Rao, N.J., Ph.D.Thesis, Univ. of Roorkee,(India)1974.
138. Richardson, J.F. and Zaki, W.N., Trans. Instn.
Chem.Engr. (London) 32, 35-53 (1954).

139. Askins, J.W., Hinds, G.P. and Kunreuther, F.,
Chem.Eng. Prog. 47(8), 401 (1951).
140. Singer, E., Todd, D.B. and Guin, V.P. Ind.Eng.
Chem. 49, 11-19 (1957).
141. Stephens, G.K., M.Eng. Sc.Thesis, Chemical Engg.
Monash University, Australia (1965) as
cited in Ref. (12).
142. Stephens, G.K., Sinclair, R.J. and Potter, O.E.,
Powder Tech. 1, 57 (1967).
143. Van Deemter, J.J., Chem.Eng.Sci 13, 143 (1960).
144. Kunii, D. and Levenspiel, O. I and E.C. Fundamentals
7, 446 (1968).
145. Mitham, R., Hamilton, C. and Potter, O.E. Brit.
Chem.Engg. 13, 666 (1968).
146. Gopichand, T., Sarma, K.J.R. and Rao, M.N. Ind.
Eng. Chem. Vol. 51, No.12, 1449 (1959).
147. Toomy, R.D. and Johnstone, H.F., Chem.Eng. Prog.
Symp Ser. 5, 51, (1953).
148. Kondukov, N.V. et al, Int. Chem.Eng. 4,43 (1964).
149. Rowe, P.N. Fuel Soc. J. Univ.Sheffield 17, 8(1966).
150. Zenz, F.A. and Katz, S., Petr. Refiner 33, 203,
(1954).
151. Lochiel, A.C. and Sutherland, J.P., Chem.Eng.
Sci. 20(12) 1041 (1965).
152. Tailby, S.R. and Cocquerel, M.A.T., Trans. Inst.
Chem.Eng. 39, 195 (1961).

153. Yagi, S. and Kunii, D., Chem. Engg. Sci 16, 380 (1961).
154. Bowling, K. and Watts, A., Austr. J. App. Sci. 12, 1413, (1961).
155. Turyayev, I. Ya and Tzailingold, A.L., Zh Prikl. Khim. 33, 1783 (1960).
156. Wolf, D. and Resnick, W. Ind. Eng. Chem. Fund. 2(4) 287 (1963).
157. Morris, D.R. et al, Tran. Instrn. Chem. Engr. 42 T323 (1964).
158. Urabe, S., Hiraki, I., Yoshida, K. and Kunii, D., Kogaku Kogaku, 4, 151 (1966).
159. Chechetkin, A.V., Pavlov, V.A., Apostolova, G.V. and Romanova, T.T. ~~Teoet~~, Osmovy Khim Tekh 8(5) 796 (1974).
160. Lewis, E.W. and Bowerman, E.W., Chem. Eng. Prog. 48, 603 (1952).
161. Bharadwaj, D.K., Ph.D. Thesis, Univ. of Roorkee, Roorkee (India) 1975.
162. Bailey, C., Unpublished work, Univ. College of Swansea, as cited in Ref. (12).
163. Matheson, G.L., U.S. Patent (1950) as cited in Ref. (12).
164. Gabor, J.D., Mecham, W.J. and Jonke, A.A., Chem. Eng. Prog. Symp. Ser. 60, 96 (1964).

165. Sutherland, J.P., Vassilatos, G., Kubota, H.
and Osberg, G. L., A.I.Ch.E. Jl. 9,
437 (1963).
166. Kang, W.K. and Osberg, G.L., Can. J. Chem.Eng.
44, 142 (1966).
167. Chen, B.H. and Osberg, G.L., Can. J. Chem.Eng.
45, 90 (1967).
168. Rao, K.M., M.E.Dissertation, Univ. of Roorkee,
Roorkee (India) 1975.

